Signotopes and Convex Drawings

Dissertation
zur Erlangung des Grades einer
Doktorin der Naturwissenschaften
(Dr. rer. nat.)

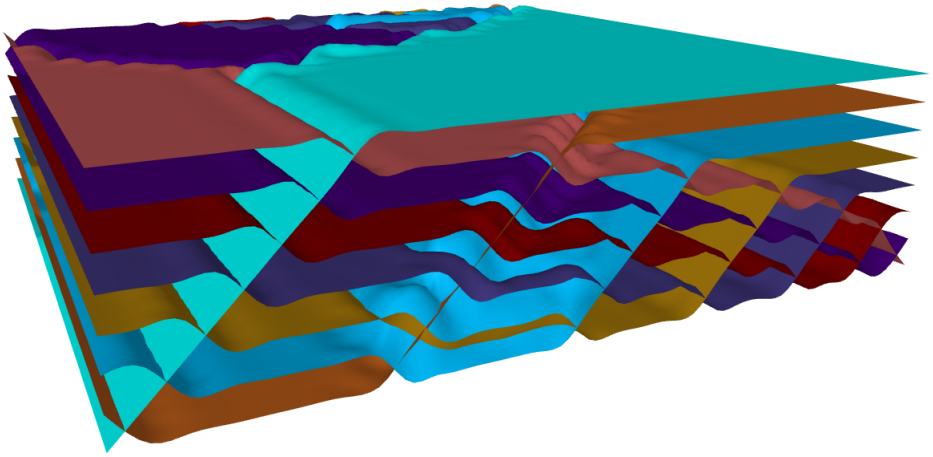

am
Fachbereich Mathematik und Informatik
der Freien Universität Berlin

vorgelegt von

Helena Bergold

Berlin, 2023

Betreuer und Erstgutachter:	Prof. Dr. Günter Rote
Zweitgutachter:	Prof. Dr. Stefan Felsner

Tag der Disputation: 19.01.2024

Abstract

In this thesis we investigate sign mappings, which for a fixed rank r map subsets of $\{1, \dots, n\}$ of size r to one of the two signs $+$ and $-$, while avoiding sign patterns on induced substructures. Particular focus will be on signotopes and generalized signotopes which originate from pseudohyperplane arrangements and simple drawings. Using those combinatorial encodings for topological objects, we prove classic results in a more general setting.

We consider Levi's extension lemma for pseudoline arrangements and prove that it generalizes to signotopes of odd rank r. Levi showed in 1926 that every pseudoline arrangement can be extended by an additional pseudoline going through two prescribed points. A generalization to dimension 3 fails as Goodman and Pollack (1981) provided an example of pseudoplane arrangements and three prescribed points which is not extendable even though for hyperplane arrangements an extension through d points in dimension d is trivial. Later Richter-Gebert (1993) showed that even an extension through two prescribed points is not possible in dimension 3. We show that signotopes, a subclass of pseudohyperplane arrangements, admit an extension theorem for all even dimensions, that is if the rank r is odd. Moreover, we provide signotopes which are not extendable for rank 4, 6, 8, 10 and 12.

Next, we focus on theorems from convex geometry such as Carathéodory's, Helly's and Kirchberger's theorem and study them in the more general setting of simple drawings of the complete graph. In particular we determine in which layer of the convexity hierarchy introduced by Arroyo et al. (2022) the statements hold, and in which layer there are counterexamples. The convexity hierarchy describes several layers between point sets in the plane and simple drawings using a generalized notion of convexity. For the proof of Kirchberger's theorem generalized signotopes, which encode the triangle orientations of simple drawings in the plane, played an essential role. Additionally to the mentioned theorems we introduce the notion of holes in the setting of simple drawings, which are classically considered in point sets. We show that convex drawings behave similarly to point sets in the sense that every sufficiently large convex drawing contains a 6-hole while there are arbitrarily large drawings without 7-holes.

Moreover, we show that Rafla's conjecture (1988) is true for convex drawings. The conjecture states that every simple drawing of the complete graph admits a plane Hamiltonian cycle. The best known partial results are plane paths of length $\Omega\left(\frac{\log(n)}{\log\log(n)}\right)$ (Suk, Zeng and Aichholzer et al. 2022) and plane matchings of size $\Omega(\sqrt{n})$ (Aichholzer et al. 2022). We investigate several variations and strengthenings of this conjecture. In particular we prove that every convex drawing admits a plane substructure consisting of a plane Hamiltonian cycle and additional $n-2$ additional edges.

Selbstständigkeitserklärung

Ich erkläre gegenüber der Freien Universität Berlin, dass ich die vorliegende Dissertation selbstständig und ohne Benutzung anderer als der angegebenen Quellen und Hilfsmittel angefertigt habe. Die vorliegende Arbeit ist frei von Plagiaten. Alle Ausführungen, die wörtlich oder inhaltlich aus anderen Schriften entnommen sind, habe ich als solche kenntlich gemacht. Diese Dissertation wurde in gleicher oder ähnlicher Form noch in keinem früheren Promotionsverfahren eingereicht.

Mit einer Prüfung meiner Arbeit durch ein Plagiatsprüfungsprogramm erkläre ich mich einverstanden.

Berlin, _____

(Helena Bergold)

Acknowledgements

First of all I want to thank my advisors Günter Rote and Stefan Felsner for giving me the opportunity to finish my PhD in Berlin as part of the graduate school Facets of complexity. Thanks for giving me the freedom to work on the research topics I like but still being available to answer questions. Thanks for giving me the opportunity to go to conferences and experience the nice environment of the community.
Additionally I want to thank my coauthors, colleagues, and friends. Particular thanks goes to my friends who I met during my bachelor and master studies in Konstanz. Despite the large Euclidean distance, we always stayed in touch.
Last but not least, I want to thank my parents, my sister and Manfred who always supported me.

Contents

Chapter 1

Introduction

The main structures considered in this thesis are pseudohyperplane arrangements and simple drawings together with their combinatorial description through sign mappings. A *sign mapping* is a function $\sigma : \binom{[n]}{r} \to \{+, -\}$ which maps a sign to every r-element subset of a ground set $[n] = \{1, \ldots, n\}$ such that particular sign patterns do not occur on induced substructures. The parameter r is called the *rank* and n is the number of *elements*. More specifically we look at so called $(r+1)$-*packets* which are sign sequences consisting of $r+1$ signs corresponding to the signs of all r-element subsets of an $(r+1)$-element subset in reversed lexicographic order. For the precise definition we refer to Chapter 2.
Various structures from combinatorial geometry can be encoded with sign mappings. Besides the axiomatization of point sets in dimension d in terms of chirotopes, the most prominent combinatorial structures are permutations. A permutation is uniquely defined by its inversion set. Moreover, if for three elements $a < b < c$ the pairs $\{a, b\}$ and $\{b, c\}$ are inversions, then $\{a, c\}$ is an inversion as well. Similarly, if $\{a, b\}$ and $\{b, c\}$ are non-inversions, then also $\{a, c\}$ is a non-inversion. Assigning "$-$" to all pairs which are an inversion in the permutation and "$+$" to the remaining pairs yields a sign mapping with a monotonicity property on 3-packets: The sign sequence $(\sigma(b, c)\ \sigma(a, c)\ \sigma(a, b))$ of a 3-element subset $\{a, b, c\}$ with $a < b < c$ is not equal to the sign patterns $+-+$ and $-+-$, i.e., is *monotone* in the sense that there is at most one sign change. It is not hard to see that all sign mappings of rank 2 with n elements avoiding the two sign patterns $+-+$ and $-+-$ are permutations on n elements. For example, the permutation $\pi = 1342$ corresponds to the 2-signotope

$$\sigma(1,2) = +, \quad \sigma(1,3) = +, \quad \sigma(1,4) = +, \quad \sigma(2,3) = -, \quad \sigma(2,4) = -, \quad \sigma(3,4) = +.$$

Signotopes

A sign mapping of rank r is an r-*signotope* if in the sign sequence of an $(r+1)$-packet, there is at most one sign change. As we have seen, permutations allow at most one sign change. Hence they are in bijection with 2-signotopes. As shown by Felsner and Weil [FW01], 3-signotopes are in bijection with Euclidean pseudoline arrangements with a marked top cell. Rank r-signotopes in general correspond to certain pseudohyperplane arrangements, which we describe in more detail in Section 2.2.4. For fixed r and n, we define a partial order on the set of all r-signotopes on n elements by comparing the preimages of $+$. For $r = 2$ this partial order is the *weak Bruhat order* of the symmetric group. In general the partial order is related to the *higher Bruhat order* which have been introduced by Manin and Schechtman [MS89] and further studied by Kapranov and Voevodsky [KV91]. The name signotopes was introduced by Felsner and Weil [FW01] to describe elements from higher Bruhat orders. While Manin and Schechtman used the transitive

hull of single step inclusion to define an order on those elements, Felsner and Weil used the inclusion. As shown by Ziegler [Zie93] those two orders do not coincide for $r \geq 4$. Both orders provide a correspondence between $(r+1)$-signotopes and maximum chains in the partial order of r-signotopes.
By the Folkman-Lawrence topological representation theorem [FL78] pseudohyperplane arrangements correspond to the combinatorial structure of oriented matroids. There are several cryptomorphic axiom systems for oriented matroids, each of them generalizing a different structure. The most important one in the context of this thesis are chirotopes which are rank r sign mappings. Oriented matroids have been studied in various contexts. For an overview see the book "Oriented Matroids" by Björner et al. [BLS+99]. We focus on signotopes which are a rich subclass since asymptocically there are $2^{\Theta(n^{r-1})}$ signotopes and oriented matroids of rank r on n elements, see Section 6.1. The precise relation between signotopes and oriented matroids is given in Section 2.2.5. While the existence of simplicial cells in oriented matroids is a famous open conjecture by Las Vergnas, all signotopes admit at least 2 simplicial cells. Since the signs of r-element subsets correspond to the orientation of the simplex spanned by those r pseudohyperplanes, a simplicial cell corresponds to an r-element subset whose sign we can change such that the new mapping is still a signotope. We call such an r-element subset in a signotope a *fliple*. While $n-2$ is a known lower bound for the minimal number of fliples in rank 3, which is tight, we show in Section 6.2 the first linear lower bound of $\frac{2n-2}{r}$ for general rank. To show this, we use structural results about signotopes and their corresponding partial order.

Extension Theorem

In his introductory paper to pseudoline arrangements from 1926, Levi [Lev26] showed that the fundamental property of line arrangements, that an arrangement can be extended by an additional line through two prescribed points, holds for pseudoline arrangements as well. It is natural to ask whether this holds in higher dimensions since clearly for proper hyperplane arrangements d points determine a hyperplane in dimension d. Goodman and Pollack [GP81] provide an example in dimension 3 and three prescribed points such that there is no extension with an additional pseudohyperplane which goes through the three prescribed points. Later Richter-Gebert [Ric93] found an example where even an extension through two prescribed points in dimension 3 is not possible. Both examples are oriented matroids but not signotopes. We study the extendability for the subclass of signotopes and show in Chapter 3 that for odd rank, that is if the dimension is even, there exists an extension through any two prescribed points. The restriction to the parity of the rank is not just a defect of the proof but for rank $r = 4, 6, 8, 10, 12$ we provide counterexamples to the extendability through two prescribed points. We expect that an infinite family of counterexamples exists. Moreover in Chapter 3 we discuss extendability through $t \geq 3$ prescribed points and show that for every rank r there are examples which are not extendable through four prescribed points.

Generalized Signotopes

For signotopes the monotonicity property allows at most one sign change on each packet. A natural generalization is to allow more than one sign change. Rank 3 sign mappings with at most

two sign changes on 4-packets are called *generalized signotopes*. The only sign pattern which do not appear in a packet of a generalized signotopes are the two alternating sign sequences $+-+-$ and $-+-+$. During the axiomatization of point sets in the plane with predicate logic, Knuth [Knu92] came across the structure of *interior triple system*, a generalization of point sets. As it turns out they correspond to generalized signotopes. In Chapter 6, we show that there are $2^{\Theta(n^3)}$ generalized signotopes. A lower bound with the same asymptotics was already shown by Knuth. However we improve the multiplicative constant and show an upper bound using Shearer's entropy lemma.
Generalized signotopes are not only a generalization of point sets but also a combinatorial generalization of simple drawings of the complete graph in the plane. In a *simple drawing* of a graph in the plane vertices are mapped to distinct points in the plane and edges are drawn as simple curves connecting the corresponding points such that two edges have at most one point in common. In this thesis we focus on simple drawings of the complete graph K_n. Tracing the boundary of a triangle in a simple drawing of K_n gives an orientation which is either clockwise or counterclockwise. To define a sign mapping on 3-subsets, we associate counterclockwise with $+$ and clockwise with $-$. In fact the sign function arising from the triangle orientation of simple drawing is a generalized signotope, which we discuss in Section 2.4. Since there are $2^{\Theta(n^3)}$ generalized signotopes but only $2^{\widetilde{O}(n^2)}$ [Kyn13] simple drawings, there are generalized signotopes which do not come from a simple drawing. Here $\widetilde{O}$ is the soft O-notation which omits polylogarithmic factors. Details are given in Section 6.4. Even though not all generalized signotopes come from simple drawings, generalized signotopes turned out to be a useful tool to prove a separation theorem in the vein of Kirchberger's theorem for simple drawings.

Classic Theorems from Convex Geometry

Generalized signotopes are the main ingredient for a separation theorem generalizing Kirchberger's theorem to simple drawings. *Kirchberger's theorem* is a classic result from convex geometry which states that every point set in $\mathbb{R}^d$ colored with two colors red and blue admits a hyperplane separating the blue from the red points if and only if every $(d+2)$-element subset admits such a separation. In Section 4.1 we give a proof of Kirchberger's theorem in the setting of generalized signotopes. Additionally, we study further classic theorems from convex geometry in the context of simple drawings. More particularly we provide a fine grained analysis in terms of the convexity hierarchy which was introduced by Arroyo et al. [AMRS22]. They provide a hierarchy for simple drawings generalizing the concept of convexity to subdrawings of K_3 which are triangles. The simplest case are geometric drawings which correspond to point sets by connecting each pair of points with their a straight-line segment. A triangle in a geometric drawing is convex in the sense of simple drawings if and only if it is convex in the classic sense. The convexity hierarchy provides subclasses such as convex, h-convex and f-convex drawings between geometric drawings and simple drawings. We show that Helly's theorem does not generalize to arbitrary simple drawings and present a family of f-convex drawings with arbitrarily large Helly number. Moreover, we give a new proof of a topological generalization of Carathéodory's theorem in the plane, which turned out to generalize to complete multipartite graphs, see [ACH$^+$23].
Another classic theorem in the study of point sets is the Erdős-Szekeres theorem which states that for every k every sufficiently large point set contains a *k-gon*, i.e., a subset of k points

in convex position. A variant of the Erdős-Szekeres theorem considers empty k-gons, so called *k-holes*. It is known that every sufficiently large point set contains a 6-hole, while there are arbitrary large point sets without 7-holes. In Section 4.4, we establish the notions of holes in simple drawings and show that there are arbitrarily large simple drawings without a 4-hole, while every sufficiently large convex drawing admits a 6-hole. Hence convex drawings are very similar to geometric point sets when it comes to holes. The key lemma for the existence of 6-holes in convex drawings is as follows: A k-gon together with its interior vertices is an f-convex drawing. We expect this lemma to be of independent interest since it provides a tool to generalize results from pseudolinear drawings to convex drawings.

Plane Hamiltonian Cycles in Convex Drawings

In Chapter 5 we show that Rafla's conjecture [Raf88] from 1988 holds for convex drawings. It states that every simple drawing of the complete graph admits a plane Hamiltonian cycle, i.e., a Hamiltonian cycle such that each pair of edges of this cycle does not cross. Even though this conjecture and related substructures attracted the attention of many researchers, so far only the existence of plane paths of length $\Omega(\log n/\log\log n)$ [AGT$^+$22, SZ22] and plane matchings of size $\Omega(\sqrt{n})$ [AGT$^+$22] are known. Clearly the existence of a plane Hamiltonian cycle would imply a plane path of length n and a plane matching of size $\lfloor \frac{n}{2} \rfloor$. Rafla's conjecture was tested for small n with the aid of computer programs. Previously it was known to be true for simple drawings of the complete graph with at most 9 vertices [ÁAF$^+$15]. We develop a SAT framework which makes it possible to show that for 10 vertices the conjecture is true as well. Based on computer experiments on data for small n, we conjecture that even a strengthening of Rafla's conjecture holds: Every simple drawing contains a plane Hamiltonian subdrawing on $2n-3$ edges. To prove Rafla's conjecture for convex drawings we used the SAT framework, especially in the early stages, to see which substructures might appear and which do not appear. This made it possible to show that convex drawings provide a layering structure. For each layer we found a path such that all of them combine to a Hamiltonian cycle.

Outline

In Chapter 2 we give the precise definitions of the mentioned structures and describe relations between various structures, starting with signotopes. The main result concerning signotopes is the 2-extendability which we discuss in Chapter 3 and is based on the publication [BFS23a]. Additionally to the results mentioned in [BFS23a], we provide an infinite family of partial signotopes which cannot be extended and discuss extendability through more than two points. The classic theorems from convex geometry in the context of simple drawings are investigated in Chapter 4. For the proof of Kirchberger's theorem, we use generalized signotopes which are introduced in Section 2.4. The results presented in the first sections of this chapter are based on [BFS$^+$23b] and the conference version is [BFS$^+$20]. Section 4.4 addresses the generalization of holes to convex drawings and is based on [BSS23b]. In Chapter 5 we further discuss convex drawings and show that they admit a plane structure consisting of a Hamiltonian cycle and a spanning star emanating of one vertex. In particular this shows that Rafla's conjecture is true for convex drawings. This chapter is based on [BFMS23]. The results concerning the asymptotic numbers of signotopes and generalized signotopes are given in Chapter 6. Moreover we give the

first linear lower bound on the number of fliples in every signotope in Section 6.2. In the last chapter of this thesis, Chapter 7, we summarize the results and give some open problems for further research.

1.1 Publications

This thesis is mostly based on the following publications.

[BFMS23] **Using SAT to study plane substructures in simple drawings**
Helena Bergold, Stefan Felsner, Meghana M. Reddy, Manfred Scheucher
Extended abstract presented at 39^{th} *European Workshop on Computational Geometry* (EuroCG 2023).

[BFS23a] **An Extension Theorem for Signotopes**
Helena Bergold, Stefan Felsner, Manfred Scheucher
Conference version appeared at 39^{th} *International Symposium on Computational Geometry* (SoCG 2023), LIPIcs 258, pages 17:1–17:14.
Extended abstract presented at 38^{th} *European Workshop on Computational Geometry* (EuroCG 2022)

[BFS$^+$20] and [BFS$^+$23b] **Topological drawings meet classical theorems from convex geometry**
Helena Bergold, Stefan Felsner, Manfred Scheucher, Felix Schröder, Raphael Steiner
Full version appeared in *Discrete & Computational Geometry* 70, pages 1121–1143, 2023.
Conference version appeared at 28^{th} *International Symposium on Graph Drawing and Network Visualization* (GD 2020), LNCS 12590, pages 281–294.
Extended abstract presented at 36^{th} *European Workshop on Computational Geometry* (EuroCG 2020)

[BSS23b] **Holes in Convex Drawings**
Helena Bergold, Manfred Scheucher, Felix Schröder
Extended abstract presented at 39^{th} *European Workshop on Computational Geometry* (EuroCG 2023).

Chapter 2

Signotopes, Drawings and Related Structures

In this chapter we give the definition of the most important structures considered in this thesis. Moreover, we discuss related structures, topological and geometric representations and important properties. We start with some basic notation. We then continue with signotopes and related structures, see Section 2.2. In the remaining part of this chapter we discuss simple drawings (cf. Section 2.3), generalized signotopes (cf. Section 2.4), rotation systems (cf. Section 2.5) and the convexity hierarchy for simple drawings (cf. Section 2.6).

2.1 Basic Notation

Throughout this thesis we use some standard notation. We summarize the most important notation:

- $[n] = \{1, \dots, n\}$ denotes the set of the first n natural numbers.
- $\binom{[n]}{r} = \{T \subseteq [n] : |T| = r\}$ is the set of all subsets of size r of $[n]$. We call the elements of $\binom{[n]}{r}$ *r-subsets*.
- $[n]^r$ denotes the r-ary Cartesian product of $[n]$, i.e., the set of all r-tuples with entries from $[n]$.
- $[n]_r$ is the subset of all r-tuples of $[n]^r$ whose entries are pairwise distinct elements from $[n]$.
- S_n denotes the symmetric group of order n, which are all permutations on n elements. We sometimes identify a permutation $\pi \in S_n$ with a linear order on $[n]$, denoted by a string $\pi = \pi(1)\pi(2)\dots\pi(n)$.
- K_n denotes the complete graph on n vertices.

Moreover, we use basic terminology from graph theory. Usually V is the set of vertices and E the set of edges of a graph. We denote an undirected edge from vertex i to vertex j by ij or $\{i, j\}$. When dealing with drawings of a graph, we do not distinguish between an edge in the abstract graph and an edge in the drawing.
Throughout this thesis, we deal with *sign functions*, which take values in $\{+, -, 0\}$. For a domain of a sign function, we consider subsets or tuples, i.e., $[n]_r$, $\binom{[n]}{r}$ or $[n]^r$ depending on the explicit function. To deal with the signs $-$ and $+$, we use basic operation $- \cdot - = + \cdot + = +$, $- \cdot + = + \cdot - = -$ and the x-fold operation $(-)^x$ which is $-$ if and only if x is odd, otherwise $+$. Moreover $0 \cdot s = 0$ for $s \in \{+, -, 0\}$.

2.2 Signotopes

Signotopes are a combinatorial structure generalizing permutations and pseudoline arrangements. They can be seen as combinatorial abstraction of various geometric objects encoded via a *sign mapping* on the domain $\binom{[n]}{r}$.

Definition 2.2.1 (Signotope)**.** *For $r \geq 1$ a* signotope *of* rank r *(short: r-signotope) on n elements is a sign function σ from all r-subsets of $[n]$ to $+$ or $-$, i.e., $\sigma : \binom{[n]}{r} \to \{+,-\}$ such that for every $(r+1)$-subset $X = \{x_1, x_2, \ldots, x_{r+1}\}$ of $[n]$ with $x_1 < x_2 < \ldots < x_{r+1}$ there is at most one sign change in the sequence*

$$(\sigma(X\backslash\{x_1\})\ \sigma(X\backslash\{x_2\})\ \ldots\ \sigma(X\backslash\{x_{r+1}\})).$$

The set of all r-signotopes on $[n]$ elements is denoted as $S(n,r)$.

Note that the sequence lists the signs of all induced r-subsets of X in reversed lexicographic order. For 3-signotopes, the following 8 sign patterns on 4-subsets are allowed:

$$(++++),\ (+++-),\ (++--),\ (+---),$$
$$(----),\ (---+),\ (--++),\ (-+++).$$

The remaining 8 sign patterns of length 4 are forbidden.
For sake of readability, we write $X = (x_1, \ldots, x_t)$ to denote a t-subset of $[n]$ with sorted elements $x_1 < x_2 < \ldots < x_t$. For such an X, the set $X_j = (x_1, \ldots, x_{j-1}, x_{j+1}, \ldots, x_t)$ denotes the set without x_j. With the convention $- < +$, the condition about sign changes in r-signotopes can be written as a *monotonicity* condition for $(r+1)$-subsets $X = (x_1, \ldots, x_{r+1})$:

$$\sigma(X_1) \leq \sigma(X_2) \leq \ldots \leq \sigma(X_{r+1}) \quad \text{or} \quad \sigma(X_1) \geq \sigma(X_2) \geq \ldots \geq \sigma(X_{r+1}).$$

We refer to such an $(r+1)$-subset as $(r+1)$-*packet* or just *packet* if the size is apparent from the context. For $r = 1$ the monotonicity is trivially fulfilled and hence every mapping $\sigma : [n] \to \{+,-\}$ is a 1-signotope. In the following, we discuss the case $r = 2$ and the correspondence to permutations. We then consider the case $r = 3$ for which we give different geometric representations and discuss related combinatorial objects. After discussing the small ranks in detail, we give some basic properties of general rank r signotopes.

2.2.1 Rank 2 – Permutations

In this section, we consider rank 2 signotopes, which correspond to permutations. A permutation π is uniquely determined by its *inversion set* $\mathrm{Inv}(\pi) = \{\{i,j\} :\ i < j \text{ and } \pi(i) > \pi(j)\}$. We define a mapping $\sigma_\pi : \binom{[n]}{2} \to \{+,-\}$ by assigning $\sigma_\pi(i,j) = -$ if and only if $\{i,j\} \in \mathrm{Inv}(\pi)$ and $\sigma_\pi(i,j) = +$ otherwise. The monotonicity condition asserts the following condition on every 3-subset $\{i,j,k\}$ with $i < j < k$: If $\sigma_\pi(i,j) = \sigma_\pi(j,k) = s \in \{+,-\}$, then $\sigma_\pi(i,k) = s$. To show this we consider the two cases $s = +$ and $s = -$. Let us start with $s = +$. In this case $\sigma_\pi(i,j) = +$ implies that $\pi(i) < \pi(j)$ and $\sigma_\pi(j,k) = +$ implies $\pi(j) < \pi(k)$ which certainly implies that $\pi(i) < \pi(k)$ by the transitivity of the order $<$ on $[n]$. Hence $\sigma_\pi(i,k) = +$. In the other case, the signs and order relations are reversed. Moreover, given a 2-signotope σ, the preimage of $-$ determines the inversion set of a permutation. This shows that 2-signotopes are in 1-to-1 correspondence with permutations. We refer to the preimage of $-$ as $-$*-set* of σ and to the preimage of $+$ as $+$*-set*. We summarize:

Lemma 2.2.2. *The set of permutations S_n on n elements is in bijection with the set $S(n,2)$ of all 2-signotopes on $[n]$. A permutation π corresponds to a 2-signotope σ with $\sigma^{-1}(-) = \mathrm{Inv}(\pi)$.*

For a fixed n, we define a partial order on the set $S(n,2)$ of all 2-signotopes on n elements by single step inclusion of the $+$-sets. Two 2-signotope σ and σ' differ in a *single step*, denoted by $\sigma \lessdot \sigma'$ if $\sigma^{-1}(+) \subset \sigma'^{-1}(+)$ and $|\sigma'^{-1}(+)| = |\sigma^{-1}(+)| + 1$. The transitive closure of this single step is the *single step inclusion* $\leq$. In particular if $\sigma \leq \sigma'$, there exist $\sigma_0, \ldots, \sigma_t$ such that

$$\sigma = \sigma_0 \lessdot \sigma_1 \lessdot \ldots \lessdot \sigma_t = \sigma'.$$

Hence the single step is the cover relation of the single step inclusion. In a partial order $\prec$, the element x *covers* y if $x \succ y$ and there is no z with $x \succ z \succ y$.
The partial order of $S(n,2)$ with the single step inclusion is the *weak Bruhat order* of the symmetric group S_n denoted by $B(n,2)$[1] and the *Hasse diagram* which is the directed graph of the cover relation. In the case of 2-signotopes this is the skeleton of the permutahedron of order n. Let $G(n,2)$ be the graph of the cover relation. The vertices are the elements of $S(n,2)$ and two vertices x and y are connected with an edge if and only if they are related through a cover relation, i.e., if they differ in a single sign. The partial order in the case $n = 4$ is shown in Figure 2.1. A subset whose value we can flip while still obtaining the monotonicity property

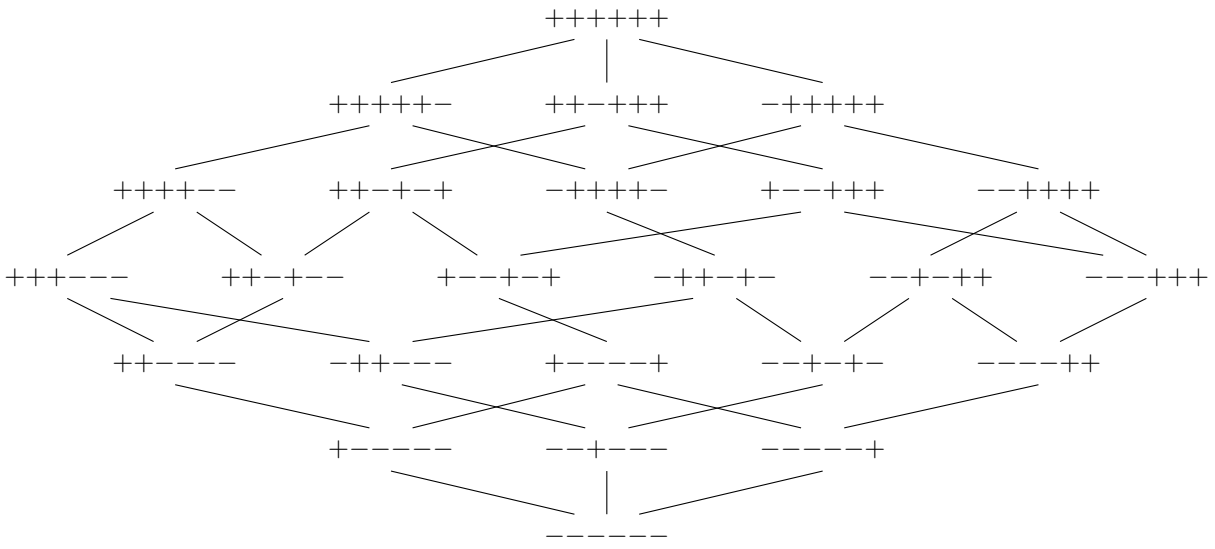

Figure 2.1: Hasse diagram of $B(4,2)$. The vertices are labeled with their 2-signotope, which are represented by the string of signs corresponding to the 2-subsets in reversed lexicographic order.

is a *fliple*. A flip, i.e., the change of a single sign, either adds one pair or removes one pair to the inversion set. This corresponds to an adjacent transposition in the permutation.
The partial order $B(n,2)$ corresponds to the *inclusion order* $\subseteq$ of the $+$-sets on $S(n,2)$ in which $\sigma \subseteq \sigma'$ if $\sigma^{-1}(+) \subseteq \sigma'^{-1}(+)$ which was shown by Yanagimoto and Okamoto [YO69].

[1] Since we define Bruhat orders for higher rank later, we introduce a second parameter which encodes the rank. In literature the weak Bruhat order is usually denoted by B_n or $B(n,1)$ where the second parameter is the dimension. To avoid confusion, we denote the partial order defined on the set $S(n,r)$ by $B(n,r)$.

2.2.2 Rank 3 – Pseudoline Arrangements

In this section, we consider the case $r = 3$, which was the main focus of the paper by Felsner and Weil [FW01], who introduced the name signotopes. They show that 3-signotopes are represented by pseudoline arrangements.

Definition 2.2.3 (Pseudoline Arrangement)**.** *A* pseudoline *is a simple curve in the Euclidean plane such that its removal from the plane results in exactly two unbounded components. A* pseudoline arrangement $\mathcal{A}$ *is a family of pseudolines such that each pair of pseudolines from* $\mathcal{A}$ *intersects in exactly one point, where the two curves cross properly. An arrangement is* simple *if no three pseudolines cross in a common point.*

In this thesis all pseudoline arrangements will be simple if not mentioned otherwise. When studying pseudoline arrangements, we only consider the combinatorics which depend on the order of crossings. Pseudoline arrangements with the same order of crossings but different embedding are considered the same. Moreover, all pseudoline arrangements considered are in the Euclidean plane[2] and hence have $2n$ unbounded cells.
The study of pseudoline arrangements goes back to Levi in the 1920's. He proved that essential properties of line arrangements also hold in the more general setting of pseudoline arrangements. The following statement generalizes the fact that two points in the plane determine a line.

Theorem 2.2.4 (Levi's extension lemma for pseudoline arrangements [Lev26])**.** *Given an arrangement* $\mathcal{A}$ *of pseudolines (not necessarily simple) and two points* p, q *in* $\mathbb{R}^2$*, not on a common pseudoline of* $\mathcal{A}$*. Then there exists a pseudoline* ℓ *containing both points* p *and* q *such that* $\mathcal{A} \cup \{\ell\}$ *is a pseudoline arrangement.*

We say that ℓ extends the pseudolines arrangement $\mathcal{A}$. In Chapter 3 we discuss a generalization of this statement to signotopes of higher rank.
Clearly pseudoline arrangements generalize line arrangements. However not all pseudoline arrangement can be represented by a line arrangement with the same combinatorics, i.e., with the same order of intersections. A pseudoline arrangement which admits such a line arrangement is *realizable*, sometimes also referred to as *stretchable*. Levi gave the non-Pappus arrangement as an example of a (non-simple) pseudoline arrangement which is not realizable. Later Ringel [Rin56] continued the line of research and presented based on the non-Pappus arrangement a simple pseudoline arrangement which is not stretchable, see Figure 2.8 on page 28 for an illustration.
Goodman and Pollack played a central role in the study of pseudoline arrangements. They showed the nowadays well-known fact that all pseudoline arrangements can be drawn with x-monotone pseudolines [Goo80]. Those x-monotone pseudoline arrangements are often also referred to as *wiring diagrams* or *sorting networks* especially if the pseudolines consist of piecewise linear curves, so called *wires* and the wires are horizontal except for small neighborhoods of their crossings with other wires. For more information concerning pseudolines, line arrangements and related structures, see the Chapter 5 of the "Handbook of Discrete and Computational Geometry" [FG17], the book "Geometric Graphs and Arrangements" by Stefan Felsner [Fel04] or the book "Lectures of Discrete Geometry" of Matoušek [Mat02, Chapter 6]. A collection of examples, problems and conjectures is given in the book "Arrangements and Spreads" of Grünbaum [Grü80].

[2] In contrast to the Euclidean version, there is the notion o pseudoline arrangements in the projective plane.

Figure 2.2: Connection between pseudoline arrangements and 3-signotopes.

Starting with a pseudoline arrangement in the Euclidean plane, we mark one of the unbounded cells as the *top cell*. Moreover, we label the pseudolines starting at the marked top cell, left of all crossings, from top to bottom by $1, \ldots, n$. Since two pseudolines cross exactly once, the pseudolines appear in reversed order on the right. The triangle sign function σ is obtained as follows: The sign of $\sigma(a, b, c)$ for $a < b < c$ indicates the orientation of the triangle formed by the three pseudolines a, b, c. If the crossing of a and c is below b, it is $\sigma(a, b, c) = +$ and if the crossing of a and c is above b, it is $\sigma(a, b, c) = -$. An illustration of the assignment is given in Figure 2.2. Since the monotonicity condition of 3-signotopes is a condition on all 4-subsets, we consider all pseudoline arrangements with 4 elements to show that the triangle sign function of all pseudoline arrangements is a 3-signotope. An illustration of the 8 possibilities of pseudoline arrangements with a fixed to cell are shown in Figure 2.3.

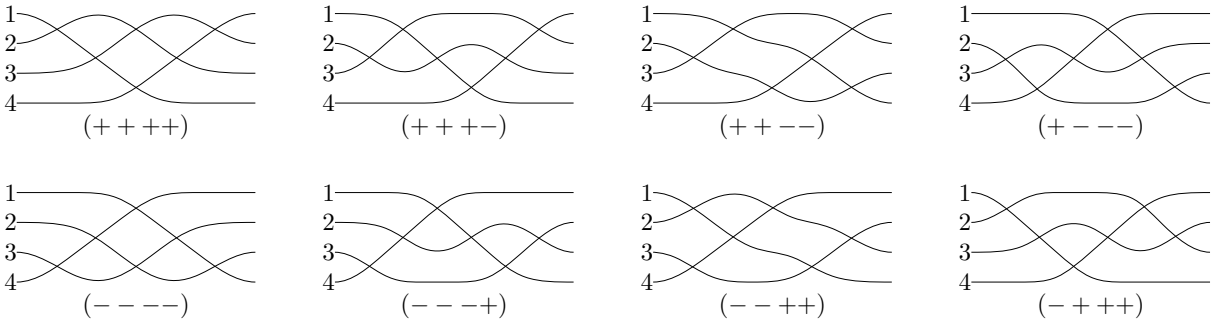

Figure 2.3: All possibilities of pseudoline arrangements with a fixed top cell and 4 pseudolines together with its 3-signotope.

Since the triangle sign function of all eight possibilities is a valid 3-signotope, all pseudoline arrangements have a corresponding 3-signotope. Moreover, Felsner and Weil showed that the reverse is true, i.e., every 3-signotope has a corresponding pseudoline arrangements whose triangle sign function is equal to the signotope.

Proposition 2.2.5 ([FW01, Theorem 7])**.** *The set of simple pseudoline arrangements in the Euclidean plane with n pseudolines and a marked top cell is in bijection with the set $S(n, 3)$ of 3-signotopes on n elements.*

To show that every 3-signotope can be realized by a pseudoline arrangement, we need structural results about general r-signotopes, which we discuss in Section 2.2.4. However we give a sketch of the proof. First consider a pseudoline arrangement. We identify the crossings of a pseudoline arrangement with the elements which cross, i.e., for 3-signotopes crossings are subsets of size 2. As usual the pseudolines are labeled from top to bottom by $1, \ldots, n$, which corresponds to the identity permutation. If two pseudolines cross, the two elements change the position. Hence we can represent a pseudoline arrangement by a sequence of permutation in which two adjacent

permutation differ in an adjacent transposition. In fact, we can define a sequence of permutation representing a pseudoline arrangement from a 3-signotope. Let σ be a 3-signotope on n elements. We define a corresponding partial order on $\binom{[n]}{2}$. If $\sigma(a,b,c) = +$, it holds $ab \prec ac \prec bc$ and if $\sigma(a,b,c) = -$, it is $bc \prec ac \prec ab$. By taking the transitive closure of this relation, we obtain a partial order on the 2-subsets. We consider a linear extension of this partial order which gives a linear order $A_1, \ldots, A_{\binom{n}{2}}$ on the 2-subsets of $[n]$. We start by constructing the pseudoline arrangement by drawing them in the order $\pi_0 = 1 \ldots n$ corresponding to the identity permutation. In every step $i = 1, \ldots, \binom{n}{2}$, we construct a new permutation π_i by reversing the order of the two elements of A_i. For the constructed pseudoline arrangements we change the order of the two corresponding pseudolines which yields a crossing. For three pseudolines $a < b < c$ the partial order asserts that either $ab \prec ac \prec bc$ or $bc \prec ac \prec ab$ which also holds in every linear extension. Hence the triangle sign function of the so constructed pseudoline arrangement corresponds to the 3-signotope. Moreover, the structure ensures that the elements of A_i are adjacent in π_{i-1}.

The chain of permutations $\pi_0, \ldots, \pi_{\binom{n}{2}}$ corresponding to a pseudoline arrangement is a maximum chain in the order $B(n,2)$ of the 2-signotopes. This connection has been studied earlier by Goodman and Pollack. They define allowable sequences as a periodic sequence of permutations to have a combinatorial abstraction of line arrangements.

Definition 2.2.6 (Allowable Sequence)**.** *For a fixed n, an* allowable sequence *is a periodic sequence of permutations on $[n]$ such that the following two properties hold:*

(1) Two consecutive permutations consist of reversing one or more non-overlapping substrings; (a substring is a sequence of consecutive elements)

(2) If two elements have been reversed, they do not switch again until everything else was reversed.

An allowable sequence is simple *if in every step, we reverse exactly one substring consisting of exactly two element, i.e., two consecutive permutations differ in an adjacent transposition.*

Not all allowable sequences have a corresponding line arrangement. An allowable sequence which cannot be realized with a line arrangement has been presented by Goodman and Pollack [GP80]. However they showed that all allowable sequences have a corresponding pseudoline arrangement [GP84].

Proposition 2.2.7 ([GP84, Theorem 4.1])**.** *For every allowable sequence of permutations on $[n]$, there is an arrangement of n pseudolines whose associated sequence equals the allowable sequence.*

As already shown by Goodman [Goo80], allowable sequences have the following two properties, which reflect the partial order of signotopes.

(a) If $i_1 j_1$ is reversed before $i_2 j_2$, then $j_1 i_1$ is reversed before $j_2 i_2$;

(b) If ij is reversed before jk, then ik is reversed in between ij and jk.

By repeating the maximum chain of permutations of a 3-signotope in a periodic sequence in the following way, we get an allowable sequence. The first half of the period is exactly the maximum

chain, i.e., we switch ij with $i < j$. For the second half, we repeat the maximum chain but instead of switching ij, with $i < j$, we switch ji. The order of the two elements represents the order in the pseudoline arrangement before the crossing. Starting with an allowable sequence which contains the identity permutation, we get a maximum chain of 2-signotopes by taking a subsequence between the identity and reversed identity permutation. Note that relabeling the elements if necessary is possible to achieve that the allowable sequence contains the identity permutation.
In Section 2.2.4, we will see that this relation between 2-signotopes and 3-signotopes is not a coincidence of small values but is a very useful structural property of signotopes. In particular, we see that maximum chains of $(r-1)$-signotopes correspond to r-signotopes. For this we define the partial order on $S(n,r)$ via single step inclusion of the $+$-set.

Additionally, we want to mention the combinatorial encoding of pseudoline arrangements via so called local sequences, introduced by Goodman and Pollack [GP84]. A *local sequence* in a marked Euclidean arrangement of pseudolines consists of n permutations π_i on $[n]\backslash\{i\}$ which give the order of the crossings with the remaining pseudolines along the i-th pseudoline. From the 3-signotope σ, we get this information, by restricting the partial order $\prec$ to all elements containing this one element. This gives a total order representing the crossings along the pseudoline. Moreover, the 2-signotope corresponding to the permutation π_i is defined by

$$\sigma_i(j,k) = \sigma(\{i,j,k\})$$

for pairwise distinct $i,j,k \in [n]$ with $j < k$.

Due to the formula of Stanley [Sta84] the precise number of allowable sequences is known and equal to

$$\binom{n}{2}! \Big/ 1^{n-1}3^{n-2}5^{n-3}\cdots(2n-3)^1.$$

In contrast to an exact formula for allowable sequences, there are only rough estimates for the number $s(n,3)$ of 3-signotopes on n elements, i.e., the number of arrangements of pseudolines. It has been shown by Goodman and Pollack [GP93] that $s(n,3) = 2^{\Theta(n^2)}$ while the number of arrangements of lines is only $2^{\Theta(n\log n)}$. Knuth [Knu92] showed that $s(n,3) \leq 3^{n-1}s(n-1,3)$ which gives $s(n,3) \leq 3^{\binom{n}{2}} = 2^{\log_2(3)\binom{n}{2}}$ where $\log_2(3) \approx 1.585$. He conjectured that $s(n,3) \leq 2^{\binom{n}{2}+o(n^2)}$, i.e., that $\log_2(s(n,3)) \leq \frac{1}{2}n^2 + o(n^2)$. Felsner and Valtr [FV11] showed that $\log_2(s(n,3)) \leq 0.6571n^2$ for sufficiently large n. The lower bound $0.2083n^2 \leq \log_2(s(n,3))$ for sufficiently large n is due to Dumitrescu and Mandal [DM19]. An improved lower bound of $0.2250n^2$ was recently shown by Cortés Kühnast, Felsner and Scheucher [CFS23]. The exact numbers are known for $n \leq 16$. The last value was computed by Günter Rote. See the entry A006245 in the OEIS [OEI].

2.2.3 Rank 3 – Pseudoconfiguration of Points

During the study of allowable sequences, Goodman and Pollack also showed a connection to point configurations. Similar to pseudolines, there is a topological generalization of point sets in the plane, which are called pseudoconfiguration of points. They are an abstract description of the fact that each pair of points in the plane determines a line. The collection of points and the so constructed lines has the following properties which hold more generally.

Definition 2.2.8 (Pseudoconfiguration of Points)**.** *A* pseudoconfiguration of points *is a set of points P in the plane together with a family of pseudolines L such that*

- *For two distinct points $p, q \in P$ there exists exactly one pseudoline L containing p and q;*
- *Every pseudoline in L contains at least two points of P;*
- *Two pseudolines have exactly one point in common, in which they cross, i.e., L is a pseudoline arrangement.*

A pseudoconfiguration of points is simple *if every pseudoline contains exactly two points of P.*

Goodman [Goo80] investigated the relation between pseudoconfigurations of points and pseudoline arrangements and showed that they have a similar duality relation as the point-line-duality in the geometric setting. Given a set of points P and a set of lines L in the plane, the duality (sometimes also referred to as polarity) is given by the following relation

$$\{p = (a, b) \in P\} \leftrightarrow \{y = ax + b \in L\}.$$

To show an analogue of this duality in the topological setting, Goodman used allowable sequences as they represent both structures, pseudoline arrangements and pseudoconfigurations of points. In Section 2.2.2, we have seen the connection between 3-signotopes, simple pseudoline arrangements and simple allowable sequences. To study the connection to pseudoconfigurations of points, we encode the allowable sequence by its substrings which get reversed. Note that this is a bijective encoding of allowable sequences. In the setting of simple arrangements, this always corresponds to adjacent transposition. If we reverse the pair ij, then we assume that i and j appear in this order before the transposition. Starting with a pseudoconfiguration of points, we draw a circle around it enclosing all points of P and all crossings of the pseudolines of L. Every pseudoline has two crossing with the circle. We identify these crossings with the points which are on the corresponding pseudoline such that the point closest to the crossing appears first. Reading those pairs in clockwise order gives a periodic sequence satisfying the axioms of allowable sequences [Goo80]. In the simple case, we get a sequence of 2-subsets. Hence for every pseudoconfiguration of points we get an allowable sequence. For an illustration see Figure 2.4. Goodman and Pollack showed that the reverse is true as well.

Proposition 2.2.9 ([GP84, Theorem 4.4])**.** *Every allowable sequence with permutations on $[n]$ can be realized as a pseudoconfiguration of n points.*

Moreover, there is an arrangement of lines with the same combinatorics if and only if there is a point configuration. This holds even in the non-simple case. For non-simple arrangements, we have the correspondence

$$\begin{aligned} & k \text{ pseudolines cross in a common point in the pseudoline arrangement} \\ \leftrightarrow\ & \text{a substring of length } k \text{ is reversed in the allowable sequence} \\ \leftrightarrow\ & k \text{ points lie on a common pseudoline in a pseudoconfiguration of points.} \end{aligned}$$

Since we focus on signotopes, we restrict our attention to simple arrangements and simple pseudoconfigurations of points.

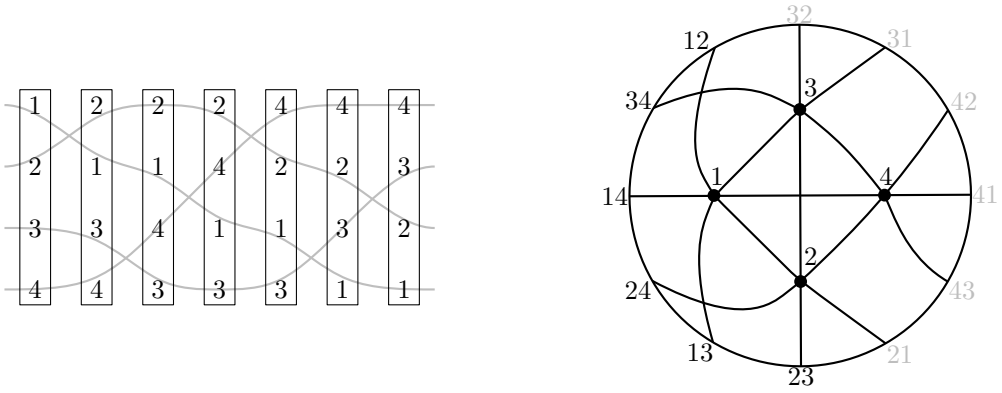

Figure 2.4: A pseudoline arrangement together with a simple allowable sequence and a corresponding pseudoconfiguration of points.

Balko, Fulek and Kynčl [BFK15] consider pseudoconfigurations of points and provide an independent proof that pseudoconfigurations of points are a topological representation of 3-signotopes. Restricting the curves to the curve segments between the two vertices yields an x-monotone pseudolinear drawing of the complete graph K_n, a subclass of simple drawings. We discuss this in more detail in Section 2.3.

2.2.4 Higher Bruhat Order

The relation between 2-signotopes and 3-signotopes discussed in the previous section is not a coincidence. For all $r \geq 2$, there is a relation between maximum chains of $(r-1)$-signotopes and r-signotopes. This property was first shown for the higher Bruhat order, which is a partial order on the set of signotopes for fixed r and n. Higher Bruhat orders were introduced by Manin and Schechtmann [MS89] in the context of discriminantal arrangements. Kapranov and Voevodsky [KV91] sketched two geometric representations for elements of higher Bruhat orders, the first in terms of single element extensions of cyclic hyperplane arrangements, and the second in terms of tight zonotopal tilings, i.e., projections of cubes. Zonotopal tilings are sometimes also called *cubillages*. Ziegler [Zie93] studies the first of these geometric interpretations and investigates the theory of higher Bruhat order. The second of the geometric interpretations of zonotopal tilings was further investigated by Thomas [Tho03] and more recently by Williams [Wil23]. We discuss those representations together with two additional topological representation in Section 2.2.6.

The easiest and well-known case is the weak Bruhat order of the symmetric group denoted by $B(n,2)$, which we discussed in Section 2.2.1. For the partial order $B(n,2)$, which is an order on the 2-signotopes $S(n,2)$, we consider the single step inclusion of the $+$-sets. Recall that the single step inclusion $\leq$ is the transitive closure of the single step $\sigma \lessdot \sigma'$ which is defined via $\sigma^{-1}(+) \subset \sigma'^{-1}(+)$ and $|\sigma'^{-1}(+)| = |\sigma^{-1}(+)| + 1$. For all r, we define the higher Bruhat order[3] $B(n,r)$ as the partial order on $S(n,r)$ induced by the single step inclusion.

Definition 2.2.10 (Higher Bruhat Order)**.** *For $r \geq 1$, the* higher Bruhat order $B(n,r)$ *is a partial order $\leq$ on the elements of $S(n,r)$ with the transitive closure of the single step inclusion $\lessdot$.*

[3] In the literature, the second parameter of the higher Bruhat order corresponds to the dimension, which is $r-1$.

The original definition of the higher Bruhat order $B(n,r)$ by Manin and Schechtman [MS89] is based on total orderings of all $(r-1)$-subsets of $[n]$, which they call *admissible orders*. In such an admissible order, the $(r-1)$-subsets appear in lexicographic or reversed lexicographic order in r-packets.
In 1969 Yanagimoto and Okamoto [YO69] showed that $B(n,2) = B_{\subseteq}(n,2)$. Here $B_{\subseteq}(n,r)$ denotes the inclusion order $\subseteq$ of the $+$-sets of the elements of $S(n,r)$. Clearly, every relation of two elements of $S(n,r)$ in $B(n_r)$ is in $B_{\subseteq}(n,r)$. In general $B(n,r)$ and $B_{\subseteq}(n,r)$ are not the same. We summarize some results regarding higher Bruhat orders.

- For all $n \geq r \geq 2$ there is a unique minimal and a unique maximal element in $B(n,r)$ and $B_{\subseteq}(n,r)$, respectively. The unique maximal element of rank r on n elements, denoted by $\sigma_{\max}$ is the constant $+$ function. In the same way the unique minimal elements, denoted by $\sigma_{\min}$ is the constant $-$ function. (see [MS89]).
- For $r \geq 1$, the diagram of $B(r+1,r) = B_{\subseteq}(r+1,r)$ is a $2(r+1)$-gon (see Figure 2.5).

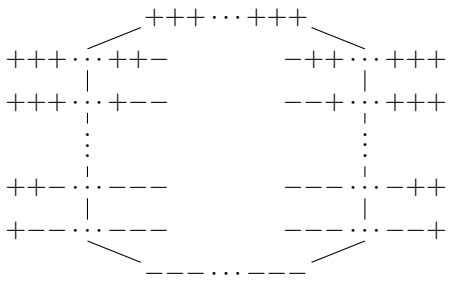

Figure 2.5: Diagram of $B(r+1,r)$.

- $B(n,r) = B_{\subseteq}(n,r)$ for $r \leq 3$ and $n-r \leq 3$ (see [Zie93] and [FW00] for the case $r=3$). However, $B(8,4) \neq B_{\subseteq}(8,4)$ (see [Zie93]).
- For all $n \geq r \geq 2$, $B(n,r)$ is a graded partial order, i.e., there is a *rank function* ρ such that for all $x < y$ it holds $\rho(x) < \rho(y)$ and for all y which cover x it holds $\rho(y) = \rho(x)+1$. For the higher Bruhat order, the rank function is the cardinality of the $+$-set (see [MS89]).
- $B(n,r)$ is a lattice for $r \leq 2$ and $n-r \leq 2$. However, the partial order $B(6,3)$ is not a lattice. (see [Zie93])

The most important property for our purposes is the following structural result of the higher Bruhat orders which gives a connections between maximum chains in $B(n,r-1)$ (respectively $B_{\subseteq}(n,r-1)$) and r-signotopes, i.e., elements in $B(n,r)$ (see [MS89, Zie93, FW01]).

Theorem 2.2.11. *For $r \geq 2$, there is a surjective mapping Π_r from the maximum chains of $(r-1)$-signotopes in $B(n,r-1)$, respectively $B_{\subseteq}(n,r-1)$, to the set of r-signotopes $S(n,r)$. Moreover, every element of $S(n,r)$ is contained in a maximum chain in $B_{\subseteq}(n,r)$.*

Note that if $B(n,r) = B_{\subseteq}(n,r)$, then for every two r-signotopes σ, σ' with $\sigma \subseteq \sigma'$, there is a maximum chain containing both. In general this is not the case.
We give a sketch of the proof by Felsner and Weil [FW01] for the inclusion order. For this we define a partial order corresponding to an r-signotope. In the case $r=3$ this is exactly the

partial order which we defined in Section 2.2.2 (page 12) describing the order of crossings from left to right in a pseudoline arrangement. We generalize this definition for arbitrary rank.

Definition 2.2.12. *For an r-signotope σ and every r-subset $X = (x_1, \dots, x_r)$, we define the partial order $\prec_\sigma$ on $\binom{[n]}{r-1}$ as the transitive closure of the following relations:*

$$X_1 \succ_\sigma X_2 \succ_\sigma \dots \succ_\sigma X_r \quad \text{if} \quad \sigma(x_1, \dots, x_r) = +, \qquad \text{and}$$
$$X_1 \prec_\sigma X_2 \prec_\sigma \dots \prec_\sigma X_r \quad \text{if} \quad \sigma(x_1, \dots, x_r) = -.$$

Recall that for $X = (x_1, \dots, x_r)$ we use the convention $x_1 < \dots < x_r$ and $X_i = X \backslash \{x_i\}$. By taking the transitive closure of all relations obtained from r-subsets, we obtain a partial order $\prec_\sigma$ on the $(r-1)$-subsets corresponding to σ [FW01, Lemma 10].
Let $\sigma_0, \dots, \sigma_{\binom{n}{r-1}}$ be a maximum chain of $(r-1)$-signotopes which we represent by the unique $(r-1)$-subsets A_i such that $\sigma_{i-1}(A_i) = -$ and $\sigma_i(A_i) = +$. This is a total order on the $(r-1)$-subsets. To eventually define an r-signotope $\bar{\sigma}$, we consider the r-subsets of $[n]$. For $X \in \binom{[n]}{r}$ the sequence $X_1, \dots, X_r$ appears either in this order or in reversed order as a subsequence of $A_0, \dots, A_{\binom{n}{r-1}}$. In the first case, we set $\bar{\sigma}(X) = +$, in the latter $\bar{\sigma}(X) = -$. This is indeed an r-signotope on $[n]$, see [FW01, Proposition 12]. For every r-signotope σ, we consider a linear extension of the partial order $\prec_\sigma$, which is a total order on the $(r-1)$-subsets corresponding to a maximum chain. Indeed the r-signotope corresponding to the maximum chain is exactly σ. This surjective map from a maximum chain of $(r-1)$-signotopes to an r-signotope is denoted by Π_r.
In the next step we identify the pre-image of an r-signotope, i.e., we want to define a relation on the maximum chains of $B_\subseteq(n, r-1)$ which map to the same r-signotope. Two maximum chains represented by the permutation $A_0, \dots, A_{\binom{n}{r}}$ and $B_0, \dots, B_{\binom{n}{r}}$ on $(r-1)$-subsets are *equivalent* if they differ in an adjacent transposition. A collection of r-signotopes is an *equivalence class* if for each pair of signotopes from the collection there is a sequence of signotopes contained in the class such that two consecutive ones are equivalent.

Proposition 2.2.13. *$\Pi_r^{-1}(\sigma)$ is a complete equivalence class.*

An equivalence class is exactly the set of linear extension of the partial order $\prec_\sigma$ corresponding to σ and the adjacent transpositions are the incomparable elements in $\prec_\sigma$.

In the higher Bruhat order $B(n, r)$, the cover relation corresponds to a flip of a sign of a single r-subset. We can define the *flip graph*, denoted as $G(n, r)$, as the graph of the cover relation. The degree of a signotope in the flip graph corresponds to the number of signs we can flip. The r-subsets whose sign we can flip are called fliple. More precisely an r-signotope σ on $[n]$, an r-subset $X \subseteq [n]$ is a *fliple* if both assignments $+$ and $-$ to $\sigma(X)$ result in a signotope. The constant signotopes have exactly $n - r + 1$ fliples which are $\{(i, i+1, \dots, i+r-1) : i = 1, \dots, n-r+1\}$ since they appear as the last or first element in every packet they are contained in. Moreover, since every r-signotope is contained in a maximum chain in $B(n, r)$ (cf. Theorem 2.2.11), every signotope contains at least two fliples. In Chapter 6, we give a linear lower bound on the number of fliples in r-signotopes for all r.
For $r = 3$, Felsner and Kriegel [FK99] showed that the minimum number of fliples is $n-2$, which is tight. Moreover, recently Alves Radtke et al. [AFO+23]) showed that the flip graph $G(n, 3)$ of 3-signotopes on n elements is in fact $(n-2)$-connected. A fliple of a 3-signotope corresponds is a

triangular cell in the pseudoline arrangement, i.e., a cell bounded by exactly three pseudolines. Triangular cells play an important role in the study of pseudoline arrangements, since it is possible to change the orientation of a triangle by moving one of the pseudolines over the crossing of the two others. Such a local perturbation is called a *triangle flip*. It does not change the orientation of any other triangle in the arrangement. For higher ranks, a fliple corresponds to a simplicial cell in the corresponding pseudohyperplane arrangement. We discuss this topological representation in Section 2.2.6. The analogon of fliples in oriented matroids, which we discuss in more detail in the next Section 2.2.5, is called *mutation*. While the existence of fliples in signotopes is known, it remains a central open problem in combinatorial geometry to decide whether every uniform oriented matroid contains a mutation [BLS+99, Chapter 7.3].

Let $s(n,r) = |S(n,r)|$ be the number of r-signotopes on n elements. A closed formula for the exact number is only given in the boundary cases $r = 1, 2$ and $n - r = 0, 1, 2$ [Zie93]:

$$\begin{aligned} s(n,1) &= 2^n \\ s(n,2) &= n! \\ s(n,n-2) &= 2^n + n2^{n-2} - 2n \\ s(n,n-1) &= 2n \\ s(n,n) &= 2 \end{aligned}$$

The number of r-signotopes for r between 4 and 10 and small values of n are listed in the sequences A60595 to A60601 in the OEIS. In the case $r = 3$ we know $0.2083n^2 \leq \log_2(s(n,3)) \leq 0.6571n^2$ for sufficiently large n, which we already discussed in Section 2.2.2.
In general we just know that $\log_2(s(n,r)) = \Theta(n^{r-1})$ for $r \geq 3$, which was shown by Balko [Bal19], who studied signotopes in terms of monotone colorings of uniform hypergraphs.

Proposition 2.2.14 ([Bal19, Theorem 3])**.** *For $r \geq 3$, the number of r-signotopes on $[n]$ is $s(n,r) = 2^{\Theta(n^{r-1})}$.*

In Chapter 6, we give a proof of Proposition 2.2.14.

2.2.5 Chirotopes – Oriented Matroids

Kapranov and Voevodsky [KV91, Theorem 4.9] already mentioned that signotopes are oriented matroids. There are several cryptomorphic axiom systems of oriented matroids. Each of them is based on a different geometric and combinatorial object. We limit ourselves to the definition of chirotopes, which arise as a combinatorial generalization of point sets. We refer the interested reader to the book "Oriented matroids" by Björner, Las Vergnas, Sturmfels, White and Ziegler [BLS+99] for further definitions and properties of oriented matroids. Given r points $p_1 \ldots, p_r$ as column vectors in $\mathbb{R}^{r-1}$, we consider the determinant of the $(r \times r)$-matrix corresponding to the homogeneous coordinates of the r points:

$$\det(p_1, \ldots, p_r) := \det \begin{pmatrix} 1 & 1 & \ldots & 1 \\ p_1 & p_2 & \ldots & p_r \end{pmatrix}.$$

The sign of the determinants describe the orientation of a simplex spanned by the r points in dimension $r - 1$. The determinant is 0 if and only if the r points are contained in a common hyperplane of $\mathbb{R}^{r-1}$. Chirotopes are an abstract description of the behavior of these determinants. They are sign functions whose domain is the set $[n]^r$ of all r-tuples with entries from $[n]$.

Definition 2.2.15 (Chirotope)**.** *A* chirotope *of* rank $r \geq 1$ *(short:* r-chirotope*) on the ground set* $[n]$ *is a sign mapping* $\chi : [n]^r \to \{+, -, 0\}$ *such that*

(1) χ *is not the constant* 0*-map;*

(2) χ *is* alternating*, i.e., for all permutations* $\pi \in S_r$ *and all* $x_1, \ldots, x_r \in [n]$ *it is*

$$\chi(x_{\pi_1}, \ldots, x_{\pi_r}) = \operatorname{sgn}(\pi)\chi(x_1, \ldots, x_r),$$

where $\operatorname{sgn}(\pi) = (-)^{|\operatorname{Inv}(\pi)|}$*;*

(3) For all $x_1, x_2, \ldots, x_r, y_1, y_2, \ldots, y_r \in [n]$ *such that*

$$\chi(y_i, x_2, x_3, \ldots, x_r) \cdot \chi(y_1, y_2, \ldots, y_{i-1}, x_1, y_{i+1}, \ldots y_r) \in \{0, +\}$$

for all $i \in \{1, \ldots, r\}$*, it is*

$$\chi(x_1, \ldots x_r) \cdot \chi(y_1, \ldots, y_r) \in \{0, +\}.$$

We refer to axiom (3) as the Grassmann-Plücker relations since it is the combinatorial version of those relations. The original *Grassmann-Plücker relation* is the following relation

$$\det(x_1, \ldots, x_r) \cdot \det(y_1, \ldots, y_r) = \sum_{i=1}^{r} \det(y_i, x_2, \ldots, x_r) \cdot \det(y_1, \ldots, y_{i-1}, x_1, y_{i+1}, \ldots, y_r)$$

on the determinants of vectors $x_1, \ldots, x_r, y_1, \ldots, y_r \in \mathbb{R}^r$. The difference of both sides is a multilinear form in the $r + 1$ variables $x_1, y_1, \ldots, y_r$. Moreover, the equation holds trivially for $y_i = y_j$ for $i \neq j$ or $x_1 = y_i$ for $i = 1, \ldots, r$, which is called alternating map in terms of linear algebra. Since an alternating multilinear from with $r+1$ variables in dimension r is the constant 0 map, the equation holds.
The chirotope axiom is the abstraction of this relation to sign properties. If all summands of the right-hand side are non-negative this corresponds to the sign + or 0, the left-hand side has to have the same sign.
A chirotope with $\chi(x_1, \ldots, x_r) \neq 0$ for r distinct elements $x_1, \ldots, x_r$ is *uniform*. In the geometric setting of point sets, this corresponds to *general position*, i.e., no r points are on a $r - 2$ dimensional hyperplane in $\mathbb{R}^{r-1}$.
For uniform chirotopes, the last axiom (3) can be replaced by the so-called 3-term Grassmann-Plücker relations [BLS$^+$99, Theorem 3.6.2]. They are a restriction of the Grassmann-Plücker relations to the case $x_i = y_i$ for $i = 3, \ldots, r$.

Theorem 2.2.16 (3-Term Grassmann-Plücker Relations [BLS$^+$99, Theorem 3.6.2])**.**
A uniform alternating map $\chi : [n]^r \to \{+, -, 0\}$ *(see axiom (2) of 2.2.15) which satisfies the following condition is a chirotope.*

- *For all* $x_1, \ldots, x_r, y_1, y_2 \in [n]$*, such that*

$$\chi(y_1, x_2, x_3, \ldots, x_r) \cdot \chi(x_1, y_2, x_3, \ldots, x_r) \in \{+, 0\} \text{ and}$$
$$\chi(y_2, x_2, x_3, \ldots, x_r) \cdot \chi(y_1, x_1, x_3, \ldots, x_r) \in \{+, 0\}$$

it holds that

$$\chi(x_1, x_2, x_3, \ldots, x_r) \cdot \chi(y_1, y_2, x_3, \ldots, x_r) \in \{+, 0\}.$$

An r-signotope σ is defined on r-subsets of $[n]$ which we can interpret as r-tuples, where the elements are pairwise different and sorted in increasing order. We define a mapping from $[n]^r$ to $\{+,-,0\}$ as follows:

$$\chi_\sigma(x_1,\ldots,x_r) = \begin{cases} 0 & \text{if } |\{x_1,\ldots,x_r\}| < r; \\ \operatorname{sgn}(\pi)\cdot\sigma(x_{\pi(1)},\ldots,x_{\pi(r)}) & \text{for } \pi\in S_r \text{ such that } x_{\pi(1)}<\ldots<x_{\pi(r)}. \end{cases}$$

for all r-tuples $(x_1,\ldots,x_r)\in[n]^r$. Note that we use the convention $\operatorname{sgn}(\pi)=(-)^{|\mathrm{Inv}(\pi)|}$. The map χ_σ is a chirotope. We could not find a proof of this particular statement even though it is known that signotopes are oriented matroids. Hence we provide the full proof.

Lemma 2.2.17. *For every r-signotope σ, the map χ_σ is a chirotope.*

Proof. Since signotopes map r-subsets to $\{+,-\}$, the map χ_σ is not identical to the 0-map. By definition χ_σ is alternating and uniform, it is sufficient to prove the 3-term Grassman-Plücker relations, see Theorem 2.2.16. Moreover, we assume without loss of generality that $x_1,\ldots,x_r,y_1,y_2$ of the 3-term Grassmann-Plücker are pairwise different. If $x_i=x_j$ for $i\neq j$, $y_1=y_2$ or $y_i=x_j$ for $i=1,2$ and $j\geq 3$, the conclusion of the condition holds since the product is 0. If $y_1=x_1$ or $y_2=x_2$, the first condition of the assumption equals the conclusion. Similarly, if $y_1=x_2$ or $y_2=x_1$ the second condition is exactly the condition of the conclusion.
In the remaining part, we assume that all elements are different and hence none of the signs which appear in the 3-term Grassmann-Plücker relation are 0. Fix $r+2$ different elements $y_1,y_2,x_1,x_2,x_3,\ldots,x_r\in[n]$. Without loss of generality we assume that $x_3<\ldots<x_r$. Otherwise we have to apply the same permutations in all of the subsets to order them. Since there are two signs multiplied, we multiply each condition by $+$. Let

$$\begin{aligned} s_1 &= \chi(y_1,x_2,x_3,\ldots,x_r) = \chi(x_1,y_2,x_3,\ldots,x_r), \\ s_2 &= \chi(y_2,x_2,x_3,\ldots,x_r) = \chi(y_1,x_1,x_3,\ldots,x_r). \end{aligned}$$

We want to show that $\chi(x_1,x_2,x_3,\ldots,x_r)=\chi(y_1,y_2,x_3,\ldots,x_r)$. In order to do this we introduce the notion

$$\mathrm{inv}(a,b) = |\{(a,x_i):\ i\geq 3,\ a>x_i\}| + |\{(b,x_i):\ i\geq 3,\ b>x_i\}|$$

for $a,b\in\{x_1,x_2,y_1,y_2\}$ to encode the number of inversion of a,b with respect to $x_3,\ldots,x_r$. Now we consider the following four packets:

$$\begin{aligned} P &= \{y_1,x_1,x_2,x_3,\ldots,x_r\}, & Q &= \{y_2,x_1,x_2,x_3,\ldots,x_r\}, \\ R &= \{y_1,y_2,x_1,x_3,\ldots,x_r\}, & S &= \{y_1,y_2,x_2,x_3,\ldots,x_r\}. \end{aligned}$$

Since we do not know the order of the elements in the packets, we write X_x for a set X without the element $x\in X$. We are only interested in the sign of σ corresponding to the subsets which correspond to deleting one of the elements y_1,y_2,x_1,x_2.
In the first step we consider P. We consider several cases. The three elements y_1,x_1,x_2 can be ordered in 6 different ways. Since all signs and the order in the packet are reversed if the

order of the three elements is reversed, we consider only three of the cases. In the first case, we assume that $y_1 > x_1 > x_2$. Hence P_{y_1}, P_{x_1}, P_{x_2} appear in this order in the sequence. It is

$$\begin{aligned}\sigma(P_{y_1}) &= (-)^{\mathrm{inv}(x_1,x_2)} \cdot \chi(x_1,\ldots,x_r);\\ \sigma(P_{x_1}) &= (-)^{\mathrm{inv}(y_1,x_2)} \cdot s_1;\\ \sigma(P_{x_2}) &= (-)^{\mathrm{inv}(y_1,x_1)} \cdot s_2.\end{aligned}$$

This shows that if the last two signs of P_{x_1} and P_{x_2} are different, then the sign of P_{y_1} must be the same as P_{x_1}. More formally if $(-)^{\mathrm{inv}(y_1,x_2)} \cdot s_1 = - \cdot (-)^{\mathrm{inv}(y_1,x_1)} \cdot s_2$, then $(-)^{\mathrm{inv}(x_1,x_2)} \cdot \chi(x_1,\ldots,x_r) = (-)^{\mathrm{inv}(y_1,x_2)} s_1$. We now consider the other two cases. For all of them we get the same condition on the sign of $\chi(x_1,\ldots,x_r)$.
In the second case, we assume that $y_1 < x_2 < x_1$. Again, we consider the three signs in the packet P. It is

$$\begin{aligned}\sigma(P_{y_1}) &= (-)^{\mathrm{inv}(x_1,x_2)+1} \cdot \chi(x_1,\ldots,x_r);\\ \sigma(P_{x_2}) &= (-)^{\mathrm{inv}(y_1,x_1)} \cdot s_2;\\ \sigma(P_{x_1}) &= (-)^{\mathrm{inv}(y_1,x_2)} \cdot s_1,\end{aligned}$$

and they appear in this order in the packet. Hence the condition from above holds. In the remaining case, we assume the order $x_1 < y_1 < x_2$. The signs are

$$\begin{aligned}\sigma(P_{x_1}) &= (-)^{\mathrm{inv}(y_1,x_2)} \cdot s_1;\\ \sigma(P_{y_1}) &= (-)^{\mathrm{inv}(x_1,x_2)} \cdot \chi(x_1,\ldots,x_r);\\ \sigma(P_{x_2}) &= (-)^{\mathrm{inv}(y_1,x_1)+1} \cdot s_2,\end{aligned}$$

which appear in this particular order. Again the condition holds. Reformulation of this dependencies and the fact that $\mathrm{inv}(a,b) = \mathrm{inv}(b,a)$ and $\mathrm{inv}(a,b) + \mathrm{inv}(a,c) \equiv \mathrm{inv}(b,c) \mod 2$ gives the following claim.

Claim 2.1. *If* $s_1 = (-)^{\mathrm{inv}(x_1,x_2)+1} \cdot s_2$, *then* $\chi(x_1,\ldots,x_r) = (-)^{\mathrm{inv}(y_1,x_1)} \cdot s_1$.

By considering the three different orders of the elements x_1, x_2, y_2 in the packet Q, we get the following relations.

Claim 2.2. *If* $s_1 = (-)^{\mathrm{inv}(x_1,x_2)} \cdot s_2$, *then* $\chi(x_1,\ldots,x_r) = (-)^{\mathrm{inv}(y_2,x_2)} \cdot s_1$.

Claim 2.1 can be applied if $s_1 = (-)^{\mathrm{inv}(x_1,x_2)+1} \cdot s_2$ and Claim 2.2 if $s_1 = (-)^{\mathrm{inv}(x_1,x_2)} \cdot s_2$. Hence s_1 and s_2 fulfill exactly one of the two conditions. In both cases we get an implication for the sign of $\chi(x_1,\ldots,x_r)$.
We proceed in the same way for the two packets R and S to get a condition of the sign $\chi(y_1,y_2,x_3,\ldots,x_r)$. Again exactly one of the two cases from the following two claims occurs.

Claim 2.3. *If* $s_1 = (-)^{\mathrm{inv}(y_1,y_2)} \cdot s_2$, *then* $\chi(y_1,y_2,x_3,\ldots,x_r) = (-)^{\mathrm{inv}(y_1,x_1)} \cdot s_1$.

Claim 2.4. *If* $s_1 = (-)^{\mathrm{inv}(y_1,y_2)+1} \cdot s_2$, *then* $\chi(y_1,y_2,x_3,\ldots,x_r) = (-)^{\mathrm{inv}(y_2,x_2)} \cdot s_1$.

To conclude the statement of the lemma, we have to go through the four possibilities to combine the different cases. Clearly, if we are in the case of Claim 2.1 and Claim 2.3, the statement follows since $\chi(x_1, \ldots, x_r)$ and $\chi(y_1, y_2, x_3, \ldots, x_r)$ have the same sign. If Claim 2.2 and Claim 2.4 holds, then the statement follows in the same way. If the case that the conditions of Claim 2.1 and Claim 2.4 are fulfilled it holds

$$(-)^{\mathrm{inv}(x_1,x_2)+1} \cdot s_2 = s_1 = (-)^{\mathrm{inv}(y_1,y_2)+1} s_2.$$

This implies that $\mathrm{inv}(x_1, x_2) + \mathrm{inv}(y_1, y_2) \equiv 0 \mod 2$ and hence

$$\begin{aligned}\chi(x_1, \ldots, x_r) &= (-)^{\mathrm{inv}(y_1,x_1)} \cdot s_1 \\ &= (-)^{\mathrm{inv}(y_1,x_1)+\mathrm{inv}(x_1,x_2)+\mathrm{inv}(y_1,y_2)} \cdot s_1 \\ &= (-)^{\mathrm{inv}(y_2,x_2)} \cdot s_1 = \chi(y_1, y_2, x_3, \ldots, x_r).\end{aligned}$$

In the last case, we assume that the conditions of Claim 2.2 and Claim 2.3 hold. This implies again $\mathrm{inv}(x_1, x_2) + \mathrm{inv}(y_1, y_2) \equiv 0 \mod 2$, which in the same way as in the preceding case leads to the statement of the lemma. □

This lemma shows that r-signotopes are a subclass of uniform r-chirotopes. Moreover, they are acyclic.

Definition 2.2.18. *A uniform chirotope is* acyclic *if and only if for every $(r+1)$-subset $X = \{x_1, \ldots, x_{r+1}\}$ (not necessarily ordered) the sign sequence*

$$(\chi(X_{x_1}) \ldots \chi(X_{x_{r+1}}))$$

is none of the alternating sign sequences $(+-+\ldots(-)^r)$ and $(-+-\ldots(-)^{r+1})$ of length $r+1$.

This definition of acyclicity is independent of the ordering of the elements.

Lemma 2.2.19. *If the sign sequence of $x_1, \ldots, x_{r+1}$ is alternating, then the sign sequence of $x_{\pi(1)}, \ldots, x_{\pi(r+1)}$ is alternating for every permutation $\pi \in S_{r+1}$.*

Proof. Since adjacent transpositions generate the symmetric group, we only need to show the statement for an adjacent transposition. Let $x_1 < \ldots < x_{r+1}$ and $\pi \in S_{r+1}$ be the permutation with $\pi(j) = j+1$, $\pi(j+1) = j$ and $\pi(i) = i$ for all $i \in [n] \backslash \{j, j+1\}$. Consider the corresponding sequence for $X = (x_1, \ldots, x_{r+1})$ and $X^\pi = (x_1, \ldots, x_{j+1}, x_j, \ldots, x_{r+1})$:

$$(\ \chi(X^\pi_1)\ \ldots\ \chi(X^\pi_{j+1})\ \chi(X^\pi_j)\ \ldots\ \chi(X^\pi_{r+1})\ ).$$

All subsets X^π_i for $i \notin \{j, j+1\}$ contain both elements j and $j+1$. However, they appear in reversed order compared to X. All other elements appear in the same order. Hence the sign of the permutation π when restricting to the elements of $\{x_1, \ldots, x_{r+1}\} \backslash \{x_i\}$ is negative. This shows that all signs except the one of $\chi(X^\pi_{j+1})$ and $\chi(X^\pi_j)$ are reversed in the considered sequence. If we restrict the permutation π to the elements $\{x_1, \ldots, x_{r+1}\} \backslash \{x_i\}$ for $i = j, j+1$, the resulting permutation is the identity whose sign is positive. However, the position of the two adjacent signs in the sequence is reversed. Hence the sign sequence is equal to

$$(\ -\chi(X_1)\ \ldots\ -\chi(X_{j-1})\ \chi(X_{j+1})\ \chi(X_j)\ -\chi(X_{j+2})\ \ldots\ -\chi(X_{r+1})\ )$$

which is alternating if and only if $(\ \chi(X_1)\ \ldots\ \chi(X_{r+1})\ )$ is alternating. □

In [BLS$^+$99] acyclicity is only given in terms of cryptomorphic axiom systems of oriented matroids. Since we could not find the definition for general r-chirotopes elsewhere, we prove that this definition matches the definition of [BLS$^+$99]. In his PhD thesis, Kliem discusses the rank 3 case even for non-uniform oriented matroids, see Definition 3.3 in Chapter 4 of [Kli22].

Lemma 2.2.20. *The definition of acyclicity for uniform chirotopes (Definition 2.2.18) is equivalent to Definition 3.4.7 in [BLS$^+$99] for uniform oriented matroids.*

Proof. By Definition 3.4.7 in [BLS$^+$99] an oriented matroid is acyclic if it does not contain a *positive circuit*. To avoid the formal definition of circuits, we use the following description. In a uniform oriented matroid there are functions $C_X : X \to \{+,-\}$ for all $(r+1)$-subsets $X \subseteq [n]$ such that

$$\chi(x_1, x_3, \ldots, x_{r+1}) = -C_X(x_1)C_X(x_2)\chi(x_2, x_3, \ldots, x_{r+1}), \tag{2.1}$$

see [BLS$^+$99, (PV) in Defintion 3.5.1]. Such a function C_X is called *circuit*. By the circuit axioms it holds: If a circuit C_X exists, then $-C_X$ is a circuit as well. A uniform oriented matroid contains a positive circuit if there is an $(r+1)$-subset $X = \{x_1, \ldots, x_{r+1}\}$ such that C_X is the constant + function.
By Definition 2.2.18 a chirotope is *not* acyclic if there is an $(r+1)$-subset $X = \{x_1, \ldots, x_{r+1}\}$ containing the alternating sign sequence. This is equivalent to

$$\chi(x_1, \ldots, x_r) = (-)^{i+r-1}\chi(x_1, \ldots, x_{i-1}, x_{i+1}, \ldots, x_{r+1}) \tag{2.2}$$

for all $i = 1, \ldots, r$.
Assume χ is not acyclic and hence (2.2) holds for an $(r+1)$-subset $X = \{x_1, \ldots, x_{r+1}\}$. As described above there is a circuit C_X which fulfills the equation (2.1). Together with the alternating property of chirotopes, it is

$$\begin{aligned}\chi(x_1, \ldots, x_r) &= (-)^{i-1} \cdot \chi(x_i, x_1, \ldots, x_{i-1}, x_{i+1}, \ldots, x_r) \\ &= (-)^{i} \cdot C_X(x_i)C_X(x_{r+1})\chi(x_{r+1}, x_1, \ldots, x_{i-1}, x_{i+1}, \ldots, x_r) \\ &= (-)^{i+r-1} \cdot C_X(x_i)C_X(x_{r+1})\chi(x_1, \ldots, x_{i-1}, x_{i+1}, \ldots, x_{r+1})\end{aligned} \tag{2.3}$$

for all $i = 1, \ldots, r$. Both equations (2.2) and (2.3) together imply

$$\begin{aligned}&(-)^{i+r-1}\chi(x_1, \ldots, x_{i-1}, x_{i+1}, \ldots, x_{r+1}) \\ &= \chi(x_1, \ldots, x_r) \\ &= (-)^{i+r-1} \cdot C_X(x_i)C_X(x_{r+1})\chi(x_1, \ldots, x_{i-1}, x_{i+1}, \ldots, x_{r+1}).\end{aligned}$$

for all $i \in \{1, \ldots, r\}$. This shows that $C_X(x_i) = C_X(x_{r+1})$ for all i and hence C is either the constant + or the constant − function. In both cases we have a positive circuit.
For the reverse direction assume there is a positive circuit, i.e., there is an $(r+1)$-subset $X = \{x_1, \ldots, x_{r+1}\}$ such and C_X is the constant + function on $\{x_1, \ldots, x_{r+1}\}$. By (2.1) and the alternating property of chirotopes as used in (2.3) it follows for all $i = 1, \ldots, r$

$$\begin{aligned}\chi(x_1, \ldots, x_r) &= -C_X(x_i)C_X(x_{r+1})(-)^{i+r-1}\chi(x_1, \ldots, x_{i-1}, x_{i+1}, \ldots, x_{r+1}) \\ &= (-)^{i+r}\chi(x_1, \ldots, x_{i-1}, x_{i+1}, \ldots, x_{r+1})\end{aligned}$$

which is exactly an alternating sequence, see (2.2). □

Rank 3 acyclic chirotopes are also known as *abstract order types* or *CC-Systems*. The latter was introduced by Knuth [Knu92] in his book "Axioms and Hulls" using counterclockwise predicates to axiomize planar point sets.
The chirotope χ_σ of a signotope σ is acyclic since there is at most one sign change on the packet if the elements are ordered. Moreover by Lemma 2.2.19 the alternating sign sequence is invariant under permutations. We summarize the results:

Theorem 2.2.21. *For every r-signotope σ, the map χ_σ is an acyclic uniform r-chirotope.*

Note that acyclic uniform chirotopes are in general not signotopes. The important part about signotopes is the linear order of the elements. For rank 3 however, there is a permutation of the elements of a chirotope such that it becomes a signotope. This follows from the fact that every chirotope can be represented by a pseudoline arrangement in which we can mark an unbounded cell as the top cell and order the pseudolines from top to bottom. We have already seen that marked Euclidean pseudoline arrangements are in correspondence with 3-signotope. For $r \geq 4$ this is no longer true, and signotopes are a proper subclass of acyclic uniform chirotopes. For example 5 points in $\mathbb{R}^3$ in general position which are not in convex position have no sorting such that the packet on all 5 elements is monotone.

It is well-known that the number of r-chirotopes on n elements is $2^{\Theta}(n^{r-1})$, see for example [BLS+99, Corollary 7.4.3]. Since the number of r-signotopes has the same asymptotics, see Proposition 2.2.14, they are indeed a rich subclass of r-chirotopes.

2.2.6 Topological Representations of r-Signotopes

The cases $r = 1$ and $r = 2$ are well-understood. For $r = 3$ we already discussed two topological representations and a similar way for a combinatorial encoding. In this section, we give several topological and geometric representations of r-signotopes. Kapranov and Voevodsky [KV91] already mentioned two topological representations for higher Bruhat orders, the first in terms of single element extensions of cyclic hyperplane arrangements, and the second in terms of tight zonotopal tilings of projections of cubes, also called *cubillages*. For rank 3 signotopes, we already discussed pseudolines and pseudoconfiguration of points as topological representation. Both presentation have a generalization for higher rank.
For each of the following four presented representations we give an illustration of the 4-signotope σ_{ex} on 6 elements. For a compact representation, we describe it as a string of its signs in reversed lexicographic order of its r-subsets:

$$\sigma_{\text{ex}} = ++---+---++++++.$$

Pseudohyperplane Arrangements

It was already observed by Kapranov and Voevodsky [KV91] that r-signotopes are a subclass of rank r oriented matroids, see Section 2.2.5 for a proof in terms of chirotopes. The Folkman-Lawrence representation theorem [FL78] asserts that every r-chirotope can be represented as a pseudohyperplane arrangement in $\mathbb{R}^{r-1}$. This in particular holds for r-signotopes as they are a subclass. Pseudohyperplane arrangements abstract the properties of proper hyperplane arrangements.

Definition 2.2.22 (Pseudohyperplane Arrangement)**.** *A* pseudohyperplane H *in* $\mathbb{R}^d$ *is homeomorphic to a hyperplane in* $\mathbb{R}^d$*, i.e., the removal of* H *divides* $\mathbb{R}^d$ *into two connected components, which are both homeomorphic to an open* d*-dimensional ball. A* pseudohyperplane arrangement *in* $\mathbb{R}^d$ *is a family of pseudohyperplanes in* $\mathbb{R}^d$ *such that for every pair* H_1, H_2 *of pseudohyperplanes the intersection is a pseudohyperplane in* $\mathbb{R}^{d-1}$ *and* H_1 *intersects both components of* $\mathbb{R}^d \backslash H_2$*.*

Signotopes are a subclass of r-chirotopes, which provide more structure. As shown by Felsner and Weil r-signotopes correspond to a maximum chain of $(r-1)$-signotopes (cf. Theorem 2.2.11). We refer to such a maximum chain as a *sweep* of the r-signotope. In terms of pseudohyperplane

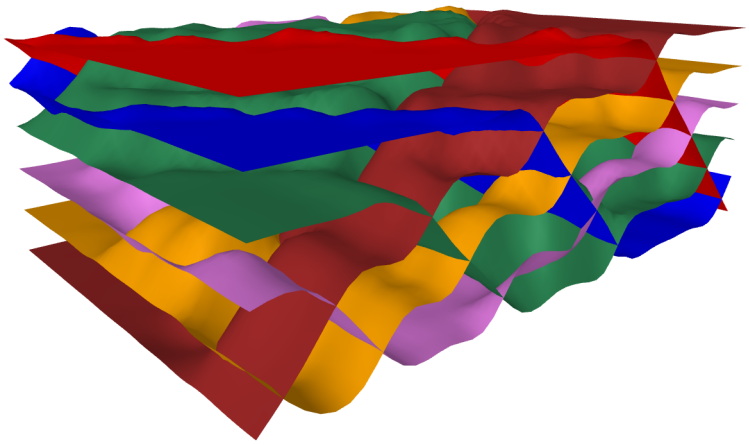

Figure 2.6: A pseudohyperplane arrangement in $\mathbb{R}^3$ of the 4-signotope σ_{ex} on 6 elements. The front is the reversed cyclic arrangement in $\mathbb{R}^2$, the start of the sweep.

arrangement, the sweep is a sequence of pseudohyperplane arrangements in $\mathbb{R}^{r-2}$, i.e., one dimension lower. The sweep of an r-signotope starts with the reversed cyclic arrangement which corresponds to the constant $-$ function and ends with the cyclic arrangement, the constant $+$ function. Two consecutive $(r-1)$-signotopes differ in exactly one sign, which is a fliple in both $(r-1)$-signotopes. For the topological setting of pseudohyperplane, this corresponds to a change of orientation of a simplicial cell. Hence the $r-1$ pseudohyperplanes cross in between. For an illustration of σ_{ex} see Figure 2.6.[4] In Section 2.2.2, we already discussed the rank 3 case in which the Euclidean pseudoline arrangement can be represented by a maximum chain of permutations such that two consecutive differ in an adjacent transposition.

Since the sweep for a signotope always starts with the reverse and ends with the cyclic arrangement of one dimension/rank less, the cyclic arrangement itself plays an important role. Clearly the cyclic arrangement in dimension d is a $(d+1)$-signotope which corresponds to the unique maximal element $\sigma_{\max}$ in the higher Bruhat order $B(n, d+1)$, the constant $+$ function. In the studies of oriented matroids it is also known as the *alternating oriented matroid*, which is based on the structure in terms of the circuit axioms.

[4] For a 3 dimensional visualization see
https://helenabergold.github.io/supp/3d_signotopes/example_pshyperplanes.html

k-Intersecting Pseudoconfiguration of Points

Recently, Miyata [Miy21] presented a representation of r-signotopes using the interaction of a point set and a family of curves. Surprisingly, this is for all ranks a representation in the plane. As it is a generalization of pseudoconfiguration of points (see Section 2.2.3 for the definition), they are called $(r-2)$-*intersecting pseudoconfiguration of points*.

Definition 2.2.23 (k-Intersecting Pseudoconfiguration of Points)**.** *A k-intersecting pseudoconfiguration of points of order n consists of a point set $P = \{p_1, \ldots, p_n\}$ in the plane ordered by increasing x coordinate and a set of x-monotone curves C such that*

- *For every curve $c \in C$ there exists at least $k+1$ points of P on c;*
- *For any $k+1$ points there exists a unique curve going through them; and*
- *Two curves have at most k common points which are proper crossings (no touchings).*

Note that 1-intersecting pseudoconfigurations of points are basically pseudoconfigurations of points. For pseudoconfiguration of points, see Definition 2.2.8, we assumed that two pseudolines have exactly one crossing. In the case of 1-intersecting pseudoconfiguration of points, we weakened this condition to at most one crossing. However, if two curves do not cross, there is an arrangement representing the same 3-signotope in which they cross.
In general, given a k-intersecting pseudoconfiguration of points the n points of P ordered with increasing x coordinate correspond to the n elements. The sign $\sigma(x_1, \ldots, x_r)$ of an r-subset $x_1 < \ldots < x_r$ is obtained by the curve c going through the $r-1$ points $x_1, \ldots, x_{r-1}$ and the above-below-relation of the r-th point x_r with respect to the curve c. If x_r is above c, the subset is mapped to $+$ and $-$ otherwise. The curve going trough the points $x_1, \ldots, x_{r-1}$ is denoted by $c(x_1, \ldots, x_{r-1})$. Note that the other $r-1$ curves determined by the remaining $(r-1)$-subsets of the r-subset contain the same information in the following way. Every curve divides the plane in exactly two connected component, both of them unbounded. Since the curves are x-monotone, one of the component is above and the other one below. We say the component above the curve is the $+$-side, and the other component is the $-$-side. We define a sign mapping on $\binom{[n]}{r}$ by

$$\begin{aligned}\sigma(x_1, \ldots, x_r) = + \quad &\Leftrightarrow \quad x_i \text{ is on the } (-)^{r-i}\text{-side of } c(x_1, \ldots, x_{i-1}, x_{i+1}, \ldots, x_r);\\ \sigma(x_1, \ldots, x_r) = - \quad &\Leftrightarrow \quad x_i \text{ is on the } (-)^{r-i+1}\text{-side of } c(x_1, \ldots, x_{i-1}, x_{i+1}, \ldots, x_r);\end{aligned}$$

which is indeed well-defined and a signotope as shown by Miyata. An illustration of σ_{ex} is given in Figure 2.7.[5]

Theorem 2.2.24 ([Miy21])**.** *For $r \geq 2$, the sign function of an $(r-2)$-intersecting pseudoconfiguration of points of order n is an r-signotope on $[n]$. Moreover, for every r-signotope σ on n elements, there is a $(r-2)$-intersecting pseudoconfiguration of points of order n such that the corresponding sign function equals σ.*

The case $r = 3$ follows by the duality of pseudoconfiguration of points and marked pseudoline arrangements discussed in Section 2.2.3. An independent proof for this special case is provided by Balko, Fulek and Kynčl [BFK15].

[5] This representation was generated using an algorithm provided by Günter Rote.

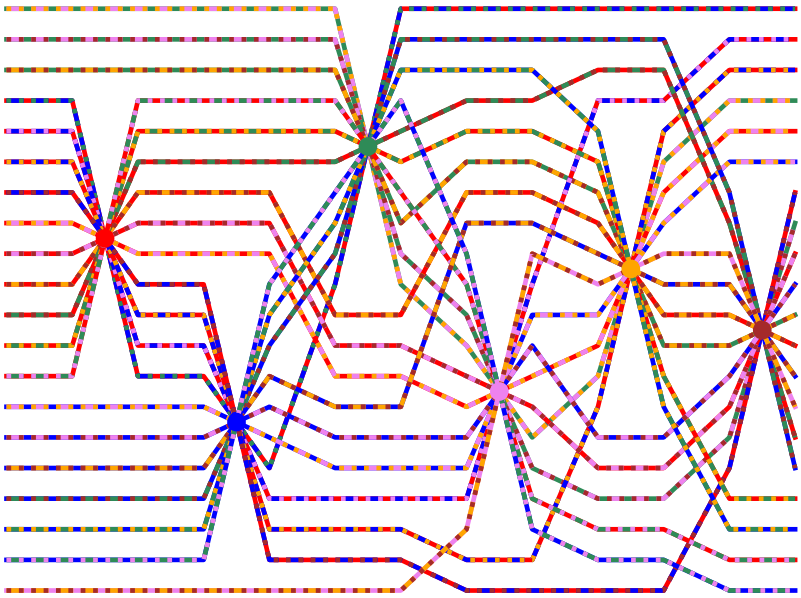

Figure 2.7: A representation of a 4-signotope σ_{ex} on 6-elements as a 2-intersecting pseudoconfiguration of points. The points represent the 6 elements, each of them marked with a different color. The curves are colored with the colors of the three points they contain.

Particular instances of $(r-2)$-intersecting pseudoconfiguration of points are obtained by taking the curves as polynomial functions of degree $r-2$ which interpolate the $(r-1)$-subsets of the point set. More precisely $r-1$ points determine a polynomial function of degree $r-2$ and two such curves cross in at most $r-2$ points. However, not all configurations are *realizable* in such a way that every curve of L is a polynomial function of degree $\leq r-2$. This already holds in the $r=3$ case, since not all pseudoline arrangements are realizable as a line arrangements which is equivalent to realizing pseudoconfiguration of points as point sets.

Zonotopal tiling

A dual representation to pseudohyperplane arrangements are *zonotopal tilings* of $r-1$ dimensional zonotopes. A *zonotope* is the Minkowski sum of vectors $V = \{v_1, \ldots, v_n\}$ in $\mathbb{R}^{r-1}$, which is then tiled by translations of the Minkowski sum of subsets of V. This geometric representation of signotopes was first studied by Kapranov and Voevodsky [KV91] and further investigated by Thomas [Tho03] and Williams [Wil23]. By the Bohne-Dress theorem every rank r-signotopes can be realized as a tight zonotopal tiling in $\mathbb{R}^{r-1}$. For a proof and further information, see for example [RZ94]. A tiling is *tight* if all tiles are Minkowski sums of $r-1$ independent vectors. In such a representation, each vector corresponds to one element of the signotope. Hence for a 3-signotope, the tiled zonotope corresponds to a $2n$-gon. Connecting the halving points of the translations of the same vector gives a pseudohyperplane arrangement. For an illustration of a 3-signotope on 9 elements as a zonotopal tiling together with its dual pseudoline arrangement, see Figure 2.8.

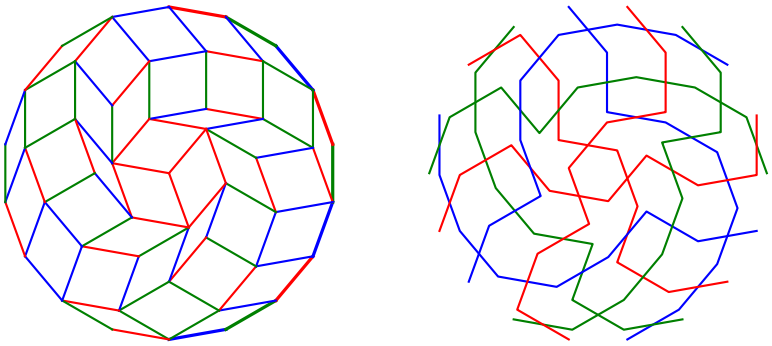

Figure 2.8: A 2-dimensional zonotope with its dual pseudoline arrangement. This is the non-realizable example by Ringel [Rin56] with 9 elements of rank 3.

The 3-dimensional zonotope representing σ_{ex} is given in Figure 2.9.[6]

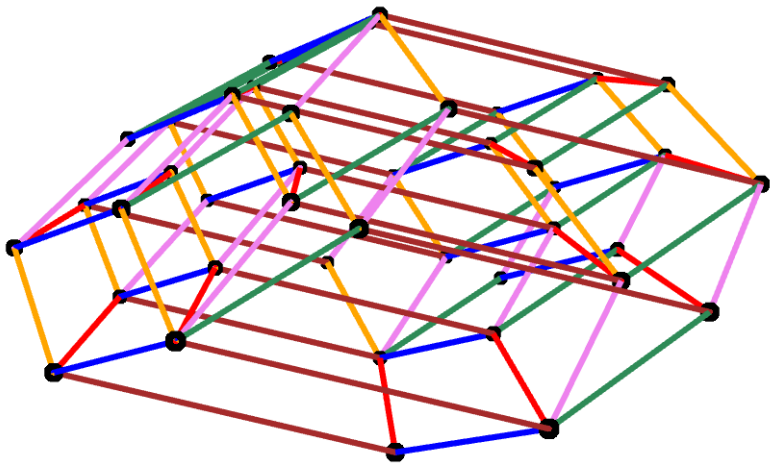

Figure 2.9: A 3-dimensional zonotopal tiling representing the 4-signotope σ_{ex} on 6 elements. Each vector corresponds to one element of the signotope. Translations of the same vector have the same color.

One element extension of the cyclic arrangement

The next representation of r-signotopes was first mentioned by Kapranov and Voevodsky [KV91] and further studied by Ziegler [Zie93]. For this an r-signotope on n elements is represented as a single element extension of the cyclic arrangement of rank $n-r+1$ on n elements. A crossing point of $n-r$ hyperplanes can be identified with its $n-(n-r)=r$ pseudoplanes which do not contain this crossing point. Along each *line* which corresponds to the crossing of $n-r-1$ elements, the r-subsets of the crossing points are ordered lexicographically. A one element extension of this cyclic arrangement corresponds to adding an additional pseudohyperplane.

[6] An interactive view of the 3-dimensional object can be found here:
https://helenabergold.github.io/supp/3d_signotopes/example_zonotope.html

Such a pseudohyperplane partitions each line into two parts, one part above the extending pseudohyperplane and one below. If a crossing point is above the extending line, the r subset of the label is mapped to $+$ and for the crossing points below to $-$. Monotonicity of this sign mapping on r-subsets follows from the order of the labels along all lines. For an illustration see Figure 2.10.

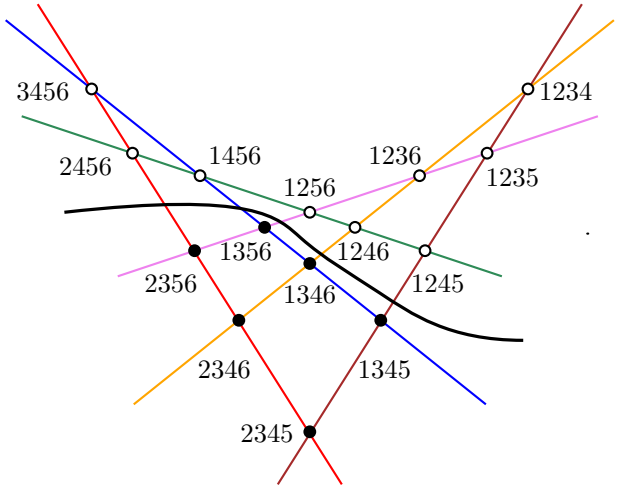

Figure 2.10: The 4-signotope σ_{ex} on 6 elements represented by a one element extension of the cyclic arrangement of rank 3 on 6 elements. The crossing points with white vertices build the $+$-set, the black vertices the $-$-set.

2.3 Simple Drawings

Starting from Turán's brick factory problem from the 1940's, which asks for the minimum number of crossings in a drawing of a complete bipartite graph, simple drawings have gained a lot of attention and became a source for many open problems and conjectures. In the literature, simple drawings are also called *good drawings*, *simple topological drawings*, and *simple topological graphs*.

Definition 2.3.1 (Simple Drawing)**.** *In a* simple drawing *of a graph in the plane (respectively on the sphere),*

- *The vertices are mapped to distinct points in the plane (respectively on the sphere);*
- *Edges are mapped to simple curves connecting the two corresponding vertices and containing no other vertices;*
- *Every pair of edges has at most one common point, which is either a common vertex or a crossing (but not a touching); and*
- *No three edges cross at a common point.*

Figure 2.11 shows the obstructions to simple drawings. In this thesis, we only consider simple

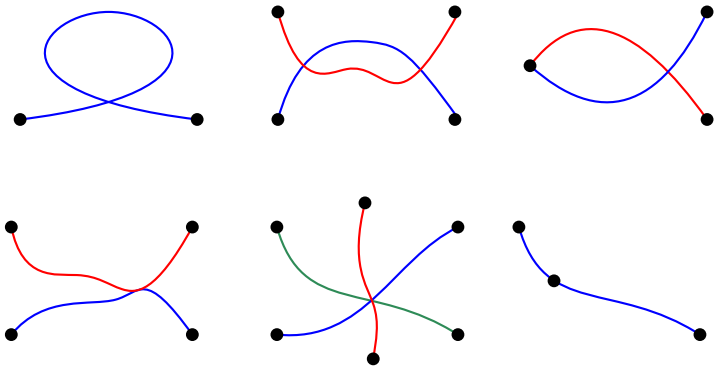

Figure 2.11: The obstructions to simple drawings.

drawings of the complete graph K_n, hence between each pair of vertices there is a curve connecting them. They can be seen as continuous projection of the d-simplex onto the plane which shows that they are a topological generalization of point sets in the plane.

When studying simple drawings, we do not consider the actual embedding of the drawing on the sphere or in the plane. There are different ways to define isomorphism classes on simple drawings, which we discuss in more detail in Section 2.5. Throughout this thesis we only consider the so called *weak isomorphism* in which two drawings are isomorphic if the same pairs of edges cross. This is an isomorphism class for drawings on the sphere. If we consider drawings in the plane, we additional fix a cell of the drawing as the unbounded cell. We refer to it as *outer cell*.

Given a point set in the plane in *general position*, i.e., no three points on a line, connecting the points with straight-line segments yields a simple drawing which is denoted as *geometric drawing*. Geometric drawings are a proper subclass of simple drawings. Moreover, we have already seen that signotopes appeared in the context of pseudolinear drawings of K_n if the vertices are ordered from left to right (see Section 2.2.3). A *pseudolinear drawing* is a drawing in which all edges can be extended to pseudolines such that the resulting configuration is a pseudoline arrangement. Pseudolinear drawings are clearly simple drawings and contain all geometric drawings. A characterization of pseudolinear drawings via an infinite family of forbidden subdrawings is given in [ABR21].

Deciding whether a pseudolinear drawing is homeomorphic to a geometric drawing corresponds to deciding whether a pseuodoline arrangement is realizable as a line arrangement. This is shown to be ETR-hard [Mnë88]. Since there are non-realizable pseudoline arrangements, geometric drawings are a proper subset of pseudolinear drawings. In Section 2.6 we give a more refined classification of classes between pseudolinear drawings and simple drawings. When extending the pseudlinear drawing to a pseudoline arrangement, we obtain a pseudoconfiguration of points. Furthermore, from a pseudoconfiguration of points we get to a pseudolinear drawing by restricting to the curves between the two vertices. Since every pseudoline arrangement can be drawn in an x-monotone way, we achieve an ordering of the vertices $1, \dots, n$ such that all pseudolines/edges are drawn x-monotone. Balko, Fulek and Kynčl [BFK15] used this setting to define triple orientations based on the above-below-relationship similar to the one of the k-intersecting pseudoconfiguration of points. In particular, for $i < j < k$, the triple i, j, k is mapped to $+$ if j is below the edge ik and if j is above the edge, we assign $-$. For an illustration, see Figure 2.12.

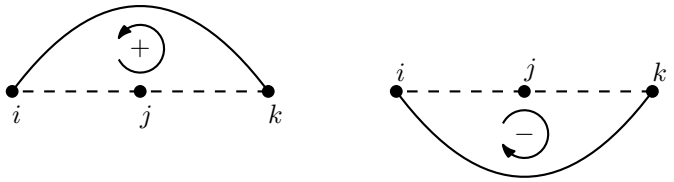

Figure 2.12: Illustration of the connection between the above below relation ship and triangle orientations in pseudolinear drawings.

This mapping is indeed a signotope as shown by Balko, Fulek and Kynčl. If we look at the extended edges to x-monotone pseudolines, the sign of a triple i, j, k determines the orientation of the triangle spanned by those three vertices in the drawing of the complete graph. Given a simple drawing $\mathcal{D}$, the subdrawing of K_3 induced by three vertices is a *triangle*. Note that the edges of a triangle in a simple drawing do not cross and they build a simple closed curve. Hence a triangle partitions the plane (respectively the sphere) into exactly two connected components. If i, j, k is assigned $+$, i.e., if j is below the edge ik, the triangle ijk is oriented counterclockwise when tracing the boundary of the triangle i, j, k in this order. If i, j, k is $-$, then the triangle orientation is clockwise. We can define the triangle orientation in arbitrary simple drawings, which we discuss in the next section.

2.4 Generalized Signotopes

Let $\mathcal{D}$ be a simple drawing of a complete graph in the plane. To each triple (a, b, c) consisting of three distinct vertices, we assign an *orientation* $\gamma(a, b, c) \in \{+, -\}$. The sign $\gamma(a, b, c)$ indicates whether we go counterclockwise or clockwise around the triangle when traversing the edges ab, bc, ca in this order.
In comparison to pseudolinear drawings, when considering simple drawings of the complete graph we have no meaningful ordering of the vertices. Exchanging the labels of two vertices reverts the orientation of all triangles containing both vertices. This suggests to look at the *alternating* extension of γ. Formally $\gamma(i_{\pi(1)}, i_{\pi(2)}, i_{\pi(3)}) = \operatorname{sgn}(\pi) \cdot \gamma(i_1, i_2, i_3)$ for any distinct labels i_1, i_2, i_3 and any permutation $\pi \in S_3$. This yields a mapping $\gamma : [n]_3 \to \{+, -\}$. Recall that $[n]_3$ denotes triples with pairwise distinct entries from $[n]$. To see whether the alternating extension of γ still has a property comparable to the monotonicity of signotopes, we have to look at 4-tuples of vertices, i.e., drawings of K_4. It turns out that the monotonicity condition is replaced by unimodality or co-unimodality, i.e., there are at most two sign changes in the sequence. On the sphere there are two types of drawings of K_4: Type I has one crossing and type II has no crossing. Type I can be drawn in two different ways in the plane: In type $\mathrm{I_a}$ the crossing is only incident to bounded cells and in type $\mathrm{I_b}$ the crossing is incident to the outer cell, see Figure 2.13 for the drawings with one possible labeling of the vertices.
The type of a drawing of K_4 with vertices a, b, c, d can be characterized in terms of the sign sequence of orientations $(\gamma(b, c, d)\ \gamma(a, c, d)\ \gamma(a, b, d)\ \gamma(a, b, c))$. The drawing is

- of type $\mathrm{I_a}$ or type $\mathrm{I_b}$ if and only if the sequence is $(++++)$, $(++--)$, $(+--+)$, $(-++-)$, $(--++)$, or $(----)$; and
- of type II if and only if the number of $+$'s (and $-$'s respectively) in the sequence is odd.

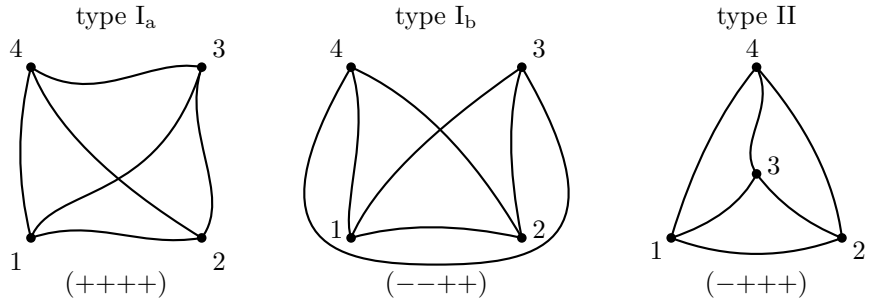

Figure 2.13: The three types of simple drawings of K_4 in the plane.

Since there are no other possibilities to draw a K_4, there are at most two sign-changes in the sequence $(\gamma(b,c,d)\ \gamma(a,c,d)\ \gamma(a,b,d)\ \gamma(a,b,c))$. Moreover, any such sequence is in fact induced by a simple drawing of K_4. Allowing up to two sign-changes is equivalent to forbidding the two alternating patterns $(+-+-)$ and $(-+-+)$. In contrast to signotopes, for which the ordering of the elements is essential, this is no longer true for generalized signotopes. If a generalized signotope γ is alternating and avoids the two patterns $(+-+-)$ and $(-+-+)$ on sorted indices, i.e., $(\gamma(j,k,l)\ \gamma(i,k,l)\ \gamma(i,j,l)\ \gamma(i,j,k))$ has at most two sign-changes for all $i<j<k<l$, then it avoids the two patterns in $(\gamma(b,c,d)\ \gamma(a,c,d)\ \gamma(a,b,d)\ \gamma(a,b,c))$ for pairwise distinct $a,b,c,d\in[n]$. This follows directly from Lemma 2.2.19 and allows us to define *generalized signotopes* as alternating mappings $\gamma\colon [n]_3\to\{+,-\}$ without alternating sign sequences.

Definition 2.4.1 (Generalized Signotope)**.** *A* generalized signotope *is a sign function* $\gamma\colon [n]_3\to\{+,-\}$ *such that for pairwise distinct elements* $a,b,c,d\in[n]$ *the sign sequence*

$$(\gamma(b,c,d)\ \gamma(a,c,d)\ \gamma(a,b,d)\ \gamma(a,b,c))$$

has at most two sign changes.

For simple drawings of the K_n in the plane, all subdrawings of K_4 admit at most two sign changes on every 4-packet. Given a simple drawing $\mathcal{D}$, a *subdrawing* is a set of curves corresponding to edges and their endvertices. A subdrawing of a graph H whose edges and vertices correspond to the incident relations of H. Hence the sign function of every simple drawing of K_n, which encodes the orientations (clockwise or anticlockwise) of the induced K_3, has at most two sign changes on every 4-packet. We conclude:

Proposition 2.4.2. *Every simple drawing of* K_n *induces a generalized signotope on* n *elements.*

The structure of generalized signotopes appears in various geometric objects. In his monograph "Axioms and Hulls" Knuth [Knu92] used ternary predicates to axiomize point sets in general position in the plane, the CC-Systems which are acyclic uniform rank 3 chirotopes, see Section 2.2.5. As a relaxation of those axioms, he studies generalized signotopes which he calls *interior triple systems*. Let g_n denote the number of generalized signotopes on n elements. Knuth showed that $\frac{1}{27}n^3\le\log_2(g_n)$. In Chapter 6 we will improve this bound to $\frac{1}{24}n^3\le\log_2(g_n)$ and give an asymptotic matching upper bound of $0.139n^3$ using Shearer's entropy lemma. While generalized signotopes contain all uniform acyclic 3-chirotopes, the alternating sign patterns $(+-+-)$ or $(-+-+)$ appear in cyclic 3-chirotope, see Section 2.2.5. Moreover, generalized signotopes appeared in the study of intersection patterns of convex sets, see [ADKP22b, ADKP22a].

In Chapter 6, we show that asymptotically there are more generalized signotopes than simple drawings. Moreover, we discuss the relation between simple drawings and generalized signotopes. While all 3-signotopes correspond to a pseudoline arrangement, this is no longer true for the generalized signotopes and simple drawings. The two drawings shown in Figure 2.14 have essential different properties. For example the drawing on the left, denoted as $\mathcal{C}_5$ is geometric and corresponds to the point set in convex position, while the drawing on the right, denoted as $\mathcal{T}_5$ is not isomorphic to a geometric drawing. However with the given labeling both generalized signotopes are the constant +-function. Moreover, the two drawings presented are the two

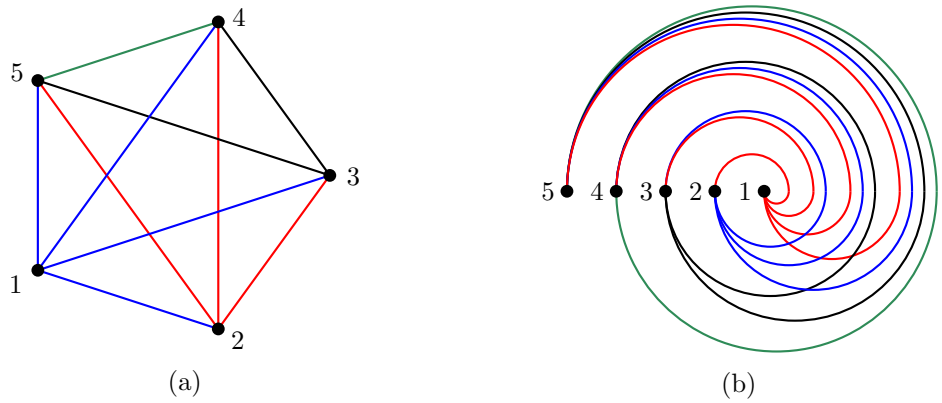

Figure 2.14: The two crossing-maximal simple drawings of K_5. For both of them the triangle orientation for triangles $\{i, j, k\}$ with $i < j < k$ is counterclockwise oriented,i.e., $\gamma(i, j, k) = +$. (a) The geometric drawing $\mathcal{C}_5$ of points in convex position. (b) The *twisted* drawing $\mathcal{T}_5$ with rotation system $\Pi^{oc}_{5,1}$. The drawing $\mathcal{T}_5$ is not geometric.

crossing maximal drawings of K_5. Given a simple drawing and its generalized signotope, we can decide on the basis of the generalized signotope, whether the K_4 has a crossing or not. Hence different simple drawings yielding the same generalized signotope have the same number of crossings. However, the generalized signotope does not provide information on the exact edges which cross. The two drawings given in Figure 2.14 have the same generalized signotope. While in the $\mathcal{C}_5$ the edge $\{1, 5\}$ is uncrossed, the edge $\{1, 5\}$ in the drawing $\mathcal{T}_5$ crosses all edges $\{j, k\}$ with $1 < j < k < 5$. Despite the lack of information, generalized signotopes turned out to be very useful and have been the essential tool for the proof of a separation theorem in the context of simple drawings. In Chapter 4, we discuss theorems from convex geometry in the context of simple drawings and give a proof of Kirchberger's theorem in terms of generalized signotopes.

2.5 Rotation Systems

Various properties of a simple drawing only depend on the combinatorics of the drawing. One way to encode the combinatorics are generalized signotopes, which encode the orientation of the induced K_3. However, as discussed in Section 2.4 generalized signotopes do not encode all information about the drawings. Another way to encode simple drawings combinatorially are rotation systems.

Definition 2.5.1 (Rotation System)**.** *For a given simple drawing $\mathcal{D}$ and a vertex v of $\mathcal{D}$, the cyclic order π_v of incident edges in counterclockwise order around v is called the* rotation of v *in $\mathcal{D}$. The collection of rotations of all vertices is called the* rotation system *of $\mathcal{D}$.*

In the case of simple drawings of the complete graph K_n, the rotation of a vertex v is a cyclic permutation on the $n-1$ vertices $V(K_n)\backslash\{v\}$. The rotation system captures the combinatorial properties of a simple drawing on the sphere – the choice of the outer cell when stereographically projecting the drawing onto a plane has no effect on the rotation system.

Definition 2.5.2 (Pre-Rotation System)**.** *A* pre-rotation system *on V consists of cyclic permutations π_v on the elements $V\backslash\{v\}$ for all $v \in V$. A pre-rotation system $\Pi = (\pi_v)_{v\in V}$ is* drawable *if there is a simple drawing of the complete graph with vertices V such that its rotation system coincides with Π.*

Two pre-rotation systems are *isomorphic* if they are the same up to relabeling and reflection (i.e., all cyclic orders are reversed). Two simple drawings are *weakly isomorphic* if their rotation systems are isomorphic.

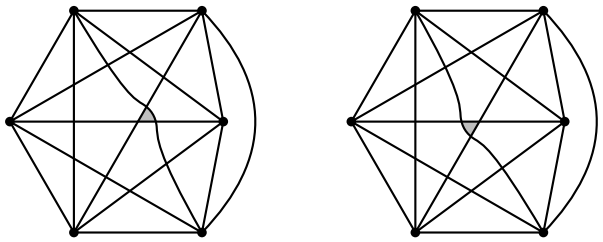

Figure 2.15: Two weakly isomorphic drawings of K_6, which can be transformed into each other by a triangle-flip. The triangle flip is marked grey.

Besides weak isomorphism, there is also the notion of strong isomorphism in literature: Two simple drawings are called *strongly isomorphic* if they induce homeomorphic cell decompositions of the sphere.
A triangular cell, which has no vertex on its boundary, is bounded by three edges. By moving one of these edges across the intersection of the two other edges, one obtains a weakly isomorphic drawing; see Figure 2.15. This operation is called *triangle-flip*. Gioan [Gio05, Gio22], see also Arroyo et al. [AMRS17], showed that any two weakly isomorphic drawings of the complete graph can be transformed into each other with a sequence of triangle-flips and at most one reflection of the drawing.
On four vertices there are three non-isomorphic pre-rotation systems. The K_4 has exactly two non-isomorphic simple drawings on the sphere: The drawing with one crossing (see type I in Figure 2.13) and the drawing with no crossing (type II in Figure 2.13). Note that the drawing of type $\mathrm{I_a}$ and type $\mathrm{I_b}$ are isomorphic on the sphere. The two pre-rotation systems corresponding to type I and type II are drawable, and the third pre-rotation system is an obstruction to drawability. It is denoted by Π_4^o and described in Figure 2.16.
By studying the drawings of K_4, see Figure 2.17, we learn that a crossing pair of edges can be identified from the underlying rotation system. Hence the weak isomorphism is consistent with the definition in the beginning of Section 2.3.

Π_4^o :	$\Pi_{5,1}^o$:	$\Pi_{5,2}^o$:
π_1 : 2 3 4	π_1 : 2 3 4 5	π_1 : 2 3 4 5
π_2 : 1 3 4	π_2 : 1 3 4 5	π_2 : 1 3 5 4
π_3 : 1 2 4	π_3 : 1 4 2 5	π_3 : 1 4 2 5
π_4 : 1 3 2	π_4 : 1 5 3 2	π_4 : 1 5 3 2
	π_5 : 1 4 2 3	π_5 : 1 2 4 3

Figure 2.16: The three obstructions Π_4^o, $\Pi_{5,1}^o$, and $\Pi_{5,2}^o$ for rotation systems.

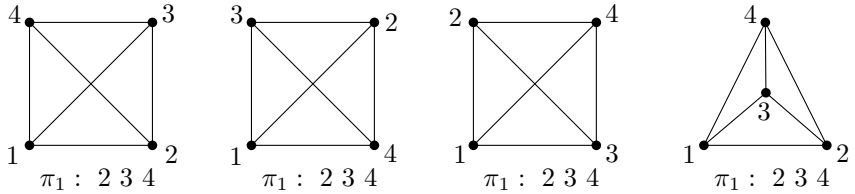

π_1 : 2 3 4	π_1 : 2 3 4	π_1 : 2 3 4	π_1 : 2 3 4
π_2 : 1 3 4	π_2 : 1 4 3	π_2 : 1 3 4	π_2 : 1 4 3
π_3 : 1 2 4	π_3 : 1 4 2	π_3 : 1 4 2	π_3 : 1 2 4
π_4 : 1 2 3	π_4 : 1 2 3	π_4 : 1 3 2	π_4 : 1 3 2

Figure 2.17: The first three drawings of type I are isomorphic, representing the different possibilities of edges crossing in a K_4. The last one represents the isomorphism class corresponding to type II.

Since every crossing pair of edges involves exactly four vertices, we have to look at subconfigurations of size 4 to identify all crossings in a simple drawing. For a pre-rotation system $\Pi = (\pi_v)_{v\in V}$ and a subset of the elements $I \subseteq V$, the *sub-configuration induced by* I is $\Pi|_I = (\pi_v|_I)_{v\in I}$, where $\pi_v|_I$ denotes the cyclic permutation obtained by restricting π_v to $I\backslash\{v\}$. A pre-rotation system Π on V *contains* Π' if there is an induced sub-configuration $\Pi|_I$ with $I \subseteq V$ isomorphic to Π'. A pre-rotation system not containing Π' is called Π'*-free*.

The pairs of crossing edges in a drawing of K_n are fully determined by its underlying rotation system.

Observation 2.5.3. *The following two statements hold:*

(i) A pre-rotation system containing Π_4^o is not drawable.

(ii) Let Π be a Π_4^o-free pre-rotation system on $[n]$. The subconfiguration induced by a 4-element subset is drawable and determines which pairs of edges cross in the drawing.

Note that part (ii) of the lemma allows to talk about the crossing pairs of edges of a Π_4^o-free pre-rotation system, even if there is no associated drawing.
Ábrego et al. [ÁAF+15] generated all pre-rotation systems for up to 9 vertices and used a drawing program based on back-tracking to classify the drawable ones. In particular, they provided the following classification.

Proposition 2.5.4 ([ÁAF+15])**.** *A pre-rotation system on $n \leq 6$ elements is drawable if and only if it does not contain Π_4^o, $\Pi_{5,1}^o$, or $\Pi_{5,2}^o$ (Figure 2.16) as a subconfiguration.*

Moreover, Kynčl showed that a pre-rotation system is drawable if and only if all induced 4-, 5-, and 6-element subconfigurations are drawable [Kyn20, Theorem 1.1]. Together with Proposition 2.5.4 this yields the following characterization:

Theorem 2.5.5. *A pre-rotation system on n elements is drawable if and only if it does not contain Π_4^o, $\Pi_{5,1}^o$ or $\Pi_{5,2}^o$ (Figure 2.16) as a subconfiguration.*

Rotation systems encode combinatorial properties of simple drawings on the sphere. To make investigation with computers, we modeled a CNF instance describing rotation systems. For more details see Chapter 5. Since rotation systems encode the crossings, and plane substructures do not depend on the actual embedding in the plane, the SAT instance lead to several new conjectures concerning plane substructures in simple drawings and in particular helped to prove that every convex drawing contains a plane Hamiltonian cycle. The existence of Hamiltonian cycles in simple drawings is known as Rafla's conjecture [Raf88] and remains open. Despite several improvements of the longest plane path in the last years, the conjecture is only shown for small classes of simple drawings. Subclasses of simple drawings such as convex drawings are defined in the next section.

2.6 Convexity Hierarchy

Geometric drawings of the K_n are a different point of view for point sets in the plane. The vertices are exactly the points, and we connect the points by their straight-line segment. Moreover, pseudoconfigurations of points are simple drawings where we only consider the segment of the curves between two points. This class of drawings is called *pseudolinear drawings*, which clearly contains all geometric drawings. We now define superclassses of pseudolinear drawings which generalize the convexity properties. They have been introduced in the convexity hierarchy by Arroyo et al. [AMRS22]. The classic notion of convexity in the plane asserts that for two points in a convex shape, the connecting line is completely contained in the convex shape. For example (geometric) triangles are convex shapes, which we can define in simple drawings as well. Given a simple drawing $\mathcal{D}$, the subdrawing induced by three vertices is a triangle. Since the edges of a triangle in a simple drawing do not cross and hence the removal of a triangle separates the plane (respectively the sphere) into two connected components. In the plane this is a bounded component and an unbounded component. We call the closure of these connected components *sides*. A side of a triangle is *convex* if every edge that has its two endvertices in the side is completely drawn in the side. Note that both sides of the triangle might be convex. In geometric drawings, the bounded side is always convex. We are now ready to introduce the *convexity hierarchy* of Arroyo et al. [AMRS22]). For $1 \leq i < j \leq 6$, drawings with property (j) also have property (i).

(1) simple drawings;

(2) *convex* drawings: Every triangle has a convex side;

(3) *hereditary-convex* drawings (short: h-convex): we can choose a convex side S_T for every triangle T such that, for every triangle T' contained in S_T, it holds $S_{T'} \subseteq S_T$;

(4) *face-convex* drawings (short: f-convex): there is a special cell c_∞ such that, for every triangle, the side not containing c_∞ is convex;

(5) *pseudolinear* drawings: there is an arrangement $\mathcal{A}$ of pseudolines such that every edge of the drawing is supported by (contained in) one of the pseudolines of $\mathcal{A}$;

(6) geometric drawings: Every edge is drawn as straight-line segments connecting its two endpoints.

Arroyo et al. [AMRS18] showed that the f-convex drawings where the special cell c_∞ is drawn as the unbounded outer cell are precisely the pseudolinear drawings. Pseudolinear drawings are generalized by pseudocircular drawings. A drawing is called *pseudocircular* if every edge can be extended to a pseudocircle (simple closed curve) such that every pair of pseudocircles either has two crossings or is disjoint. Since stereographic projections preserve (pseudo)circles, pseudocircularity is a property of drawings on the sphere. Pseudocircular drawings were studied in an article by Arroyo, Richter, and Sunohara [ARS21]. They provided an example of a simple drawing which is not pseudocircular. Moreover, they proved that hereditary-convex drawings are precisely the *pseudospherical* drawings, i.e., pseudocircular drawings with the additional two properties that

- every pair of pseudocircles intersects, and
- for any two edges $e \neq f$ the pseudocircle γ_e has at most one crossing with f.

The relation between convex drawings and pseudocircular drawings remains open.

To see this, note that the existence of a convex side is not affected by changing the outer cell or by transferring the drawing to the sphere. Moreover, convex sides are not affected by triangle-flips. Hence, these properties only depend on the rotation system of the drawing.

Observation 2.6.1. *Convexity, hereditary-convexity, and face-convexity are properties of the weak isomorphism classes.*

For pseudolinear and geometric drawings, however, the choice of the outer cell plays an essential role. In [ABR21], Arroyo, Bensmail and Bruce Richter give characterization of pseudolinear drawings which yields a polynomial-time algorithm for the recognition. Arroyo et al. [AMRS22] showed that convex and h-convex drawings can be characterized via finitely many forbidden subconfigurations.

Proposition 2.6.2 ([AMRS22])**.** *A simple drawing is convex if and only if it does not contain* $\Pi^{\text{oc}}_{5,1}$ *or* $\Pi^{\text{oc}}_{5,2}$ *(cf. Figure 2.18) as a subconfiguration. Moreover, a convex drawing is h-convex if and only if it does not contain* Π^{oh}_{6} *(cf. Figure 2.19) as a subconfiguration.*

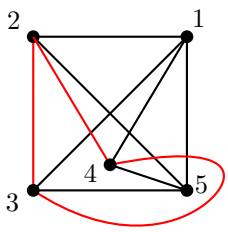

$\Pi^{oc}_{5,1}$:
π_1 : 2 3 4 5
π_2 : 1 3 4 5
π_3 : 1 2 4 5
π_4 : 1 2 5 3
π_5 : 1 2 4 3

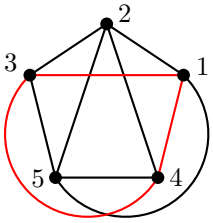

$\Pi^{oc}_{5,2}$:
π_1 : 2 3 4 5
π_2 : 1 3 5 4
π_3 : 1 2 4 5
π_4 : 1 2 5 3
π_5 : 1 4 2 3

Figure 2.18: The two obstructions $\Pi^{oc}_{5,1}$ (left) and $\Pi^{oc}_{5,2}$ (right) for convex drawings. A non-convex triangle is highlighted red.

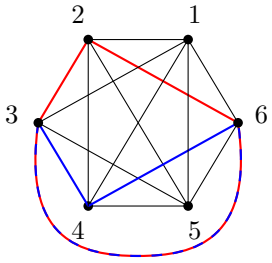

Π^{oh}_{6} :
π_1 : 2 3 4 5 6
π_2 : 1 3 4 5 6
π_3 : 1 2 6 4 5
π_4 : 1 2 3 5 6
π_5 : 1 2 3 4 6
π_6 : 1 2 4 5 3

Figure 2.19: The obstruction Π^{oh}_{6} for h-convex drawings. The convex side of the red triangle is the bounded side and for the blue triangle its the unbounded side. Hence the blue triangle is contained in the convex side of the red one but its convex side is not.

Chapter 3

An Extension Theorem for Signotopes

In 1926, Levi proved in his pioneering article on pseudoline arrangements that the fundamental extendability of line arrangements applies to the more general setting of pseudoline arrangements [Lev26].

Theorem 2.2.4 (Levi's extension lemma for pseudoline arrangements [Lev26])**.** *Given an arrangement $\mathcal{A}$ of pseudolines (not necessarily simple) and two points p, q in $\mathbb{R}^2$, not on a common pseudoline of $\mathcal{A}$. Then there exists a pseudoline ℓ containing both points p and q such that $\mathcal{A} \cup \{\ell\}$ is a pseudoline arrangement.*

Several proofs for Levi's extension lemma are known today. Besides [Lev26], see also [AMRS18, FW01, Sch19].
Generalizations to higher dimensions have been studied in the context of oriented matroids, which by the representation theorem of Folkman and Lawrence [FL78] have representations as projective pseudohyperplane arrangements. Given a family of hyperplanes $\mathcal{H}$ in $\mathbb{R}^d$, any d points in $\mathbb{R}^d$, not all on a common hyperplane of $\mathcal{H}$, define a hyperplane which is distinct from the hyperplanes in $\mathcal{H}$. Goodman and Pollack [GP81] presented an arrangement of 8 pseudoplanes in $\mathbb{R}^3$ and a selection of three points, not all on a common pseudoplane, such that there is no extension of the arrangement with a pseudoplane containing the selected points. Richter-Gebert [Ric93] then investigated a weaker version with only two disjoint prescribed points in dimension 3. He presents an example of a rank 4 oriented matroid on 12 elements which is not extendable. In this chapter, we present a proof of Levi's extension lemma in a purely combinatorial setting, which works for higher dimensions. The geometry is represented by r-signotopes, which are a rich subclass of oriented matroids (see Proposition 2.2.14, Theorem 2.2.21). We show that r-signotopes are extendable through two prescribed points in even dimensions d, that is, when the rank $r = d + 1$ is odd; see Theorem 3.1.2. Surprisingly, there are non-extendable signotopes in rank 4, 6, 8, 10, and 12, which lead to the conjecture that there is no extension theorem for any even rank $r \geq 4$, see Conjecture 3.1.

Outline. In Section 3.1, we discuss how to formulate extendability in terms of signotopes and give the main results of this chapter. A special case, where the extending element is at the last position is studied in Section 3.2. This turns out to be the essential tool in combination with the rotation operator, which is introduced in Section 3.3. In Section 3.4, we finally give the proof of the extension theorem for odd rank. Some technical lemmata are deferred to Section 3.5. In Section 3.6 we discuss the properties for the counterexamples. Up to this point the results presented in this chapter are based on [BFS23a] which is joint work with Stefan Felsner and Manfred Scheucher. Last but not least, we discuss generalizations of this extendability by prescribing more than two points, in Section 3.7.

3.1 Extendability of Signotopes

In Levi's extension lemma for pseudoline arrangements, each of the two prescribed points can either lie in a cell of the arrangement, on one pseudoline, or be the crossing point of two or more pseudolines. To formulate an extension lemma in terms of 3-signotopes we restrict our considerations to *simple* pseudoline arrangements and to crossing points as prescribed points. Since the pseudoline extending the arrangement passes through the two prescribed crossing points, the extension yields a non-simple arrangement. However, perturbing the extending pseudoline at the non-simple crossing points yields a simple arrangement. Figure 3.1 gives an illustration.

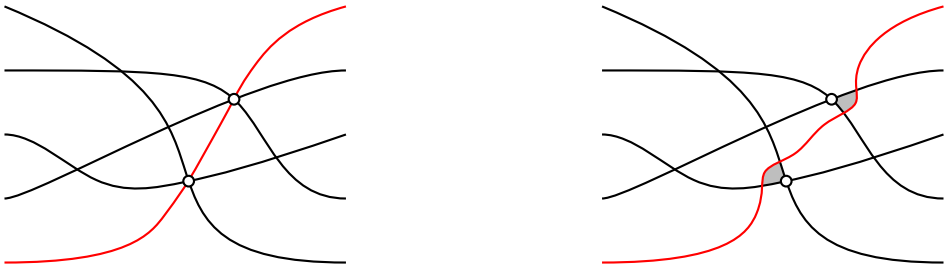

Figure 3.1: Perturbing an extending pseudoline at the two non-simple crossing points.

In terms of signotopes we identify the crossing points via the set of the two pseudolines crossing in this point. Since two pseudolines cross exactly once, the crossing points are in bijection to the 2-subsets, i.e. to $\binom{[n]}{2}$. A perturbation at a prescribed crossing together with the new inserted pseudoline yields a *triangular cell* incident to the crossing. This cell is bounded by the two pseudolines defining the crossing and the extending pseudoline. In terms of 3-signotopes this corresponds to a *fliple* containing the extending element. For the definition and more information, see Section 2.2.4.
Similarly for general rank r, we prescribe two disjoint crossing points of $r-1$ pseudohyperplanes, corresponding to $\binom{[n]}{r-1}$. For the additional element extending the signotope we require that it builds a fliple together with the prescribed $(r-1)$-subsets.
Let $\mathcal{A}$ be an arrangement of pseudolines drawn in an x-monotone way, which are labeled $1,\dots,n$ from top to bottom on the left. When applying Levi's extension lemma to extend $\mathcal{A}$ the left endpoint of the extending line ℓ will be between two consecutive endpoints of pseudolines of $\mathcal{A}$. To re-establish the properties of the labeling, we have to set the label of ℓ accordingly and increase the label of every pseudoline that starts below ℓ by one. To cope with this relabeling-issue in terms of signotopes, we introduce the reverse operation, i.e., deleting an element. For $k \in [n]$ and a subset X of $[n]$, we define

$$X\downarrow_k := \{x \mid x \in X, x < k\} \cup \{x-1 \mid x \in X, x > k\}.$$

Note that the cardinality of X and $X\downarrow_k$ is the same if and only if $k \notin X$. If $k \in X$ it is $|X\downarrow_k| = |X| - 1$. For an r-signotope σ on $[n]$, we define the *deletion* of an element $k \in [n]$ as $\sigma\downarrow_k$ on r-subsets of $[n-1]$ by

$$\sigma\downarrow_k (X\downarrow_k) := \sigma(X)$$

for all r-subsets $X \subseteq [n]$ with $k \notin X$. This is an r-signotope on $[n-1]$ because each $(r+1)$-packet has been an $(r+1)$-packet for σ. The deletion of several elements $k_1 < \ldots < k_\ell$ at the same time is the repeated application of the deletion starting with the largest element to avoid additional index shifts. This is denoted by $\sigma\downarrow_{\{k_1,\ldots,k_\ell\}}$.

Definition 3.1.1. *An r-signotope σ on $[n]$ is* t-extendable *if for all pairwise disjoint $(r-1)$-subsets $I_1, \ldots, I_t \in \binom{[n]}{r-1}$, there exists $k \in [n+1]$ and an r-signotope σ^* on $[n+1]$ with fliples $I_1^*, \ldots, I_t^*$ such that $\sigma^*\downarrow_k = \sigma$, and $I_j^*\downarrow_k = I_j$ for all $j = 1, \ldots, t$. Hence the element k* extends *σ to σ^** through *$I_1, \ldots, I_t$.*

Note that a t-extendable r-signotope on $n \geq (r-1)t$ elements is clearly $(t-1)$-extendable. While the 1-extendability is a simple exercise the first interesting part is the 2-extendability, which we discuss in Section 3.4 of this chapter. Moreover, in Section 3.7 we go even further and consider t-extendability for $t \geq 3$.
For 1-extendability, the strategy in the setting of pseudolines is to add a pseudoline just below one of the two pseudolines crossing in the prescribed point and parallel to this pseudoline in the sense that they have exactly the same crossing points. At the prescribed point the newly inserted pseudoline crosses the two pseudolines involved in the crossing and in the remaining part we again go parallel but just above the same pseudoline. For an illustration, see Figure 3.2.

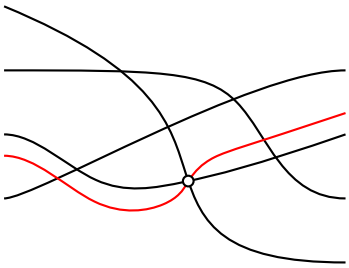

Figure 3.2: Adding a new pseudoline extending the arrangement (black) through the marked crossing point by adding a parallel pseudoline (red) to one of the pseudolines involved in the crossing.

From the theory developed in the following, 1-extendability for signotopes of all ranks is an easy corollary, see Corollary 3.2.2. The extension we get, adds the additional element at the last position which does not yield the same extension as described above in terms of pseudolines.
In the following, we focus on 2-extendability. As it turns out, 2-extendability can be guaranteed for odd rank signotopes.

Theorem 3.1.2 (Extension theorem for signotopes of odd rank)**.** *For every odd rank $r \geq 3$, every r-signotope is 2-extendable.*

The proof of Theorem 3.1.2 (see Section 3.4) generalizes to the more general setting, where the $(r-1)$-subsets I and J, which are fliples in the extension, may intersect.

Corollary 3.1.3. *For $r \geq 3$, let σ be an r-signotope on $[n]$, and I, $J \subseteq [n]$ two $(r-1)$-subsets such that $|I \cap J| + r$ is odd. Then σ is extendable to an r-signotope σ^* on $[n+1]$ with fliples I^*, J^* and an extending element $k \in [n+1]$ such that $\sigma^*\downarrow_k = \sigma$, and $I^*\downarrow_k = I$, and $J^*\downarrow_k = J$.*

For 2-signotopes, which are permutations, the prescribed sets are singletons. Hence we are in the setting of prescribed disjoint 1-subsets. Extendability through t elements corresponds to

inserting an element next to the t prescribed elements in the permutation. Hence 2-signotopes are not 2-extendable. However, the statement of Corollary 3.1.3 is still true for $r = 2$ since the two sets I, J have to be equal.

When considering the extension through $t \geq 3$ prescribed points, a possible generalization is that the intersection of all $(r-1)$-subsets is empty. In the geometric setting this corresponds to prescribed points which are not all on the same pseudohyperplane. This however does not imply that each pair is disjoint. In the non-extendable example presented by Goodman and Pollack [GP81] the intersection of all prescribed points is empty, however two of them are on a common pseudohyperplane.

Despite the restrictions to simple arrangements and crossing points as prescribed points we can derive Levi's extension lemma (Theorem 2.2.4) in its full generality with little extra work from Theorem 3.1.2.

If the prescribed points are not crossing points, we take a crossing incident to the pseudoline segment (or cell). Perturbing the inserted pseudoline slightly at the crossing points one can achieve to cross a pseudoline segment (or cell) incident to the crossing point.

Moreover, given a non-simple arrangement, we can perturb the multiple crossing points (as depicted in Figure 3.1) to obtain a simple arrangement. We obtain simplicial cells instead of the multiple crossings. This simple arrangement can then be extended, and each of the multiple crossing points of the original arrangement can again be obtained by contracting the simplicial cells to a point.

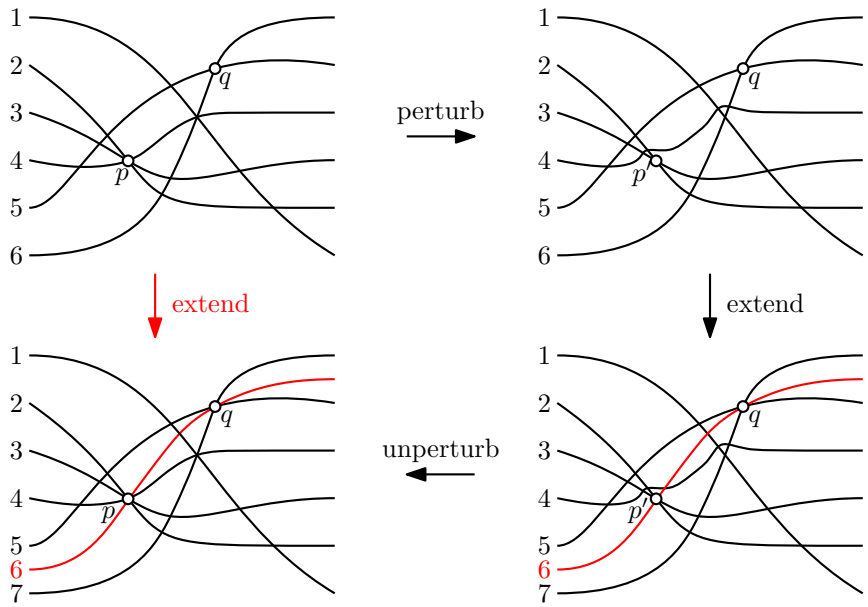

Figure 3.3: Illustration how Theorem 3.1.2 implies Levi's extension lemma (Theorem 2.2.4). When perturbing the top-left arrangement, the multi-crossing point p (the intersection of 2, 3, and 4) is split into three simple crossing points, including the point p' (the intersection of 2 and 3). After the extension, we again contract these three crossing points to one multi-crossing point.

The statement of Theorem 3.1.2 applies only to signotopes of odd rank. This is not just a defect of our proof because signotopes in even rank indeed behave differently. For ranks $r = 4, 6, 8, 10, 12$ we found r-signotopes on $n = 2r$ elements, which are not 2-extendable. In Section 3.6 we describe them in more detail and give properties for all even r which imply that an r-signotope with those properties is not 2-extendable. Based on these examples, we dare the conjecture:

Conjecture 3.1 (No extension theorem for signotopes of even rank)**.** *For every even rank $r \geq 2$, there is an r-signotope which is not 2-extendable.*

If this conjecture is true, then there are r-signotopes which are not extendable through two prescribed crossing points I and J if and only if $|I \cap J| + r$ is even. This is an analog to Corollary 3.1.3. The key for the non-extendable examples is that the projection to the common intersection $I \cap J$ is a signotope of even rank in which the prescribed points are disjoint. In particular, this signotope should be one of the counterexamples where there is no extension through the two sets $I\downarrow_{(I\cap J)}$ and $J\downarrow_{(I\cap J)}$.
For this we define the projection of a signotope on one of its elements. This operation commonly used in matroid theory and geometry and also known as *contraction*. In the resulting signotope the rank and the number of elements are both decreased by one.[1] For an r-signotope σ on $[n]$, we define the *projection* to an element $k \in [n]$ as $\sigma \downdownarrows_k$ by

$$\sigma \downdownarrows_k (X\downarrow_k) := \sigma(X)$$

for all r-subsets $X \subseteq [n]$ with $k \in X$. This is an $(r-1)$-signotope on $[n-1]$ because each r-packet was part of an $(r+1)$-packet for σ. Similar as for the deletion, the projection on a subset of elements $k_1 < \ldots < k_\ell$ is defined by successively applying the projection, starting with the largest element k_ℓ. This projection is denoted by $\sigma \downdownarrows_{\{k_1,\ldots,k_\ell\}}$. Clearly, we can determine fliples in the projection from the fliples in the original signotope.

Observation 3.1.4. *Let F be a fliple of the r-signotope σ and $K \subseteq F$. Then $F\downarrow_K$ is a fliple of $\sigma \downdownarrows_K$.*

To construct the counterexamples, we define a signotope which fulfills the projection properties described above. For the proof of the following proposition, see Section 3.4.

Proposition 3.1.5. *Let σ be an r-signotope on $[n]$ which is* not *2-extendable through the two disjoint $(r-1)$-subsets I, J. For every $m \in \mathbb{N}$, there exists an r'-signotope σ' on $[n']$ with $r' = r + m$ and $n' = n + m$ and two $(r'-1)$-subsets I', J' of $[n']$ with $|I' \cap J'| = m$ such that*

$$\sigma' \downdownarrows_{I'\cap J'} = \sigma, \quad I'\downarrow_{I'\cap J'} = I \quad \text{and} \quad J'\downarrow_{I'\cap J'} = J.$$

Moreover, there is no extending r'-signotope σ^* of σ' on $[n'+1]$ with fliples I^*, J^* such that there is a $k \in [n+1]$ with $\sigma^*\downarrow_k = \sigma'$, $I^*\downarrow_k = I'$, and $J^*\downarrow_k = J'$.

Note that the sum $r' + m = r' + |I' \cap J'|$ is even, since there are only examples which are not 2-extendable for even rank $r = r' - m$ and hence r' and m have the same parity.

[1] Since both, the rank and the number of elements are decreased, this operation is denoted by two down arrows. For the deletion, which is only one down arrow, only the number of elements is decreased while the rank stays the same.

3.2 Extendability and Incomparable Elements

For the proof of the extension theorem for odd rank signotopes, there are two central ingredients. One of them is discussed in this section. If the two prescribed crossing points are incomparable elements in the partial order $\prec_\sigma$ corresponding to the r-signotope σ, then we can easily find an extension, by adding an element at the last position. Figure 3.4 gives an illustration for the rank 3 case. For the definition of the partial order $\prec_\sigma$ on all $(r-1)$-subsets corresponding to a signotope σ see Section 2.2.4.

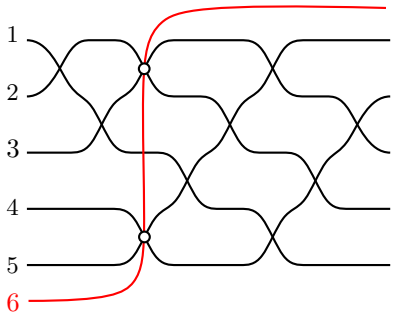

Figure 3.4: The extension through two incomparable crossing points in the setting of pseudolines.

More abstractly we can extend the signotope if there is a down-set in the partial order on $(r-1)$-subsets which has I and J as maximal elements. A *down-set* of a partial order $(\mathcal{P}, \prec)$ is a subset $\mathcal{D} \subseteq \mathcal{P}$ such that for all $p \in \mathcal{P}$ and $d \in \mathcal{D}$ with $p \preceq d$ it holds $p \in \mathcal{D}$. Similarly, an *up-set* is a subset $\mathcal{U} \subseteq \mathcal{P}$ such that for all $p \in \mathcal{P}$ and $u \in \mathcal{U}$ with $p \succeq u$ it holds $p \in \mathcal{U}$.

Proposition 3.2.1 (Extension for incomparable elements)**.** *Let $\prec$ be the partial order on $\binom{[n]}{r-1}$ corresponding to an r-signotope σ on $[n]$. For every down-set $\mathcal{D} \subseteq \binom{[n]}{r-1}$ there exists an r-signotope σ^* on $[n+1]$ such that for all maximal elements M of $\mathcal{D}$, the r-subset of the form $M \cup \{n+1\}$ is a flip of σ^* and $\sigma^*{\downarrow_{n+1}} = \sigma$.*

Proof. Define the extended r-signotope σ^* on $[n+1]$ for $x_1 < \ldots < x_r$ as follows

$$\sigma^*(x_1, \ldots, x_r) := \begin{cases} \sigma(x_1, \ldots, x_r) & \text{if } x_1, \ldots, x_r \in [n]; \\ + & \text{if } x_r = n+1 \text{ and } \{x_1, \ldots, x_{r-1}\} \in \mathcal{D}; \\ - & \text{if } x_r = n+1 \text{ and } \{x_1, \ldots, x_{r-1}\} \notin \mathcal{D}. \end{cases}$$

Clearly it holds $\sigma^*{\downarrow_{n+1}} = \sigma$. In the following we show that σ^* is an r-signotope on $[n+1]$. For every $(r+1)$-subset $P = (x_1, \ldots, x_{r+1})$, we show that the sequence

$$(\sigma^*(P_1)\ \sigma^*(P_2)\ \ldots\ \sigma^*(P_{r+1}))$$

has at most one sign change. If $x_{r+1} \leq n$, then all signs on the considered r-subsets are the same as for σ. Since σ is an r-signotope, there is at most one sign change in the sequence.
In the other case, we have $x_{r+1} = n+1$. For all $j \leq r$ we have $n+1 \in P_j$. Furthermore, $\sigma^*(P_{r+1}) = \sigma(P_{r+1})$ because $n+1 \notin P_{r+1}$. We consider two cases. First, if $\sigma(P_{r+1}) = +$ by definition of the partial order it is

$$P\backslash\{x_{r+1}, x_i\} = P_{r+1}\backslash\{x_i\} \succ P_{r+1}\backslash\{x_j\} = P\backslash\{x_{r+1}, x_j\} \qquad \text{for } i < j.$$

By the property of a down-set this means that, whenever $P\backslash\{x_{r+1}, x_i\} \in \mathcal{D}$, we also have $P\backslash\{x_{r+1}, x_j\} \in \mathcal{D}$ for $i < j$. Let i^* be the smallest integer such that $P\backslash\{x_{r+1}, x_{i^*}\} \in \mathcal{D}$. Then by definition of σ^* it is $\sigma^*(P_j) = +$ for all $j \geq i^*$ and $\sigma^*(P_j) = -$ for all $j < i^*$.
Similar arguments apply if $\sigma(P_{r+1}) = -$. Then we have

$$P\backslash\{x_{r+1}, x_i\} \prec P\backslash\{x_{r+1}, x_j\} \qquad \text{for } i < j.$$

This time let i^* be the smallest integer such that $P\backslash\{x_{r+1}, x_{i^*}\} \notin \mathcal{D}$. Then by definition of σ^* we have $\sigma^*(P_j) = +$ for all $j < i^*$ and $\sigma^*(P_j) = -$ for all $j \geq i^*$.
Let M be a maximal element of the down-set $\mathcal{D}$. Then by definition it is $\sigma^*(M \cup \{n+1\}) = +$. In every packet in which $M \cup \{n+1\}$ appears, it is the maximal element which is still in $\mathcal{D}$. By the analysis above it follows that $M \cup \{n+1\}$ is adjacent to a sign change in each packet. Hence it is a fliple. □

From this proposition and the fact that every element in a partial order defines a down-set in which it is the maximal element, it directly follows that all r-signotopes with $r \geq 2$ are 1-extendable by adding a new element at the last position.

Corollary 3.2.2 (1-extendability)**.** *For $r \geq 2$ let σ be an r-signotope on $[n]$ and $I \subseteq [n]$ an $(r-1)$-subset. Then there is an extending r-signotope σ^* on $[n+1]$ elements such that $I \cup \{n+1\}$ is a fliple and $\sigma^*{\downarrow_{n+1}} = \sigma$.*

Proposition 3.2.1 states that we can add a new element at position $n+1$ such that the maximal elements of the partial order become fliples. For this extension, we assign $+$ to those r-subset which consists of $n+1$ and an $(r-1)$-subset which is contained in the down-set of the fliple with respect to the corresponding partial order. Otherwise we assign $-$.
As the following lemma shows, this is the only possibility in order to extend a signotope in this way. In particular, if there is an extension of a signotope such that the added element is at the last position, then a fliple including this last element prescribes the signs of all subsets which are smaller or larger in the partial order.

Lemma 3.2.3. *For $r \geq 2$, let σ be an r-signotope on $[n]$ and $\prec$ the corresponding partial order. For all $(r-1)$-subsets I and all r-signotopes σ^* on $[n+1]$ such that ${\sigma^*}{\downarrow_{n+1}} = \sigma$ and $I \cup \{n+1\}$ is a fliple of σ^* it holds*

$$\sigma^*(J \cup \{n+1\}) = \begin{cases} +, & \text{if } J \prec I; \\ -, & \text{if } J \succ I, \end{cases}$$

for all $(r-1)$-subsets $J \neq I$ of $[n]$.

Proof. We consider the case $J \prec I$. The other case with $J \succ I$ works analogously by reversing the relations and the signs. By the definition of the partial order, there is a chain of $(r-1)$-subsets of $[n]$ such that $J = J_m \prec \ldots \prec J_2 \prec J_1 = I$ such that for each pair of consecutive subsets the intersections $J_i \cap J_{i+1}$ consists of exactly $r-2$ elements. Note that the r-subset $I \cup \{n+1\} = J_1 \cup \{n+1\}$ is a fliple and hence assigning $\sigma^*(J_1 \cup \{n+1\}) = +$ is a valid signotope, which we assume from now on. For all $i = 2, \ldots, m$, we show that $\sigma^*(J_i \cup \{n+1\}) = +$ by induction. For a fixed $i \geq 2$, consider the $(r+1)$-packet $P = J_{i-1} \cup J_i \cup \{n+1\}$. Since $n+1$ is the largest element in this $(r+1)$-packet, it is $P_{r+1} = J_{i-1} \cup J_i$. Note that $n+1 \notin J_i$ for

all i which implies together with the assumption $\sigma^*\downarrow_{n+1}=\sigma$ that the sign of P_{r+1} is determined by σ, i.e.,

$$\sigma^*(J_{i-1}\cup J_i)=\sigma(J_{i-1}\cup J_i).$$

Let $j<r+1$ be the index such that $P_j=J_{i-1}\cup\{n+1\}$. We consider the relation between J_i and J_{i-1} in the lexicographic order.
If J_i is lexicographically smaller than J_{i-1}, then $J_i\cup\{n+1\}=P_k$ for a $k\in\{j+1,\dots,r\}$ and appears after the sign of P_j in the sequence. By the construction of the chain it is $J_{i-1}\succ J_i$. Since J_i is l4xicographically smaller than J_{i-1}, it is $\sigma^*(P_{r+1})=\sigma^*(J_i\cup J_{i-1})=+$. The sign of $J_i\cup\{n+1\}$ appears in the sequence between the one of $J_{i-1}\cup\{n+1\}$ and $J_i\cup J_{i-1}$. Since $\sigma^*(J_{i-1}\cup\{n+1\})=+$ by induction hypothesis, it holds $\sigma^*(J_i\cup\{n+1\})=+$.
If J_i is lexicographically larger than J_{i-1}, then $J_i\cup\{n+1\}=P_k$ for a $k=1,\dots,j-1$. Moreover it is $\sigma^*(P_{r+1})=\sigma^*(J_i\cup J_{i-1})=-$. By induction hypthesis it is still $\sigma^*(P_j)=\sigma^*(J_{i-1}\cup\{n+1\})=+$. Hence the sign change has to be between P_j and P_{r+1} which again implies that $\sigma^*(J_i\cup\{n+1\})=+$. □

If there are two maximal elements in a down set, they are incomparable. This gives a condition to ensure that a signotope is not extendable by an element added at the last position.

Proposition 3.2.4. *For $r\geq 3$, let σ be an r-signotope on $[n]$ and for $t\geq 2$ let $I_1,\dots,I_t$ be disjoint $(r-1)$-subsets. Then there is an r-signotope σ^* on $[n+1]$ with $\sigma^*\downarrow_{n+1}=\sigma$ such that for all $j=1,\dots,t$ the r-subsets $I_j\cup\{n+1\}$ are fliples if and only if $I_1,\dots,I_t$ are pairwise incomparable in the partial order corresponding to σ.*

Proof. The reverse direction, i.e., the existence of an extension if the prescribed subsets are pairwise incomparable follows from Proposition 3.2.1.
For the other direction assume there is an extension σ^* with $\sigma^*\downarrow_{n+1}=\sigma$. Then σ^* is a 1-extension for every I_j as in the assumptions of Lemma 3.2.3. Towards a contradiction assume there are two $(r-1)$-subsets I_i and I_j which are comparable. Without loss of generality $I_i\prec I_j$. Hence I_i is in the down-set of I_j and $I_j\cup\{n+1\}$ is a fliple of σ^*. By Lemma 3.2.3 the sign of $I_i\cup\{n+1\}$ has to be a $+$ in σ^*. Moreover, $I_i\cup\{n+1\}$ is a fliple by assumption. Hence flipping the sign to $-$ yields a valid signotope. Since we assume $r\geq 3$ and I_i and I_j are disjoint, the two r-subsets $I_i\cup\{n+1\}$ and $I_j\cup\{n+1\}$ do not appear in a common $(r+1)$-packet. Hence flipping $I_i\cup\{n+1\}$ from $+$ to $-$ does not affect whether $I_j\cup\{n+1\}$ is a fliple. In particular $I_j\cup\{n+1\}$ is still a fliple in the signotope in which $I_i\cup\{n+1\}$ was flipped to $-$. This is not possible by Lemma 3.2.3. A contradiction. □

Note that for $r=2$, the sets $\{i,n+1\}$ and $\{j,n+1\}$ for $i\neq j$ appear in a common 3-packet. Hence there are extensions for two successive elements in the total order given by the 2-signotope which are extendable even though they are not incomparable.

In general the two prescribed $(r-1)$-subsets are not incomparable. Still we can use Proposition 3.2.1 to proof the extendability result. For this we need an operation on signotopes which still preserves the basic properties of the signotope such as the fliples. We introduce this operation, which we call *rotation* in the following section.

3.3 Rotation Operator

We now prepare for the proof of Theorem 3.1.2. For this we introduce the rotation operator. If we rotate an arrangement of pseudolines in the plane, i.e., we choose another unbounded cell as the top cell, we get a pseudoline arrangement with the same cell structure. However, the signotope does not stay the same and the linear order of the elements changes. If we rotate only a single pseudoline, then the orientation of the triangle spanned by 3 pseudolines stays the same if and only if the rotated pseudoline is not involved. See for example the triangle spanned by $\{2,3,4\}$ in the left arrangement, which corresponds to the triangle spanned by $\{1,2,3\}$ in the right arrangement in Figure 3.5. When rotating *clockwise*, the first element of σ becomes the last one in the rotated signotope σ_{rot}. In terms of the 3-signotope σ the signs of the rotated signotope σ_{rot} are: $\sigma_{\text{rot}}(a,b,c) = \sigma(a+1,b+1,c+1)$ if $c \neq n$ and $\sigma_{\text{rot}}(a,b,n) = -\sigma(1,a+1,b+1)$.

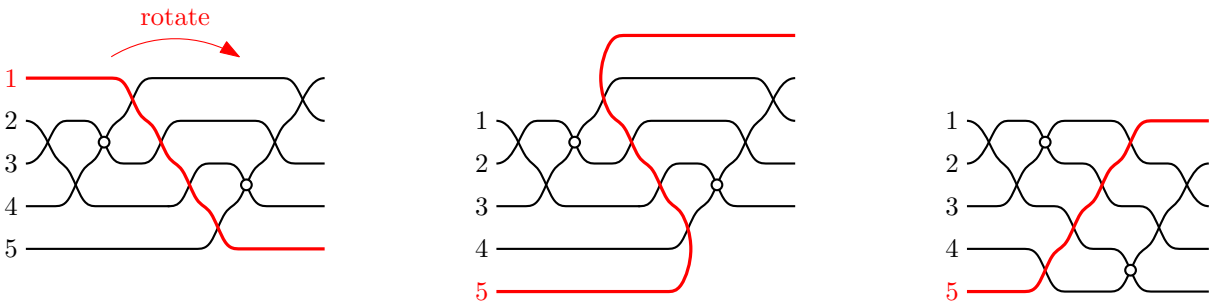

Figure 3.5: Illustration of a clockwise rotation of pseudolines. The rotated pseudoline is highlighted red. The two marked crossings became incomparable in the rotated arrangement.

For general r, we define the *clockwise rotated* signotope σ_{rot} of a given r-signotope σ as:

$$\sigma_{\text{rot}}(x_1,\ldots,x_r) := \begin{cases} -\sigma(1,x_1+1,\ldots,x_{r-1}+1) & \text{if } x_1 < x_2 < \ldots < x_r = n, \\ \sigma(x_1+1,\ldots,x_r+1) & \text{if } x_1 < x_2 < \ldots < x_r < n. \end{cases}$$

To keep track of the index shift caused by a clockwise rotation, we define $x_{\text{rot}} = x-1$ if $x \neq 1$ and $1_{\text{rot}} = n$. It is

$$X_{\text{rot}} = \{x_{\text{rot}} : x \in X\} = \begin{cases} (x_1-1, x_2-1, \ldots, x_k-1) & \text{if } x_1 > 1; \\ (x_2-1, \ldots, x_k-1, n) & \text{if } x_1 = 1 \end{cases}$$

for any subset $X = (x_1,\ldots,x_k)$ of $[n]$ with $x_1 < \ldots < x_k$. Note that this allows us to write $\sigma_{\text{rot}}(X_{\text{rot}}) = \sigma(X)$ if $1 \notin X$ and $\sigma_{\text{rot}}(X_{\text{rot}}) = -\sigma(X)$ if $1 \in X$. The *k-folded clockwise rotation* is denoted by $\sigma_{\text{rot}(k)}$. Note that the rotation operation depends on the number of elements n of a signotope. While n is known when rotating a signotope itself, we have to be careful when rotating a subset $X \subseteq [n]$. As the following lemmas show, the rotated signotope is indeed an r-signotope, which moreover has essentially the same fliples.

Lemma 3.3.1. *Let σ be an r-signotope on $[n]$. Then σ_{rot} is an r-signotope on $[n]$.*

Proof. Consider an $(r+1)$-packet $P' = (x'_1,\ldots,x'_{r+1})$. Since rotation is a bijection on the $(r+1)$-packets of $[n]$ there is a $P = (x_1,\ldots,x_{r+1})$ such that $P' = P_{\text{rot}}$.

If the rotated element 1 is not in P, i.e., $x'_{r+1} < n$, then $x_i = x'_i + 1$ for all $i = 1, \ldots, r+1$ and the signs of the r-subsets of packet P' have to be considered in the same order

$$\begin{array}{rrrrr} & (\ \sigma_{\text{rot}}(P'_1) & \sigma_{\text{rot}}(P'_2) & \ldots & \sigma_{\text{rot}}(P'_r) \quad \sigma_{\text{rot}}(P'_{r+1})\ ) \\ = & (\ \sigma(P_1) & \sigma(P_2) & \ldots & \sigma(P_r) \quad \sigma(P_{r+1})\ ). \end{array}$$

as for P. The latter has at most one sign change since σ is an r-signotope.
If the rotated element 1 is in P, that is, $x'_{r+1} = n$ and $x_1 = 1$, then we have $x_{i+1} = x'_i + 1$ for all $i = 1, \ldots, r$. Note that $n \in P'_i$ for $i = 1, \ldots, r$ and hence $1 \in P_j$ for $j = 2, \ldots, r+1$. The sign sequence of P' is

$$\begin{array}{rlllll} & (\ \sigma_{\text{rot}}(P'_1) & \sigma_{\text{rot}}(P'_2) & \ldots & \sigma_{\text{rot}}(P'_r) & \sigma_{\text{rot}}(P'_{r+1})\ ) \\ = & (\ \sigma_{\text{rot}}(P'\backslash\{x_2 - 1\}) & \sigma_{\text{rot}}(P'\backslash\{x_3 - 1\}) & \ldots & \sigma_{\text{rot}}(P'\backslash\{x_{r+1} - 1\}) & \sigma_{\text{rot}}(P'\backslash\{n\})\ ) \\ = & (\ -\sigma(P_2) & -\sigma(P_3) & \ldots & -\sigma(P_{r+1}) & \sigma(P\backslash\{1\})\ ) \\ = & (\ -\sigma(P_2) & -\sigma(P_3) & \ldots & -\sigma(P_{r+1}) & \sigma(P_1)\ ), \end{array}$$

which has at most one sign change because $(\sigma(P_1)\ \sigma(P_2)\ \ldots\ \sigma(P_r)\ \sigma(P_{r+1}))$ has at most one sign change due to the signotope property of σ. □

The following lemma shows that the rotated signotope σ_{rot} has essentially the same properties as σ when it comes to fliples. We only need to handle the index shift.

Lemma 3.3.2. *Let σ be an r-signotope and let F be a flip of σ. Then F_{rot} is a flip in the clockwise rotated signotope σ_{rot}.*

Proof. To prove that an r-subset F_{rot} is a flip, we need to check all $(r+1)$-packets P' with $F_{\text{rot}} \subset P'$. Let P' be such a packet and let P be such that $P_{\text{rot}} = P'$. Since F is a flip in σ we know that if we change the sign of $\sigma(F)$ there is still at most one sign change in the sequence $\sigma(P_1), \sigma(P_2), \ldots, \sigma(P_r), \sigma(P_{r+1})$, we abbreviate this by saying that F is *flipable* in P.
If $1 \notin P$, then $\sigma(P_i) = \sigma_{\text{rot}}(P'_i)$ for all i. Moreover if j is such that $F = P_j$ then $F_{\text{rot}} = P'_j$. Since the signs in the sequence stay the same F_{rot} is flipable in P'.
Otherwise we have $1 \in P$. Then as shown in the proof of Lemma 3.3.1 it is

$$\begin{array}{rrrrr} & (\ \sigma_{\text{rot}}(P'_1) & \sigma_{\text{rot}}(P'_2) & \ldots & \sigma_{\text{rot}}(P'_r) \quad \sigma_{\text{rot}}(P'_{r+1})\ ) \\ = & (\ -\sigma(P_2) & -\sigma(P_3) & \ldots & -\sigma(P_{r+1}) \quad \sigma(P_1)\ ). \end{array}$$

If $F = P_1$ the sequence $(\sigma(P_2)\ \ldots\ \sigma(P_{r+1}))$ is constant. This implies that the sign of $\sigma_{\text{rot}}(F_{\text{rot}}) = \sigma_{\text{rot}}(P'_{r+1}) = \sigma(P_1)$ can be flipped. If $F = P_{r+1}$ the sign sequence $(\sigma(P_1)\ \ldots\ \sigma(P_r))$ is constant. This shows that the sign of $\sigma_{\text{rot}}(F_{\text{rot}}) = \sigma_{\text{rot}}(P'_r)$ is adjacent to different signs and can thus be flipped. If $F = P_2$ then $\sigma(P_1) \neq \sigma(P_3)$ and the signs $\sigma_{\text{rot}}(P'_i)$ for $2 \leq i \leq r+1$ are the same. Hence $F_{\text{rot}} = P'_1$ is flipable in P'. If $F = P_j$ with $3 \leq j \leq r$, then $F_{\text{rot}} = P'_{j-1}$ is clearly flipable in P'. This shows that F_{rot} is flipable in all packets containing it and hence a flip of σ_{rot}. □

3.4 2-Extendability for Odd Rank

In this section, we show that for each pair of disjoint crossing points, respectively $(r-1)$-subsets, odd rank signotopes admit a rotation in which the crossing points are incomparable. In this case, we use Proposition 3.2.1 to define an extension. To achieve an extension of the original signotope, we then rotate in the reverse direction.
For a signotope σ and its rotation σ_{rot}, the partial orders are denoted by $\prec$ and $\prec_{\text{rot}}$, respectively. Moreover, if two elements x, y are incomparable in $\prec$ (respectively $\prec_{\text{rot}}$), it is denoted by $x \| y$ (respectively $x \|_{\text{rot}} y$). We summarize the interaction between the rotation operator and the partial order in the following proposition. For the proof, we need some additional technical lemmata, which are deferred to Section 3.5.

Proposition 3.4.1. *Let σ be an r-signotope on $[n]$ with partial order $\prec$. For two $(r-1)$-subsets I, J with $I \prec J$ and $1 \notin I \cap J$, it holds $I_{\text{rot}} \|_{\text{rot}} J_{\text{rot}}$ or $I_{\text{rot}} \prec_{\text{rot}} J_{\text{rot}}$.*

For two $(r-1)$-subsets I and J which have a common intersection of $r-2$ elements, the relation is reversed if and only if the intersection contains the rotated element. Otherwise the relation stays the same.

Lemma 3.4.2. *Let σ be an r-signotope with partial order $\prec$ and σ_{rot} the rotated signotope with corresponding partial order $\prec_{\text{rot}}$. For two $(r-1)$-subsets I, J such that $|I \cap J| = r-2$ and $I \prec J$ it holds*

$$\begin{aligned} I_{\text{rot}} &\prec_{\text{rot}} J_{\text{rot}} \quad \text{if } 1 \notin I \cap J, \quad \text{and} \\ I_{\text{rot}} &\succ_{\text{rot}} J_{\text{rot}} \quad \text{if } 1 \in I \cap J. \end{aligned}$$

Proof. If $1 \notin I$ and $1 \notin J$, then $1 \notin I \cup J$ and the sign of $I \cup J$ is the same for σ and σ_{rot}, i.e., $\sigma(I \cup J) = \sigma_{\text{rot}}(I_{\text{rot}} \cup J_{\text{rot}})$. Furthermore the order of I and J in the r-subset $I \cup J$ is the same as the order of I_{rot} and J_{rot} in the r-subset $I_{\text{rot}} \cup J_{\text{rot}}$. If I is lexicographically larger than J, then I_{rot} is lexicographically larger than J_{rot} which implies that the sign of $I \cup J$ in σ and $I_{\text{rot}} \cup J_{\text{rot}}$ in σ_{rot} is the same. Hence $I_{\text{rot}} \prec_{\text{rot}} J_{\text{rot}}$.
If $1 \in I$ but $1 \notin J$ then I is lexicographically smaller than J. By assumption it is $J \succ I$ and thus $\sigma(I \cup J) = +$. After rotating clockwise, I_{rot} is lexicographically larger than J_{rot} since $n \in I_{\text{rot}}$ and $n \notin J_{\text{rot}}$. Furthermore the sign of the r-subset changes, i.e., $\sigma(I \cup J) = -\sigma_{\text{rot}}(I_{\text{rot}} \cup J_{\text{rot}}) = -$. This shows that the relation stays the same, i.e., $I_{\text{rot}} \prec_{\text{rot}} J_{\text{rot}}$. The case $1 \in J$ but $1 \notin I$ works analogously.
If $1 \in I$ and $1 \in J$ the lexicographic order of I and J is the same as the lexicographic order of I_{rot} and J_{rot} but the sign of the r-subset gets is reversed, i.e., $\sigma(I \cup J) = -\sigma_{\text{rot}}(I_{\text{rot}} \cup J_{\text{rot}})$. Thus the order between I_{rot} and J_{rot} is reversed as claimed. □

Indeed Proposition 3.4.1 ensures that for odd rank there exists a rotation such that the two prescribed $(r-1)$-subsets are incomparable.

Proposition 3.4.3. *Let $r \geq 3$ be an odd integer, let σ be an r-signotope on $[n]$ and let I, J be two disjoint $(r-1)$-subsets. After $k \leq n-1$ clockwise rotations, σ, I, and J are transformed into $\sigma_{\text{rot}(k)}$, $I_{\text{rot}(k)}$, and $J_{\text{rot}(k)}$, respectively, such that $I_{\text{rot}(k)} \|_{\text{rot}(k)} J_{\text{rot}(k)}$.*

Proof. Assume I and J are comparable in the partial order $\prec$ corresponding to the r-signotope σ. otherwise $k = 0$ is the desired rotation. Without loss of generality assume $I \prec J$. We show that after n clockwise rotations, i.e., when every element was rotated once, all signs of σ are reversed. Hence the partial order $\prec_{\mathrm{rot}(n)}$ rotated signotope $\sigma_{\mathrm{rot}(n)}$ is the reversed relation to $\prec$.
The sign of an r-subset $(z_1, \ldots, z_r)$ of $[n]$ changes from $+$ to $-$ or vice versa if and only if the rotated element is contained in $(z_1, \ldots, z_r)$, i.e., if we rotate z_1. Hence after rotating n times in total every z_i was rotated and thus the sign of an r-subset changes exactly r times. Since r is odd, the sign after rotating n times is reversed. The obtained signotope $\sigma_{\mathrm{rot}(n)}$ is the reverse of the original signotope σ and the corresponding partial order is also reversed.
Furthermore by Proposition 3.4.1 we cannot reverse the order of two disjoint $(r-1)$-subsets in a single rotation. Hence there will be a rotation with $k < n$ such that the two disjoint sets are incomparable. □

With similar arguments as in the previous proof it follows that for all ranks r applying $2n$ rotations yields the same signotope. Hence we can define the counterclockwise rotation which corresponds to $2n-1$ clockwise rotations, which is denoted as $\sigma_{\mathrm{rot}(-1)}$. Applying k rotations in the reverse direction is consequently denoted with $\sigma_{\mathrm{rot}(-k)}$.
Although the following lemma is trivial in the setting of pseudoline arrangements, we need to prove it in the context of general r-signotopes. We show that the extension of a rotated signotope when rotated back contains the original signotope. To show this we need to investigate the interaction between the rotation and deletion of elements and show that the two operators behave in an almost commutative way.

Lemma 3.4.4. *Let σ be an r-signotope on $[n]$. Then it is $\sigma_{\mathrm{rot}}\downarrow_n = \sigma\downarrow_1$ and $\sigma_{\mathrm{rot}}\downarrow_{x_{\mathrm{rot}}} = (\sigma\downarrow_x)_{\mathrm{rot}}$ for $x \in \{2, \ldots, n\}$.*

Proof. Because of the index shift it does not matter whether we delete the first element or we rotate σ such that the first element becomes the last and delete the last element in this rotated signotope. Formally, the deletion operator is defined by $\sigma\downarrow_1 (X\downarrow_1) = \sigma(X)$ for all r-subsets $X \subseteq [n]$ with $1 \notin X$. Since $1 \notin X$, it is $\sigma(X) = \sigma_{\mathrm{rot}}(X_{\mathrm{rot}})$ and $n \notin X_{\mathrm{rot}}$. Hence deleting the element n does not affect X_{rot}, i.e., it is $X_{\mathrm{rot}} = (X_{\mathrm{rot}})\downarrow_n$. This shows $\sigma_{\mathrm{rot}}(X_{\mathrm{rot}}) = \sigma_{\mathrm{rot}}\downarrow_n (X_{\mathrm{rot}}\downarrow_n) = \sigma_{\mathrm{rot}}\downarrow_n (X_{\mathrm{rot}})$. Assembling the steps shows

$$\sigma\downarrow_1 (X\downarrow_1) = \sigma_{\mathrm{rot}}\downarrow_n (X_{\mathrm{rot}}).$$

Since $1 \notin X$, it is $X\downarrow_1 = X_{\mathrm{rot}}$. Hence the first part $\sigma_{\mathrm{rot}}\downarrow_n = \sigma\downarrow_1$ holds.
Let $x > 1$ which implies $x_{\mathrm{rot}} \neq n$. Let X be an r-subset of $[n-1]$ and let X^* be an r-subset of $[n]$ with $x_{\mathrm{rot}} \notin X^*$ and $X^*\downarrow_{x_{\mathrm{rot}}} = X$. We obtain

$$\sigma_{\mathrm{rot}}\downarrow_{x_{\mathrm{rot}}} (X) = \sigma_{\mathrm{rot}}\downarrow_{x_{\mathrm{rot}}} (X^*\downarrow_{x_{\mathrm{rot}}}) = \sigma_{\mathrm{rot}}(X^*).$$

We will now rewrite the term to get the statement. Since $x_{\mathrm{rot}} \notin X^*$, we have $x \notin (X^*)_{\mathrm{rot}(-1)}$. It is

$$\begin{aligned}\sigma_{\mathrm{rot}}\downarrow_{x_{\mathrm{rot}}} (X) = \sigma_{\mathrm{rot}}(X^*) &= s \cdot \sigma\left((X^*)_{\mathrm{rot}(-1)}\right) = s \cdot \sigma\downarrow_x \left(\left((X^*)_{\mathrm{rot}(-1)}\right)\downarrow_x\right) \\ &= s \cdot \sigma\downarrow_x \left((X^*\downarrow_{x_{\mathrm{rot}}})_{\mathrm{rot}(-1)}\right) = s \cdot \sigma\downarrow_x \left(X_{\mathrm{rot}(-1)}\right) = (\sigma\downarrow_x)_{\mathrm{rot}}(X),\end{aligned}$$

where the sign $s = +$ (respectively $s = -$) if $n \notin X^*$ (resp. $n \in X^*$). Note that $n \in X^*$ is equivalent to $1 \in X_{\mathrm{rot}(-1)}$ for $x \neq 1$. □

With Proposition 3.2.1, Proposition 3.4.3 and Lemma 3.4.4 we are now ready to prove Theorem 3.1.2.

3.4.1 Extension Theorem for Odd Rank (Theorem 3.1.2)

For convenience we restate the theorem.

Theorem 3.1.2 (Extension theorem for signotopes of odd rank)**.** *For every odd rank $r \geq 3$, every r-signotope is 2-extendable.*

Proof. Let σ be an r-signotope on $[n]$ and let I, J be a pair of disjoint $(r-1)$-subsets. By Proposition 3.4.3 there exists $k \in \{0, \dots, n-1\}$ such that the k-fold rotated $(r-1)$-subsets $I_{\mathrm{rot}(k)}$, $J_{\mathrm{rot}(k)}$ are incomparable in the k-fold rotated signotope $\sigma_{\mathrm{rot}(k)}$.
To extend the signotope $\sigma_{\mathrm{rot}(k)}$, we use the down-set $\mathcal{D}$ consisting of $I_{\mathrm{rot}(k)}$, $J_{\mathrm{rot}(k)}$, and all $(r-1)$-subsets which are smaller in $\prec_{\mathrm{rot}(k)}$. In this down-set $I_{\mathrm{rot}(k)}$ and $J_{\mathrm{rot}(k)}$ are maximal elements since they are incomparable. Hence we can apply Proposition 3.2.1 in order to add a new element at position $n+1$ in the rotated signotope $\sigma_{\mathrm{rot}(k)}$ such that $I_{\mathrm{rot}(k)} \cup \{n+1\}$ and $J_{\mathrm{rot}(k)} \cup \{n+1\}$ are fliples. Let $\sigma^*_{\mathrm{rot}(k)}$ denote the extended signotope with $\sigma^*_{\mathrm{rot}(k)}{\downarrow_{n+1}} = \sigma_{\mathrm{rot}(k)}$.
For an illustration of the considered signotopes, see Figure 3.6.

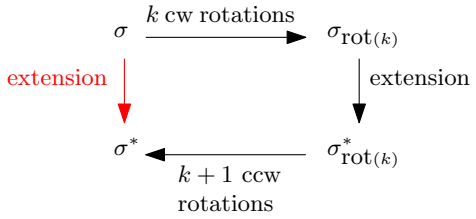

Figure 3.6: Illustration of the connections between the considered signotopes in the proof of Theorem 3.1.2. The red arc is the conclusion of the statement.

Finally, we need to find a rotation of $\sigma^*_{\mathrm{rot}(k)}$ which contains the original signotope σ. For this we perform $k+1$ counterclockwise rotations (or equivalently, $2n+1-k$ clockwise rotations) and denote the so-obtained signotope by σ^*. Note that we perform $k+1$ counterclockwise rotations since the newly added element needs to be rotated and the k-fold clockwise rotation needs to be undone.
After the first counterclockwise rotation, the added element $n+1$ in $\sigma^*_{\mathrm{rot}(k)}$ becomes the first element 1 in $(\sigma^*_{\mathrm{rot}(k)})_{\mathrm{rot}(-1)}$. By Lemma 3.4.4 it holds $((\sigma^*_{\mathrm{rot}(k)})_{\mathrm{rot}(-1)}){\downarrow_1} = (\sigma^*_{\mathrm{rot}(k)}){\downarrow_{n+1}} = \sigma_{\mathrm{rot}(k)}$.
After additional k counterclockwise rotations, the added element $n+1$ in $\sigma^*_{\mathrm{rot}(k)}$ becomes the element $k+1$ in σ^*.
Furthermore, the fliples $I_{\mathrm{rot}(k)} \cup \{n+1\}$ and $J_{\mathrm{rot}(k)} \cup \{n+1\}$ of σ^*_{rot} correspond to the fliples $I \cup \{k+1\}$ and $J \cup \{k+1\}$ in σ^* (cf. Lemma 3.3.2). When handling the rotation of those sets, we need to be careful since the number of elements changed which affects the rotation operator. Since we do not rotate the extending element, the second part of Lemma 3.4.4 applied multiple times shows $((\sigma^*_{\mathrm{rot}(k)})_{\mathrm{rot}(-1)}){\downarrow_1} = (\sigma^*{\downarrow_{k+1}})_{\mathrm{rot}(k)}$. Together with the previous equation this shows $\sigma_{\mathrm{rot}(k)} = (\sigma^*{\downarrow_{k+1}})_{\mathrm{rot}(k)}$, which further implies $\sigma = \sigma^*{\downarrow_{k+1}}$. Hence we obtain the signotope σ when deleting $k+1$ from σ^*, which shows that σ^* is an extension of σ. □

3.4.2 Extendability with Intersection (Corollary 3.1.3)

Corollary 3.1.3. *For $r \geq 3$, let σ be an r-signotope on $[n]$, and I, $J \subseteq [n]$ two $(r-1)$-subsets such that $|I \cap J| + r$ is odd. Then σ is extendable to an r-signotope σ^* on $[n+1]$ with fliples I^*, J^* and an extending element $k \in [n+1]$ such that $\sigma^*{\downarrow_k} = \sigma$, and $I^*{\downarrow_k} = I$, and $J^*{\downarrow_k} = J$.*

Proof. To prove Corollary 3.1.3, we proceed similar as in the proof of Theorem 3.1.2. By Proposition 3.2.1, it suffices to show that after some rotations the $(r-1)$-subsets corresponding to I and J are incomparable.
Let $m = |I \cap J|$. Since Theorem 3.1.2 covers the case $m = 0$, we may assume $m \geq 1$. We consider the following two cases.
First, assume that r is odd and m is even. For odd rank r, we have already seen that after n rotations, the signotope is reversed and hence the corresponding partial order is reversed. For even m, the relation between I and J is reversed m times whenever we rotate one element $x \in I \cap J$, see Lemma 3.4.2. If we rotate an element $x \notin I \cap J$, the relation cannot be reversed, see Proposition 3.4.1. Hence the relation is reversed exactly m times in one single rotation. Since m is even and the order is reversed after n rotations, the corresponding $(r-1)$-subsets must be incomparable in between.
If r is even and m is odd, the n-fold rotation leaves the signotope unchanged and hence the partial order is the same. Since m is odd, we reverse the orientation of I and J exactly m times in a single rotation step. Hence they must be incomparable in between. The statement now follows from Proposition 3.2.1 and Lemma 3.4.4 similar as in the proof in Section 3.4.1. □

3.4.3 Non-Extendability with Intersection (Proposition 3.1.5)

Proposition 3.1.5. *Let σ be an r-signotope on $[n]$ which is* not *2-extendable through the two disjoint $(r-1)$-subsets I, J. For every $m \in \mathbb{N}$, there exists an r'-signotope σ' on $[n']$ with $r' = r + m$ and $n' = n + m$ and two $(r'-1)$-subsets I', J' of $[n']$ with $|I' \cap J'| = m$ such that*

$$\sigma' \downdownarrows_{I' \cap J'} = \sigma, \quad I'{\downarrow_{I' \cap J'}} = I \quad \text{and} \quad J'{\downarrow_{I' \cap J'}} = J.$$

Moreover, there is no extending r'-signotope σ^* of σ' on $[n'+1]$ with fliples I^*, J^* such that there is a $k \in [n+1]$ with $\sigma^*{\downarrow_k} = \sigma'$, $I^*{\downarrow_k} = I'$, and $J^*{\downarrow_k} = J'$.

Proof. In a first step, assume there is an extension σ^* of σ' on $[n'+1]$ with fliples I^*, J^* and an extending element $k \in [n+1]$ such that $\sigma^*{\downarrow_k} = \sigma'$, $I^*{\downarrow_k} = I'$, and $J^*{\downarrow_k} = J'$. Let k' be the label of k after deleting $I' \cap J'$. Clearly, $(I^*{\downarrow_{I' \cap J'}}){\downarrow_{k'}} = (I^*{\downarrow_k}){\downarrow_{I' \cap J'}} = I'{\downarrow_{I' \cap J'}} = I$ and analogously for J^* and σ^*. Moreover, I^* and J^* are fliples of σ^* which implies by Observation 3.1.4 that $I^*{\downarrow_{I' \cap J'}}$ and $J^*{\downarrow_{I' \cap J'}}$ are fliples in the projection $\sigma^* \downdownarrows_{I' \cap J'}$. This shows that $\sigma^* \downdownarrows_{I' \cap J'}$ is an extension of σ by the element k' such that $I \cup \{k'\}$ and $J \cup \{k'\}$ are fliples. A contradiction to the assumption that σ is not 2-extendable.
To show that such an signotope σ' exists, we construct a signotope by reversing the projection. For this we add the new m elements at the last position $n+1, \ldots, n' = n+m$. For r'-subsets X which contain all new elements, the sign is given by the sign of $X{\downarrow_{\{n+1,\ldots,n'\}}}$ in σ. For the remaining r'-subsets we have to assign them in a different manner. For this, consider the case $m = 1$. By repeating the following construction m times, the case $m \geq 2$ is solved.
Let C be a maximum chain $\sigma_0 \prec \ldots \prec \sigma_{\binom{n}{r}}$ of r-signotopes containing $\sigma = \sigma_i$ for an $i \in \{0, \ldots, \binom{n}{r}\}$ which exists by Theorem 2.2.11. Moreover σ_0 is the constant $-$ function and $\sigma_{\binom{n}{r}}$

the constant + function. From σ_j to σ_{j+1} there is exactly one r-subset flipped from $-$ to $+$. Let $A_1, \ldots, A_{\binom{n}{r}}$ be the order of flipped subsets. Hence in $\sigma = \sigma_i$ all r-subset $A_1, \ldots, A_i$ are mapped to $+$ and the remaining $A_{i+1}, \ldots, A_{\binom{n}{r}}$ are $-$, i.e.,

$$\sigma(A_j) = \begin{cases} + & \text{if } j \leq i; \\ - & \text{if } j > i. \end{cases}$$

Again by Theorem 2.2.11, there is an $(r+1)$-signotope σ_C on $[n]$ corresponding to the maximum chain C for which $A_1, \ldots, A_{\binom{n}{r}}$ is a sweep. In particular the order is a linear extension of the partial order $\prec_C$ corresponding to σ_C. This shows that for an $(r+1)$-subset X and some $1 \leq j < \ell \leq r+1$

$$\sigma_C(X) = \begin{cases} + & \text{if } X_j \succ_C X_\ell; \\ - & \text{if } X_j \prec_C X_\ell. \end{cases}$$

Note that by the properties of a signotope, the choice of j and ℓ is irrelevant. Using σ_C, we define σ' as $(r+1)$-signotope on $[n+1]$ elements as follows:

$$\sigma'(X) := \begin{cases} \sigma_C(X) & \text{if } X \subseteq [n]; \\ \sigma(A_j) & \text{if } n+1 \in X \text{ and } X \backslash \{n+1\} = A_j. \end{cases}$$

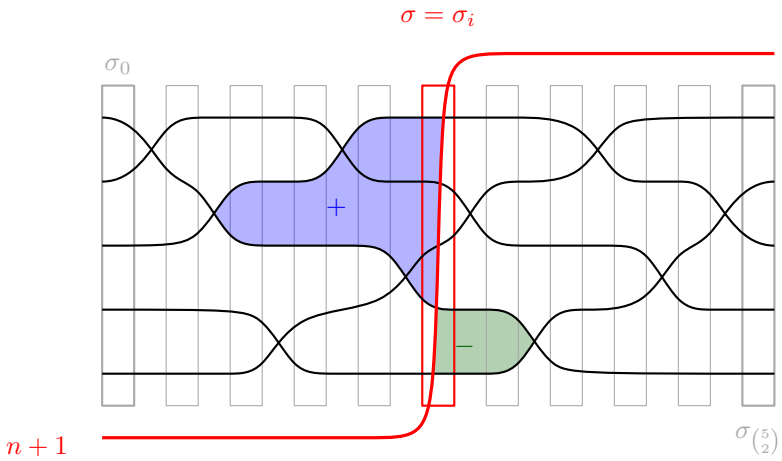

Figure 3.7: Illustration of the construction. The assignment for the 3-signotope depends on the maximum chain of permutations. The 3-signotope projected to $n+1$ (red) yields the starting 2-signotope σ.

Clearly $\sigma' \downdownarrows_{n+1} = \sigma$. To see that σ' is indeed a signotope and fulfills the monotonicity condition, we check all $(r+2)$-subsets P of $[n+1]$. For the illustration of the case $r = 2$, see Figure 3.7. If P does not contain $n+1$, then the packet is monotone because σ_C is a signotope. If $n+1 \in P$, then $n+1 \in P_j$ for all $j = 1, \ldots, r+1$ and $n+1 \notin P_{r+2}$. Since σ is an r-signotope on $[n]$ in the first $r+1$ signs there is at most one sign change. Deleting another element of P_{r+2} yields an r-subset which is one of the A_j. Let $P_1 = A_j \cup \{n+1\}$ and $P_{r+1} = A_\ell \cup \{n+1\}$. This implies that A_j is lexicographically larger than A_ℓ.

First assume $j > \ell$, i.e., $A_j \succ A_\ell$. Since A_j is lexicographically larger than A_ℓ, it is $\sigma'(P_{r+2}) = \sigma_C(A_j \cup A_\ell) = +$. If moreover $\ell > i$, then $j > i$ and $\sigma'(P_1) = \sigma(A_j) = -$, $\sigma'(P_{r+1}) = \sigma(A_\ell) = -$. Hence there is only one sign change which is between P_{r+1} and P_{r+2}. If $\ell < i$, then $\sigma'(P_{r+1}) = \sigma(A_\ell) = +$. This shows that there is at most one sign change between P_1 and P_{r+1}.
If $j < \ell$. This implies $\sigma'(P_{r+2}) = \sigma_C(A_j \cup A_\ell) = -$. If $\ell < i$, then $j < i$ and $\sigma'(P_1) = \sigma(A_j) = +$, $\sigma'(P_{r+1}) = \sigma(A_\ell) = +$. Hence there is only one sign change between P_{r+1} and P_{r+2}. If $\ell > i$, then $\sigma'(P_{r+1}) = \sigma(A_\ell) = -$. This shows that there is at most one sign change between P_1 and P_{r+1}. This completes the proof that σ' is an $(r+1)$-signotope on $n+1$ elements. □

3.5 Technical Lemmata

In this section, we proof Proposition 3.4.1 which implies that two disjoint $(r-1)$-subsets cannot be reversed in a single rotation. In Lemma 3.4.2, we showed that the relation between two $(r-1)$-subsets, which share $r-2$ elements, is reversed if and only if the intersection contains the rotated element. Since those $(r-1)$-subsets are directly in relation and hence not incomparable, the orientation stays the same if the rotated element is not contained in the intersection.
For this, we introduce the following two partitions of the family of all $(r-1)$-subsets. With respect to the first element 1, we partition the $(r-1)$-subsets $\binom{[n]}{r-1}$ into the following three sets:

$$\begin{aligned}
\mathcal{H}_1^\sigma &= \{\ I \subset [n] : |I| = r-1,\ 1 \in I\ \};\\
\mathcal{U}_1^\sigma &= \{\ I \subset [n] : |I| = r-1,\ 1 \notin I,\ \sigma(I \cup \{1\}) = +\ \};\\
\mathcal{D}_1^\sigma &= \{\ I \subset [n] : |I| = r-1,\ 1 \notin I,\ \sigma(I \cup \{1\}) = -\ \}.
\end{aligned}$$

Similarly, with respect to the last element n, we partition $\binom{[n]}{r-1}$ into the following three sets:

$$\begin{aligned}
\mathcal{H}_n^\sigma &= \{\ I \subset [n] : |I| = r-1,\ n \in I\ \};\\
\mathcal{U}_n^\sigma &= \{\ I \subset [n] : |I| = r-1,\ n \notin I,\ \sigma(I \cup \{n\}) = -\ \};\\
\mathcal{D}_n^\sigma &= \{\ I \subset [n] : |I| = r-1,\ n \notin I,\ \sigma(I \cup \{n\}) = +\ \}.
\end{aligned}$$

We want to emphasize the sign change in the definition, that is, every $I \in \mathcal{U}_1^\sigma$ has the sign $\sigma(I \cup \{1\}) = +$ while every $I \in \mathcal{U}_n^\sigma$ fulfills $\sigma(I \cup \{n\}) = -$.

Lemma 3.5.1. *$\mathcal{U}_1^\sigma$ and $\mathcal{U}_n^\sigma$ are up-sets and $\mathcal{D}_1^\sigma$ and $\mathcal{D}_n^\sigma$ are down-sets of the partial order $\prec$ corresponding to the r-signotope σ.*

Proof. In the following we show that $\mathcal{U}_1^\sigma$ is an up-set. Analogous arguments show that $\mathcal{U}_n^\sigma$ is an up-set and that $\mathcal{D}_1^\sigma$ and $\mathcal{D}_n^\sigma$ are down-sets. Let I be an element of $\mathcal{U}_1^\sigma$. By definition, it is $1 \notin I$ and $\sigma(I \cup \{1\}) = +$. Let J be an $(r-1)$-subset with $J \succ I$.
If the intersection $I \cap J$ contains $r-2$ elements, we cannot have $1 \in J$, as otherwise J was lexicographic smaller than I, which implies with the assumption $J \succ I$

$$- = \sigma(I \cup J) = \sigma(I \cup \{1\}) = +,$$

a contradiction. Therefore, $1 \notin J$ and we have $r+1$ elements in $I \cup J \cup \{1\}$. If I is lexicographic smaller than J, then the following sets are sorted in decreasing lexicographic order $I \cup J$, $J \cup \{1\}$, $I \cup \{1\}$ which corresponds to the order in the $(r+1)$-packet $I \cup J \cup \{1\}$. Since we have

$\sigma(I \cup \{1\}) = +$ by assumption and $\sigma(I \cup J) = +$ because $J \succ I$, it follows $\sigma(J \cup \{1\}) = +$. Hence $J \in \mathcal{U}_1^\sigma$.
In the other case, if J is lexicographical smaller than I, we have the following decreasing order with respect to the lexicographical order $I \cup J$, $I \cup \{1\}$, $J \cup \{1\}$. Since we have $\sigma(I \cup \{1\}) = +$ and $\sigma(I \cup J) = -$, it follows $\sigma(J \cup \{1\}) = +$ and hence again $J \in \mathcal{U}_1^\sigma$.
If the intersection $I \cap J$ contains less than $r-2$ elements, we proceed by induction. There is a chain $I = I_1 \prec I_2 \prec \ldots \prec I_k = J$ such that any two consecutive I_i have an intersection of $r-2$ elements. For $i = 2, \ldots, k$, since $I_{i-1} \in \mathcal{U}_1^\sigma$, we conclude that $I_i \in \mathcal{U}_1^\sigma$, and in particular, $J \in \mathcal{U}_1^\sigma$. This completes the proof that $\mathcal{U}_1^\sigma$ is an up-set. □

We now study the effect of a clockwise rotation to the partial order. In the partial order $\prec_{\mathrm{rot}}$ corresponding to the rotated signotope σ_{rot}, the sets $(\mathcal{U}_1^\sigma)_{\mathrm{rot}}$ and $(\mathcal{D}_1^\sigma)_{\mathrm{rot}}$ remain up-set and down-set, respectively. Here $\mathcal{X}_{\mathrm{rot}} = \{X_{\mathrm{rot}} \colon X \in \mathcal{X}\}$ denotes the clockwise rotated sets of a set-system $\mathcal{X}$.

Lemma 3.5.2. *It holds* $(\mathcal{H}_1^\sigma)_{\mathrm{rot}} = \mathcal{H}_n^{\sigma_{\mathrm{rot}}}$, $(\mathcal{U}_1^\sigma)_{\mathrm{rot}} = \mathcal{U}_n^{\sigma_{\mathrm{rot}}}$, *and* $(\mathcal{D}_1^\sigma)_{\mathrm{rot}} = \mathcal{D}_n^{\sigma_{\mathrm{rot}}}$.

Proof. An $(r-1)$-subset I contains the first element 1 if and only if its clockwise rotation I_{rot} contains the last element n. Therefore, we have

$$(\mathcal{H}_1^\sigma)_{\mathrm{rot}} = \mathcal{H}_n^{\sigma_{\mathrm{rot}}} \text{ and } (\mathcal{U}_1^\sigma \cup \mathcal{D}_1^\sigma)_{\mathrm{rot}} = \mathcal{U}_n^{\sigma_{\mathrm{rot}}} \cup \mathcal{D}_n^{\sigma_{\mathrm{rot}}}.$$

To show $(\mathcal{U}_1^\sigma)_{\mathrm{rot}} = \mathcal{U}_n^{\sigma_{\mathrm{rot}}}$ and $(\mathcal{D}_1^\sigma)_{\mathrm{rot}} = \mathcal{D}_n^{\sigma_{\mathrm{rot}}}$, it suffices to prove the two subset relations $(\mathcal{U}_1^\sigma)_{\mathrm{rot}} \subseteq \mathcal{U}_n^{\sigma_{\mathrm{rot}}}$ and $(\mathcal{D}_1^\sigma)_{\mathrm{rot}} \subseteq \mathcal{D}_n^{\sigma_{\mathrm{rot}}}$.
For the first subset relation $(\mathcal{U}_1^\sigma)_{\mathrm{rot}} \subseteq \mathcal{U}_n^{\sigma_{\mathrm{rot}}}$, let $I \in \mathcal{U}_1^\sigma$, i.e., $\sigma(I \cup \{1\}) = +$. After rotating the element 1, we obtain

$$+ = \sigma(I \cup \{1\}) = -\sigma_{\mathrm{rot}}((I \cup \{1\})_{\mathrm{rot}}).$$

Hence $\sigma_{\mathrm{rot}}(I_{\mathrm{rot}} \cup \{n\}) = -$ which implies $I_{\mathrm{rot}} \in \mathcal{U}_n^{\sigma_{\mathrm{rot}}}$. An analogous argument shows $(\mathcal{D}_1^\sigma)_{\mathrm{rot}} \subseteq \mathcal{D}_n^{\sigma_{\mathrm{rot}}}$. □

It is worth noting that for $I, J \in \mathcal{H}_1^\sigma$ (i.e., $1 \in I \cap J$) with $I \prec J$ Lemma 3.5.1 implies that any chain $I = I_1 \prec \ldots \prec I_k = J$ lies entirely in $\mathcal{H}_1^\sigma$ (i.e. $I_1, \ldots, I_k \in \mathcal{H}_1^\sigma$). Since a clockwise rotation converts comparability of elements containing the element 1, we have $I_{\mathrm{rot}} = (I_1)_{\mathrm{rot}} \succ_{\mathrm{rot}} \ldots \succ_{\mathrm{rot}} (I_k)_{\mathrm{rot}} = J_{\mathrm{rot}}$.
With the above lemmas, we can now prove Proposition 3.4.1.

Proposition 3.4.1. *Let σ be an r-signotope on $[n]$ with partial order $\prec$. For two $(r-1)$-subsets I, J with $I \prec J$ and $1 \notin I \cap J$, it holds $I_{\mathrm{rot}} \| _{\mathrm{rot}} J_{\mathrm{rot}}$ or $I_{\mathrm{rot}} \prec_{\mathrm{rot}} J_{\mathrm{rot}}$.*

Proof. Assume towards a contradiction that I, J are two $(r-1)$-subsets with $I \prec J$ and $I_{\mathrm{rot}} \succ_{\mathrm{rot}} J_{\mathrm{rot}}$.
If $I \in \mathcal{U}_1^\sigma$, then by Lemma 3.5.1, $J \in \mathcal{U}_1^\sigma$. If $I \in \mathcal{D}_1^\sigma$, then by Lemma 3.5.2, $I_{\mathrm{rot}} \in \mathcal{D}_n^{\sigma_{\mathrm{rot}}}$ and by Lemma 3.5.1 and the assumption that $I_{\mathrm{rot}} \succ_{\mathrm{rot}} J_{\mathrm{rot}}$ it is $J_{\mathrm{rot}} \in \mathcal{D}_n^{\sigma_{\mathrm{rot}}}$. Applying Lemma 3.5.2 again yields $J \in \mathcal{D}_1^\sigma$. Analogous arguments show that, if $J \in \mathcal{D}_1^\sigma$ (resp. $J \in \mathcal{U}_1^\sigma$), then $I \in \mathcal{D}_1^\sigma$ (resp. $I \in \mathcal{U}_1^\sigma$).
Since $1 \notin I \cap J$ not both I and J can be in $\mathcal{H}_1^\sigma$. Hence I and J are both in $\mathcal{D}_1^\sigma$ or both in $\mathcal{U}_1^\sigma$. Since $I \prec J$, there is a chain $I = I_1 \prec \ldots \prec I_k = J$. By Lemma 3.5.1 it is $I_1, \ldots, I_k \in \mathcal{D}_1^\sigma$ (resp. $\mathcal{U}_1^\sigma$). After a clockwise rotation, we have $(I_1)_{\mathrm{rot}}, \ldots, (I_k)_{\mathrm{rot}} \in \mathcal{D}_n^{\sigma_{\mathrm{rot}}}$ (resp. $\mathcal{U}_n^{\sigma_{\mathrm{rot}}}$) and hence $I_{\mathrm{rot}} = (I_1)_{\mathrm{rot}} \prec_{\mathrm{rot}} \ldots \prec_{\mathrm{rot}} (I_k)_{\mathrm{rot}} = J_{\mathrm{rot}}$, which is a contradiction to $I_{\mathrm{rot}} \succ_{\mathrm{rot}} J_{\mathrm{rot}}$. □

3.6 Non-2-Extendable Examples for Even Rank

Since the proof for the extension theorem (Theorem 3.1.2) applies only for odd ranks, we had to investigate even ranks in a different manner. For even rank signotopes, rotating every element once yields the same signotope. Hence two $(r-1)$-subsets are generally not incomparable in any rotation.
To study extendability in rank 4, we used computer assistance to enumerate all signotopes and then tested each of the signotopes for 2-extendability. On 6 and 7 elements all 4-signotopes are 2-extendable. On 8 elements we found non-2-extendable 4-signotopes.
Using this two-level-SAT approach we managed to find the first examples of 4-signotopes which are not 2-extendable. Among the non-extendable rank 4 examples on 8 elements, we discovered some with high symmetries and nice properties. Those examples have a similar structure as the example of Richter-Gebert in the context of extendability in oriented matroids [Ric93] even though the non-extendable oriented matroid by Richter-Gebert has no sorting of the element such that it is a signotope. The common property is the following: There are two disjoint simplicial cells (i.e. fliples, respectively mutations) such that the choice of each of the crossing points for both simplicial cells witnesses the non-extendability. In fact, we constructed the signotope examples in such a way that those simplicial cells are built by the odd and even elements, respectively. For such examples it is sufficient to check two $(r-1)$-subsets I, J to verify the non-2-extendability. This is a speed up for the extendability-test by a factor of $\Theta(r^2)$ since not all pairs of $(r-1)$-subsets I, J need to be tested.
In order to keep symmetries and similarities of our nicely structured example of rank 4, we restricted our search space to examples in rank r on $2r$ elements. While for rank 4 all signotopes on 8 elements can be enumerated within a few seconds, the complete enumeration in higher ranks is unpractical as the number of r-signotopes on $2r$ elements grows faster than doubly exponential in r (cf. Proposition 2.2.14). Hence, to be able to approach higher ranks, we further analyzed the structure of our non-2-extendable rank 4 examples together with an analysis of the already found rank 6 examples. In Section 3.6.1 we give a brief summary of the SAT framework and explain how we encode signotopes.
With the observed properties as additional constraints, we further restricted the search space. Under these restrictions, we managed to find examples for rank 6, 8, 10, and 12 which are not 2-extendable, which we describe in Section 3.6.2. Investigating those properties, we can prove non-extendability, see Section 3.6.3. With this proof of non-extendability, we do not need the second SAT instance to test extendability. It remains to find signotopes with the specified properties. The existence of non-extendable examples for even $r \geq 14$ remains open.

3.6.1 SAT Encoding

We give a short description of the encoding of r-signotopes on n elements in terms of a SAT instance. Such an instance consists of a Boolean formula which has a valid assignment if and only if there is a signotope with the specified properties. In particular we model the instance with a Boolean formula in *conjunctive normal form* (short: CNF), which is a conjunction of clauses. Each *clause* is a disjunction of variables and their negation (called literals). We then use state-of-the-art SAT solvers such as CaDiCaL [Bie19] to decide whether a solution exists.
To model a signotopes σ on $[n]$ and its fliples as a CNF formula, we define Boolean variables S_X for every r-subset $X \in \binom{[n]}{r}$ and interpret the value $\sigma(X) = +$ as $S_X = \textsc{True}$ and $\sigma(X) = -$

as $S_X = \text{FALSE}$. Moreover, we have to ensure the monotonicity on $(r+1)$-packets. For this we list all possibilities of valid sign sequences, i.e., sign sequences of length $r+1$ with only one sign change. There are exactly $2r+2$ possible assignment of this sequence. Let $\mathcal{T}$ be the list of all those types. To encode which packet corresponds to which sequence and to ensure that every packet has exactly one of the sequences, we introduce auxiliary variables $T_{P,t}$ for every $P \in \binom{[n]}{r+1}$ and $t \in \mathcal{T}$ which we synchronize with the values of the corresponding r-subsets. Let $t(i)$ be the sign of t at position i. For $t(i) = -$ and a Boolean variable X we say $t(i) \cdot X$ is $\neg X$. Moreover, if $t(i) = +$, then $t(i) \cdot X$ is X. The variable $T_{P,t}$ is TRUE if and only if the sign sequence of the $(r+1)$-packet P is the same as the sign sequence $t \in \mathcal{T}$. In particular $T_{P,t} \Leftrightarrow \bigwedge_{j=1,\dots,r+1} t(j) \cdot S_{P_j}$. For the CNF we have to add the clauses

$$\neg T_{P,t} \ \vee \ t(j) \cdot S_{P_j} \text{ for all } j = 1, \dots, r+1; \text{ and}$$
$$T_{P,t} \ \vee \bigvee_{j=1,\dots,r+1} \neg\, t(j) \cdot S_{P_j}.$$

Note that the first direction of the implication is modeled by the $r+1$ clauses while the reverse direction is modeled by the clause in the second line.
An important part of the extendability are fliples. In a first step we define variables $F_{X,P}$ for every $(r+1)$-packet $P \in \binom{[n]}{r+1}$ and every r-subset $X \in \binom{P}{r}$ to indicate whether X is a fliple when σ is restricted to P. If $F_{X,P} = \text{TRUE}$, the r-subset X is flipable in the packet P, i.e., is next to a sign change or at the beginning, respectively end, of a constant sign sequence. The information about the sign change is already encoded in $T_{P,t}$. Assume X is at position $j \in \{1, \dots, r+1\}$ of the packet P. Then X is flipable in P if and only if the sign sequence t of P has the sign change between position $j-1$ and j or between position j and $j+1$. For this let $\mathcal{T}_j$ be the set of sign sequences such that the j'th sign can be flipped without violating the monotonicity condition. Now it is $F_{X,P} \Leftrightarrow \bigvee_{t \in \mathcal{T}_j} T_{P,t}$. Hence for the CNF, we add the clauses

$$\neg F_{X,P} \vee \bigvee_{t \in \mathcal{T}_j} T_{P,t}; \text{ and}$$
$$F_{X,P} \vee \neg T_{P,t} \ \text{ for all } t \in \mathcal{T}_j.$$

Using the $F_{X,P}$ variables, we can assert the variables $F_X = \bigwedge_{P \in \binom{[n]}{r+1} :\, X \subset P} F_{X,P}$ for every $X \in \binom{[n]}{r}$ to indicate whether X forms a fliple in the signotope. Again we add the following clauses to the CNF

$$\neg F_X \vee F_{X,P} \text{ for all } P \supset X; \text{ and}$$
$$F_X \vee \bigvee_{P \supset X} \neg F_{X,P}.$$

For more details the supplemental code see [BFS23a].[2]

3.6.2 Structure of the Examples supporting Conjecture 3.1

For the first witnessing examples of Conjecture 3.1 in rank 4, we used a two-step SAT approach. To make investigations in higher ranks, we had to get a better understanding of the examples

[2] `https://github.com/manfredscheucher/supplemental-signotope-extension`

found in rank 4. Hence we filtered those with regularities and symmetries to come up with a generalization of the observed properties and analyzed their structure.
One of the first and crucial observations was that there exist signotopes such that for every choice of $r-1$ even indices $I \subset E_r := \{2, 4, \ldots, 2r\}$ and every choice of $r-1$ odd indices $J \subset O_r := \{1, 3, \ldots, 2r-1\}$ there is no extension.
While we came up with further observations one by one over the time, we give a summary of all properties, which we desire from the examples in rank r with $n = 2r$ elements. Let $X = (x_1, x_2, \ldots, x_r)$ be an r-subset.

(a) $\sigma = \sigma_{\mathrm{rot}(4)}$.

(b) $\sigma(2, 4, \ldots, 2r) = -$ and $\sigma(1, 3, \ldots, 2r-1) = +$.

(c) If the r-subset X contains exactly one even element of E_r, respectively only one odd element of O_r, then the sign $\sigma(X)$ depends only on the position of that element in the increasing order of the elements of X. More specifically:
- If $e = x_i \in E_r$ is the only even element in X, then $\sigma(X) = (-)^i$.
- If $o = x_i \in O_r$ is the only odd element in X, then it is $\sigma(X) = (-)^{i+1}$.

(d) If $x_1, \ldots, x_i \in E_r$ and $x_{i+1}, \ldots, x_r \in O_r$ with $2 \leq i \leq r-2$, then $\sigma(X) = (-)^{i+1}$.

(e) Let $x_1, \ldots, x_i \in O_r$ and $x_{i+1}, \ldots, x_r \in E_r$ for $2 \leq i < r-2$.
- If $x_r < 2r$, then $\sigma(X) = -$.
- If $x_j = 2j$ for all $j = i+1, \ldots, r$, then $\sigma(X) = +$.

Furthermore, we fix the following set of 8 fliples for rank 4.

$$F_4 = \{(1,3,5,7), (2,4,6,8), (2,3,7,8), (1,3,4,8), \\ (1,2,4,7), (3,5,6,8), (4,5,7,8), (3,4,6,7)\}$$

Together with the *4-fold symmetry*, see Property (a), it is sufficient to mention only some of them:

$$\widehat{F}_4 = \{(1,3,5,7), (2,4,6,8), (4,5,7,8), (3,4,6,7), (1,2,4,7)\}$$

In rank 4, there are only four signs which are not determined by the above properties:

$$(1,3,4,8), \qquad (4,5,7,8), \qquad (2,3,7,8), \qquad (3,4,6,7)$$

By the 4-fold symmetry, the assignment of $(1,3,4,8)$ also determines the sign of $(4,5,7,8)$, and vice versa. The third and fourth subset have a similar interaction. Hence, there are precisely 4 signotopes in rank 4 which fulfill the above properties. We fix the configuration where all four undetermined signs are $-$ and refer to it as σ_4 in the following. However, the choice does not play a role. For higher rank, there are several signs undetermined by the above properties. Except a set of prescribed fliples, our aim was to find a relation between examples in different ranks, for example using projection and deletion arguments. For this we investigated the structure of our rank 4 examples together with some already found rank 6 examples. We found the following correlation.

(f) For $r \geq 6$, let σ_{r-2} be an example of rank $r-2$ on $2r-4$ elements. For an r-subset $X \subseteq [2r]$ with $1, 3 \notin X$ and $2, 4 \in X$, we define the sign

$$\sigma_r(X) = \sigma_{r-2}(X{\downarrow_{\{1,2,3,4\}}}).$$

Note that $X{\downarrow_{\{1,2,3,4\}}}$ is obtained by deleting the elements 2 and 4 from X and a further index shift by -2 caused by deleting 1 and 3, which are not contained in X. In other words, σ_{r-2} is obtained from σ_r by a projection to $1, 3$ and a deletion of $2, 4$.

If we start with one example in rank 4 and recursively construct examples in higher ranks with the desired properties and further prescribe an exact set of $(r/2)^2 + (r/2) + 4$ fliples for rank r, it finally turned out that there is a unique example in each of the ranks $r = 6, 8, 10, 12$. The description of the fliples are provided in the paragraph "Higher Ranks". All examples and the source code to verify their correctness are available at the supplemental data of [BFS23a]. Note that even though E_r and O_r are fliples of the defined signotopes, changing the sign of one of them yields a signotope with different properties. In particular for $r = 4$ the signotope becomes 2-extendable. The set of even elements E_r and the set of odd elements O_r are fliples are always contained among the prescribed fliples, which follows from property (c).

Rank 4

We explicitly give the rank 4 example and give a visualization as pseudohyperplane arrangement. We fix σ_4 as the examples, which is not 2-extendable and has the properties (a)–(f). For this example we map the four subsets, which are not determined yet, to $-$. Representing the signotope with a string of its signs in reversed lexicographic order of its 4-subsets, the complete signotope has the signs

$$\sigma_4 = +++--+++-++-+++++--+--++--------- \\ +++-++-+++++-+++---+-+-++++-+-++++.$$

The representation of σ_4 is given as supplemental data as 3-dimensional object[3]. This is generated using a SageMath program which computes the sweep of the signotope and for every rank 3 signotope a wiring diagram of fixed length. In particular, there is only one crossing at a time in the wiring diagram. This helps to make the boundaries of the 3-dimensional visualization nice. A projection to 2 dimensions is given in Figure 3.8. The single wiring diagrams are given as in Figure 3.9 with the same colors assigned to the elements. We start with the reversed cyclic arrangement at the top left position and then continue line by line until we reach the cyclic arrangement. In each step we highlight the triangular cells, which are flipped either from the previous arrangement or to the following arrangement been flipped.

[3] https://helenabergold.github.io/supp/3d_signotopes/nonextendable_sign48_pshyperplane.html

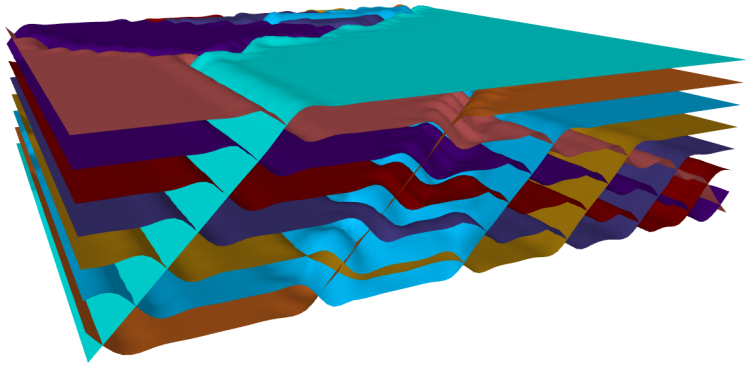

Figure 3.8: A projection of the 3-dimensional pseudohyperplane arrangement of σ_4. In the front, we start with the reversed cyclic arrangement. The odd elements $1, 3, 5, 7$ have a color from the red color family, whereas, the even elements $2, 4, 6, 8$ are colored with shades of blue and purple.

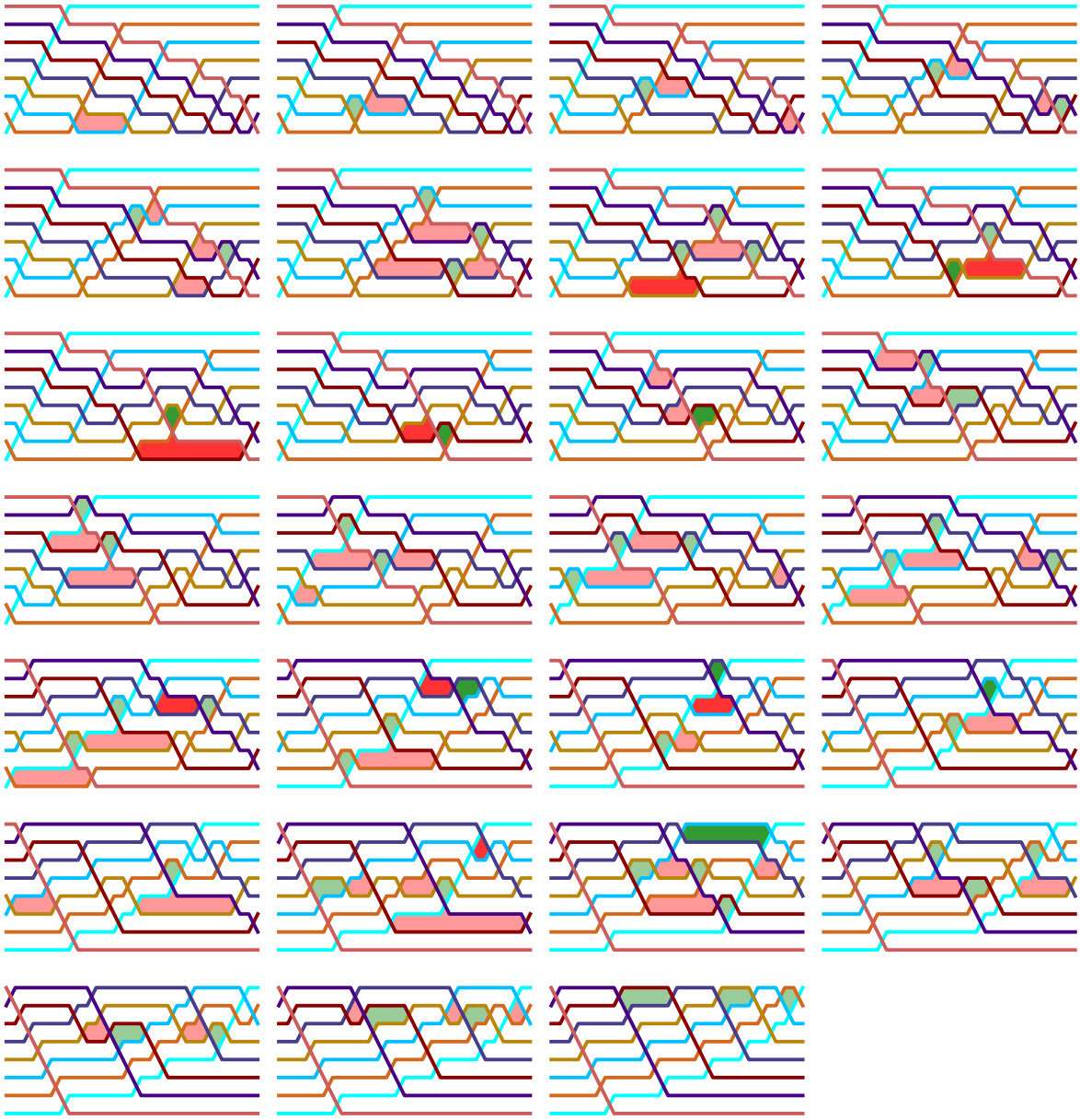

Figure 3.9: The sweep of pseudolines corresponding to σ_4 starting with the reversed cyclic arrangement in the top left. The odd elements $1, 3, 5, 7$ have a color from the red color family, whereas, the even elements $2, 4, 6, 8$ are colored with shades of blue and purple. Triangular cells which get flipped in comparison to the next signotope are marked red, if they have been flipped from the previous one they are green. Moreover we highlight the triangles consisting only of odd or only of even elements.

Higher Ranks

For higher ranks, we refer to the supplemental data [BFS23a] for the explicit sign sequence of the signotopes, since even represented as a string would be a lot of space and pages filled with + and − signs. However we give the set of fliples of the signotopes, since this is the only missing information. For the fliples we only give one representative for every 4-fold symmetry class.

Besides the two fliples, consisting of all even and all odd elements, we have a recursive construction for the remaining fliples. Starting with the three additional fliples $\widehat{F}_4$ of σ_4, which we represent as a string of "|" and "x" of length $2r$. If the i-th element is contained in the fliple, we write "x" at the i-th position, "|" otherwise. Hence this string consists of exactly r characters "x" and r characters "|". The three fliples of $\widehat{F}_4$ are represented by the strings "$|||xx|xx$", "$||xx|xx|$", and "$xx|x||x|$".
Given the set of fliples $\widehat{F}_r$ for an even $r \geq 4$, we construct $\widehat{F}_{r+2}$ as follows. If in the string of "x" and "|" there is a substring "$||xx$", we construct a string of size $2(r+2) = 2r+4$ by replacing the substring

$$\text{“}||xx\text{” by “}||||xxxx\text{”},$$

which adds additional four characters to the string. Moreover we replace the substring

$$\text{“}x||x\text{” by “}x|||xx|x\text{”}.$$

Note that both replacement add two additional elements to the fliple itself since we add two times "x" and two times "|". Note that starting with $r = 4$, we only get three patterns "$|||||xxxx|xx$", "$||||xxxx|xx|$", and "$xx|x|||xx|x|$" for $r = 6$. In addition we prescribe the string "$||xxxx|x||x|$" (corresponding to the fliple $(3, 4, 5, 6, 8, 11)$ for which both rules can be applied increasing the number of fliples for every r.
The fliples of $\widehat{F}_r$ for $r = 4, 6, 8, 10, 12$ together with its string representations are:

$$\begin{aligned}\widehat{F}_4 = \{&(1,3,5,7),(2,4,6,8),\\ &(1,2,4,7),(3,4,6,7),(4,5,7,8),\}\end{aligned}$$

$$\begin{aligned}\widehat{F}_6 = \{&(1,3,5,7,9,11),(2,4,6,8,10,12),\\ &(1,2,4,8,9,11),(5,6,7,8,10,11),(6,7,8,9,11,12),(3,4,5,6,8,11),\}\end{aligned}$$

$$\begin{aligned}\widehat{F}_8 = \{&(1,3,5,7,9,11,13,15),(2,4,6,8,10,12,14,16),\\ &(1,2,4,10,11,12,13,15),(3,4,5,6,8,12,13,15),(5,6,7,8,9,10,12,15),\\ &(7,8,9,10,11,12,14,15),(8,9,10,11,12,13,15,16)\}\end{aligned}$$

$$\widehat{F}_{10} = \{(1,3,5,7,9,11,13,15,17,19),(2,4,6,8,10,12,14,16,18,20),$$
$$(1,2,4,12,13,14,15,16,17,19),(3,4,5,6,8,14,15,16,17,19),$$
$$(5,6,7,8,9,10,12,16,17,19),(7,8,9,10,11,12,13,14,16,19),$$
$$(9,10,11,12,13,14,15,16,18,19),(10,11,12,13,14,15,16,17,19,20),\}$$

$$\widehat{F}_{12} = \{(1,3,5,7,9,11,13,15,17,19,21,23),(2,4,6,8,10,12,14,16,18,20,22,24),$$
$$(1,2,4,14,15,16,17,18,19,20,21,23),(3,4,5,6,8,16,17,18,19,20,21,23),$$
$$(5,6,7,8,9,10,12,18,19,20,21,23),(7,8,9,10,11,12,13,14,16,20,21,23),$$
$$(9,10,11,12,13,14,15,16,17,18,20,23),(11,12,13,14,15,16,17,18,19,20,22,23),$$
$$(12,13,14,15,16,17,18,19,20,21,23,24)\}$$

Until now there is no explanation why this construction works and whether it works for arbitrary rank. However this is the construction of the set of fliples for up to $r = 12$ which gives together with the remaining property a unique example.

3.6.3 Towards an Infinite Family of Counterexamples

In this section, we construct a *partial signotope* ρ_r for every even rank r, i.e., we only assign signs to a subset $\mathcal{X} \subseteq \binom{[n]}{r}$ of all r-subsets. In particular those signs imply that every signotope which contains the partial signotope is not 2-extendable. We say a signotope σ *contains* a partial signotope ρ whose domain is $\mathcal{X} \subseteq \binom{[n]}{r}$ if $\sigma(X) = \rho(X)$ for all $X \in \mathcal{X}$. We define a partial signotope ρ_r on $n = 2r$ elements for even rank r and show that the non-extendable signotopes σ_r (see Section 3.6.2) for $r = 4, 6, 8, 10, 12$ contain ρ_r. However the existence of signotopes with the specified properties remains open for all even $r \geq 14$.

The question whether there exists a signotope σ containing ρ_r for all even r is an instance of the *completion problem*. For related structures such as acyclic uniform 3-chirotopes, uniform 3-chirotopes, and generalized signotopes the completion problem is NP-hard. The first was shown by Knuth [Knu92]. Later Baier [Bai05] showed that the proof of Knuth transfers to uniform rank 3 chirotopes. Tschirschnitz [Tsc03] independently showed the result with a reduction from alternating 3SAT. This reduction might transfer to the setting of 3-signotopes. The NP-hardness of generalized signotopes was recently shown by Bergold, Scheucher and Schröder [BSS23a] who also showed the hardness for 40 related completion problems. We expect that the completion problem for signotopes is NP-hard as conjectured by Felsner, Gärtner and Tschirschnitz [FGT05].

For even r, we define a partial mapping ρ_r on $\binom{[2r]}{r}$. The $n = 2r$ elements are partitioned into the odd elements $O_r = \{o_1, \ldots, o_r\}$ and the even elements $E_r = \{e_1, \ldots, e_r\}$ with $o_i = 2i - 1$ and $e_i = 2i$ for $i = 1, \ldots, r$. Hence it holds $o_i < e_i < o_{i+1} < e_{i+1}$ for all $i = 1, \ldots, r-1$. Even though ρ_r is only a partial signotope, we use the operations as defined for r-signotopes such as rotation $(\rho_r)_{\mathrm{rot}}$, deletion and projection. Instead of $(\rho_r)_{\mathrm{rot}(k)}$, we write $\rho_r^{(k)}$ for the k-fold rotation. Without loss of generality, we assume

(1) $\rho_r(o_1, o_2, \ldots, o_r) = +$.

Otherwise, we just reverse all the signs. Furthermore, we define the following signs of ρ_r.

(2) $\rho_r(e_1, e_2, \ldots, e_r) = -$,

(3) $\rho_r(e_{i_1}, \ldots, e_{i_k}, o_j, e_{i_{k+1}}, \ldots, e_{i_{r-1}}) = (-)^k$ for $k = 0, \ldots, r-1$, and $i_1 < \ldots < i_k < j \leq i_{k+1} < i_{r-1} \leq r$,

(4) $\rho_r(o_{i_1}, \ldots, o_{i_k}, e_j, o_{i_{k+1}}, \ldots, o_{i_{r-1}}) = (-)^{k+1}$ for $k = 0, \ldots, r-1$, and $i_1 < \ldots < i_k \leq j < i_{k+1} < i_{r-1} \leq r$.

Note that those conditions together imply that O_r and E_r are fliples. The only packets in which O_r appears are the ones consisting of all elements from O_r and exactly one element from E_r. The signs which appear in those $(r+1)$-packets are all determined by (1)–(4) and do not contradict the monotonicity property. Moreover, the sign change is next to O_r. The same argument holds for E_r by exchanging the roles of E_r and O_r. For more details see the proof of Proposition 3.6.1 (page 70).
In the geometric sense of pseudohyperplane arrangements O_r and E_r being fliples means that the simplex spanned by each of the r pseudohyperplanes is not crossed by any other pseudohyperplane, i.e., is a simplicial cell. The conditions (3) and (4) show that each crossing of only even elements is above every pseudohyperplane corresponding to an odd hyperplane and each crossing of the pseudohyperplane of only odd elements is below each pseudohyperplane of an even element.
Another important structural property making the example very symmetric and therefore easier to analyze is the *4-fold symmetry*. The partial mapping ρ_r satisfies

(5) $\rho_r = \rho_r^{(4)}$.

The 4-fold symmetry is equivalent to

$$\rho_r(x_1, \ldots, x_r) = (-)^i \rho_r(x_{i+1} - 4, \ldots, x_r - 4, n - 4 + x_1, \ldots, n - 4 + x_i)$$

for all $1 \leq x_1 < \ldots < x_i \leq 4 < x_{i+1} < \ldots < x_r \leq 2r$ and does not contradict the properties (1)–(4). We discuss this in more detail in the proof of Proposition 3.6.1 (page 70). Further signs of ρ_r are

(6) $\rho_r(o_{i_1}, \ldots, o_{i_k}, e_{k+1}, e_{k+2}, \ldots, e_r) = +$ for $k = 2, \ldots, r-2$ and $i_1 < \ldots < i_k \leq k+1$,

(7) $\rho_r(o_1, o_2, e_2, \ldots, e_k, o_{k+2}, \ldots, o_r) = -$ for $k = 3, \ldots, r-1$.

The signs determined in (1)–(7) define $\Omega(r^3)$ signs of r-subsets of a total of $\binom{2r}{r}$ signs and do not contradict the monotonicity property of signotopes. We defer the proof of the following proposition to the end of this section (page 70).

Proposition 3.6.1. *For all even $r \geq 4$, the partial mapping ρ_r is a partial r-signotope, i.e., the determined signs do not contradict the monotonictiy property on $(r+1)$-packets.*

In the following we show that for even $r = 4, \ldots, 12$, there exist signotopes containing ρ_r. In particular the signotopes σ_r described in Section 3.6.2 contain ρ_r. For even rank $r \geq 14$ the existence remains unknown.

Lemma 3.6.2. *The signotopes σ_r of rank r for $r = 4, 6, 8, 10, 12$ (defined in Section 3.6.2), which are not 2-extendable, contain ρ_r. In particular they fulfill properties* (1)–(7).

Proof. Clearly conditions (1)–(5) are fulfilled by those examples as they are exactly (a)–(c). Moreover, (6) corresponds to the second part of (e). To show the remaining property (7), we apply the rotation operator multiple times to obtain an r-subset to which property (e) applies. We distinguish two cases depending on the parity of k, such that e_k is the largest element of E_r in the r-subset $(o_1, o_2, e_2, \dots, e_k, o_{k+2}, \dots, o_r)$.
First assume k is odd. Since r is even, the number of elements $o_{k+2}, \dots, o_r$ is even. By the 4-fold symmetry of σ_r (a) the application of four rotations yields the same signotope. In every step in which we apply four (backwards) rotations, we rotate exactly two of the elements o_{r-1}, o_r which become o_1, o_2. Since the number of rotated elements is even, the sign stays the same. To rotate all elements $o_{k+2}, \dots, o_r$, we apply $4 \cdot \frac{r-k-1}{2} = 2(r-k-1)$ rotations in total. Using the 4-fold symmetry, it holds

$$\sigma_r(o_1, o_2, e_2, \dots, e_k, o_{k+2}, \dots, o_r) = \sigma_r(o_1, \dots, o_{r-k+1}, e_{r-k+1}, \dots, e_{r-1}) = -.$$

The sign of the latter r-subset is $-$ because of the first part of (e).
If k is even, we apply $4 \cdot \frac{r-k-2}{2} = 2(r-k-2)$ rotations. In each set of four rotations exactly the two elements o_{r-1}, o_r are rotated and become o_1, o_2. In the end the considered r-subset still contains o_r. Hence we apply another set of four rotations in which only o_r is rotated which implies a reversion of the sign. By second part of (e), we can determine the sign of the resulting set.

$$\begin{aligned}\sigma_r(o_1, o_2, e_2, \dots, e_{k+2}, o_{k+4}, \dots, o_r) &= \sigma_r(o_1, \dots, o_{r-k-2}, e_{r-k-2}, \dots, e_{r-2}, o_r) \\ &= -\sigma_r(o_2, \dots, o_{r-k}, e_{r-k}, \dots, e_r) \\ &= - \cdot + = -.\end{aligned}$$

This shows that σ_r fulfills (7) and hence σ_r contains ρ_r for $r = 4, \dots, 12$. □

ρ_r is not 2-extendable

The next step is to show that for even r every r-signotope containing ρ_r is not 2-extendable. In order to show the non-extendability, we show a stronger statement. As for the signotopes σ_r, we show that every r-signotope σ which contains ρ_r and for every choice of an $(r-1)$-subset $\widetilde{E} \subseteq E_r$ and an $(r-1)$-subset $\widetilde{O} \subseteq O_r$ there is no extension in which $\widetilde{E}$ and $\widetilde{O}$ are fliples together with the new element.

Theorem 3.6.3. *Let $\widetilde{O} \subset O_r = \{o_1, \dots, o_r\}$, $\widetilde{E} \subset E_r = \{e_1, \dots, e_r\}$ be two disjoint $(r-1)$-subsets. For even $r \geq 4$ and all r-signotopes σ on $[2r]$ which contain ρ_r there is no extending r-signotope $\hat{\rho}_r$ on $[2r+1]$ such that there is an $z \in [2r+1]$ with $(\hat{\rho}_r)\downarrow_z = \sigma$ and $\widetilde{O} \cup \{z\}$ and $\widetilde{E} \cup \{z\}$ are fliples of $\hat{\rho}_r$.*

For the proof, we need to show that we cannot extend a signotope containing ρ_r with an additional element z such that the two considered disjoint $(r-1)$-subsets $\widetilde{E}$ and $\widetilde{O}$ are fliples in the extension. Since the elements are sorted in linear order, we need to make sure that we cannot add z at any position. We start by showing that we cannot extend ρ_r with z inserted at the last position $n+1$. In order to avoid the index shift, we go through all rotations and show in the considered rotation, that no extension with the last element exists. If we show for the i-th rotation of ρ_r with $i = 0, \dots, n-1$ that we cannot extend $\rho_r^{(i)}$ with an element at the last

position, than ρ_r is not extendable. Since our constructed partial signotope ρ_r is 4-symmetric (see (5)) it suffices to show the non-extendability with an element at the last position for signotopes containing one of the four rotations $\rho_r = \rho_r^{(0)}, \rho_r^{(1)}, \rho_r^{(2)}, \rho_r^{(3)}$. Note that $(E_r)_{\text{rot}} = O_r$ and $(O_r)_{\text{rot}}$. Hence the prescribed fliples stay the same for every rotation.

For each of the four rotations, we proceed as follows. To show that there is no extension with an element $z = n+1$ such that $\widetilde{E}$ and $\widetilde{O}$ are fliples, we assume towards a contradiction that there is an extension by the element $n+1$ in such a way that one of the two sets $\widetilde{E} \cup \{n+1\}$ and $\widetilde{O} \cup \{n+1\}$ is a fliple. By deducing signs using the monotonicity property, we show that the other set cannot be a fliple at the same time. All arguments work for each choice of $\widetilde{E}$ and $\widetilde{O}$. We consider the four rotations separately. In order to make it easier to follow, we rewrite the conditions (1)–(7) in terms of the considered rotation. This makes it easier to use the condition in the proof for the non-extendability. Moreover, we only mention the properties which are necessary for the considered rotation.

Rotation 0

In a first step, we look at a signotope containing ρ_r, i.e., with the original properties (1)–(7). We only mention the properties we use for the proof. Note that the elements of each r-subset are sorted.

(0.1) $\rho_r(o_1, \ldots, o_r) = +$ (cf. property (1))

(0.2) $\rho_r(e_1, \ldots, e_r) = -$ (cf. property (2))

(0.3) $\rho_r(o, e_{i_1}, \ldots, e_{i_{r-1}}) = (-)^0 = +$ for $o \in O_r$ and $e_{i_j} \in E_r$ (cf. property (3))

(0.4) $\rho_r(o_{i_1}, \ldots, o_{i_{r-1}}, e) = (-)^r = +$ for $o_{i_j} \in O_r$ and $e \in E_r$ (cf. property (4))

(0.5) $\rho_r(o_{i_1} \ldots o_{i_k}, e_{k+1}, \ldots, e_r) = +$ for $o_{i_j} \in O_r$ and $k = 2, \ldots, r-2$. (cf. property (6))

Note that for property (0.4) we used that r is even. We show that every signotope which contains ρ_r cannot be extended by an element $z = n+1$ at the last position to an r-signotope $\hat{\rho}_r$ such that $\widetilde{O} \cup \{z\}$ and $\widetilde{E} \cup \{z\}$ are both fliples. Since $\hat{\rho}_r$ is an extension, the deletion $\hat{\rho}_r \downarrow_{n+1}$ of the last element contains the partial signotope ρ_r. Hence if there is an extension, the conditions (0.1)–(0.5) hold for $\hat{\rho}_r$.
We assume that there is an extension $\hat{\rho}_r$ with $z = n+1$ such that there is a fliple $\widetilde{E} \cup \{z\}$ for an $(r-1)$-subset $\widetilde{E}$ of E_r. By deducing further signs using the monotonicity property, we show that for all $\widetilde{O} \subset O_r$, the r-subset $\widetilde{O} \cup \{z\}$ is not a fliple of $\hat{\rho}_r$. Since $\widetilde{E} \cup \{z\}$ is a fliple, the sign change of the $(r+1)$-subset $P = \{e_1, \ldots, e_r, z\}$ is before or after the position of $\widetilde{E} \cup \{z\}$ in the packet. In the case that the subset $P_1 = \{e_2, \ldots, e_r, z\}$ is the fliple, there might be no sign change since the fliple is at the first position. However, since P_1 is a fliple, we can flip the sign of the subset in order to get a sign change between P_1 and P_2. Flipping the sign of P_1 does not affect whether subsets of the form $\widetilde{O} \cup \{z\}$ are flipable. By (0.2) it is $\rho_r(e_1, \ldots, e_r) = \rho(P_{r+1}) = -$. Hence we assume

(0.6) $\hat{\rho}_r(e_2, \ldots, e_r, z) = +$.

Since $\hat{\rho}_r$ is an r-signotope, we use the monotonicity of signotopes to show $\hat{\rho}_r(o_2, \ldots, o_r, z) = +$ in the following Claim 3.1. By (0.1) it is $\rho_r(o_1, \ldots, o_r) = +$. Hence in the packet $\{o_1, \ldots, o_r, z\}$ the only possible fliple of the form $\widetilde{O} \cup \{z\}$ is $(o_2, \ldots, o_r, z)$. As we show in Claim 3.1 this r-subset is not a fliple. Hence there is no extension such that $\widetilde{E} \cup \{z\}$ and $\widetilde{O} \cup \{z\}$ are both fliples, which completes the proof for this rotation.
To prove that $\hat{\rho}_r(o_2, \ldots, o_r, z) = +$, we increase the number of odd elements in our r-subset in order to use the monotonicity on a common $(r+1)$-packet.

Claim 3.1. *For $k = 0, \ldots, r-1$ and $o_{i_1} < \ldots < o_{i_k} \leq o_{k+1}$ it is*

$$\hat{\rho}_r(o_{i_1}, \ldots, o_{i_k}, e_{k+2}, \ldots, e_r, z) = +.$$

Furthermore, for $k = 1, \ldots, r-1$ the r-subset $(o_{i_1}, \ldots, o_{i_k}, e_{k+2}, \ldots, e_r, z)$ is not a fliple.

Proof. We prove the claim by induction on k and start the base case with $k = 0$. In this case the claim follows by assumption (0.6). Now let $k > 0$. We want to determine the sign of the r-subset $(o_{i_1}, \ldots, o_{i_k}, e_{k+2}, \ldots, e_r, z)$. Since $o_{i_k} \leq o_{k+1} < e_{k+1}$ we can add the element e_{k+1} between o_{i_k} and e_{k+2} and consider the sign sequence of the $(r+1)$-subset

$$P = (o_{i_1}, \ldots, o_{i_k}, e_{k+1}, e_{k+2}, \ldots, e_r, z).$$

By induction hypothesis, it is $\hat{\rho}_r(P_k) = \hat{\rho}_r(o_{i_1}, \ldots, o_{i_{k-1}}, e_{k+1}, e_{k+2}, \ldots, e_r, z) = +$. Furthermore by the properties of ρ_r, we have $\hat{\rho}_r(P_{r+1}) = \hat{\rho}_r(o_{i_1}, \ldots, o_{i_k}, e_{k+1}, e_{k+2}, \ldots, e_r) = +$. For $2 \leq k \leq r-2$, this is by property (0.5). For $k = 1$ and $k = r-1$, this follows from property (0.3) and property (0.4), respectively. Since P_{k+1} appears in the sequence between P_k and P_{r+1}, which have both the sign $+$, it is $\hat{\rho}_r(P_{k+1}) = \hat{\rho}_r(o_{i_1}, \ldots, o_{i_k}, e_{k+2}, \ldots, e_r, z) = +$. Furthermore, since $(o_{i_1}, \ldots, o_{i_k}, e_{k+2}, \ldots, e_r, z)$ is not adjacent to a sign change in this sequence, it cannot be a fliple of $\hat{\rho}_r$. Hence the claim follows by induction. □

Rotation 1

We rotate $o_1 = 1$ of ρ_r which becomes $n = e_r$ for $\rho_r^{(1)}$. Moreover in the rotated signotope, the role of the odd and even elements change and with them some signs. The following properties we will need to show that there is no extension with $z = n + 1$.

(1.1) $\rho_r^{(1)}(o_1, \ldots, o_r) = \rho_r(e_1, \ldots, e_r) = -$ (cf. property (2))

(1.2) $\rho_r^{(1)}(e_1, \ldots, e_r) = - \cdot \rho_r(o_1, \ldots, o_r) = - \cdot + = -$ (cf. property (1))

(1.3) $\rho_r^{(1)}(e_1, \ldots, e_{r-1}, o_r) = \rho_r(o_2, \ldots, o_r, e_r) = (-)^r = +$ (cf. property (3))

(1.4) $\rho_r^{(1)}(e_1, o_2, \ldots, o_r) = \rho_r(o_2, e_2, \ldots, e_r) = (-)^0 = +$ (cf. property (4))

(1.5) $\rho_r^{(1)}(e_1, \ldots e_k, o_{k+1}, \ldots, o_r) = \rho_r(o_2, \ldots, o_{k+1}, e_{k+1}, \ldots, e_r) = +$ for $k = 2, \ldots, r-2$. (cf. property (6))

We proceed in a similar way as for the last rotation and show that there is no extension $\hat{\rho}_r^{(1)}$ of this rotation, where the extended element z is inserted at the last position $n+1$ such that $\widetilde{E} \cup \{z\}$ and $\widetilde{O} \cup \{z\}$ are fliples.

We assume there is an extension $\hat{\rho}_r^{(1)}$ with a fliple of the form $\widetilde{E} \cup \{z\}$ and show that it is not possible that a set of the form $\widetilde{O} \cup \{z\}$ is a fliple in the same extension. Since $\rho_r^{(1)}(e_1, \ldots, e_r) = -$, we assume without loss of generality.

$$(1.6) \quad \hat{\rho}_r^{(1)}(e_1, \ldots, e_{r-1}, z) = -.$$

If $\widetilde{E} \neq (e_1, \ldots, e_{r-1})$, this equation holds, since the signs of $(e_1, \ldots, e_{r-1}, z)$ and $(e_1, \ldots, e_r)$ are adjacent in the sign sequence of the packet $(e_1, \ldots, e_r, z)$. Moreover they are on the same side of the fliple $\widetilde{E} \cup \{z\}$. Hence they have the same sign. Moreover if $\widetilde{E} = (e_1, \ldots, e_{r-1})$, we can flip the sign of $(e_1, \ldots, e_{r-1}, z)$ if necessary without affecting the other properties. In particular it does not change whether there is a fliple of the form $\widetilde{O} \cup \{z\}$.
By increasing the number of odd elements, we conclude the following signs. As in the first part, we prove this claim by induction.

Claim 3.2. *For $k = r-1, \ldots, 0$ it is*

$$\hat{\rho}_r^{(1)}(e_1, \ldots, e_k, o_{k+2}, \ldots, o_r, z) = -.$$

Furthermore, for $k = r-2, \ldots, 0$ the r-subset $(e_1, \ldots, e_k, o_{k+2}, \ldots, o_r, z)$ is not a fliple.

Proof. For $k = r-1$, the sign of $(e_1, \ldots, e_{r-1}, z)$ is $-$ by assumption (1.6). For $k < r-1$, we consider the sign sequence of the $(r+1)$-subset

$$P = (e_1, \ldots, e_k, e_{k+1}, o_{k+2}, \ldots, o_r, z).$$

By induction hypothesis, it is $\hat{\rho}_r^{(1)}(P_{k+2}) = \hat{\rho}_r^{(1)}(e_1, \ldots, e_k, e_{k+1}, o_{k+3}, \ldots, o_r) = -$. Furthermore, by (1.5), it is $\hat{\rho}_r^{(1)}(P_{r+1}) = \hat{\rho}_r^{(1)}(e_1, \ldots, e_k, e_{k+1}, o_{k+2}, \ldots, o_r) = +$ for $k = 1, \ldots, r-3$. For $k = r-2$ and $k = 0$ this follows by (1.3) and (1.4), respectively. The subset $P_{k+1} = (e_1, \ldots, e_k, o_{k+2}, \ldots, o_r, z)$ is on the same side of the sign change as P_{k+2} and hence it maps to $-$. Moreover, it is not adjacent to the sign change. The latter shows that P_{k+1} is not flipable in this sequence and hence not a fliple of $\hat{\rho}_r^{(1)}$. □

The claim shows that $\hat{\rho}_r^{(1)}(o_2, \ldots, o_r, z) = -$ and $(o_2, \ldots, o_r, z)$ is not a fliple. Considering the sign sequence corresponding to the $(r+1)$-subset $(o_1, \ldots, o_r, z)$, we can conclude with (1.1) that this sequence consist only of $-$ signs. Hence there cannot be a fliple of the form $\widetilde{O} \cup \{z\}$ other than $(o_2, \ldots, o_r, z)$ which is not a fliple by Claim 3.2. This shows that after one rotation we cannot insert an element at the last position. This correspond to adding the new element z between the first and the second element in the signotope containing ρ_r.

Rotation 2

After a second rotation, $\rho_r^{(2)}$ has the following properties.

$$(2.1) \quad \rho_r^{(2)}(o_1, \ldots, o_r) = - \; \rho_r(o_1, \ldots, o_r) = - \qquad \text{(cf. property (1))}$$

$$(2.2) \quad \rho_r^{(2)}(e_1, \ldots, e_r) = - \; \rho(e_1, \ldots, e_r) = + \qquad \text{(cf. property (2))}$$

$$(2.3) \quad \rho_r^{(2)}(o_1, e_1, \ldots, e_{r-1}) = \rho_r(o_2, e_2, \ldots, e_r) = (-)^0 = + \qquad \text{(cf. property (3))}$$

(2.4) $\rho_r^{(2)}(o_1,\dots,o_{r-1},e_{r-1}) = \rho_r(o_2,\dots,o_r,e_r) = (-)^r = +$ (cf. property (4))

(2.5) $\rho_r^{(2)}(o_1,\dots,o_k,e_k,\dots,e_{r-1}) = \rho_r(o_2,\dots,o_{k+1},e_{k+1},\dots,e_r) = +$ for $k = 2,\dots,r-2$. (cf. property (6))

As before, we show that we cannot add an element z at the last position $n+1$ such that $\widetilde{O}\cup\{z\}$ and $\widetilde{E}\cup\{z\}$ are fliples. Assume there is an extension $\hat{\rho}_r^{(3)}$ such that $\widetilde{E}\cup\{z\}$ is a fliple. By (2.2) the sign of $(e_1,\dots,e_r)$ is $+$. Hence we may assume

(2.6) $\hat{\rho}_r^{(3)}(e_1,\dots,e_{r-1},z) = +$.

If $\widetilde{E} \neq (e_1,\dots,e_{r-1})$ it clearly holds. Moreover if $\widetilde{E} = (e_1,\dots,e_{r-1})$, we can flip the sign of $(e_1,\dots,e_{r-1},z)$ if necessary without affecting whether $\widetilde{O}\cup\{z\}$ is flipable.

Claim 3.3. *For $k = 0,\dots,r-1$ it is*

$$\hat{\rho}_r^{(2)}(o_1,\dots,o_k,e_{k+1},\dots,e_{r-1},z) = +.$$

Furthermore, for $k = 1,\dots,r-1$ the r-subset $(o_1,\dots,o_k,e_{k+1},\dots,e_{r-1},z)$ is not a fliple.

Proof. As in the preceding part, we prove this claim by induction and we increase the number of odd elements in the sequence one by one. For $k = 0$, by (2.6) it is $\hat{\rho}_r^{(2)}(e_1,\dots,e_{r-1},z) = +$. For $k > 1$, we consider the packet

$$P = (o_1,\dots,o_k,e_k,e_{k+1},\dots,e_{r-1},z).$$

The sign of P_k is $\hat{\rho}_r^{(2)}(o_1,\dots,o_{k-1},e_k,e_{k+1},e_{r-1},z) = +$ by induction hypothesis. Furthermore by construction of ρ_r, it is $\hat{\rho}_r^{(2)}(P_{r+1}) = \hat{\rho}_r^{(2)}(o_1,\dots,o_k,e_k,\dots,e_{r-1}) = +$ for $k = 1,\dots,r-1$. To be more precise, for $k = 2,\dots,r-2$ it follows by (2.5). For $k = 1$ and $k = r-1$, it follows by (2.3) and (2.4), respectively. Since the considered subset P_{k+1} is in between P_k and P_{r+1}, it follows $\hat{\rho}_r^{(2)}(P_{k+1}) = +$ and P_{k+1} is not flipable in P and hence is not a fliple. □

Considering the packet $(o_1,\dots,o_r,z)$ shows that none of the r-subsets $\widetilde{O}\cup\{z\}$ can be a fliple.

Rotation 3

For the last considered rotation, we use the following properties.

(3.1) $\rho_r^{(3)}(o_1,\dots,o_r) = -\rho_r(e_1,\dots,e_r) = +$ (cf. property (2))

(3.2) $\rho_r^{(3)}(e_1,\dots,e_r) = \rho_r(o_1,\dots,o_r) = +$ (cf. property (1))

(3.3) $\rho_r^{(3)}(o_1,e_2,\dots,e_r) = \rho_r(o_1,o_2,e_2,o_4,\dots,o_r) = (-)^3 = -$ (cf. property (4))

(3.4) $\rho_r^{(3)}(o_1,\dots,o_{r-1},e_r) = - \cdot \rho_r(o_2,e_2,\dots,e_r) = - \cdot (-)^0 = -$ (cf. property (3))

(3.5) $\rho_r^{(3)}(o_1,\dots,o_k,e_{k+1},\dots,e_r) = \rho_r(o_1,o_2,e_2,\dots,e_{k+1},o_{k+3},\dots,o_r) = -$ for $k = 2,\dots,r-2$. (cf. property (7))

Note that this is the only rotation for which we need property (7). Again, we assume that there is a fliple $\widetilde{E} \cup \{z\}$ and hence we may assume without loss of generality that

$$\hat{\rho}_r^{(3)}(e_2, \dots, e_r, z) = -. \tag{3.6}$$

Using those properties, we show by induction, that the following subsets are determined due to the monotonicity of signotopes.

Claim 3.4. *For $k = 0, \dots, r-1$, it is*

$$\hat{\rho}_r^{(3)}(o_1, \dots, o_k, e_{k+2}, \dots, e_r, z) = -.$$

Furthermore, for $k = 1, \dots, r-1$ the r-subset $(o_1, \dots, o_k, e_{k+2}, \dots, e_r, z)$ is not a fliple.

Proof. By (3.6) it is $\hat{\rho}_r^{(3)}(e_2, \dots, e_r, z) = -$ which is the statement for $k = 0$. For $k > 1$, we consider the packet

$$P = (o_1, \dots, o_k, e_{k+1}, \dots, e_r, z).$$

By induction the sign of $P_k = (o_1, \dots, o_{k-1}, e_{k+1}, e_r, z)$ is determined and is $\hat{\rho}_r^{(3)}(P_k) = -$. Furthermore for $k = 2, \dots, r-2$ the sign of $P_{r+1} = (o_1, \dots, o_k, e_{k+1}, \dots, e_r)$ is $\hat{\rho}_r^{(3)}(P_{r+1}) = -$ by (3.5). By (3.3) and (3.4) it is $\hat{\rho}_r^{(3)}(P_{r+1}) = -$ for $k = 1$ and $k = r-1$. Since the sign of P_{k+1} is between the sign of P_k and P_{r+1} the claim follows. □

Analogously to the preceding rotations it follows that $\hat{\rho}_r^{(3)}$ has no fliple of the form $\widetilde{O} \cup \{z\}$ by considering the packet $(o_1, \dots, o_r, z)$. This completes the proof of Theorem 3.6.3.

ρ_r is a partial signotope (Proof of Proposition 3.6.1)

In this part we provide the missing part and prove Proposition 3.6.1. For this we show that the signs given by properties (1)–(7) do not contradict the monotonicity of signotopes. For the proof we consider packets in which the signs of r-subsets are determined by one or more conditions. In a first step we consider the properties (1)–(4). We consider $(r+1)$-subsets containing exactly one element from O_r and r elements from E_r (or vice versa). Let P be the packet having an even element e at position $k+1$ and all others are odd. In this case it is

$$\begin{aligned} \rho_r(P_i) &= (-)^{k-1} && \text{for } i \le k \\ \rho_r(P_{k+1}) &= \rho_r(o_1, \dots, o_r) = + \\ \rho_r(P_j) &= (-)^k && \text{for } j \ge k+2. \end{aligned}$$

All signs are determined and do not contradict the monotonicity. Since these are the only packets in which O_r appears and the sign change is next to the sign of O_r, it is a fliple. Similar arguments hold for E_r.

Let us now consider the 4-symmetry (cf. property (5)). Property (1) and (2) are invariant under the 4-fold rotation. For (4) we consider the r-subset $X = (o_{i_1}, \dots o_{i_k}, e, o_{i_{k+1}}, \dots, o_{i_{r-1}})$. If $e > 4$, then we only rotate some of the o_i's. Let ℓ be the index such that $o_{i_\ell} < 4$ but $o_{i_{\ell+1}} > 4$.

Hence ℓ elements get rotated during the four rotations and the position of the even element is decreased by ℓ. Hence it holds

$$\begin{aligned}\rho_r(X) &= \rho_r(X_{\mathrm{rot}(4)})\\ &= (-)^{\ell} \cdot \rho_r(o_{i_{\ell+1}}-4,\ldots,o_{i_k}-4,e-4,o_{i_{k+1}}-4,\ldots,o_{i_{r-1}}-4,n-4+o_{i_1},\ldots,n-4+o_{i_\ell})\\ &= (-)^{\ell}(-)^{k+1-\ell} = (-)^{k+1}\end{aligned}$$

which coincides with the sign according to (4). If $e \leq 4$, we rotate additional elements. Again let ℓ be the index such that $o_{i_\ell} < e_j \leq 4$ and $o_{i_{\ell+1}} > 4$. In this case we rotate $\ell+1$ elements and the position of e in $X_{\mathrm{rot}(4)}$ is $r-(\ell+1)+k+1$ and hence it holds for even r

$$\begin{aligned}\rho_r(X) &= \rho_r(X_{\mathrm{rot}(4)})\\ &= (-)^{\ell+1} \cdot \rho_r(o_{i_{\ell+1}}-4,\ldots,o_{i_{r-1}}-4,n-4+o_{i_1},\ldots,n-4+o_{i_k},n-4-e,\\ &\quad n-4+o_{i_{k+1}},\ldots,n-4+o_{i_\ell})\\ &= (-)^{\ell+1} \cdot (-)^{r-(\ell+1)+k+1} = (-)^{k+1}\end{aligned}$$

which again coincides with the sign according to (4). This shows that (4) is invariant with respect to the 4-symmetry. Analogously it follows that (3) is invariant.
Now we apply the 4-symmetry property (5) to the two remaining properties (6) and (7). Hence the following signs are determined.

(6*) $\rho_r(e_1,\ldots,e_{2\ell},o_{i_1},\ldots,o_{i_k},e_{2\ell+k+1},\ldots,e_r) = +$
with $k=2,\ldots,r-2$, $2\ell+k \leq r$, and $i_1,\ldots,i_k \in \{2\ell,\ldots,2\ell+k+1\}$; and

$\rho_r(o_{i_1},\ldots,o_{i_j},e_i,\ldots,e_{2\ell},o_{i_{j+1}},\ldots,o_{i_k}) = (-)^{j+2\ell-i+1} = (-)^{j-i+1}$
with $k+2\ell-i+1=r$, $2\ell-i \geq 2$, $k \geq 2$, $i_1,\ldots,i_j \in \{1,\ldots,i\}$, $i_{j+1},\ldots,i_k \in \{2\ell+1,\ldots,r\}$

Note that in the second version, the sign depends on how many elements are rotated. In the first version this is always an odd number. If we do the same for property (7), we get the following more general rules

(7*) $\rho_r(o_1,\ldots,o_{2\ell},e_{2\ell},\ldots,e_{2\ell+k},o_{2\ell+k+2},\ldots,o_r) = -$
with $\ell \geq 1$ and $k \geq 2$ such that $2\ell+k \leq r$; and

$\rho_r(e_1,\ldots,e_\ell,o_{\ell+2},\ldots,o_{2k},e_{2k},\ldots,e_r) = +$
with $0 \leq \ell \leq 2k-3$, $k \geq 4$, $\ell+r-2k+1 \geq 2$.

The subsets $(o_1,\ldots,o_{2\ell},e_{2\ell},\ldots,e_{2k},o_{2k+2},\ldots,o_r)$ and $(e_1,\ldots,e_{2\ell},o_{2\ell+2},\ldots,o_{2k},e_{2k},\ldots,e_r)$ appear in both rules (6*) and (7*) and get the same sign $-$ and $+$, respectively, in both rules.
Furthermore we study the interaction of (6*) and (7*) and the other properties. If two rules affect each other, subsets for which the rule applies appear in the same $(r+1)$-packet. More precisely they need to have $r-1$ elements in common.
Subsets for which (6*) or (7*) apply contain at least two elements from O_r and two from E_r. Hence they do not appear with $(o_1,\ldots,o_r)$ and $(e_1,\ldots,e_r)$ in a same $(r+1)$-packet.
In a first step, we consider packets which contain exactly two elements from O_r and a subset for which rule (6*) applies. Deleting one of the elements of O_r from the packet leads to a subset for which property (3) gives the sign. To ensure that we can apply (6*) for one of the other

r-subsets, we start with a subset of (6*) with only two elements from O_r. There are two different types $(e_1, \ldots, e_{2\ell}, o_{i_1}, o_{i_2}, e_{2\ell+3}, \ldots, e_r)$ and $(o_1, e_1, \ldots, e_{r-2}, o_{i_2})$. We now list all $(r+1)$-packets which contain at least one of them and exactly two elements from O_r and check the determined signs in order to see whether they contradict the partial signotope property. If the sign of an r-subset is determined by any of the rules, we will write it to the right and give the number of the corresponding rule.

P		
$(e_1, \ldots, e_{2\ell}, e_{2\ell+1}, o_{2\ell+2}, o_{2\ell+3}, e_{2\ell+3}, \ldots, e_r)$	$\rho_r(P_{2\ell+1}) = +$	(6*)
	$\rho_r(P_{2\ell+2}) = (-)^{2\ell+1} = -$	(3)
	$\rho_r(P_{2\ell+3}) = (-)^{2\ell+1} = -$	(3)
$(e_1, \ldots, e_{2\ell}, o_{i_1}, e_j, o_{i_2}, e_{2\ell+3}, \ldots, e_r)$	$\rho_r(P_{2\ell+1}) = (-)^{2\ell+1} = -$	(3)
	$\rho_r(P_{2\ell+2}) = +$	(6*)
	$\rho_r(P_{2\ell+3}) = (-)^{2\ell} = +$	(3)
$(e_1, \ldots, e_{2\ell}, o_{2\ell+1}, o_{2\ell+2}, e_{2\ell+2}, e_{2\ell+3}, \ldots, e_r)$	$\rho_r(P_{2\ell}) = +$	(7*)
	$\rho_r(P_{2\ell+1}) = (-1)^{2\ell} = +$	(3)
	$\rho_r(P_{2\ell+2}) = (-1)^{2\ell} = +$	(3)
	$\rho_r(P_{2\ell+3}) = +$	(6*)
$(o_1, e_1, \ldots, e_{r-2}, e_{r-1}, o_r)$	$\rho_r(P_1) = (-1)^{r-1} = -$	(3)
	$\rho_r(P_r) = -$	(6*)
	$\rho_r(P_{r+1}) = (-1)^0 = +$	(3)
$(o_1, e_1, \ldots, e_{r-2}, o_{i_2}, e_j)$	$\rho_r(P_1) = (-1)^{r-2} = +$	(3)
	$\rho_r(P_r) = (-1)^0 = +$	(3)
	$\rho_r(P_{r+1}) = -$	(6*)

In the next step, we consider packets containing a subset of the form (6*) and exactly two elements from E_r. Subsets for which we can apply rule (6*) which have only two elements from E_r have the form

$$(o_{i_1}, \ldots, o_{i_j}, e_{2\ell-1}, e_{2\ell}, o_{i_{j+1}}, \ldots, o_{i_{r-2}}).$$

for $0 \leq j \leq r-2$ and compatible $\ell = 1, \ldots, r$. Their sign in ρ_r is $(-)^j$ according to (6*). There are only three possibilities to add another element from O_r.

P			
$(o_{i_1}, \ldots, o_{i_{j+1}}, e_{2\ell-1}, e_{2\ell}, o_{i_{j+2}}, \ldots, o_{i_{r-1}})$	$\rho_r(P_k) = (-)^j$	$k \leq j+1$	(6*)
	$\rho_r(P_{j+2}) = (-)^{j+2}$		(4)
	$\rho_r(P_{j+3}) = (-)^{j+2}$		(4)
	$\rho_r(P_k) = (-)^{j+1}$	$k \geq j+4$	(6*)
$(o_{i_1}, \ldots, o_{i_j}, e_{2\ell-1}, o_{2\ell}, e_{2\ell}, o_{i_{j+1}}, \ldots, o_{i_{r-2}})$	$\rho_r(P_{j+1}) = (-)^{j+2}$		(4)
	$\rho_r(P_{j+2}) = (-)^j$		(6*)
	$\rho_r(P_{j+3}) = (-)^{j+1}$		(4)
$(o_{i_1}, \ldots, o_{i_j}, e_{2\ell-1}, e_{2\ell}, o_{i_{j+1}}, \ldots, o_{i_{r-1}})$	$\rho_r(P_k) = (-)^{j-1}$	$k \leq j$	(6*)
	$\rho_r(P_{j+1}) = (-)^{j+1}$		(4)
	$\rho_r(P_{j+2}) = (-)^{j+1}$		(4)
	$\rho_r(P_k) = (-)^j$	$k \geq j+3$	(6*)

In a similar way, we proceed for rule (7*). First we consider packets in which r-subsets appear for which rule (7*) applies and which have exactly two odd elements. If there are only two elements from O_r, the subsets for which rule (7*) applies are $(o_1, o_2, e_2, \ldots, e_{r-1})$ and $(e_1, \ldots, e_{2k-3}, o_{2k-1}, o_{2k}, e_{2k}, \ldots, e_r)$ for $k = 1, \ldots, \frac{r}{2}$. They are contained in the following two $(r+1)$-packets

P	
$(o_1, e_1, o_2, e_2, \ldots, e_{r-1})$	$\rho_r(P_1) = -$ (3) $\rho_r(P_2) = -$ (7*) $\rho_r(P_3) = +$ (3)
$(o_1, o_2, e_2, \ldots, e_{r-1}, e_r)$	$\rho_r(P_1) = +$ (3) $\rho_r(P_2) = +$ (3) $\rho_r(P_3) = (-1)^2 = +$ (6*) $\rho_r(P_{r+1}) = -$ (7*)
$(e_1, \ldots, e_{2k-3}, e_{2k-2}, o_{2k-1}, o_{2k}, e_{2k}, \ldots, e_r)$	$\rho_r(P_{2k-2}) = +$ (7*) $\rho_r(P_{2k-1}) = (-)^{2k-2} = +$ (3) $\rho_r(P_{2k}) = (-)^{2k-2} = +$ (3) $\rho_r(P_{2k+1}) = +$ (6*)
$(e_1, \ldots, e_{2k-3}, o_{2k-1}, e_{2k-1}, o_{2k}, e_{2k}, \ldots, e_r)$	$\rho_r(P_{2k-2}) = (-)^{2k-2} = +$ (3) $\rho_r(P_{2k-1}) = +$ (7*) $\rho_r(P_{2k}) = (-)^{2k-3} = -$ (3)

Let us now consider packets with only two elements from E_r containing an r-subset for which rule (7*) applies. Subsets from (7*) we have to consider are $(o_1, \ldots, o_{2\ell}, e_{2\ell}, e_{2\ell+1}, o_{2\ell+3}, \ldots, o_r)$ and $(e_1, o_3, \ldots, o_r, e_r)$ and they appear in the following $(r+1)$-packets with only two elements from E_r.

P	
$(o_1, \ldots, o_{2\ell}, e_{2\ell}, o_{2\ell+1}, e_{2\ell+1}, o_{2\ell+3}, \ldots, o_r)$	$\rho_r(P_{2\ell+1}) = (-)^{2\ell+2} = +$ (4) $\rho_r(P_{2\ell+2}) = -$ (7*) $\rho_r(P_{2\ell+3}) = (-)^{2\ell+1} = -$ (4)
$(o_1, \ldots, o_{2\ell}, e_{2\ell}, e_{2\ell+1}, o_{2\ell+2}, o_{2\ell+3}, \ldots, o_r)$	$\rho_r(P_{2\ell+1}) = (-)^{2\ell+1} = -$ (4) $\rho_r(P_{2\ell+2}) = (-)^{2\ell+1} = -$ (4) $\rho_r(P_{2\ell+3}) = -$ (7*)
$(o_1, e_1, o_3, \ldots, o_r, e_r)$	$\rho_r(P_1) = +$ (7*) $\rho_r(P_2) = (-)^r = +$ (4) $\rho_r(P_{r+1}) = (-)^2 = +$ (4)
$(e_1, o_2, o_3, \ldots, o_r, e_r)$	$\rho_r(P_1) = (-1)^r = +$ (4) $\rho_r(P_2) = +$ (7*) $\rho_r(P_{r+1}) = (-1)^1 = -$ (4)

The remaining part are packets which contain subsets of the form (6*) and (7*), respectively, with at least three elements from O_r and three elements from E_r. In all of those cases the only rules which might apply are (6*) and (7*). We consider two cases. Some packets we consider might appear in both. We start with packets containing subsets of the form (7*). We start with the r-subset

$$(o_1, \ldots, o_{2\ell}, e_{2\ell}, \ldots, e_{2\ell+k}, o_{2\ell+l+2}, \ldots, o_r).$$

For the packet we add another element, we start with the possibilities to add an element from O_r. If we add an element $o_{2\ell+j}$ with $j \in \{1, \dots, 2\ell + k\}$, the only way to get consecutive blocks of only elements from O_r followed by only elements from E_r (considered cyclically) is to delete this element again. Hence the only subset for which we can apply one of the rules contained in this packet is the one we started with. Moreover the odd elements $o_1, \dots, o_{2\ell}$ are already contained in the subset.
Hence there is only one remaining option:

$$P = (o_1, \dots, o_{2\ell}, e_{2\ell}, \dots, e_{2\ell+k}, o_{2\ell+k+1}, o_{2\ell+k+2}, \dots, o_r).$$

If $2\ell + k$ is even, we can apply rule (6*) and get the following signs.

$$\begin{aligned}
\rho_r(P_j) = (-)^{2\ell-1-2\ell+1} = + \qquad & \text{for all } 1 \le j \le 2\ell && (6^*)\\
\rho_r(P_{2\ell+1}) = (-)^{2\ell-(2\ell-1)+1} = + & && (6^*)\\
\rho_r(P_{2\ell+k+2}) = - & && (6^*)\&(7^*)\\
\rho_r(P_j) = (-1)^{2\ell-(2\ell)+1} = - \qquad & \text{for all } 2\ell + k + 3 \le j \le r. && (6^*)
\end{aligned}$$

In the other case, if $2\ell + k$ is odd, we can only determine the two following signs

$$\begin{aligned}
\rho_r(P_{2\ell+k+2}) = - & && (6^*)\&(7^*)\\
\rho_r(P_{2\ell+k+3}) = -. & && (7^*)
\end{aligned}$$

If instead we add an element from E_r, there is again only one possibility.

$$P' = (o_1, \dots, o_{2\ell}, e_{2\ell}, \dots, e_{2\ell+k}, e_{2\ell+k+1}, o_{2\ell+k+2}, \dots, o_r)$$

If $2\ell + k + 1$ is even, all sign of the packet are determined and are

$$\begin{aligned}
\rho_r(P'_j) = (-)^{2\ell-1-(2\ell)+1} = + \text{ for all } 1 \le j \le 2\ell & && (6^*)\\
\rho_r(P'_{2\ell+1}) = + & && (6^*)\\
\rho_r(P'_{2\ell+k+2}) = - & && (7^*)\\
\rho_r(P'_{2\ell+k+3}) = - & && (7^*)\\
\rho_r(P'_j) = (-)^{2\ell-2\ell+1} = - \text{ for all } 1\ell + k + 2 \le j \le r. & && (6^*)
\end{aligned}$$

On the other hand, if $2\ell + k + 1$ is odd, we only have two determined signs. For both we apply property (7*).

$$\begin{aligned}
\rho_r(P'_{2\ell+k+2}) = - & && (7^*)\\
\rho_r(P'_{2\ell+k+3}) = -. & && (7^*)
\end{aligned}$$

Let us now have a look at the second version of (7*) which are subsets of the following form $(e_1, \dots, e_\ell, o_{\ell+2}, \dots, o_{2k}, e_{2k}, \dots, e_r)$. If we insert an $o \in O_r$, we have one possibility to add it in order to have consecutive blocks of elements in O_r an elements in E_r. We get an $(r + 1)$-packet of the following form

$$Q = (e_1, \dots, e_\ell, o_{\ell+1}, o_{\ell+2}, \dots, o_{2k}, e_{2k}, \dots, e_r)$$

with the determined signs

$$\begin{aligned}
\rho_r(Q_\ell) &= + && && (7^*)\\
\rho_r(Q_{\ell+1}) &= + && && (7^*)\\
\rho_r(Q_j) &= + && \text{for all } \ell+2 \le j \le 2k; && \text{only if } \ell \text{ is even} && (6^*)\\
\rho_r(Q_{2k+1}) &= + && && \text{only if } \ell \text{ is even} && (6^*)
\end{aligned}$$

Adding another element from E_r gives the packet

$$Q' = (e_1, \ldots, e_\ell, e_{\ell+1}, o_{\ell+2}, \ldots, o_{2k}, e_{2k}, \ldots, e_r)$$

which has the signs

$$\begin{aligned}
\rho_r(Q'_{\ell+1}) &= + && && (7^*)\\
\rho_r(Q'_{\ell+2}) &= + && && (7^*)\\
\rho_r(Q_j) &= + && \text{for all } \ell+2 \le j \le 2k; && \text{only if } \ell+1 \text{ is even} && (6^*)\\
\rho_r(Q_{2k+1}) &= + && && \text{only if } \ell \text{ is even .} && (6^*)
\end{aligned}$$

Similarly, we investigate packets containing subsets of the form (6*). Since there are two different versions of this property we consider them separately. Again, for each of them we add first an element from O_r and then one from E_r which gives us two different packets whose sign sequence we analyze in the following. Let us first consider the $(r+1)$-packet $P = (e_1, \ldots, e_{2\ell}, o_{i_1}, \ldots, o_{i_k}, o_{i_{k+1}}, e_{2\ell+k+1}, \ldots, e_r)$. Then the signs of P_j for $j = 2\ell+1, \ldots, 2\ell+k+2$ are determined by (6*) and all of them are +, which does not contradict the monotonicity of signotopes. Similar for the packet $P = (e_1, \ldots, e_{2\ell}, e_{2\ell+1}, o_{i_1}, \ldots, o_{i_{k+1}}, e_{2\ell+k+1}, \ldots, e_r)$ the sign of $P_{2\ell+1}$ is + by (6*). Possibly depending on the values the signs of P_j with $j = 2\ell+2, \ldots, 2\ell+1+k$ are determined by (7*) and are also +. Now let us consider the second variant of (6*). The $(r+1)$-packet $P = (o_{i_1}, \ldots, o_{i_j}, o_{i_{j+1}}, e_i, \ldots, e_{2\ell}, o_{i_{j+1}}, \ldots, o_{i_k})$ has the signs which are determined by the property given at the end of the line

$$\begin{aligned}
\rho_r(P_m) &= (-)^{j-i+1} && \text{for } m \le j+1 && (6^*)\\
\rho_r(P_{j+2}) &= (-)^{j-i+1} && && (6^*)\\
\rho_r(P_m) &= (-)^{j-i+2} && \text{for } m \ge 2\ell+j+1. && (6^*)
\end{aligned}$$

As a last packet, we consider $P = (o_{i_1}, \ldots, o_{i_j}, e_{i-1}, e_i, \ldots, e_{2\ell}, o_{i_{j+1}}, \ldots, o_{i_k})$, which has the following signs:

$$\begin{aligned}
\rho_r(P_m) &= (-)^{j-i+1} && \text{for } m \le j && (6^*)\\
\rho_r(P_{j+1}) &= (-)^{j-i+1} && && (6^*)\\
\rho_r(P_m) &= (-)^{j-i+2} && \text{for } m \ge 2\ell+j. && (6^*)
\end{aligned}$$

If we instead add $e_{2\ell+1}$ to the r-subset, there is only one sign determined.
This completes the proof and shows that ρ_r is a partial signotope.

3.7 t-Extendability

In the previous section, we studied 1- and 2-extendability. Moreover, we developed techniques to investigate general t-extendability. In this section, we discuss examples which show that signotopes with rank $r \geq 4$ are not 4-extendable. Moreover, for $r = 3$ and $r = 5$, we present an example which is not 3-extendable.

Line arrangements are trivially not extendable by a line through three prescribed points. However, it might be possible that a line arrangement is extendable by a pseudoline. Is it not hard to see, that this is in general not the case. An example for this is the cyclic arrangement, see Figure 3.10. There is no possibility to add a pseudoline going through the three marked crossing

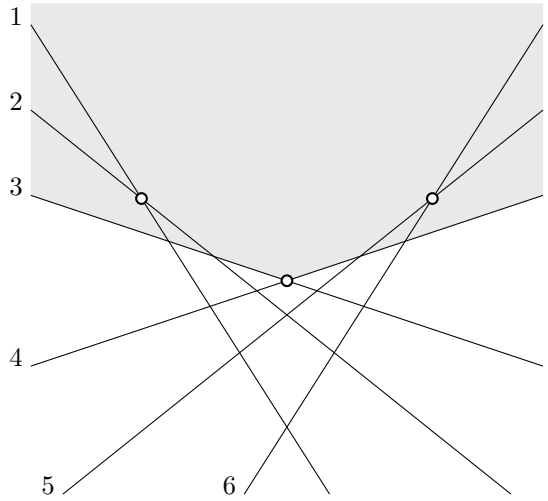

Figure 3.10: The cyclic line arrangement with 6 lines. There is no extension to a pseudoline arrangements with a pseudoline passing through the three marked points. The sector of one crossing point containing the other two points is marked grey.

points. If there was a pseudoline going through all three points, this new pseudoline has to contain the three points in a linear order. Hence one of the crossing points has to be in between the other two on the newly added pseudoline. For this we study *sectors* which are spanned by two pseudolines. Two pseudolines which cross once divide the plane into four connected components. We call those connected components sectors. The prescribed point which is in between the other two on the newly added pseudoline must have the two remaining points in two different sectors. However, this is not the case. For each of the three points, the other two points are in the same sector. This shows that the rank 3 signotope on 6 elements where every triple is mapped to $+$, i.e., the unique maximal signotope $\sigma_{\max}$ of $B(6, 3)$ is not 3-extendable. The above arguments with the sectors, essentially use the partial order corresponding to a signotope. Hence we can write the proof in terms of signotopes. Moreover, we can generalize this to higher ranks in which this construction only gives that $\sigma_{\max} \in B(n, r)$ for $r \geq 4$ is not 4-extendable.

Proposition 3.7.1. *Let $\sigma_{\max} \in B(n, r)$ be the constant $+$ signotope with $n = 4(r-1)$ elements and odd rank r. For $r \geq 3$ the signotope $\sigma_{\max}$ is not 4-extendable. Moreover, for $r = 3$, $n = 6$ and $r = 5$, $n = 12$, the signotope $\sigma_{\max}$ is not 3-extendable.*

To study the extendability we use Proposition 3.2.4 which gives a condition for the extendability by an element at the last position. We extend this characterization by going through all rotations.

Corollary 3.7.2. *An r-signotope σ on $[n]$ is t-extendable for $t \geq 2$ if and only if for all pairwise disjoint $(r-1)$-subsets $I_1, \ldots, I_t$ there exists a rotation in which they are pairwise incomparable.*

Hence the strategy to prove Proposition 3.7.1 is to prescribe $(r-1)$-subsets such that in each rotation at least two of them are comparable. For $\sigma_{\max}$, we consider the four $(r-1)$-subsets

$$I_i = ((i-1)\cdot(r-1)+1, \ldots, i\cdot(r-1))$$

for $i = 1, 2, 3, 4$. Note that they are disjoint and consecutive in the sense that all elements contained in I_i are smaller than all elements of I_j for $i < j$. We consider all rotations, and investigate which of the subsets are incomparable. For rank 3, we only consider I_1, I_2, I_3. For rank 5 with the same prescribed $(r-1)$-subsets there exists a 3-extension. However, if we instead consider the three 4-subsets $I = (1,3,4,5), J = (2,10,11,12), K = (6,7,8,9)$ on $n = 12$ elements, $\sigma_{\max}$ is not 3-extendable.
To show comparability between two $(r-1)$-subsets, it is enough to consider a smaller signotope. If they are comparable in the restriction, they are comparable in the original signotope.

Lemma 3.7.3. *Let σ be an r-signotope on $[n]$ and I, J two disjoint $(r-1)$-subsets of $[n]$. Furthermore let $\sigma' = \sigma{\downarrow_{[n]\setminus(I\cup J)}}$ be the restriction to the elements of $I \cup J$, i.e., an r-signotope on $n' = 2(r-1) < n$ elements. For the partial order $\prec$ of σ and $\prec'$ of σ', it holds: If $I' \prec' J'$, then $I \prec J$.*

Proof. If I' and J' are comparable in σ', i.e., $I' \prec' J'$, there is a chain of $(r-1)$-subsets $I' = I'_0 \prec I'_1 \prec' \ldots \prec' I'_k = J'$ such that $|I'_i \cap I'_{i+1}| = r-2$ and $I_i \subseteq [n]$. For each of the I'_i there is a corresponding set I_i of σ such that $(I_i){\downarrow_{[n]\setminus(I\cup J)}} = I'_i$. Now clearly $I_i \prec I_{i+1}$ for all i which implies the statement. □

Since for each two of the four prescribed $(r-1)$-subsets I_1, I_2, I_3, I_4 the order of the elements is the same, we study the comparability between them in $\sigma_{\max}$.

Lemma 3.7.4. *For $i < j$, it holds $I_i \prec I_j$ in the partial order $\prec$ corresponding to $\sigma_{\max}$.*

Proof. By the Lemma 3.7.3 it is enough to show that the two $(r-1)$-subsets $I_1 = (1, \ldots, r-1)$ and $I_2 = (r, \ldots, 2(r-1))$ are comparable concerning the signotope of rank r on $n = 2(r-1)$ elements. Since the sign of all r-subsets $X^i = (i, \ldots, i+r)$ is $+$, it is $X^i_1 \prec X^i_r$ which shows that $(i, \ldots, i+r-1) \prec (i+1, \ldots, i+r)$ for all $i = 1, \ldots, r-1$. With the transitivity of $\prec$, the claim follows. □

In the next step, we study the comparability of the $(r-1)$-subsets in the rotations. For every rotation k let $I_i^{(k)}$ denote the k-th rotation of I_i, i.e., $I_i^{(k)} = (I_i)_{\mathrm{rot}(k)}$. Moreover, let $\prec_{(k)}$ be the partial order corresponding to the k-th rotation $\sigma_{\mathrm{rot}(k)}$ of σ. We investigate for which rotation k the $(r-1)$-subsets $I_i^{(k)}$ and $I_j^{(k)}$ are comparable.

Lemma 3.7.5. *Let $I_i = (x_1, \ldots, x_{r-1})$ and $I_j = (y_1, \ldots, y_{r-1})$ with $x_{r-1} < y_1$. The two disjoint $(r-1)$-subsets $I_i^{(k)}$ and $I_j^{(k)}$ are comparable if $x_1^{(k)}, x_2^{(k)}$ or $y_{r-1}^{(k)}$ are the smallest elements in the k-th rotation among the elements $I_i^{(k)} \cup I_j^{(k)} = \{x_1^{(k)}, \ldots, x_{r-1}^{(k)}, y_1^{(k)}, \ldots, y_{r-1}^{(k)}\}$.*

Proof. We consider the three cases separately. We restrict to the first n rotations since afterwards everything is the same except that all signs might be reversed which does not affect the comparability. If $x_1^{(k)}$ is the smallest element, we have

$$x_1^{(k)} < \ldots < x_{r-1}^{(k)} < y_1^{(k)} < \ldots < y_{r-1}^{(k)}.$$

In this case the statement follows from Lemma 3.7.4. In the next case, we assume $x_2^{(k)}$ is the smallest element. Hence the ordering of the considered elements is

$$x_2^{(k)} < \ldots < x_{r-1}^{(k)} < y_1^{(k)} < \ldots < y_{r-1}^{(k)} < x_1^{(k)}.$$

Since we only consider r-subset of the considered $2(r-1)$ elements by Lemma 3.7.3, the only signs which are $-$ are the ones of the r-subsets containing $x_1^{(k)}$. Considering the set $(x_2^{(k)}, \ldots, x_{r-1}^{(k)}, y_1^{(k)}, x_1^{(k)})$ whose sign is $-$ in $\sigma_{\mathrm{rot}(k)}$. It holds

$$(x_3^{(k)}, \ldots, x_{r-1}^{(k)}, y_1^{(k)}, x_1^{(k)}) \prec_{(k)} (x_2^{(k)}, \ldots, x_{r-1}^{(k)}, y_1^{(k)})$$

All remaining signs which we considered in the proof of Lemma 3.7.4 are still $+$ and hence it holds

$$(x_2^{(k)}, \ldots, x_{r-1}^{(k)}, y_1^{(k)}) \prec_{(k)} (y_1^{(k)}, \ldots, y_{r-1}^{(k)}).$$

This completes the second part of the lemma. Hence it remains to consider the last ordering of elements in which we have

$$y_{r-1}^{(k)} < x_1^{(k)} < \ldots < x_{r-1}^{(k)} < y_1^{(k)} < \ldots < y_{r-2}^{(k)}.$$

In this case all signs are $-$ except the ones of the r-subsets containing $y_{r-1}^{(k)}$. Hence we have $\sigma_{\mathrm{rot}(k)}(x_\ell^{(k)}, \ldots, x_{r-1}^{(k)}, y_1^{(k)}, \ldots, y_{\ell-1}^{(k)}) = -$ for all $\ell = 1, \ldots, r-2$ which implies

$$(x_{\ell+1}^{(k)}, \ldots, x_{r-1}^{(k)}, y_1^{(k)}, \ldots, y_{\ell-1}^{(k)}) \prec_{(k)} (x_\ell^{(k)}, \ldots, x_{r-1}^{(k)}, y_1^{(k)}, \ldots, y_{\ell-2}^{(k)}).$$

Moreover it is $\sigma_{\mathrm{rot}(k)}(y_{r-1}^{(k)}, x_{r-1}^{(k)}, y_1^{(k)}, \ldots, y_{r-2}^{(k)}) = +$ which implies

$$(y_{r-1}^{(k)}, y_1^{(k)}, \ldots, y_{r-2}^{(k)}) \prec_{(k)} (x_{r-1}^{(k)}, y_1^{(k)}, \ldots, y_{r-2}^{(k)}).$$

Combining the relations, the claim follows. □

We are now ready to prove Proposition 3.7.1. We will first consider the case $r = 3$ with the prescribed sets I_1, I_2, I_3 to show the moreover part and then show that the choice of I_1, I_2, I_3, I_4 implies the not 4-extendability for general rank. The remaining part for $r = 5$ uses a different choice of prescribed fliples which we give in the end.

Proof of Proposition 3.7.1. In the case $r = 3$, we consider the three pairs $I_1 = (1, 2)$, $I_2 = (3, 4)$ and $I_3 = (5, 6)$. By the previous Lemma 3.7.5 $I_1^{(k)}$ and $I_2^{(k)}$ are comparable in the signotope after $k = 0, 1, 3, 4, 5$ rotations. Hence the only possible rotation in which they might be incomparable is $\sigma_{\mathrm{rot}(2)}$. Furthermore Lemma 3.7.5 shows that $I_2^{(k)}$ and $I_3^{(k)}$ are comparable for

$k = 0, 1, 2, 3, 5$. Hence they cannot be incomparable after 2 rotations. This shows the moreover part of Proposition 3.7.1.

For odd rank $r \geq 5$, we show that $I_1^{(k)}$, $I_2^{(k)}$, $I_3^{(k)}$, and $I_4^{(k)}$ cannot be incomparable at the same rotation k. By Lemma 3.7.5 the two sets $I_1^{(k)}$, $I_2^{(k)}$ are comparable if either one of the two smallest of I_1 or the largest of I_2 are the first element in the rotation. Hence they can only be incomparable for $k \in \{2, \ldots, 2r-4\}$. However $I_3^{(k)}$ and $I_4^{(k)}$ are comparable for all $k \in \{2, \ldots, 2r-4\}$ since in this case we still have the smallest one of I_3 as a first element. Hence they cannot be incomparable at the same time.

To show that $\sigma_{\max}$ of rank 5 is not 3-extendable, we consider the disjoint 4-subsets $I = (1, 3, 4, 5)$, $J = (2, 10, 11, 12)$, $K = (6, 7, 8, 9)$. Since all elements from I are smaller than the one from K, Lemma 3.7.5 implies that they are comparable for rotation $k = 0, 1, 2, 8, 9, 10, 11$.
$K_{\mathrm{rot}(k)}$ and $J_{\mathrm{rot}(k)}$ are comparable for rotation $k = 2, 3, 4, 5, 6, 7, 11$. Hence the three subsets are not pairwise incomparable in the same rotation. For $k = 2$ this is because

$$J_{\mathrm{rot}(2)} = (8, 9, 10, 12) \prec_{\mathrm{rot}(2)} (5, 9, 10, 12) \prec_{\mathrm{rot}(2)} (4, 5, 9, 12) \prec_{\mathrm{rot}(2)} (4, 5, 7, 12) \prec_{\mathrm{rot}(2)} (4, 5, 6, 7) = K_{\mathrm{rot}(2)}$$

All of the relations hold since the r-subset of the union of two consecutive $(r-1)$-subsets contains the 12 which is the only element rotated and hence the sign is $-$ in $\sigma_{\mathrm{rot}(2)}$. The same chain but shifted holds for rotation $k = 3, 4, 5, 6$. For $k = 7$, the chain

$$J_{\mathrm{rot}(7)} = (3, 4, 5, 7) \prec_{\mathrm{rot}(7)} (2, 3, 5, 7) \prec_{\mathrm{rot}(7)} (2, 3, 5, 12) \prec_{\mathrm{rot}(7)} (1, 2, 3, 12) \prec_{\mathrm{rot}(7)} (1, 2, 11, 12) = K_{\mathrm{rot}(7)}$$

and for $k = 11$ the chain

$$J_{\mathrm{rot}(11)} = (1, 3, 11, 12) \prec_{\mathrm{rot}(11)} (1, 9, 11, 12) \prec_{\mathrm{rot}(11)} (9, 10, 11, 12) \prec_{\mathrm{rot}(11)} (8, 9, 10, 12) \prec_{\mathrm{rot}(11)} (7, 8, 9, 10) = K_{\mathrm{rot}(11)}$$

witnesses the comparability. □

Chapter 4

Classic Theorems from Convex Geometry in Simple Drawings

In this chapter, we discuss classic theorems from convex geometry such as Kirchberger's, Helly's, and Carathéodory's theorem and variants of the Erdős-Szekeres theorem in terms of the *convexity* hierarchy of simple drawings, which was developed by Arroyo, McQuillan, Richter, and Salazar [AMRS22]. For the definition of the layers, see Section 2.6. In particular we make use of the combinatorial structure of generalized signotopes as introduced in Section 2.4 which describe combinatorially the triangle orientations of simple drawings in the plane. The classic version of the theorems we consider in this chapter are originally in the setting of point sets in the plane or more generally in $\mathbb{R}^d$. When considering point sets in general position, connecting the points via straight-line segments yields a geometric drawing of the K_n. Hence the classic versions of the theorems for the plane imply a result for geometric drawings of the K_n. Moreover, generalizations of the classic theorems have been proven by Goodman and Pollack [GP82] who dualized the original statements and proved Radon's, Kirchberger's, Helly's and Carathéodory's Theorem for arrangements of pseudolines. As mentioned in their paper (cf. [GP82, Remark 5.2]) all statements can be formulated in terms of allowable sequences and hence transfer to pseudoconfiguration of points. By restricting the pseudolines to the segments of the curves between the two points, the results transfer to pseudolinear drawings. Recently, Keszegh [Kes23] developed a theory of pseudoconvex sets in the plane based on hypergraphs, which again turns out to be equivalent to rank 3 oriented matroids. He gives alternatives proofs for the mentioned theorems and discussed Helly's theorem in more detail.

Outline This chapter is mostly based on [BFS$^+$23b] and its conference version [BFS$^+$20]. The results are joint work with Stefan Felsner, Manfred Scheucher, Felix Schröder and Raphael Steiner. Section 4.4 is based on [BSS23b] and further unpublished joint work with Joachim Orthaber, Manfred Scheucher and Felix Schröder.
In Section 4.1, we use the structure of generalized signotopes to prove a version of Kirchberger's theorem for simple drawings in the plane. Section 4.2 deals with a generalization of Carathéodory's theorem to simple drawings and in Section 4.3, we present a family of simple drawings with arbitrarily large Helly number. In Section 4.4, we consider a variant of the classic Erdős-Szekeres theorem concerning empty k-gons, so called k-holes. The existence of holes of size $k \leq 6$ is known for points sets in the plane. Moreover, there are arbitrarily large points sets without 7-holes. For simple drawings, so far only empty triangles, i.e., 3-holes, have been studied. We generalize the notion of k-holes for simple drawings in the plane and discuss variants of the definition. In particular, we present arbitrarily large simple drawings without 4-holes and show that 6-holes exist in convex drawings.

4.1 Kirchberger's Theorem

Two closed sets $A, B \subseteq \mathbb{R}^d$ are called *separable* if there exists a hyperplane H separating them, i.e., $A \subset H_+$ and $B \subset H_-$ with H_+, H_- being the two closed half-spaces defined by H. It is well-known that, if two non-empty compact sets A, B are separable, then they can be separated by a hyperplane H containing points of A and B. *Kirchberger's theorem* [Kir03] asserts that two finite point sets $A, B \subseteq \mathbb{R}^d$ are separable if and only if for every $C \subseteq A \cup B$ with $|C| = d+2$, $C \cap A$ and $C \cap B$ are separable.
As mentioned above, Goodman and Pollack (cf. Theorem 4.8 and Remark 5.2 in [GP82]) proved Kirchberger's theorem for arrangements of pseudolines, which transfers to pseudolinear drawings of K_n. A version of Kirchberger's theorem for Complexes of oriented matroids has been shown in [HKK23].
The 2-dimensional version of Kirchberger's theorem can be formulated in terms of triple orientations which indicate whether a point lies on the right or left side of a chosen line. Note that for this we assign an orientation to the line and moreover, we assume that the point set is in general position as otherwise there could be a third point on a line. We show a generalization for simple drawings using the triangle orientations, which are encoded in generalized signotopes. For a generalized signotope γ on n elements, two sets $A, B \subseteq [n]$ are *separable* if there exist $i, j \in A \cup B$ such that $\gamma(i, j, x) = +$ for all $x \in A \setminus \{i, j\}$ and $\gamma(i, j, x) = -$ for all $x \in B \setminus \{i, j\}$. In this case we say that ij *separates* A from B and write $\gamma(i, j, A) = +$ and $\gamma(i, j, B) = -$. Moreover, if we can find $i \in A$ and $j \in B$, we say that A and B are *strongly separable*.

Theorem 4.1.1 (Kirchberger for Generalized Signotopes)**.** *Let $\gamma : [n]_3 \to \{+, -\}$ be a generalized signotope, and let $A, B \subseteq [n]$ be two non-empty sets. If for every $C \subseteq A \cup B$ with $|C| = 4$, the sets $A \cap C$ and $B \cap C$ are separable, then A and B are strongly separable.*

Since every simple drawing yields a generalized signotope (cf. Proposition 2.4.2), Theorem 4.1.1 implies Kirchberger's theorem for simple drawings of the complete graphs. In terms of simple drawings *separability* means that there exists an edge ij such that all triangles induced by i, j, a for $a \in A$ are oriented counterclockwise if the vertices appear in this particular order and all triangles induced by i, j, b for $b \in B$ are oriented clockwise.

Corollary 4.1.2 (Kirchberger for Simple Drawings)**.** *Let $\mathcal{D}$ be a simple drawing of the K_n in the plane whose vertices are partitioned into A and B. If for every $C \subseteq A \cup B$ with $|C| = 4$, the vertex sets $A \cap C$ and $B \cap C$ are separable, then there exist two vertices $a \in A$ and $b \in B$ such that the edge ab separates A from B.*

By the following lemma the roles of A and B are interchangeable even in the strong separating context.

Lemma 4.1.3. *Let γ be a generalized signotope on n elements partitioned into A and B. If there is a strong separator ab with $a \in A$ and $b \in B$ separating A from B, then ba strongly separates B from A.*

Proof. A strong separator ab fulfills $\gamma(a, b, A) = +$ and $\gamma(a, b, B) = -$. In this case it is $\gamma(b, a, B) = +$ and $\gamma(b, a, A) = -$ showing that ba is a strong separator separating B from A. □

On 4-tuples separability is the same as strong separability. This shows that we can assume that all 4-tuples are strongly separable.

Lemma 4.1.4. *Let $\gamma : [4]_3 \to \{+,-\}$ be a generalized signotope with $[4] = A \cup B$ a partition into two non-empty sets A and B. Then A and B are separable if and only if they are strongly separable.*

Proof. Clearly if A and B are strongly separable, they are separable. For the reverse direction we assume that $|A| \leq |B|$. Otherwise exchange the roles of A and B which is possible by Lemma 4.1.3. Assume A and B are separable. Table 4.1 and 4.2 show that in all separable generalized signotopes on $\{a, b_1, b_2, b_3\}$ and $\{a_1, a_2, b_1, b_2\}$, respectively, there is a strong separator of the sets $\{a\}$ and $\{b_1, b_2, b_3\}$ or $\{a_1, a_2\}$ and $\{b_1, b_2\}$, respectively. □

4.1.1 Reverse Direction

In the classic version of Kirchberger's theorem for point sets in $\mathbb{R}^d$, the converse statement of Theorem 4.1.1 is trivially true. A separating hyperplane for the point set separates all subsets. However, in the setting of generalized signotopes the reverse direction is no longer true. A separating pair ij for A, B is not necessarily contained in a 4-element subset $C \subset A \cup B$. In Figure 4.1(b), we provide a generalized signotope on 6 elements with a separator for a fixed partition into $A = \{1, 2\}$ and $B = \{3, 4, 5, 6\}$. However for the subset $C = \{2, 4, 5, 6\}$ the two sets $A \cap C = \{2\}$ and $B \cap C = \{4, 5, 6\}$ are not separable. Moreover, this generalized signotopes comes from a simple drawing, which is drawn in Figure 4.1(a). The edge marked bold separates the blue from the red vertices. However, the subdrawing of the K_4 marked with dashed edges has no separator.

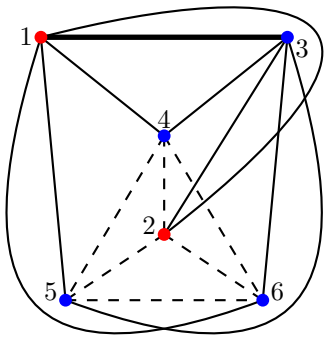

(a)

$\gamma(4,5,6)$	$=$	$+$	$\gamma(1,5,6)$	$=$	$-$
$\gamma(3,5,6)$	$=$	$-$	$\gamma(1,4,6)$	$=$	$-$
$\gamma(3,4,6)$	$=$	$-$	$\gamma(1,4,5)$	$=$	$-$
$\gamma(3,4,5)$	$=$	$-$	$\gamma(1,3,6)$	$=$	$-$
$\gamma(2,5,6)$	$=$	$-$	$\gamma(1,3,5)$	$=$	$-$
$\gamma(2,4,6)$	$=$	$-$	$\gamma(1,3,4)$	$=$	$-$
$\gamma(2,4,5)$	$=$	$+$	$\gamma(1,2,6)$	$=$	$-$
$\gamma(2,3,6)$	$=$	$-$	$\gamma(1,2,5)$	$=$	$-$
$\gamma(2,3,5)$	$=$	$-$	$\gamma(1,2,4)$	$=$	$-$
$\gamma(2,3,4)$	$=$	$+$	$\gamma(1,2,3)$	$=$	$-$

(b)

Figure 4.1: (a) Simple drawing showing that the reverse direction of Kirchberger is not true. The bold edge is a separator for the drawing on all 6 vertices. However, the subdrawing of the K_4 marked with the dashed edges has no separator. The vertices of A are marked red and the vertices of B blue. (b) Orientations of the drawing yielding the generalized signotope γ.

$\gamma(b_1,b_2,b_3)$	$\gamma(a,b_2,b_3)$	$\gamma(a,b_1,b_3)$	$\gamma(a,b_1,b_2)$	list of separators
+	+	+	+	$\underline{ab_3}, b_1a, b_1b_3$
−	+	+	+	$\underline{ab_3}, b_1a, b_1b_2, b_2b_3$
+	−	+	+	$\underline{ab_2}, b_1a, b_1b_3, b_3b_2$
−	−	+	+	$\underline{ab_2}, b_1a, b_1b_2$
+	+	−	+	(no separator)
+	−	−	+	$\underline{ab_2}, b_3a, b_3b_2$
−	−	−	+	$\underline{ab_2}, b_1b_2, b_3a, b_3b_1$
+	+	+	−	$\underline{ab_3}, b_1b_3, b_2a, b_2b_1$
−	+	+	−	$\underline{ab_3}, b_2a, b_2b_3$
−	−	+	−	(no separator)
+	+	−	−	$\underline{ab_1}, b_2a, b_2b_1$
−	+	−	−	$\underline{ab_1}, b_2a, b_2b_3, b_3b_1$
+	−	−	−	$\underline{ab_1}, b_2b_1, b_3a, b_3b_2$
−	−	−	−	$\underline{ab_1}, b_3a, b_3b_1$

Table 4.1: Separators for generalized signotopes on $\{a, b_1, b_2, b_3\}$. Strong separators are underlined.

$\gamma(a_2,b_1,b_2)$	$\gamma(a_1,b_1,b_2)$	$\gamma(a_1,a_2,b_2)$	$\gamma(a_1,a_2,b_1)$	list of separators
+	+	+	+	$a_2a_1, \underline{a_2b_2}, b_1a_1, b_1b_2$
−	+	+	+	$a_2a_1, \underline{a_2b_1}, b_1a_1$
+	−	+	+	$a_2a_1, \underline{a_2b_2}, b_2a_1$
−	−	+	+	$a_2a_1, \underline{a_2b_1}, b_2a_1, b_2b_1$
+	+	−	+	$\underline{a_1b_2}, b_1a_1, b_1b_2$
+	−	−	+	(no separator)
−	−	−	+	$\underline{a_2b_1}, b_2a_2, b_2b_1$
+	+	+	−	$\underline{a_2b_2}, b_1a_2, b_1b_2$
−	+	+	−	(no separator)
−	−	+	−	$\underline{a_1b_1}, b_2a_1, b_2b_1$
+	+	−	−	$a_1a_2, \underline{a_1b_2}, b_1a_2, b_1b_2$
−	+	−	−	$a_1a_2, \underline{a_1b_2}, b_2a_2$
+	−	−	−	$a_1a_2, \underline{a_1b_1}, b_1a_2$
−	−	−	−	$a_1a_2, \underline{a_1b_1}, b_2a_2, b_2b_1$

Table 4.2: Separators for generalized signotopes on $\{a_1, a_2, b_1, b_2\}$. Strong separators are underlined.

4.1.2 Proof in Point Sets

In order to make the proof of Theorem 4.1.1 more accessible we first discuss the proof idea which is based on induction in the geometric setting and analyze which of the given structures already help us in the more abstract setting of generalized signotopes. This already covers some parts of the proof. However, we give a full proof for Theorem 4.1.1 using only the notion of generalized signotopes in Section 4.1.3.

Let P be a point set in general position, whose points are partitioned into A and B. For the illustration we assume that the points of A are colored red and the points of B are colored blue. A separating line in the plane for the geometric setting is a line l such that all points from A are in one half-plane spanned by l and the points of B in the other half-plane. The definition of a strong separation of generalized signotopes in the setting of point sets is a separating line l spanned by one point of A and one point of B. Clearly a set of points in general position has a separating line if and only if there exists a line containing a point of A and a point of B. Further we give the separating line a direction and show that there is a line spanned by a point $a \in A$ and a point $b \in B$ such that all other points of A are on the left side of the line when orienting the line from a to b. This oriented line is denoted by $\overrightarrow{ab}$. If $\overrightarrow{ab}$ is a separator, A is on the left-hand side of $\overrightarrow{ab}$ and B is on right-hand side of $\overrightarrow{ab}$. Note that if x is right of $\overrightarrow{ab}$ then the triangle a, b, x is oriented clockwise and hence a is right of $\overrightarrow{bx}$ and b is right of $\overrightarrow{xa}$.
Throughout the proof we assume that all 4-element subsets are separable. Without loss of generality we assume that $|A| \leq |B|$. We prove the statement using induction on the size of the set A.

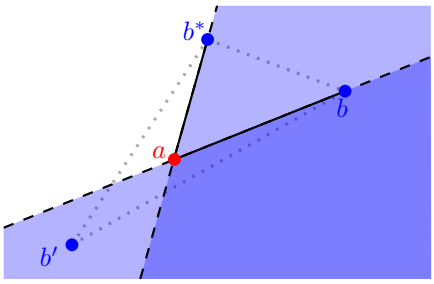

$$\begin{aligned} \gamma(a, b, B') &= - \\ \gamma(a, b, b^*) &= + \\ \gamma(a, b^*, b') &= + \end{aligned}$$

$a, b, b^*, b' :$ $\quad + + - +$

no separator

Figure 4.2: Illustration of the proof in the geometric setting, with only one red vertex, together with the implied orientations.

For the induction base, let A consists of exactly one point a. For every $b \in B$, let $N(b)$ be the number of points $b' \in B$ which are on the right-hand side of the $\overrightarrow{ab}$. Let $b \in B$ be a point which maximizes the value $N(b)$. Let B' be the set of points right of $\overrightarrow{ab}$ including b itself. Assume $\{a\}$ is not separable from B. Then $B' \subsetneq B$ and hence there is $b^* \in B \backslash B'$ which is left of $\overrightarrow{ab}$. If all elements of B', which are on the right-hand side of the line $\overrightarrow{ab}$, are on the right-hand side of $\overrightarrow{ab^*}$, then $N(b^*) \geq N(b) + 1$. A contradiction to the maximality assumption of $N(b)$. Hence there is a vertex $b' \in B'$ which is on the right-hand side of $\overrightarrow{ab}$ but on the left-hand side of $\overrightarrow{ab^*}$. This implies that a is left of $\overrightarrow{b^*b'}$ and $\overrightarrow{b'b}$. Moreover, b^* is left of $\overrightarrow{ab}$ and hence a is left of $\overrightarrow{bb^*}$. This implies that a is in the convex hull of b, b', b^*. This is a contradiction to the assumption that all 4-tuples are separable. For an illustration see Figure 4.2.

Since the point set is in general position, it holds:

- For every $a \in A$ there is exactly one $b = b(a) \in B$ such that $\overrightarrow{ab}$ separates $\{a\}$ from B.

In the above proof, we only used the triple orientations and hence the result transfers to generalized signotopes. The summary of the triple orientations is given in Figure 4.2. By assumption all points of B' are right of $\overrightarrow{ab}$. For all elements b' of B' the triple a, b, b' is oriented clockwise, i.e., $\gamma(a, b, B') = -$. Furthermore there is a vertex $b^* \in B \backslash B'$ with $\gamma(a, b, b^*) = +$, otherwise, we are done. By the choice of b, we assumed that there exists $b' \in B'$ such that $\gamma(a, b^*, b') = +$. This shows that the sign sequence induced by the four element subset $\{a, b, b^*, b'\}$ is $?+-+$. Here "?" denotes that the triple orientation is not known. By the properties of a generalized signotope it is $\gamma(b, b^*, b') = +$ to avoid the alternating sign pattern. Hence the considered subset has no separator, see Table 4.1. This shows that the induction base works analogously for generalized signotopes.

For the induction step, assume that $|A| \geq 2$ and every set of $|A| - 1$ points is separable from B. Let $A' = A \backslash \{a^*\}$ be a subset of A with $|A| - 1$ points. By induction hypothesis, there are points $a \in A'$ and $b \in B$ such that all elements from A' are left of $\overrightarrow{ab}$ and all elements from B are right of $\overrightarrow{ab}$.
If a^* is left of $\overrightarrow{ab}$, the line $\overrightarrow{ab}$ is the separator. Assume that a^* is right of $\overrightarrow{ab}$. Then there is a unique $b^* = b(a^*)$ such that a^*b^* separates separates $\{a^*\}$ from B. We consider the following three cases:

(i) Assume $b^* = b$. In this case a is left of $\overrightarrow{a^*b}$ and all elements from B are on the right-hand side. If all elements from A are left of $\overrightarrow{a^*b}$, we have a separator. Otherwise there is a vertex a' which is left of $\overrightarrow{ab}$ but right of $\overrightarrow{a^*b}$. See Figure 4.3 for an illustration. In this case b is in the convex hull of a, a^*, a' which is a contradiction to the assumption that all 4-element subsets are separable.

(ii) Assume $b^* \neq b$ and a is right of $\overrightarrow{a^*b^*}$. Then the four points a, b, a^*, b^* are not separable. Since there is exactly one possibility to separate a single element from A from a subset of B, the only possible separators of the subset $\{a, a^*, b, b^*\}$ are ab and a^*b^*. By the assumption they do not separate. A contradiction to the assumption. For an illustration, see Figure 4.4.

(iii) Assume $b^* \neq b$ and a is left of $\overrightarrow{a^*b^*}$. If all points of A' are left of $\overrightarrow{ab}$ and left of $\overrightarrow{a^*b^*}$, the separator line is a^*b^*. Otherwise there is a vertex $a' \in A'$ which is left of $\overrightarrow{ab}$ and right of $\overrightarrow{a^*b^*}$, see Figure 4.5. The fact that a' is left of the line $\overrightarrow{ab}$ and right of the line $\overrightarrow{a^*b^*}$ implies that the line-segment from a^* to the crossing of the two lines is contained in the convex hull of a, a^*, a'. Since B^* is right of $\overrightarrow{ab}$, the point b^* is on this line segment. Hence b^* is in the convex hull of a, a^*, a'. Again a contradiction.

As in the induction base, we check whether the triple orientation given through our assumptions in the three different cases are sufficient to prove Kirchberger's theorem for generalized signotopes. Note that all triple orientations are summarized next to the corresponding figures. For all three cases we have the following signs. Since $\overrightarrow{ab}$ separates A' from B, it holds $\gamma(a, b, B) = -$ and $\gamma(a, b, A') = +$. Furthermore if a^* is left of $\overrightarrow{ab}$, i.e., $\gamma(a, b, a^*) = +$, we have a separator,

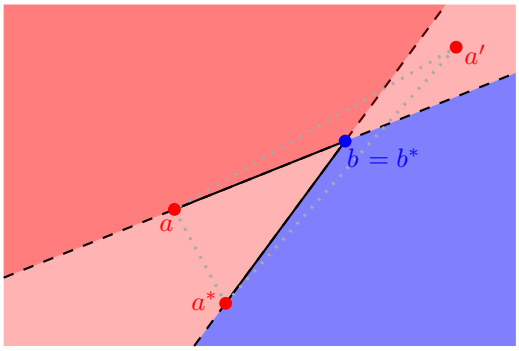

$$\begin{aligned}\gamma(a,b,B) &= -\\ \gamma(a,b,A') &= +\\ \gamma(a,b,a^*) &= -\\ \gamma(a^*,b,B) &= -\\ \gamma(a^*,b,a') &= -\end{aligned}$$

$a, a^*, a', b:$ $+-++$

no separator

Figure 4.3: Illustration of case (i), where $b = b^*$ in the geometric version of the induction step. In this case $b^* = b$ with the given orientations. In the depicted case there is no separator of the four points since b is in the convex hull of a, a^*, and a'.

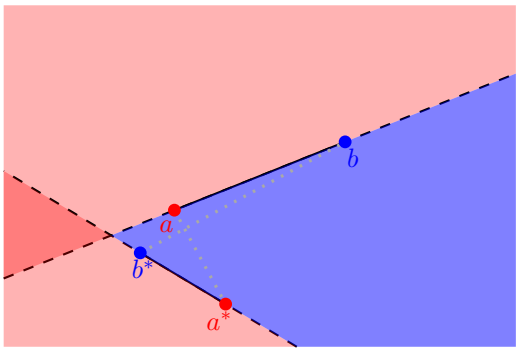

$$\begin{aligned}\gamma(a,b,B) &= -\\ \gamma(a,b,A') &= +\\ \gamma(a,b,a^*) &= -\\ \gamma(a^*,b^*,B) &= -\\ \gamma(a^*,b^*,a) &= -\end{aligned}$$

$a, a^*, b, b^*:$ $+--+$

no separator

Figure 4.4: Illustration of second case (ii) of the geometric version together with the given orientations. We assume $b^* \neq b$ and a is right of $\overrightarrow{a^*b^*}$. In this case there is no separator of the four depicted elements as the convex hull of a and a^* intersects the convex hull of b and b^*.

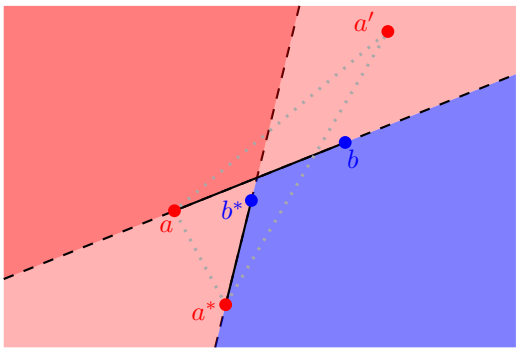

$$\begin{aligned}\gamma(a,b,B) &= -\\ \gamma(a,b,A') &= +\\ \gamma(a,b,a^*) &= -\\ \gamma(a^*,b^*,B) &= -\\ \gamma(a^*,b^*,a) &= +\\ \gamma(a^*,b^*,a') &= -\end{aligned}$$

$a, a^*, a', b:$ $+?+?$

Figure 4.5: Case (iii) of the geometric version of the proof. It is $b^* \neq b$ and a is left of $\overrightarrow{a^*b^*}$. The only case where we have no separator is the case depicted above. In this case b^* is in the convex hull of a, a^*, and a'. In this case, there could be still a separator in the setting of generalized signotopes.

and hence we only consider the case $\gamma(a, b, a^*) = -$. For the three cases, we get the following additional conditions.

(i) If $b = b^*$, by definition it holds $\gamma(a^*, b, B) = -$. In the non-trivial case there is a vertex a' with $\gamma(a^*, b, a') = -$. This shows that the packet consisting of a, a^*, a', b has the sign sequence $+-+?$. To avoid $+-+-$, it is $\gamma(a, a^*, a') = +$. However this 4-element subset has no separator, see Table 4.1.

(ii) For the second case, it is $b \neq b^*$ and by definition all elements from B are right of $\overrightarrow{a^*b^*}$ and hence $\gamma(a^*, b^*, B) = -$. Furthermore, we assume that a is to the right of $\overrightarrow{a^*b^*}$, which gives the triple orientation $\gamma(a^*, b^*, a) = -$. The four element subset $\{a, a^*, b, b^*\}$ has the sign sequence $+--+$. Using Table 4.2, we see that this packet has no separator.

(iii) As in the previous case, we assume $b^* \neq b$ and $\gamma(a^*, b^*, B) = -$. Moreover, the point a is to the left of $\overrightarrow{a^*b^*}$, which gives $\gamma(a^*, b^*, a) = +$. In the non-trivial case, there is an $a' \in A'$ which is right of $\overrightarrow{a^*b^*}$. This translates into the sign $\gamma(a^*, b^*, a') = -$. As suggested in the proof of the geometric setting, we look at the 4 elements a, a^*, a', b^* whose sign sequence is $+?+?$.

In contrast to the geometric case,there is not enough information to show that this four element subset is not separable. In a simple drawing of this subconfiguration, the edge aa' could be drawn differently, see Figure 4.6. In this case, the four elements have a separator which is $a'b^*$ marked with a fat line.

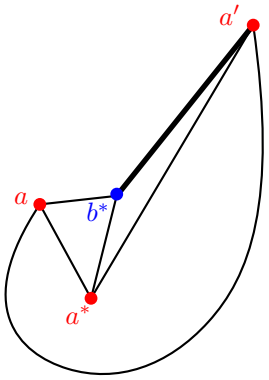

Figure 4.6: Illustration of a possible drawing where $\gamma(a^*, b^*, a) = +$ and $\gamma(a^*, b^*, a') = -$. However in contrast to the geometric setting (see Figure 4.5), where b^* is in the convex hull of a, a^*, a', the edge $a'b^*$ is a separator for this 4-element subset.

4.1.3 Proof of Kirchberger's Theorem for Generalized Signotopes (Theorem 4.1.1)

By Lemma 4.1.4, we assume that all 4-tuples from $A \cup B$ are strongly separable. Moreover, by symmetry we assume $|A| \leq |B|$. First we consider the cases $|A| = 1, 2, 3$ individually and then the case $|A| \geq 4$.

Let $A = \{a\}$, let B' be a maximal subset of B such that B' is strongly separated from $\{a\}$, and let $b \in B'$ be such that $\gamma(a, b, B') = -$. Suppose that $B' \neq B$, then there is a $b^* \in B \backslash B'$ with

$$\gamma(a, b, b^*) = +. \tag{4.1}$$

By maximality of B' we cannot use the pair a, b^* for a strong separation of $\{a\}$ and $B' \cup \{b^*\}$. Hence, for some $b' \in B'$:

$$\gamma(a, b^*, b') = +. \tag{4.2}$$

Since γ is alternating (4.1) and (4.2) together imply $b' \neq b$. Since $b' \in B'$ we have $\gamma(a, b, b') = -$. From this together with (4.1), (4.2), and Table 4.1 it follows that the four-element set $\{a, b, b', b^*\}$ has no separator. This is a contradiction, hence $B' = B$.

As a consequence we obtain:

- Every one-element set $\{a\}$ with $a \in A$ can be strongly separated from B. Since γ is alternating there is a unique $b(a) \in B$ such that $\gamma(a, b(a), B) = -$.

Now consider the case $A = \{a_1, a_2\}$. Let $b_i = b(a_i)$, i.e., $\gamma(a_i, b_i, B) = -$ for $i = 1, 2$. If $\gamma(a_1, b_1, a_2) = +$ or if $\gamma(a_2, b_2, a_1) = +$, then a_1b_1 or a_2b_2, respectively, is a strong separator for A and B. Therefore, we may assume that it holds $\gamma(a_1, b_1, a_2) = -$, and $\gamma(a_2, b_2, a_1) = -$. By the alternating property, it is $b_1 \neq b_2$. We get the sequence $+--+$ for the four-element set $\{a_1, a_2, b_1, b_2\}$ which has no strong separator (cf. Table 4.2), a contradiction.

Let $A = \{a_1, a_2, a_3\}$. Suppose that A is not separable from B. For $i = 1, 2, 3$, let $b_i = b(a_i)$, i.e., $\gamma(a_i, b_i, B) = -$. For $i, j \in \{1, 2, 3\}$, $i \neq j$ we define $s_{ij} = \gamma(a_i, b_i, a_j)$. Moreover, if $s_{ij} = +$ for some i and all $j \neq i$, then a_ib_i separates A from B. Hence, for each i there exists $j \neq i$ with $s_{ij} = -$.
If $s_{ij} = s_{ji} = -$ for some i, j, then since γ is alternating $b_i \neq b_j$ and the packet a_i, a_j, b_i, b_j corresponds to the sign sequence $+--+$ in Table 4.2. Hence there is no strong separator and at least one of s_{ij} and s_{ji} is $+$.
These two conditions imply that we can relabel the elements of A such that $s_{12} = s_{23} = s_{31} = +$ and $s_{13} = s_{21} = s_{32} = -$. Suppose that $b_i = b_j = b$ for $i, j \in \{1, 2, 3\}$ with $i \neq j$. Since $b \in \{b_1, b_2\}$ it is $\gamma(b, a_1, a_2) = \gamma(a_2, b_2, a_1) = -$ or $\gamma(b, a_1, a_2) = - \cdot \gamma(a_1, b_1, a_2) = -$. Similar, we get $\gamma(b, a_1, a_3) = +$ and $\gamma(b, a_2, a_3) = -$ which yields the sign pattern $?-+-$ for the packet b, a_1, a_2, a_3. Avoiding the alternating sign pattern, we get $--+-$. Table 4.1 shows there is no strong separator. This contradiction shows that b_1, b_2, b_3 must be pairwise distinct.
From $s_{32} = -$ and $s_{31} = +$ we find that b_3, a_1, a_2, a_3 corresponds to a row of type $?-+?$ in Table 4.1. Since every 4-element subset has a separator by assumption, we conclude that the strong separator of $\{b_3, a_1, a_2, a_3\}$ is a_2b_3. In both cases, it holds

$$\gamma(b_3, a_1, a_2) = +. \tag{4.3}$$

Now consider $\{a_1, a_2, b_1, b_3\}$. From $s_{12} = +$, equation (4.3), and $\gamma(a_1, b_1, b_3) = -$ we obtain the pattern $?-+-$. Since $+-+-$ is forbidden we obtain

$$\gamma(a_2, b_1, b_3) = -. \tag{4.4}$$

The set $\{a_2, a_3, b_1, b_3\}$ needs a strong separator. The candidate pair a_3b_1 is made impossible by $\gamma(a_3, b_1, b_3) = +$, a_3b_3 is made impossible by $s_{32} = -$, and a_2b_3 is made impossible by (4.4). Hence a_2b_1 is the strong separator and, in particular, it holds

$$\gamma(a_2, b_1, a_3) = +. \tag{4.5}$$

But now the set $\{a_1, a_2, a_3, b_1\}$ has no strong separator. The candidate pair a_1b_1 is impossible because of $s_{13} = -$, a_2b_1 does not separate because $s_{12} = +$, and (4.5) shows that a_3b_1 cannot separate the set. This contradiction proves the case $|A| = 3$.

For the remaining case $|A| \geq 4$ consider a counterexample (γ, A, B) minimizing the size of the smaller of the two sets. We have $4 \leq |A| \leq |B|$.
Let $a^* \in A$. By minimality $A' = A \backslash \{a^*\}$ is separable from B. Let $a \in A'$ and $b \in B$ such that $\gamma(a, b, A') = +$ and $\gamma(a, b, B) = -$. Hence

$$\gamma(a, b, a^*) = -. \tag{4.6}$$

Let $b^* = b(a^*)$, i.e., $\gamma(a^*, b^*, B) = -$. There is some $a' \in A'$ such that

$$\gamma(a^*, b^*, a') = -. \tag{4.7}$$

Assume $a' = a$, then $b \neq b^*$ because of (4.6) and (4.7). From (4.6), (4.7), $\gamma(a, b, B) = -$, and $\gamma(a^*, b^*, B) = -$ it follows that the four-element set $\{a, a^*, b, b^*\}$ has the sign pattern $+--+$, hence there is no separator, see Table 4.2. This shows that $a' \neq a$.
Let $b' = b(a')$. If $b \neq b'$ we look at the four elements $\{a, b, a', b'\}$. The packet corresponds to the sign sequence $-?-+$ so that we can conclude $\gamma(a, a', b') = -$ to avoid the forbidden pattern. If $b = b'$, then $a' \in A'$ implies $\gamma(a, b, a') = +$ which yields $\gamma(a', b', a) = \gamma(a', b, a) = -$.
Hence, regardless whether $b = b'$ or $b \neq b'$ we have

$$\gamma(a', b', a) = - \ . \tag{4.8}$$

Since $|A| \geq 4$, we know by the minimality of the instance (γ, A, B) that the set $\{a, b, a', b', a^*, b^*\}$, which has 3 elements of A and at least 1 element of B, is separable. It follows from $\gamma(a, b, B) = \gamma(a', b', B) = \gamma(a^*, b^*, B) = -$ that the only possible strong separators are ab, $a'b'$, and a^*b^*. They, however, do not separate because of (4.6), (4.7) and (4.8) respectively. This contradiction shows that there is no counterexample and Kirchberger's theorem holds in the setting of generalized signotopes.

4.2 Carathéodory's Theorem

Carathéodory's theorem asserts that, if a point x lies in the convex hull of a point set P in $\mathbb{R}^d$, then x lies in the convex hull of at most $d + 1$ points of P.
As already mentioned in the beginning of this chapter, Goodman and Pollack [GP82] proved a dual of Carathéodory's theorem, which transfers to pseudolinear drawings. A more general version in the plane is due to Balko, Fulek, and Kynčl [BFK15, Lemma 4.7], who provided a proof of Carathéodory's theorem for simple drawings of K_n. In this section, we present a shorter proof for their theorem. Recently Aichholzer, Chiu, Hoang, Hoffmann, Kynčl, Maus, Vogtenhuber and Weinberger [ACH+23] showed that our proof generalizes to simple drawings of complete multipartite graphs.

Theorem 4.2.1 (Carathéodory for Simple Drawings)**.** *Let $\mathcal{D}$ be a simple drawing of K_n in the plane and let $x \in \mathbb{R}^2$ be a point contained in a bounded connected component of $\mathbb{R}^2 - \mathcal{D}$. Then there is a triangle in $\mathcal{D}$ that contains x in the bounded side.*

Note that, in the classic version of Carathéodory's theorem for points in $\mathbb{R}^d$, the case $|A| = 1$ of Kirchberger's theorem implies Carathéodory's theorem, and vice versa. This is not true for the generalized versions. The vertex 1 in Figure 4.7 is in the triangle spanned by $2, 3, 4$. However, partitioning the four vertices into $A = \{1\}$ and $B = \{2, 3, 4\}$ gives a separating pair $(1, 2)$ because the triples $(1, 2, 3)$ and $(1, 2, 4)$ are oriented the same way.

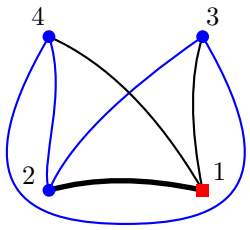

Figure 4.7: Example that Kirchberger's theorem with one red point does not imply Carathéodory's theorem for simple drawings. The vertex 1 is in region bounded by the blue triangle. However, there is still an edge separating the blue from the red vertices.

Proof. Suppose towards a contradiction that there is a pair $(\mathcal{D}, x)$ consisting of a simple drawing $\mathcal{D}$ of K_n and a point x in a bounded cell of the drawing, violating the claim. We choose $\mathcal{D}$ minimal with respect to the number of vertices n.
Let a be a vertex of the drawing. If we remove all incident edges of a from $\mathcal{D}$, then, by minimality of the example, x becomes a point of the outer cell. Therefore, if we remove the incident edges of a one by one, we find a last subdrawing $\mathcal{D}'$ such that x is still in a bounded cell. Let ab be an edge such that in the drawing $\mathcal{D}' - ab$ the point x is in the outer cell. Hence there is a simple curve P connecting x to infinity, which does not cross any of the edges in $\mathcal{D}' - ab$. By the choice of $\mathcal{D}'$, the curve P has at least one crossing with the edge ab. We choose P minimal with respect to the number of crossings with ab.

Claim 4.1. *P intersects ab exactly once.*

Proof. Suppose that P crosses ab more than once. Then there is a *lense* C formed by P and ab, that is, two crossings of P and ab such that the simple closed curve ∂C, composed of a connected subcurve P_1 of P and a part P_2 of the edge ab between the crossings, encloses a simply connected region C, see Figure 4.8(a).
Now consider the simple curve P' from x to infinity which is obtained from P by replacing the subcurve P_1 by a curve P_2' which is a close copy of P_2 in the sense that it has the same crossing pattern with all edges in $\mathcal{D}$ and the same simple properties, but is disjoint from ab. As P was chosen minimal with respect to the number of crossings with ab, there has to be an edge e of the drawing $\mathcal{D}'$ that intersects P_2' and by the choice of P_2' also P_2. By construction, this edge e has no crossing with P and crosses ab at most once. Hence one of its endpoints is inside the lense C and one outside C. If $b \in C$, we choose c_1 to be the endpoint of e which is not in C and if $b \notin C$, we choose the endpoint of e which is in C. Hence the edge bc_1 in $\mathcal{D}'$ intersects ∂C. But since they are adjacent, bc_1 cannot intersect ab and by the choice of P it does not intersect P.

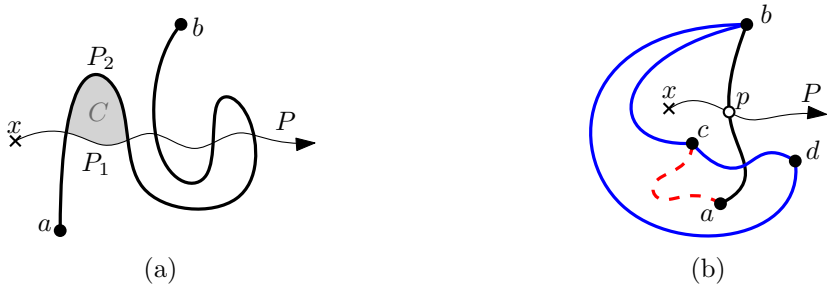

Figure 4.8: (a) and (b) give an illustration of the proof of Theorem 4.2.1.

A contradiction. This shows that P crosses ab in a unique point p. ■

If a has another neighbor c_2 in the drawing $\mathcal{D}'$ then, since only edges incident to a have been removed there is an edge connecting b to c_2 in $\mathcal{D}'$. Both edges ac_2 and bc_2 do not cross P, so x is in the interior of the triangle spanned by a, b, c_2, which is a contradiction to the assumption that $(\mathcal{D}, x)$ is a counterexample.
Hence there is no edge ac_2 in $\mathcal{D}'$ and $\deg(a) = 1$ in $\mathcal{D}'$. As x is not in the outer cell of $\mathcal{D}'$, there must be an edge cd in $\mathcal{D}'$ which intersects the partial segment of the edge ab starting in a and ending in the unique crossing point p of P and ab, in its interior. Let c be the vertex on the same side of ab as x; see Figure 4.8(b). The edges bc and bd of $\mathcal{D}'$ cross neither P nor ab. Consequently, the triangle spanned by b, c, d (drawn blue) must contain a in its interior.

Claim 4.2. *The edge ac in the original drawing $\mathcal{D}$ (drawn red dashed) lies completely in the bounded side of the triangle spanned by b, c, d.*

Proof. The bounded region defined by the edges ab, cd, and bd of $\mathcal{D}'$ contains a and c. Since $\mathcal{D}$ is a simple drawing, ac has no crossing with ab and cd. This implies ac has an even number of crossings with bd. Since the drawing is simple, ab has no crossing with bd, which proves the claim. ■

Now the curve P does not intersect ac, and the only edge of the triangle induced by a, b, c intersected by P is ab. Therefore, x lies in the interior of the triangle spanned by a, b, c. This contradicts the assumption that $(\mathcal{D}, x)$ is a counterexample. □

4.2.1 Colorful Carathéodory Theorem

Bárány [Bár82] generalized Carathéodory's theorem as follows: Given finite point sets $P_0, \ldots, P_d$ from $\mathbb{R}^d$ such that there is a point $x \in \text{conv}(P_0) \cap \ldots \cap \text{conv}(P_d)$, then x lies in a simplex spanned by $d+1$ points $p_0 \in P_0, \ldots, p_d \in P_d$. The sets P_i are often referred to as colors and hence we call such a simplex *colorful*. The theorem is known as the *Colorful Carathéodory theorem*. Choosing $P_0 = \ldots = P_d$ gives the classic statement of Carathéodory's theorem.
A strengthening, known as the *Strong Colorful Carathéodory theorem*, was shown by Holmsen, Pach and Tverberg [HPT08] and independently by Arocha et al. [ABB+09]: It is sufficient if there is a point x with $x \in \text{conv}(P_i \cup P_j)$ for all $i \neq j$, to find a colorful simplex. The Strong Colorful Carathéodory theorem was further generalized to oriented matroids by Holmsen [Hol16]. In particular, the theorem applies to pseudolinear drawings which are in correspondence with oriented matroids of rank 3.

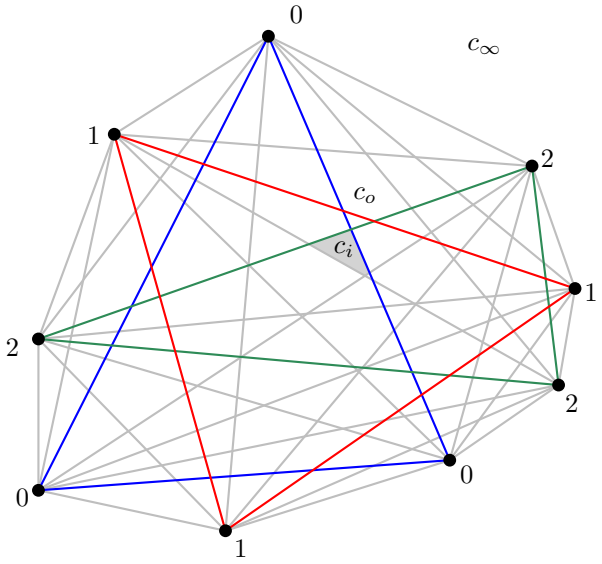

Figure 4.9: A f-convex drawings of K_9. If the cell c_o is chosen as the outer cell, then Colorful Carathéodory theorem does not hold for the colored triangles and every point x from the cell c_i. To obtain a pseudolinear drawing, the cell c_∞ has to be the unbounded cell.

Holmsen's proof [Hol16] uses sophisticated methods from topology. However, Bárány's algorithmic proof [Bár82] of the Colorful Carathéodory theorem can be adapted to pseudoconfigurations of points in the plane. Instead of the Euclidean distance, one can use a discrete metric that counts the minimum number of cells to traverse. In the following we give a sketch.
Start with an arbitrary colorful triangle T. If x is in the bounded side of the chosen triangle T, we are done. Otherwise, we choose a shortest path from x to the bounded side of the current colorful triangle T. In Bárány's original proof the shortest path is considered as the Euclidean distance. In the setting of pseudoconfiguration of points this is not a precise measure. Instead, we measure the distance by the number of edges we cross. Let P be the shortest path from x to the bounded side of T. Then P crosses exactly one of the triangle edges of T. Let e be this edge. Since T is colorful, the two endpoints of T have two different colors. The third vertex v_k of the triangle has the remaining third color k considered. By assumption x is contained in a bounded cell of the subdrawing induced by all vertices of color k. Using Carathéodory's theorem this implies that there is a triangle spanned by three vertices of color k, such that x is contained in the bounded side. Moreover the shortest path in a pseudoline arrangement crosses every pseudoline at most once (cf. [BLS$^+$99, Proposition 4.2.3]). Hence there is a vertex v'_k which is in the halfspace of the pseudoline spanned by e which does not contain v_k. Clearly the triangle T' spanned by the vertex v'_k and the two endvertices of e is again colorful. Moreover, the length of the shortest path P' from x to the interior of T' decreases since we can take P and remove the crossing with the edge e. We proceed in a similar way. Since the distance decreases in every step, we achieve distance 0 after a finite number of steps, which yields a colorful triangle containing x.

The following result shows that in the convexity hierarchy of simple drawings of K_n the Colorful Carathéodory theorem is not valid beyond the class of pseudolinear drawings.

Proposition 4.2.2. *There exists a f-convex drawing of the K_9, whose vertices are colored with three colors and a point x in the bounded side of each of the three monochromatic triangle, but there is no colorful triangle containing x.*

Proof. The drawing depicted in Figure 4.9 is a geometric drawing. By changing the outer cell from c_∞ to c_o the drawing remains f-convex, see Observation 2.6.1. Let x be an arbitrary point from the cell c_i. The point x is contained in the three monochromatic triangles and is separated from the outer cell only by three monochromatic edges. Therefore, there is no triangle in the drawing spanned by a red, a green, and a blue point such that x is contained in the triangle formed by these three points. □

4.3 Helly's Theorem

The *Helly number* of a family of sets $\mathcal{F}$ with empty intersection is the size of the smallest subfamily of $\mathcal{F}$ with empty intersection. *Helly's theorem* asserts that the Helly number of a family of n convex sets $S_1, \ldots, S_n$ from $\mathbb{R}^d$ is at most $d+1$, i.e., the intersection of $S_1, \ldots, S_n$ is non-empty if the intersection of every subfamily of size $d+1$ is non-empty [Hel30].
In the following we discuss the Helly number in the context of simple drawings and the convexity hierarchy. For this we assume that the sets S_i are the bounded sides of triangles of the drawing in the plane.
From the results of Goodman and Pollack [GP82] it follows that Helly's theorem generalizes to pseudoconfigurations of points in two dimensions, and thus for pseudolinear drawings. A more general version of Helly's theorem was shown by Bachem and Wanka [BW88]. They prove Helly's and Radon's theorem for oriented matroids with the "intersection property" (i.e. the existence of an adjoint). All oriented matroids of rank 3 have this property since they have a representation as pseudoline arrangements and as pseudoconfiguration of points. Hence both theorems, Helly's and Radon's hold for pseudolinear drawings. We discuss Radon's theorem in more detail in Section 4.5.

We show that Helly's theorem does not hold for f-convex drawings. Moreover, the Helly number can be arbitrarily large in f-convex drawings. Note that the following proposition does not contradict the Topological Helly theorem (see [Hel30] for connected sets and [GPP$^+$17] for a connection to the Betti-numbers) because in our construction the number of connected components of the intersection can grow arbitrarily large. More precisely, if the number of triangles n is even, the intersection of the $n/2$ triangles with even index has $n/2$ connected components, see Figure 4.10 for an illustration.

Proposition 4.3.1. *For every integer $n \geq 3$, there exists an f-convex drawing of K_{3n} in the plane whose Helly number is at least n, i.e., there are n triangles such that the bounded sides of any $n-1$ triangles have a common interior point, but the intersection of the bounded sides of all n triangles is empty. In particular, Helly's theorem does not generalize to f-convex drawings.*

Proof. Consider the geometric drawing $\mathcal{D}$ of K_{3n} with n triangles T_i as shown for the case $n = 7$ in Figure 4.10. All edges are drawn straight-line. Let $\mathcal{D}'$ be the drawing obtained from $\mathcal{D}$ by making the cell c_o the outer cell. Since it arises from a geometric drawing by changing the outer cell, $\mathcal{D}'$ is f-convex. Let B_i be the side of T_i that is bounded in $\mathcal{D}'$. For $1 \leq i < n$ the set B_i corresponds to the unbounded side of T_i in $\mathcal{D}$ while B_n corresponds to the bounded side of T_n.

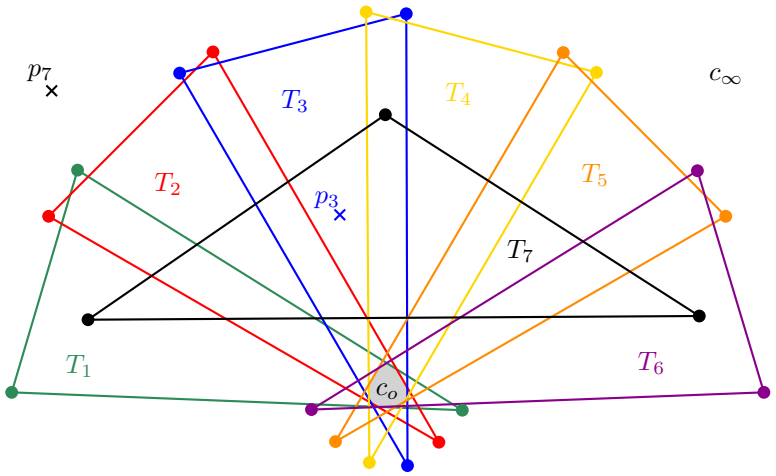

Figure 4.10: A drawing $\mathcal{D}$ of K_{21} is obtained by adding the remaining edges as straight-line segments. Making the gray cell c_o the outer cell, we obtain an f-convex drawing with Helly number 7. We omit some edges for sake of readability.[1]

In $\mathcal{D}'$ we have $\bigcap_{i=1}^{n-1} B_i \neq \emptyset$, indeed any point p_n which belongs to the outer cell of $\mathcal{D}$ is in this intersection. For each $i \in \{1, \ldots, n-1\}$ there is a point $p_i \in \bigcap_{j=1;j\neq i}^{n} B_j$ which is not in B_i. Since $B_n \subset \bigcup_{i=1}^{n-1} B_i^c$, we have $B_n \cap \bigcap_{i=1}^{n-1} B_i = \emptyset$, i.e., $\bigcap_{i=1}^{n} B_i = \emptyset$. In summary, the intersection of any $n-1$ of the n sets $B_1, \ldots, B_n$ is non-empty but the intersection of all of them is empty. □

4.3.1 Colorful Helly's Theorem

Lovász (cf. Bárány [Bár82]) generalized Helly's theorem as follows: Let $\mathcal{C}_0, \ldots, \mathcal{C}_d$ be families of compact convex sets from $\mathbb{R}^d$ such that for every "colorful" choice of sets $C_0 \in \mathcal{C}_0, \ldots, C_d \in \mathcal{C}_d$ the intersection $C_0 \cap \ldots \cap C_d$ is non-empty. Again the choice of $\mathcal{C}_0 = \ldots = \mathcal{C}_d$ implies the classic version of Helly's theorem. Then, for some k, the intersection $\bigcap \mathcal{C}_k$ is non-empty. This result is known as the *Colorful Helly theorem*. Kalai and Meshulam [KM05] presented a simple version of the Colorful Helly theorem, which, in particular, carries over to pseudolinear drawings. Since Helly's theorem does not generalize to f-convex drawings (cf. Proposition 4.3.1), neither does the Colorful Helly theorem.

4.4 Holes in Convex Drawings

This section is based on [BSS23b] and further unpublished research together with Joachim Orthaber, Manfred Scheucher and Felix Schröder.
Another classic theorem from convex geometry is the Erdős–Szekeres theorem [ES35]. It states that for every $k \in \mathbb{N}$ every sufficiently large point set P in general position contains a subset of k points which are the vertices of a convex polygon. Such a convex polygon with k vertices is called *k-gon*. The *Erdős–Szekeres number* is the smallest integer $ES(k)$ such that every set of $ES(k)$

[1] A special thanks goes to Patrick Schnider for his simplification of this construction.

points contains a k-gon. Erdős and Szekeres [ES35] showed the upper bound $ES(k) \leq \binom{2k-4}{k-2}+1$ and conjectured that it holds $ES(k) = 2^{k-2}+1$ for every $k \geq 2$. Later they proved the matching lower bound $ES(k) \geq 2^{k-2}+1$ [ES60]. The conjecture was verified for $k \leq 6$ by exhaustive computer search [SP06] and remains open for $k \geq 7$. The currently best known upper bound of $ES(k) \leq 2^{k+O(\sqrt{k \log k})}$ is due to Holmsen, Mojarrad, Pach, and Tardos [HMPT20] who improved the small error term of the break through result by Suk [Suk17]. While determining $ES(k)$ continues to be a challenging problem, various variants have attracted the attention of many researchers in the last decades.
A prominent variation of the Erdős–Szekeres theorem suggested by Erdős himself [Erd78] is about the existence of k-gons which do not contain vertices in the interior of their convex hull, so called *k-holes*. The existence of 5-holes in sufficiently large point sets was shown by Harborth [Har78]. An easier textbook proof can be found in Martoušek's book [Mat02]. Proposition 4.4.8 shows that the latter transfers to pseudolinear drawings. Moreover, Horton [Hor83] gives a construction of arbitrarily large point sets without a 7-hole. The case $k = 6$ remained open until Gerken [Ger08] and Nicolás [Nic07] proved independently the empty hexagon theorem, i.e., the existence of 6-holes for sufficiently large point sets. Gerken showed that every 9-gon in a point set yields a 6-hole while Nicolás showed that a 25-gon yields a 6-hole. The proof of Gerken only uses the order type of the point sets and not the exact coordinates and generalizes to pseudolinear drawings [Sch23].

We establish the notion of holes in simple drawings and investigate the existence of holes in various layers of the convexity hierarchy, see Section 2.6. The only case which was previously studied in simple drawings are empty triangles, i.e., 3-holes. A triangle is *empty* if one of its two sides does not contain any vertex in its interior. For simple drawings, Harborth [Har98] proved that there are at least two empty triangles and conjectured that the minimum among all simple drawings of K_n is $2n-4$. This is a tight upper bound which is witnessed by the twisted drawing $\mathcal{T}_n$ [Har98]. Recently García, Tejel, Vogtenhuber and Weinberger [GTVW22] showed that *generalized twisted drawings*, which is a class of simple drawings containing the twisted drawing $\mathcal{T}_n$, contain exactly $2n-4$ empty triangles. The best known lower bound is n which is due to Aichholzer, Hackl, Pilz, Ramos, Sacristán and Vogtenhuber [AHP+15]. In the geometric setting, the number of empty triangles behave differently: Every point set has $\Omega(n^2)$ empty triangles, and this bound is asymptotically optimal [BF87]. Note that the notion of empty triangles in point sets slightly differs from the one in simple drawings since the complement of the convex hull of a point set can be an empty triangle. The class of convex drawings behaves similarly to the geometric setting as the minimum number of empty triangles is asymptotically quadratic [AMRS18, Theorem 5].

To define k-holes in simple drawings, we first consider the notion of k-gons in simple drawings of the complete graph K_n. A *k-gon* is a subdrawing weakly isomorphic to the geometric drawing $\mathcal{C}_k$ of k points in convex position, see Figure 4.11(a). In terms of crossings, a k-gon $\mathcal{C}_k$ is a (sub)drawing with vertices $v_1, \ldots, v_k$ such that $\{v_i, v_\ell\}$ crosses $\{v_j, v_m\}$ for $i < j < \ell < m$. In contrast to the geometric setting where every sufficiently large geometric drawing contains a k-gon, simple drawings of complete graphs do not necessarily contain k-gons [Har98]. For example, the twisted drawing $\mathcal{T}_n$ depicted in Figure 4.11(b) does not contain a 5-gon. In terms of crossings, $\mathcal{T}_n$ can be characterized as a drawing of K_n with vertices $v_1, \ldots, v_n$ such that $\{v_i, v_m\}$ crosses $\{v_j, v_\ell\}$ for $i < j < \ell < m$. Even though there are arbitrarily large simple drawings with-

out a k-gon, a theorem by Pach, Solymosi and Tóth [PST03] states that every sufficiently large simple drawing of K_n contains $\mathcal{C}_k$ or $\mathcal{T}_k$. The currently best known estimate is due to Suk and Zeng [SZ22] who showed that every simple drawing of K_n with $n > 2^{9 \cdot \log_2(a) \log_2(b) a^2 b^2}$ contains $\mathcal{C}_a$ or $\mathcal{T}_b$. Since convex drawings do not contain $\mathcal{T}_5$ as a subdrawing, every convex drawing of K_n contains a k-gon $\mathcal{C}_k$ with $k = (\log_2 n)^{1/2-o(1)}$.

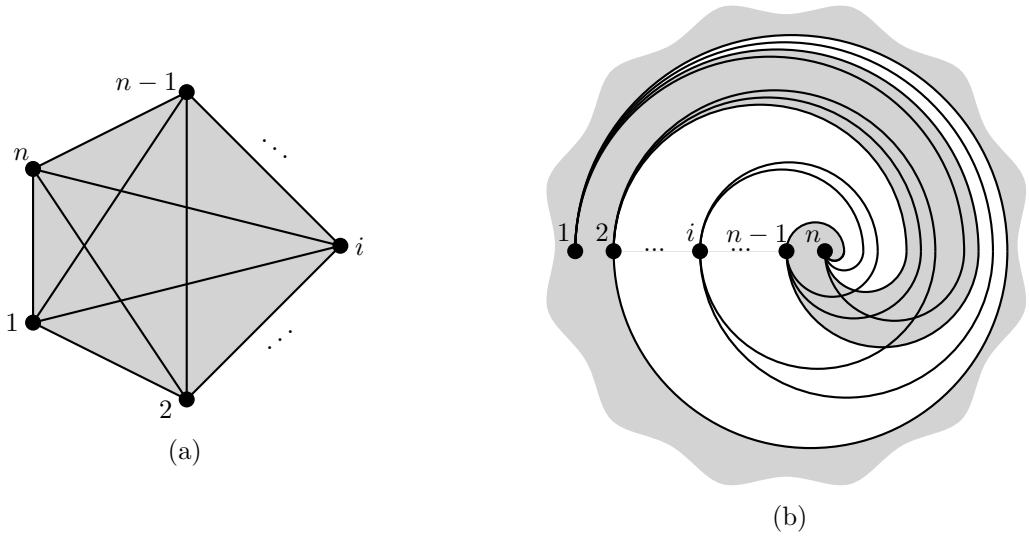

Figure 4.11: (a) The geometric drawing $\mathcal{C}_n$ with n points in convex position also referred to as n-gon. The convex side is drawn gray.
(b) The twisted drawing $\mathcal{T}_n$ which has exactly one 4-hole, whose convex side is drawn gray.

In the drawing $\mathcal{C}_k$ with $k \geq 4$, all triangles have exactly one empty side which is the unique convex side. The *convex side* of $\mathcal{C}_k$ is the union of the convex sides of its triangles; see the gray shaded region in Figure 4.11(a). Given a k-gon $\mathcal{C}_k$ in a simple drawing of K_n, we call vertices in its convex side *interior vertices*. Arroyo, McQuillan, Richter and Salazar [AMRS22, Section 3] started the investigations of interior vertices of k-gons in convex drawings and showed that edges from an interior vertex to a vertex of $\mathcal{C}_k$ and edges between two interior vertices are contained in the convex side of $\mathcal{C}_k$, which the concept of convexity of triangles.

Lemma 4.4.1 ([AMRS22, Lemma 3.5])**.** *Let $\mathcal{C}_k$ be a k-gon in a convex drawing of K_n with vertices $v_1, \ldots, v_k$ and $k \geq 4$. Then for each two vertices u, v contained in the convex side of $\mathcal{C}_k$ the edge $\{u, v\}$ is contained in the convex side of $\mathcal{C}_k$. Moreover, for each interior vertex u, the vertices $v_1, \ldots, v_k$ appear in this cyclic order in the rotation around the vertex u.*

We present a definition for k-holes in simple drawings for all $k \geq 3$.

Definition 4.4.2 (Holes in Simple Drawings)**.** *A* k-hole *in a simple drawing of K_n is a k-gon which has no interior vertices.*

For example, the vertices $1, 2, n-1, n$ form a 4-hole in $\mathcal{T}_n$ which is highlighted gray in Figure 4.11(b). In the following, we resolve the questions of the existence of 4-, 5- and 6-holes in simple and convex drawings.

4.4.1 Simple Drawings without a 4-Hole

The twisted drawing $\mathcal{T}_n$ with $n \geq 4$ depicted in Figure 2.14(b) has exactly $2n-4$ empty triangles which are spanned by the vertices $\{1, 2, i\}$ for $3 \leq i \leq n$ and $\{i, n-1, n\}$ for $1 \leq i \leq n-2$ [Har98]. Clearly a 4-hole $\{a, b, c, d\}$ implies that all triangles spanned by three of its vertices are empty. Indeed the drawing $\mathcal{T}_n$ has exactly one 4-hole, which is spanned by $\{1, 2, n-1, n\}$. However, in simple drawings the existence of 4-holes cannot be guaranteed.

For $n \geq 5$, let $\widetilde{\mathcal{T}_n}$ denote the simple drawing of K_n that is obtained by rerouting the edge $\{1, n\}$ in the drawing $\mathcal{T}_n$ as illustrated in Figure 4.12. More precisely, while in $\mathcal{T}_n$ the edge $\{1, n\}$ crosses every edge $\{i, j\}$ with $2 \leq i < j \leq n-1$, in $\widetilde{\mathcal{T}_n}$ it only crosses the edges $\{i, j\}$ with $2 \leq i < j \leq n-2$. Recall that the pairs of crossing edges determine the weak isomorphism class, see Theorem 2.5.5.

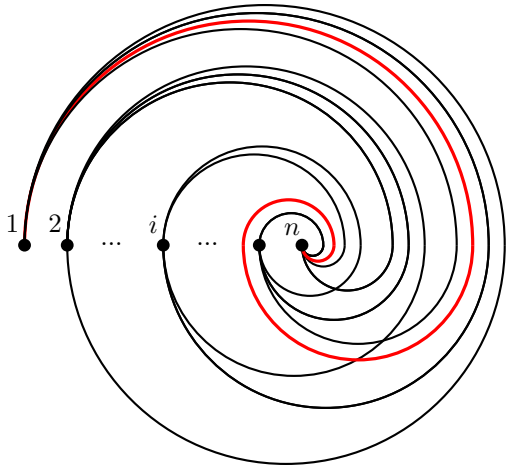

Figure 4.12: Illustration of $\widetilde{\mathcal{T}_n}$ without 4-holes. The edge $\{1, n\}$ is highlighted red.

Proposition 4.4.3. *For $n \geq 5$ the drawing $\widetilde{\mathcal{T}_n}$ does not contain a 4-hole.*

Proof. Rerouting the edge $\{1, n\}$ only affects the emptiness of triangles incident to both vertices 1 and n. More precisely, it only affects the vertex $n-1$ which changes the side of every triangle incident to $\{1, n\}$. In particular the triangle spanned by $\{1, 2, n\}$ is not empty in $\widetilde{\mathcal{T}_n}$. Hence $\{1, 2, n-1, n\}$ is not a 4-hole anymore. A new 4-hole would be of the form $\{1, a, b, n\}$ with $2 \leq a < b \leq n-1$ since the new empty triangles have to contain the vertices 1 and n. However $\{1, a, b\}$ is only empty if $a = 2 < b < n$ and $\{a, b, n\}$ is only empty if $1 < a < b = n-1$. Since no four vertices span four empty triangles, $\widetilde{\mathcal{T}_n}$ does not contain a 4-hole. □

4.4.2 Holes in Convex Drawings

In this section, we show that convex drawings behave similarly to geometric point sets when it comes to the existence of holes. We show that every sufficiently large convex drawing contains a 6-hole, and hence a 5-hole and a 4-hole.

Theorem 4.4.4 (Empty Hexagon theorem for Convex Drawings)**.** *Every convex drawing of K_n with sufficiently large n contains a 6-hole.*

Moreover, 6-holes are the largest unavoidable holes because the construction by Horton [Hor83] gives arbitrarily large point sets and hence convex drawings without 7-holes. Before we give the proof we discuss structural results of convex drawings.
For 4-holes, we show that there is a quadratic number of 4-holes in convex drawings, which generalizes a result by Bárány and Füredi [BF87, Lemma 11.1].

Theorem 4.4.5. *It holds* $h_4^{\text{conv}}(n) \geq \frac{n^2}{4} - O(n)$.

Proof. Let $\mathcal{D}$ be a convex drawing of K_n. We show that every edge which is crossed is a diagonal of a 4-hole in the sense that it is one of the crossing edges of the underlying 4-gon. Let e be an edge which is crossed by another edge f. The four endvertices of e and f build a 4-gon $\mathcal{C}_4$ in $\mathcal{D}$. We assume the vertices are labeled with v_1, v_2, v_3, v_4 such that $e = \{v_1, v_3\}$ and $f = \{v_2, v_4\}$. If $\mathcal{C}_4$ does not contain vertices in its interior it is empty and hence a 4-hole. Otherwise, let x be an interior vertex of $\mathcal{C}_4$ as illustrated in Figure 4.13.

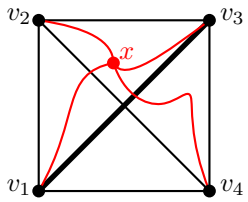

Figure 4.13: Illustration of the proof of Theorem 4.4.5.

By the properties of a 4-gon, x lies in the convex side of exactly two of its four triangles. Without loss of generality, we assume that x is in the convex side of the two triangles $\{v_1, v_2, v_3\}$ and $\{v_2, v_3, v_4\}$. By Lemma 4.4.1, all edges $\{x, v_i\}$ for $i = 1, 2, 3, 4$ are fully contained in the convex side of $\mathcal{C}_4$. Since the edge $\{x, v_4\}$ is fully contained in the convex side of the triangle spanned by $\{v_2, v_3, v_4\}$, but has to leave the triangle induced by $\{v_1, v_2, v_3\}$ to get to v_4, it crosses the edge $e = \{v_1, v_3\}$. Hence v_1, x, v_3, v_4 spans another 4-gon in which $\{v_1, v_3\}$ is one of the crossing edges. Furthermore, since the edges $\{x, v_1\}, \{x, v_2\}, \{x, v_3\}$ are contained in the convex side of $\mathcal{C}_4$, the convex side of the 4-gon spanned by $\{v_1, x, v_3, v_4\}$ is contained in the convex side of $\mathcal{C}_4$. Hence the number of interior vertices of this 4-gon is strictly smaller. Since n is finite, we can iteratively determine a smaller 4-gon with diagonal e until we reach a 4-hole with diagonal e.
Every drawing of K_n has $\binom{n}{2}$ edges and at most $2n - 2$ edges are uncrossed [Rin64], see also Section 5.2.4. Since every 4-hole has two diagonals, each 4-hole is counted twice. Altogether, the number of 4-holes in $\mathcal{D}$ is at least

$$\frac{1}{2}\left(\binom{n}{2} - 2n + 2\right) = \frac{1}{4}n^2 - \frac{5}{4}n + 1.$$

□

In the proof of Theorem 4.4.5, we used minimal 4-gons to show the existence of 4-holes with a particular diagonal. More generally, we consider *minimal* k-gons, i.e., k-gons whose convex side do not contain the convex side of another k-gon. For the sake of readability, we refer to the vertices $v_1, \ldots, v_k$ of a k-gon with indices modulo k.

Lemma 4.4.6. *Let $\mathcal{C}_k$ be a minimal k-gon in a convex drawing of K_n with vertices $v_1, \ldots, v_k$ and $k \geq 4$. Then for all $i = 1, \ldots, k$ there are no interior vertices in the convex sides of the triangles spanned by $\{v_i, v_{i+1}, v_{i+2}\}$.*

Proof. Assume towards a contradiction there is an interior vertex v in the convex side of the triangle determined by $\{v_i, v_{i+1}, v_{i+2}\}$. Clearly, the vertices $v_1, \ldots, v_i, v_{i+2}, \ldots, v_k$ span a $(k-1)$-gon and the triangle spanned by v_i, v, v_{i+2} is not contained in the convex side of that $(k-1)$-gon. In order to show that $v_1, \ldots, v_i, v, v_{i+2}, \ldots, v_k$ spans a k-gon, we need to show that the rotation system is the same as the one of $\mathcal{C}_k$. Let v_j for $j \in \{1, \ldots, i-1, i+3\}$ be one of the vertices of $\mathcal{C}_k$. By Lemma 4.4.1, the edge $\{v, v_j\}$ does not leave the convex side of $\mathcal{C}_k$ and the rotation of v is $v_1, \ldots, v_k$. Therefore, the edge $\{v, v_j\}$ has to enter v_j from the convex side of $\mathcal{C}_k$ in the rotation, which is the same as the convex side of the $(k-1)$-gon. Moreover, the convex side of the $(k-1)$-gon is entered by crossing the edge $\{v_i, v_{i+2}\}$. By the properties of a simple drawing the edge $\{v, v_j\}$ does not cross any of the edges adjacent to v_j. Hence v lies between v_i and v_{i+2} in the rotation around v_j. Figure 4.14 gives an illustration. Since this is the rotation system of a k-gon, we showed that $v_1, \ldots, v_i, v, v_{i+2}, \ldots, v_k$ span the k-gon $\mathcal{C}'_k$. Furthermore since no edge leaves the convex side of the k-gon, the convex side of the $\mathcal{C}'_k$ is contained in the convex side of $\mathcal{C}_k$ and hence $\mathcal{C}_k$ was not minimal – a contradiction. □

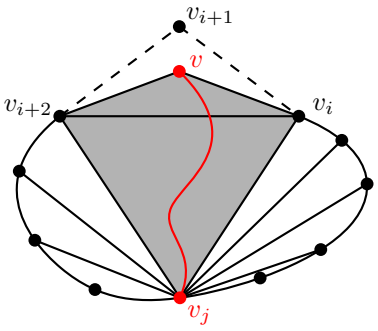

Figure 4.14: A k-gon with an interior vertex v in the convex side of the triangle spanned by v_i, v_{i+1}, v_{i+2}.

As it turns out minimal k-gons are useful to determine the existence of holes. The following theorem about the convex side of minimal k-gons might be of independent interest to transfer results on pseudolinear drawing to the more general setting of convex drawings.

Theorem 4.4.7. *Let $\mathcal{C}_k$ be a minimal k-gon in a convex drawing $\mathcal{D}$ of K_n with $n \geq k \geq 5$. Then the subdrawing induced by the vertices in the convex side of $\mathcal{C}_k$ is f-convex with the marked cell c_∞ not in the convex side of $\mathcal{C}_k$.*

Note that the statement of Theorem 4.4.7 does not hold without minimality assumption. Figure 4.15 shows an example of a 4-gon which is not minimal and the subdrawing induced by the convex side is not even h-convex.

Proof. Recall that a drawing is f-convex if there is a cell c_∞ such that, for every triangle the side not containing c_∞ is convex.
Let $\mathcal{C}_k$ be a minimal k-gon with vertices $v_1, \ldots, v_k$ in $\mathcal{D}$ and c_∞ be a cell in the non-convex side of the k-gon $\mathcal{C}_k$. The convex side of the triangles spanned by three vertices v_i, v_j, v_ℓ of

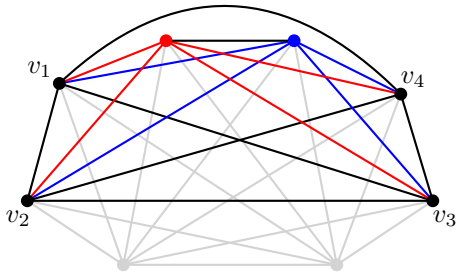

Figure 4.15: A 4-gon (black) which is not minimal and has two interior vertices (red and blue) such that the vertices in the convex side are not h-convex since it contains Π_6^{oh}.

the k-gon is the side not containing c_∞. Suppose towards a contradiction that there exists a triangle T determined by three vertices t_1, t_2, t_3 from the convex side of $\mathcal{C}_k$, such that the side not containing c_∞ is not convex. Hence the non-convex side S_N is contained in the convex side of $\mathcal{C}_k$. Since $\mathcal{D}$ is convex, the side S_C containing c_∞ and all vertices $v_1, \dots, v_k$ has to be convex. In the following we show that the three vertices t_1, t_2, t_3 are contained in the closure of a single cell of the subdrawing induced by $\mathcal{C}_k$. Assume towards a contradiction that this is not the case. Then some edge $\{v_i, v_j\}$ has a crossing with at least one of the triangle edges $\{t_\ell, t_m\}$. Since v_i and v_j are in the convex side S_C of the triangle T, this is a contradiction to the convexity. Hence S_N lies in the closure of a cell of $\mathcal{C}_k$.
By the minimality of $\mathcal{C}_k$ and Lemma 4.4.6, there are no interior vertices in the convex side of a triangle spanned by $\{v_i, v_{i+1}, v_{i+2}\}$. Moreover, since all cells in the convex side of $\mathcal{C}_k$ incident to the vertex v_{i+1} are inside this triangle, the vertex v_{i+1} is not part of T. This holds for every index i and hence the vertices t_1, t_2, t_3 are interior vertices of $\mathcal{C}_k$. Hence S_N lies in a cell of the convex side of $\mathcal{C}_k$, which is not covered by the convex side of one of the triangles spanned by $\{v_i, v_{i+1}, v_{i+2}\}$.
Since S_N is not convex, there exists a vertex z in the interior of S_N such that the subdrawing induced by $\{t_1, t_2, t_3, z\}$ has a crossing [AMRS22, Corollary 2.5]. We assume without loss of generality that the edge $\{t_1, z\}$ crosses $\{t_2, t_3\}$. Moreover, exactly one of the following two conditions holds:

- The triangle spanned by $\{t_1, t_3, z\}$ separates t_2 and c_∞.
- The triangle spanned by $\{t_1, t_2, z\}$ separates t_3 and c_∞.

Without loss of generality, we assume that the first case holds. Otherwise we exchange the roles of t_2 and t_3. Figure 4.16 gives an illustration.
Now we consider all edges from t_2 to the vertices $v_1, \dots, v_k$ of $\mathcal{C}_k$. Since S_C is convex and contains $v_1, \dots, v_k$, the edges $\{t_2, v_i\}$ are fully contained in S_C. This shows that none of the edges $\{t_2, v_i\}$ has a crossing with the boundary of T. In particular, they do not cross $\{t_1, t_3\}$.
The edges $\{t_2, v_1\}, \dots, \{t_2, v_k\}$ partition the convex side of $\mathcal{C}_k$ into triangles spanned by the three vertices t_2, v_i, v_{i+1} for $i = 1, \dots, k$. Hence there is an index i such that the three vertices t_1, t_3, z lie in one of the sides of the triangle spanned by $\{t_2, v_i, v_{i+1}\}$. The edge $\{v_i, v_{i+2}\}$ witnesses that the side of the triangle spanned by $\{t_2, v_i, v_{i+1}\}$ containing v_{i+2} is not convex. Moreover, the edge $\{t_1, z\}$ is not fully contained in the side containing t_1 and z. Hence the triangle spanned by $\{t_2, v_i, v_{i+1}\}$ has no convex side. A contradiction to the convexity. □

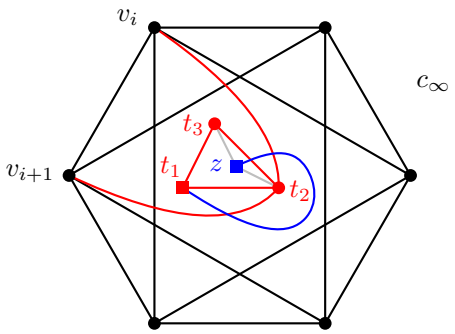

Figure 4.16: Illustration of the proof of Lemma 4.4.7. The vertices t_1, t_2, t_3 are highlighted red and vertex z is highlighted blue. The blue edge violates the convexity.

Using Theorem 4.4.7, the proof of Theorem 4.4.4 follows with the existence of k-gons and the existence of 6-holes in k-gons of pseudolinear drawings. The original proof of Gerken's empty hexagon theorem [Ger08] is in the geometric setting and shows that every 9-gon contains a 6-hole. The proof only uses the combinatorics of the point set and generalizes to pseudolinear drawings [Sch23]. Even though the existence of 6-holes directly implies the existence of 5-holes, when adapting the proof to 5-holes one obtains a better bound. Similarly as for the 6-holes, the proof for the existence of 5-holes in every 6-gon of a point set (see [Mat02, Section 3.2]) applies to pseudolinear drawings as it only uses triple orientations, which we give in the following.

Proposition 4.4.8. *Every pseudolinear drawing with a 6-gon contains a 5-hole.*

Proof. Let $\mathcal{D}$ be a pseudolinear drawing of K_n containing a 6-gon. We start with a minimal 6-gon $\mathcal{C}_6$ with vertices $v_1, \dots, v_6$. If $\mathcal{C}_6$ does not have interior points, we clearly have a 6-hole and hence a 5-hole. If $\mathcal{C}_6$ has exactly one interior vertex x, we consider the edge $\{v_1, v_4\}$ connecting two vertices through a diagonal. This diagonal is fully contained in the convex side of $\mathcal{C}_6$ and hence partitions the convex side into two parts. The vertex x is in one part and, together with the four vertices from the k-gon from the other part, it spans a 5-hole. For an illustration see Figure 4.17(a).
Let us now assume that $\mathcal{C}_6$ has at least two interior vertices. Let x, y be two interior vertices such that the remaining interior vertices are on the same side of the pseudoline ℓ extending the edge $\{x, y\}$. Note that this is possible since there is a notion of convex hull in the setting of pseudolinear drawings.
We now consider two different cases, depending on which two edges $\{v_i, v_{i+1}\}$ this pseudoline crosses to leave $\mathcal{C}_6$. If ℓ intersects two opposite edges of $\mathcal{C}_6$, then all other interior vertices lie on one side of this prolonged pseudoline. In this case there are three vertices of $\mathcal{C}_6$ which are on the opposite side as the remaining interior vertices. Those three vertices together with x, y determine a 5-hole; see Figure 4.17(b). Otherwise, if ℓ intersects two other boundary edges, there are at least four vertices of $\mathcal{C}_6$ on one of the two sides and hence there is a 6-gon with fewer interior vertices as illustrated in Figure 4.17(c) – a contradiction to the minimality of $\mathcal{C}_6$. □

We are finally ready to prove the main theorem of this section which is the existence of 6-holes in convex drawings. For this we use the existence of k-gons in large enough drawings, which imply the existence of a minimal k-gon and therefore we can apply the existence of holes in pseudolinear drawings.

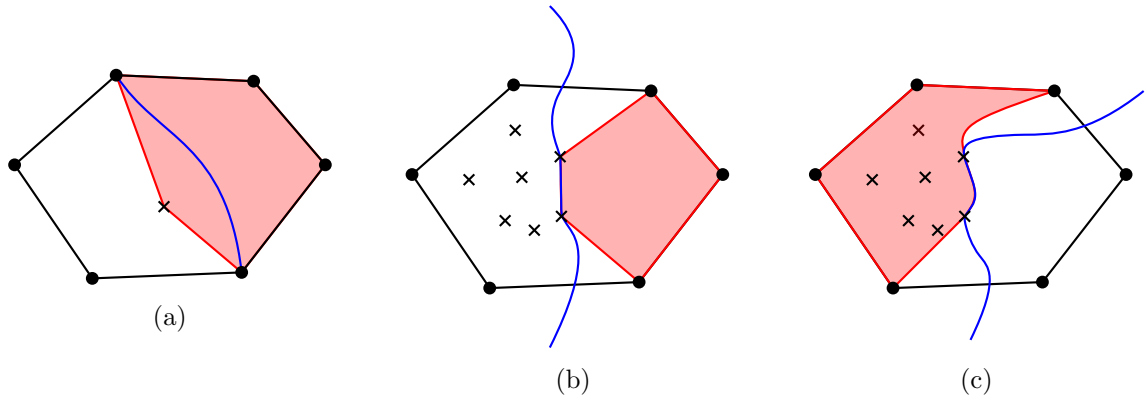

Figure 4.17: Illustration of the proof for the existence of 5-holes in pseudolinear drawings.

Proof of Theorem 4.4.4. Every convex drawing of K_n with $n > 2^{225\log_2(5)\cdot k^2\log_2(k)}$ contains a k-gon [SZ22]. In order to find a 6-hole, we apply this result for $k = 9$. (To find a 5-hole, we use $k = 6$.) Consider a minimal k-gon. By Lemma 4.4.7, the subdrawing induced by the vertices from the convex side of the k-gon is f-convex. Since the existence of holes is invariant under the choice of the outer cell, we can choose the cell containing c_∞ as the unbounded cell to make the subdrawing pseudolinear. Next we apply the results concerning the existence of a 6-hole (resp. 5-hole) in pseudolinear drawings and conclude that the subdrawing induced by the k-gon and the interior vertices contains a 6-hole (resp. 5-hole). This 6-hole (resp. 5-hole) in the subdrawing does not contain vertices of the original drawing of K_n since those vertices would be interior vertices of the k-gon. Therefore it is a 6-hole (resp. 5-hole) in the original drawing. This completes the argument. □

Even though the existence of 6-holes is shown, it remains to determine the minimal integer such that every drawing contains a 5-hole respectively, 6-hole. Let $h^{\text{conv}}(k)$ (resp. $h^{\text{geom}}(k)$) denote the smallest integer such that every convex (resp. geometric) drawing of size $n \geq h^{\text{conv}}(k)$ contains a k-hole. Every K_4 spanned by the four vertices of a crossing, contains a 4-hole (see Theorem 4.4.5). Hence it holds $h^{\text{conv}}(4) = h^{\text{geom}}(4) = 5$. In the geometric setting it holds $h^{\text{geom}}(5) = 10$ [Har78] and $30 \leq h^{\text{geom}}(6) \leq ES(9) \leq 1717$ [Ger08, Ove03]. Our proof (Theorem 4.4.4) shows

$$h^{\text{conv}}(5) \leq 2^{225\cdot 6^2\cdot\log_2(5)\cdot\log_2(6)} + 1 \quad \text{and;}$$
$$h^{\text{conv}}(6) \leq 2^{225\cdot 9^2\cdot\log_2(5)\cdot\log_2(9)} + 1.$$

4.4.3 Generalized Holes

Aichholzer, Hackl, Huemer, Hurtado and Vogtenhuber [AHH+10] showed that every sufficiently large bicolored point set $P = A \dot\cup B$ contains a generalized 4-hole spanned only by points of A or only by points of B. A *generalized k-hole* is a simple polygon (not necessarily convex) which is spanned by k points of P and does not contain points of P in its interior. Since there are no coordinates involved in the proof, the proof transfers to the pseudolinear setting. For simple drawings we need to adapt the definition of generalized holes. A simple polygon in a point set is basically a plane cycle, which we can define for simple drawings. This motivates the first

definition of empty cycles. However, in the geometric setting, a simple polygon always admits a triangulation. This is not the case for plane cycles in simple drawings. For the second more restrictive variant, we consider empty triangulations.

Empty Cycles

As a first generalization of polygons, we consider plane cycles. Similar to triangles, they divide the plane into two components whose closures we call *sides*. An *empty k-cycle* in a simple drawing is a plane cycle of length k such that one of its two sides is empty. For $k = 3$ this definition coincides with empty triangles. As for empty triangles, the complement of the convex hull of a point set is counted as an empty k-cycle even though it is not a generalized k-hole in the point set. In the following we show the existence of empty 4-cycles.

Theorem 4.4.9. *Let $\mathcal{D}$ be a simple drawing of K_n with $n \geq 4$ and let v be a vertex of $\mathcal{D}$. Then $\mathcal{D}$ contains an empty 4-cycle passing through v.*

Proof. For a fixed vertex v, we consider the star S_v centered at v and consisting of all incident edges. By [GTP21, Corollary 3.4], there is a plane subdrawing $\mathcal{D}'$ that consists of the star S_v and some spanning tree T on the remaining $n-1$ vertices. Moreover, $\mathcal{D}'$ is 2-connected [GTP21, Theorem 3.1]. Every face F of $\mathcal{D}'$ contains v on its boundary because the tree T is cycle-free. Hence the subdrawing $\mathcal{D}'$ has exactly $2n-3$ edges and $n-1$ faces. If there is a face of $\mathcal{D}'$ with exactly 4 edges on its boundary, then this yields an empty 4-cycle passing through v. Similarly if two triangular faces are adjacent, then this yields an empty 4-cycle passing through v. In the other cases, we derive a contradiction by counting the number of edges E in $\mathcal{D}'$. Since no two triangular faces are adjacent, there are at most $\lfloor \frac{n-1}{2} \rfloor$ triangles. Let f_3 denote the number of triangles. All other faces have at least 5 edges on their boundary, whose number is denoted by $f_{\geq 5}$. Since every edge is incident to exactly two faces, this yields

$$|E| \geq \frac{1}{2}\left(5f_{\geq 5} + 3f_3\right) = \frac{1}{2}\left(5(n-1-f_3) + 3f_3\right) \geq \frac{1}{2}\left(5(n-1) - 2\left\lfloor \frac{n-1}{2} \right\rfloor\right) \geq 2n-2.$$

This is a contradiction to the fact that $\mathcal{D}'$ contains exactly $2n-3$ edges. □

Similar to the minimum number of empty triangles which is asymptotically linear [AHP+15], the above theorem implies a linear lower bound on the number of empty 4-cycles.

Corollary 4.4.10. *Every simple drawing of K_n with $n \geq 4$ contains at least $\frac{n}{4}$ empty 4-cycles.*

Note that the twisted drawing $\mathcal{T}_n$ contains cubically many empty 4-cycles. A plane 4-cycle of $\mathcal{T}_n$ is illustrated in Figure 4.18. Such a 4-cycle is empty if and only if one of the two sides is empty. This is the case if the 4-cycle consists of the vertices $1, 2, n-1, n$ or $i, j, j+1, \ell$ for $i < j < j+1 < \ell$.
While the empty 3-cycles and empty 4-cycles exists in all simple drawings ([Har98] and Theorem 4.4.9), the existence of k-cycles remains open for $k \geq 5$.

Question 4.1. *Does every simple drawing of K_n contain an empty k-cycle for each $3 \leq k \leq n$?*

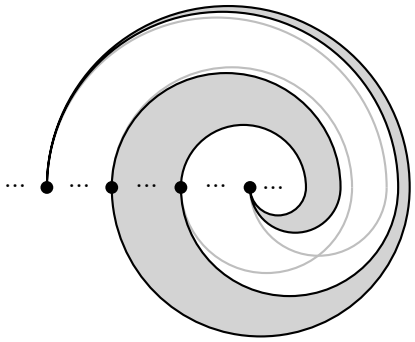

Figure 4.18: A plane 4-cycle in $\mathcal{T}_n$.

An empty n-cycle is a plane Hamiltonian cycle. Rafla [Raf88] conjectured that every simple drawing of K_n contains a plane Hamiltonian cycle.
An affirmative answer to Question 4.1 restricted to convex drawings follows immediately from Theorem 5.2.2, which we discuss in more detail in the Chapter 5. In particular Theorem 5.2.2 states that every star S_v in a convex drawing of K_n can be planarly extended by a Hamiltonian path P on the remaining $n-1$ vertices. By closing the subpath of P on the first $k-1$ vertices via v, one obtains the desired empty k-cycle.

Corollary 4.4.11. *Let $\mathcal{D}$ be a convex drawing of K_n and let $3 \leq k \leq n$. Then $\mathcal{D}$ contains an empty k-cycle.*

Empty Triangulations

Recall that a generalized hole in a point set is a simple empty polygon, and that polygons can be triangulated. To restrict the definition of generalized holes in simple drawings, we may further require that the empty side of an empty k-cycle can be *triangulated*, i.e., is the disjoint union of empty triangles. We call such a structure *empty k-triangulation*. For example, in the drawing $\widetilde{\mathcal{T}_n}$ constructed in Section 4.4.1 the vertices $1, n-1, 2, n$ form an empty 4-triangulation. While Theorem 4.4.9 asserts that every simple drawing of K_n contains an empty 4-cycle, there are simple drawings without empty 4-triangulations. To construct an infinite family of such drawings $\mathcal{T}'_n$, we start with the twisted drawing $\mathcal{T}_n$ and reroute some edges as illustrated in Figure 4.19.

Proposition 4.4.12. *For $n \geq 6$ the drawing $\mathcal{T}'_n$ contains no empty 4-triangulation.*

Using the result by Aichholzer et al. [AHH$^+$10] about the existence of monochromatic generalized 4-holes in bicolored point sets (resp. pseudolinear drawing of K_n), we show the existence of empty 4-triangulations in convex drawings. In particular, since every sufficiently large convex drawing of K_n contains a minimal k-gon whose convex side induces an f-convex subdrawing (Lemma 4.4.7), we can apply the existence in the pseudolinear setting to obtain that every sufficiently large bicolored convex drawing contains a monochromatic empty 4-triangulation.

Corollary 4.4.13. *Every sufficiently large convex drawing on vertices $V = A \dot\cup B$ has an empty 4-triangulation induced only by vertices from A or only by vertices from B.*

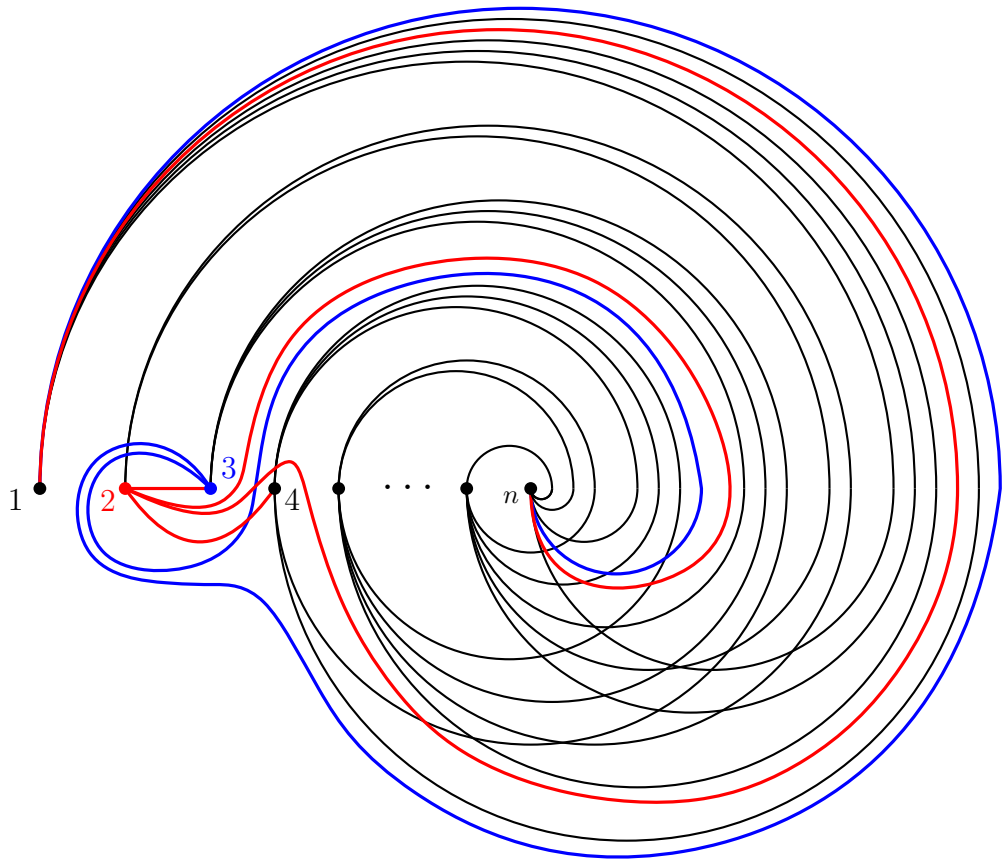

Figure 4.19: The drawing $\mathcal{T}'_n$ without empty 4-triangulations for $n \geq 6$.

Proof of Proposition 4.4.12. Note that the drawing induced by the vertices $1, 3, \dots, n$ is the twisted drawing $\mathcal{T}_{n-1}$. Even though the remaining drawing is not $\mathcal{T}_n$, it is crossing maximal.

Claim 4.3. *$\mathcal{T}'_n$ contains $\binom{n}{4}$ crossings.*

Proof. The following proof gives the exact crossing pairs and hence describes the drawing up to weak isomorphism.

The vertices $1, 3, 4, \dots, n$ build a twisted drawing $\mathcal{T}_{n-1}$ and hence every 4-tuple from $[n]\backslash\{2\}$ contains a crossing, giving $\binom{n-1}{4}$ crossings. More specifically, the edges $\{i, \ell\}$ and $\{j, k\}$ cross for $i, j, k, \ell \in [n] \setminus \{2\}$ with $i < j < k < \ell$.

It remains to describe the crossings in 4-subsets which contain vertex 2. The edge $\{1, 2\}$ crosses the edges $\{3, n\}, \{3, 4\}, \{4, i\}$ for $i = 5, \dots n$ which are $n - 2$ crossings. The edge $\{2, 3\}$ has no crossing and $\{2, 4\}$ crosses only the edge $\{3, n\}$. For $j = 5, \dots, n-1$ the edge $\{2, j\}$ crosses the two edges $\{1, 3\}, \{3, n\}$, the $n-j$ edges $\{1, j+1\}, \dots, \{1, n\}$ and the edges $\{i, k\}$ for $2 < i < k < j$, of which there are $\binom{j-3}{2}$. Finally, the edge $\{2, n\}$ crosses the $\binom{n-4}{2}$ edges $\{i, j\}$ for $3 < i < j \leq n-1$. In total there are

$$\begin{aligned}
&\binom{n-1}{4} + (n-2) + 1 + \sum_{j=5}^{n-1} \left(2 + (n-j) + \binom{j-3}{2}\right) + \binom{n-4}{2} \\
&= \binom{n-1}{4} + 3n - 11 + \binom{n-4}{2} + \sum_{j=2}^{n-4} \binom{j}{2} + \binom{n-4}{2} \\
&= \binom{n-1}{4} + 2n - 7 + \binom{n-3}{2} + \binom{n-3}{3} + \binom{n-4}{2} \\
&= \binom{n-1}{4} + 1 + (n-4) + \binom{n-3}{2} + \binom{n-2}{3} \\
&= \binom{n-1}{4} + \binom{n-1}{3} = \binom{n}{4}
\end{aligned}$$

crossings because of the hockey-stick identity $\sum_{j=r}^{n} \binom{j}{r} = \binom{n+1}{r+1}$ and its relative $\sum_{k=0}^{m} \binom{n+k}{k} = \binom{n+m+1}{n+1}$. ■

Because of the crossing maximality every empty 4-triangulation is a 4-hole. The only possibility to achieve an empty 4-triangulation which is not a 4-hole, is a crossing-free subdrawing. In the twisted subdrawing $\mathcal{T}_{n-1}$ induced by $1, 3, \dots, n$ the empty triangles are $1, 3, i$ for $i = 4, \dots, n$ and $i, n-1, n$ for $i = 1, 3 \dots n-2$ and the only 4-hole is $1, 3, n-1, n$ which is not a 4-hole in $\mathcal{T}'_n$, since the vertex 2 is in the triangle spanned by $\{3, n-1, n\}$. Hence if there is a 4-hole, it consists of the vertex 2 and three vertices of an empty triangle of the induced subdrawing $\mathcal{T}_{n-1}$. However, since all empty triangles from the induced subdrawing $\mathcal{T}_{n-1}$ are induced by 1 and 3 or both vertices $n-1, n$, at least one of the two triangle spanned by $1, 2, 3$ or $2, n-1, n$ must be empty. This is not the case in the constructed drawing. □

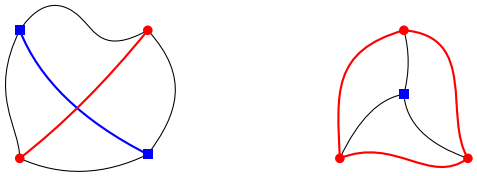

Figure 4.20: Illustration of the two partitions for Radon's theorem.

4.5 More Classic Theorems

We conclude this chapter with remarks on additional classic theorems from convex geometry which are not discussed yet. Most prominently we discuss Tverberg's theorem and the (p, q)-theorem, a Helly-type theorem. We start with a special case of Tverberg's theorem.

4.5.1 Radon's Theorem

Radon's theorem asserts that every set of $d + 2$ points in $\mathbb{R}^d$ can be partitioned into two sets whose convex hulls intersect. Clearly Radon's theorem holds for all simple drawings since every simple drawing of the K_4 can be partitioned into two sets which intersect. Instead of convex sets, we consider the bounded region enclosed by all edges connecting vertices of the same color. If the drawing has a crossing, we partition the vertices such that the endvertices of a crossing edge have the same color. In the crossing-free drawing of the K_4, we divide the vertices in the outer triangle and the vertex being in the bounded side of this triangle. For an illustration of the cases see Figure 4.20.

4.5.2 Tverberg and related Theorems

In 1959 Birch [Bir59] showed that for every r and every geometric drawing of K_{3r} there are r vertex disjoint triangles such that the intersection of their bounded side is not empty. For more information see for example [Zie11]. Indeed it is possible to reduce the number of points to $3r-2$ such that there is a partition in r parts whose convex hulls have a common intersection. Later Tverberg [Tve66] generalized this to point sets in dimension d. *Tverberg's theorem* asserts that every set V of at least $(d+1)(r-1)+1$ points in $\mathbb{R}^d$ can be partitioned into $V = V_1 \dot\cup \ldots \dot\cup V_r$ such that $\text{conv}(V_1) \cap \ldots \cap \text{conv}(V_r)$ is non-empty. The case $r = 2$ of Tverberg is exactly Radon's theorem.

The topological version of Tverberg's theorem remains unsolved. If r is prime [BSS81] or if r is a prime-power [Öza87], the topological Tverberg is true for any dimension. Moreover for every r which is not a prime power, there is a counterexample in some dimension d [BFZ19, MW14].

For pseudolinear drawings (dimension 2) the generalization was proven by Roudneff [Rou88]. An approach for a generalization of Birch's theorem for simple drawings of complete graphs is given in [FS20][2]. For a recent survey on generalizations of Tverberg's theorem, we refer to [BS18].

[2] As the authors state at the arXiv version, the proof seems to be incomplete.

4.5.3 (p, q)-Theorem

The (p, q)-*Theorem* was conjectured by Hadwiger and Debrunner and proved by Alon and Kleitman [AK92]. For improved bounds see [KST18]. It says that for any $p \geq q \geq d + 1$ there is a finite number $c(p, q, d)$ with the following property: If $\mathcal{C}$ is a family of convex sets in $\mathbb{R}^d$, with the property that among any p of them, there are q that have a common point, then there are $c(p, q, d)$ points that cover all the sets in $\mathcal{C}$. Helly's theorem is the case with $p = q = d + 1$, i.e., $c(d + 1, d + 1, d) = 1$. We are not aware whether a (p, q)-Theorem for triangles in general simple drawings exists, however, an anonymous reviewer pointed us to a proof for pseudolinear drawings. Here is an outline: A triangle in a pseudolinear drawing is the intersection of three pseudo-halfplanes. Hence, the intersection of multiple triangles is the intersection of pseudo-halfplanes, and is therefore either empty or path-connected. A (p, q)-Theorem for triangles in pseudolinear drawings now follows directly from Patáková's (p, q)-Theorem [Pat20, Theorem 6]. Moreover, Keszegh [Kes22] studied the case of pseudo-halfplanes and showed that $c(3, 3, 2) = 2$ and several related results.

Chapter 5

Plane Hamiltonian Subgraphs in Convex Drawings

In the study of simple drawings, unavoidable structures gained a lot of attention in the last years. In the last chapter, Section 4.4 we have seen that every sufficiently large simple drawing of K_n contains either a $\mathcal{T}_k$ or a $\mathcal{C}_k$. Moreover, it is well known that for complete graphs with 5 or more vertices we cannot avoid a crossing. Besides crossing structures, plane substructures in simple drawings have been studied. In a drawing $\mathcal{D}$ of K_n, the subdrawing $\mathcal{D}[H]$ induced by a subgraph H of K_n is *plane* if no two edges of H have a crossing in $\mathcal{D}$. One of the most well-known conjectures regarding plane substructures may be Rafla's conjecture. In his PhD thesis he showed that every simple drawing with $n \leq 7$ contains a plane Hamiltonian cycle and conjectured that this holds for all n.

Conjecture 5.1 ([Raf88])**.** *Every simple drawing of K_n with $n \geq 3$ contains a plane Hamiltonian cycle.*

Later Ábrego et al. [ÁAF+15] enumerated all rotation systems for $n \leq 9$ and verified the conjecture for $n \leq 9$. Note that all geometric drawings clearly have a plane Hamiltonian cycle as we can start with an arbitrary vertex and visit the remaining vertices in the order in which they appear cyclically around this particular vertex. For an illustration see Figure 5.1. For points in convex position, i.e., a point set with no point inside the convex hull, there is a unique plane Hamiltonian cycle traversing the convex hull. Since this is the only point configuration with exactly one plane Hamiltonian cycle, the number of plane Hamiltonian cycles in a point set is a measure of non-convexity, which has been studied extensively. The question of the maximum number of plane Hamiltonian cycles in a set of n points was first introduced by Newborn and Moser [NM80] (see also [BMP05, Chapter 8.4]). For the current best lower bound of $\Omega(4.642^n)$

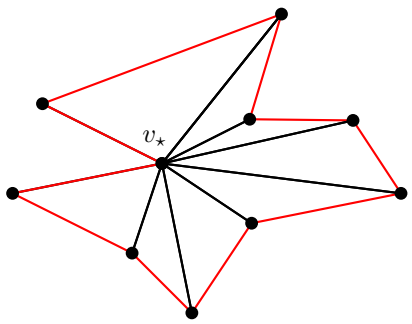

Figure 5.1: Hamiltonian cycle in a geometric drawing.

see García, Noy and Tejel [GNT00] and for the upper bound of $O(55.839^n)$ see Sharir, Sheffer and Welzl [SSW13].
Another subclass of simple drawings for which Rafla's conjecture is true are monotone drawings. Recently, Orthaber [Ort22] proved in his master thesis that cylindrical and strongly c-monotone drawings have a plane Hamiltonian cycle (see also [AOV24]). This in particular includes monotone and geometric drawings. Aichholzer et al. [AGT$^+$22] furthermore showed that generalized twisted drawings with an odd number of vertices contain a plane Hamiltonian cycle.
Besides the positive results concerning subclasses, weaker results on general simple drawing have been investigated. Clearly if there is a plane Hamiltonian cycle, then the drawing also admits a plane Hamiltonian path and a plane matching. In 2022, Suk and Zeng [SZ22] and Aichholzer et al. [AGT$^+$22] independently showed that simple drawings contain a plane path of length $(\log n)^{1-o(1)}$. Additionally, Suk and Zeng showed that every simple drawing of K_n contains a plane copy of every tree on $(\log n)^{1/4-o(1)}$ vertices. Aichholzer et al. moreover showed the existence of a plane matching of size $\Omega(\sqrt{n})$, improving previous bounds from [PST03, PT05, FS09, Suk12, FR13, Ful14, Rui17].

Outline This chapter is based on [BFMS23] which is joint work with Stefan Felsner, Meghana M. Reddy and Manfred Scheucher. We consider several variations and strengthenings of Rafla's conjecture, see Section 5.2. The main result (see Theorem 5.2.2) is a proof of the existence of plane Hamiltonian cycles in convex drawings which moreover can be extended by a spanning star consisting of additional $n-3$ edges. This is a combination of Rafla's conjecture and the result by Fulek and Ruiz-Vargas [FR13, Lemma 2.1] that every simple drawing of K_n admits a plane subdrawing of size $2n-3$. The proof of Theorem 5.2.2 is constructive and comes with a quadratic time algorithm. We use special edges denoted as *bad edges*, which admit a layering structure and reduce the problem to finding a plane path in every layer. The proof is given in Section 5.3. For the important layering structure we use computer assistance in form of a SAT framework to avoid large case distinction. In this thesis, we additionally provide a classic proof without computer in Section 5.4. Note that all problems considered in this chapter only depend on the pairs of crossing edges and not on the actual embedding. This allows to work with rotation systems, which makes it possible to investigate the problems with SAT. In Section 5.1, we give a short description of the SAT encoding. With the help of the SAT framework, we show that Rafla's conjecture is true for $n \leq 10$.

5.1 SAT Encoding for Rotation Systems

To study substructures in general simple drawings and subclasses such as convex or h-convex drawings, we develop a Python program which generates a Boolean formula that is satisfiable if and only if there exists a simple drawing of K_n with prescribed properties for a specified value of n. Moreover, the solutions of these instances are in one-to-one correspondence with non-isomorphic simple drawings with the prescribed properties. To be more specific, for a given problem of the form "does there exist a simple drawing of K_n with the property ...", the Python program generates a Boolean formula in conjunctive normal form (CNF). We then use state-of-the-art SAT solvers such as CaDiCaL [Bie19] to decide whether a solution exists and to enumerate solutions. While solutions can be verified, the correctness in the *unsatisfiable* case has

no obvious certificate. Nevertheless, we verify our unsatisfiability results using the independent proof checking tool DRAT-trim [WHH14].

To encode pre-rotation systems on n elements as a Boolean satisfiability problem for a constant n, we use Boolean variables and clauses to encode the rotations of the vertices. Since we only consider complete graphs, the rotation of a vertex $a \in [n]$ is a cyclic permutation on $[n]\backslash\{a\}$. We introduce a Boolean variable X_{aib} for every pair of distinct vertices $a, b \in [n]$ and every index $i \in [n-1]$, to indicate whether $\pi_a(i) = b$. To encode that for all $a \in [n]$ and for all $i \in [n-1]$ there is at least a value $\pi_a(i) \in [n]\backslash\{a\}$, we add the clauses

$$\bigvee_{b \neq a} X_{aib}$$

to our CNF. Moreover, we want that there is exactly one value $\pi_a(i)$ and hence $X_{aib_1} \Rightarrow \neg X_{aib_2}$ for all $b_1 \neq b_2$. This implication gives that there is at most one value $\pi_a(i) \in [n]\backslash\{a\}$ for all $a \in [n]$ and for all $i \in [n-1]$. As a clause this is

$$\neg X_{aib_1} \vee \neg X_{aib_2}.$$

Moreover, since a permutation is a bijective function, every b is taken exactly once. This is encoded with the following clauses for all $a, b \in [n]$.

$$\bigvee_{i \in [n-1]} X_{aib}; \quad \text{and}$$
$$\neg X_{ai_1b} \vee \neg X_{ai_2b} \quad \text{for all } i_1 \neq i_2.$$

Since rotations around an element are cyclic permutations, there are $n-1$ possibilities for the permutations encoded with the clauses. All of them encode the same rotation. To break the symmetries, we assume without loss of generality that we start the rotation with the smallest element, i.e., the rotation around the first element starts with 2, and for every other element the rotation starts with 1. For the CNF, we encode it as follows:

$$X_{1,1,2}; \text{ and}$$
$$X_{a,1,1} \text{ for all } a \neq 1.$$

With those clauses, we encode a pre-rotation system. To restrict the search space to rotation systems, we need to forbid the subconfigurations Π_4^o, $\Pi_{5,1}^o$, $\Pi_{5,2}^o$ depicted in Figure 2.16, see Theorem 2.5.5. To encode this, we introduce auxiliary variables $S_{a,bcd}$ to encode that bcd appear in this order in the rotation of a. We synchronize the auxiliary variables $S_{a,bcd}$ with the variables X_{aib} which encode already our rotation system. For this we add for all distinct elements $a, b, c, d \in [n]$ the clauses

$$\neg X_{aib} \vee \neg X_{ajc} \vee \neg X_{akd} \vee \quad S_{a,bcd} \quad \text{if } i < j < k, k < i < j, \text{ or } j < k < i; \text{ and}$$
$$\neg X_{aib} \vee \neg X_{ajc} \vee \neg X_{akd} \vee \neg S_{a,bcd} \quad \text{if } i < k < j, k < j < i, \text{ or } j < i < k.$$

To forbid the obstruction Π_4^o as a subconfiguration, we add the two clauses for each set of four vertices $a, b, c, d \in [n]$

$$\neg S_{a,bcd} \vee \neg S_{b,acd} \vee \neg S_{c,abd} \vee \neg S_{d,acb}; \text{ and}$$
$$S_{a,bcd} \vee \quad S_{b,acd} \vee \quad S_{c,abd} \vee \quad S_{d,acb}.$$

Here we ensure that neither Π_4^{o} nor the reversed rotation system appears as a substructure. In an analogous manner, we can assert that $\Pi_{5,1}^{\mathrm{o}}$ and $\Pi_{5,2}^{\mathrm{o}}$ are not contained. In total, we have $\Theta(n^5)$ clauses which assert that the pre-rotation system is indeed a rotation system, i.e., drawable.
Similar it is possible to restrict the search space to convex or h-convex drawings, respectively. By Proposition 2.6.2 and Observation 2.6.1 it is enough to forbid the subconfigurations $\Pi_{5,1}^{\mathrm{oc}}$, and $\Pi_{5,2}^{\mathrm{oc}}$ for convexity and additionally Π_6^{oh} for h-convexity. This can be done in an analogous manner as the drawability obstructions.

With this encoding every solution of the CNF formula corresponds to a (convex, h-convex) rotation system of a simple drawing of K_n. To ensure that the solutions are in one-to-one correspondence with isomorphism classes of rotation systems, we implement a static symmetry breaking in which we classify a unique representative.
In a first step, we consider so called natural pre-rotation systems. A pre-rotation system on $[n]$ is *natural* if the rotation of the first element is the identity permutation, that is, the rotation around 1 is $2, 3, \ldots, n$. By permuting the labels of the elements $3, \ldots, n$ we can make any pre-rotation system natural. Figure 5.2 shows the four natural rotation systems of K_4 and their corresponding drawings, while Figure 5.3 shows the four natural non-drawable pre-rotation system on [4].

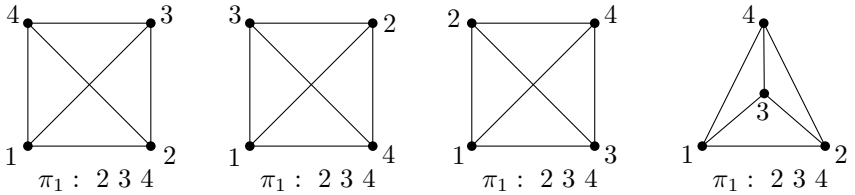

Figure 5.2: The four natural rotation systems on 4 elements with their drawings. The first, second, and third are isomorphic and the first is the lexicographic minimum representative. Note that this is the same as Figure 2.17.

π_1 : 2 3 4	π_1 : 2 3 4	π_1 : 2 3 4	π_1 : 2 3 4
π_2 : 1 3 4	π_2 : 1 4 3	π_2 : 1 3 4	π_2 : 1 4 3
π_3 : 1 2 4	π_3 : 1 4 2	π_3 : 1 4 2	π_3 : 1 2 4
π_4 : 1 3 2	π_4 : 1 3 2	π_4 : 1 2 3	π_4 : 1 2 3

Figure 5.3: The four natural pre-rotation systems on 4 elements, which are not drawable. The first is the lexicographic minimum representative, see also Figure 2.16.

As Figure 5.2 and Figure 5.3 show this encoding is still not a 1-to-1 correspondence between solutions of the CNF and isomorphism classes of the pre-rotation systems. For each pre-rotation system on $[n]$ we can obtain up to $2n!$ isomorphic pre-rotation systems by permuting the elements and by reflection (which reverses all cyclic orders). We further restrict the SAT encoding to only consider one representative for each isomorphism class.
A pre-rotation system Π can be encoded as an $n \times (n-1)$ matrix M_Π, where the a-th row encodes the rotation of the a-th element, or as a vector v_Π of length $n \cdot (n-1)$ that is obtained

by concatenating the rows of the matrix. Note that we assume that the first element in every row of M_Π is the smallest one of the cyclic permutation, i.e., the first row starts with 2 and all other rows start with 1. In order to find a unique representative for an isomorphism class, we take the pre-rotation system with the lexicographically minimal vector.
In a lexicographically minimal pre-rotation system Π, the first row of the matrix M_Π is the identity permutation on $[n]\backslash\{1\}$. It is necessary that a lexicographical minimum is natural, but not sufficient; see for example the three rotation systems corresponding to a crossing K_4 in Figure 5.2. At first glance, it seems that we have to check $n!$ relabellings whenever we test whether a given pre-rotation system Π is a lexicographic minimum. However, since the relabeling has to be natural, the choice of the first and second vertices fully determines the first row and thus the full permutation of the vertices. Hence, we only have to test $n(n-1)$ relabellings plus their reflections to test isomorphism.

In the course of this chapter, we study plane substructures in simple drawings of the complete graph. To use the SAT encoding for this investigations, we have to encode crossings and non-crossings. For this we introduce variables $C_{ab,cd} = C_{ef}$ to indicate whether two non-adjacent edges $e = \{a, b\}$ and $f = \{c, d\}$ cross (cf. Observation 2.5.3(ii)). If the drawing of K_4 with vertices $\{a, b, c, d\}$ is crossing-free, the rotation system is unique up to relabeling or reflection. Otherwise, if there is a crossing, we have one of the following: ab crosses cd, ac crosses bd, or ad crosses bc and this is fully determined by the rotation system. For each of these three cases, there are two subcases. If ab crosses cd, then the directed edge $\overrightarrow{cd}$ either traverses $\overrightarrow{ab}$ from the left to the right or vice versa. Each subcase corresponds to a unique rotation system. The three cases are depicted in Figure 5.2. The other cases are the reversed rotation systems which correspond to the reflected drawings. For the implementation, we introduce an auxiliary variable $D_{ab,cd}$ to indicate whether we are in the first subcase and set

$$C_{ab,cd} = D_{ab,cd} \vee D_{ab,dc}.$$

Moreover, we add the clauses

$$\begin{aligned} \neg S_{a,bdc} \vee \neg S_{b,acd} \vee \neg S_{c,abd} \vee \neg S_{d,acb} \vee \quad & D_{ab,cd} \\ & S_{a,bdc} \vee \neg D_{ab,cd} \\ & S_{b,acd} \vee \neg D_{ab,cd} \\ & S_{c,abd} \vee \neg D_{ab,cd} \\ & S_{d,acb} \vee \neg D_{ab,cd} \end{aligned}$$

to encode the directed crossing.
We assert that a subset of the edges $E' \subset E(K_n)$ forms a plane subdrawing by setting the auxiliary crossing variables corresponding to pairs of edges from E to FALSE, that is, we have a clause $\neg C_{e,f}$ for every pair of non-adjacent edges $e, f \in E'$. Similarly, we can assert that E' does not form a plane subdrawing with the constraint

$$\bigvee_{e,f \in E' \colon e \cap f = \emptyset} C_{e,f}.$$

For instance, to assert that a rotation system does not contain a plane Hamiltonian cycle, we need that for every cyclic permutation π on $[n]$ there is at least one crossing pair of edges in the

set of edges $E_\pi = \{(\pi(i), \pi(i+1)) : i \in [n]\}$, where the elements are considered modulo n, i.e. $n+1 = 1$. Note that this gives $(n-1)!$ clauses and is therefore only suited for relatively small values of n. Similarly, we can deal with plane Hamiltonian subdrawings on $2n-3$ edges: We assert that there is at least one crossing formed by every edge set $E' \in \binom{E(K_n)}{2n-3}$ which contains the edges E_π of some Hamiltonian cycle π. The framework is given in [BFMS23].[1]

5.2 Plane Hamiltonian Substructures

In this section we consider various questions and conjectures concerning plane substructures in simple drawings and more specifically in convex drawings. One of the most prominent conjectures concerning plane substructures is by Rafla, see Conjecture 5.1, which asks for a plane Hamiltonian cycle in drawings of K_n. In the following we investigate strengthenings and variations of this conjectures. Using the SAT framework presented in Section 5.1 we showed that Rafla's conjecture is true for all $n \leq 10$. Previously it was known to be true for $n \leq 9$ [ÁAF+15].

Theorem 5.2.1. *All simple drawings of K_n with $n \leq 10$ contain a plane Hamiltonian cycle.*

In contrast to the previous approach by Ábrego et al. who enumerated all rotation systems and tested the data base for a plane Hamiltonian cycle, we do not need the large data base of 7 198 391 729 rotation systems for $n = 9$ [ÁAF+15]. Since the growth rate of rotation systems is $2^{\Omega(n^2)}$, it is not possible with today's resources to store the database in the current form for rotation systems with $n = 10$ elements. Using the SAT framework made it possible to check the conjecture for $n = 10$, which took about 6 CPU days to show unsatisfiability for the instance. The DRAT certificate for $n = 10$ is about 78GB and the verification with DRAT-trim took additionally 6 CPU days.

In the following we discuss variants and a strengthening of the conjecture. In a first step we consider the largest plane subdrawing. In the general context this was investigated by Fulek and Ruiz-Vargas [FR13, Lemma 2.1]. They showed that every simple drawing of K_n contains a plane subdrawing with $2n-3$ edges, which is best-possible as witnessed by the geometric drawing $\mathcal{C}_n$ of n points in convex position depicted in Figure 2.14(a). Moreover, for a prescribed connected plane spanning subdrawing, an augmentation with the maximum number of edges can be computed in cubic time [GTP21, Theorem 4.1]. In general it is NP-complete to determine the size of the largest plane subdrawing [GTP21, Theorem 4.2]. We investigated a combination of both properties, a plane Hamiltonian cycle and a plane subdrawing of $2n-3$ edges. Hence we consider plane Hamiltonian subdrawings of size $2n-3$. A *plane Hamiltonian subdrawing* is a plane subdrawing which contains a Hamiltonian cycle. Such a subdrawing exists for all simple drawings with $n \leq 8$ which we showed using the SAT framework and we conjecture that this pattern continues.

Conjecture 5.2. *Every simple drawing of K_n with $n \geq 3$ contains a plane Hamiltonian subdrawing with $2n-3$ edges.*

For convex drawings, we prove Conjecture 5.2, where the plane Hamiltonian subdrawing consists of a Hamiltonian cycle and a spanning star. This clearly implies the existence of a plane Hamiltonian cycle in every convex drawing. The proof of the theorem is deferred to Section 5.3.

[1] https://github.com/manfredscheucher/supplemental-rafla

Theorem 5.2.2. *Let $\mathcal{D}$ be a convex drawing of K_n with $n \geq 3$ and let $v_\star$ be a vertex of $\mathcal{D}$. Then $\mathcal{D}$ contains a plane Hamiltonian cycle C which does not cross any edge incident to $v_\star$. This Hamiltonian cycle can be computed in $O(n^2)$ time. Moreover, if $\mathcal{D}$ is h-convex, then C traverses the neighbors of $v_\star$ in the order of the rotation around $v_\star$.*

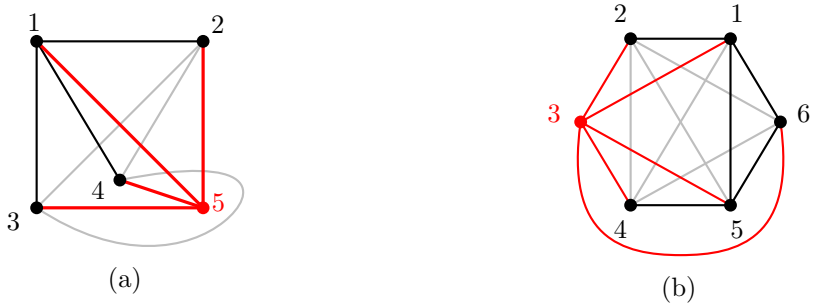

Figure 5.4: (a) The $\mathcal{T}_5$ showing that there is no Hamiltonian cycle which does not cross star edges incident to $v_\star = 5$. All edges which do not cross the star edges (black) are incident to the vertex 2; (b) The smallest convex but not h-convex drawing for which there is no Hamiltonian cycle traversing the vertices corresponding to the rotation around the vertex 3.

The Hamiltonian cycle from Theorem 5.2.2 together with the spanning star centered at $v_\star$ forms a plane subdrawing on $2n-3$ edges. The statement of Theorem 5.2.2 is not true for non-convex drawings. For example, if $v_\star$ is chosen as vertex 5 of $\mathcal{T}_5$ in Figure 5.4(a), then the only edges not crossing star-edges are incident to vertex 1. Moreover, Figure 5.4(b) shows a convex drawing which is not h-convex and where no plane Hamiltonian cycle traverses the neighbors of $v_\star = 3$ in the order of the rotation around $v_\star$.

5.2.1 Extending Hamiltonian Cycles

Another way to read Theorem 5.2.2 is the following: given a spanning star in a convex drawing, we can extend this star by additional $n-2$ edges to a plane Hamiltonian subdrawing on $2n-3$ edges. As a variant of this formulation, we tested whether the other direction is true, i.e., whether every given plane Hamiltonian cycle can be extended by $n-3$ edges to a plane subdrawing with $2n-3$ edges. It is worth noting that the special case in which the $n-3$ edges build a star already fails in the geometric setting; see Figure 5.5(a).
While for convex drawings such an extension exists for all $n \leq 10$, for general simple drawings it does not; see the example on 8 vertices depicted in Figure 5.5(b).

Conjecture 5.3. *Let $\mathcal{D}$ be a convex drawing. Then every plane Hamiltonian cycle can be extended to a plane Hamiltonian subdrawing on $2n-3$ edges.*

5.2.2 Hamiltonian Paths with a prescribed Edge

Clearly every plane Hamiltonian cycle in a simple drawings admits a plane matching with $\lfloor \frac{n}{2} \rfloor$ edges. Again, we tested whether the reverse is true, i.e., whether a prescribed plane matching can be augmented to a plane Hamiltonian cycle. In general it is not possible to find a Hamiltonian cycle containing a prescribed edge. For example, the edge $\{1,3\}$ of $\mathcal{C}_5$ depicted in Figure 2.14(a)

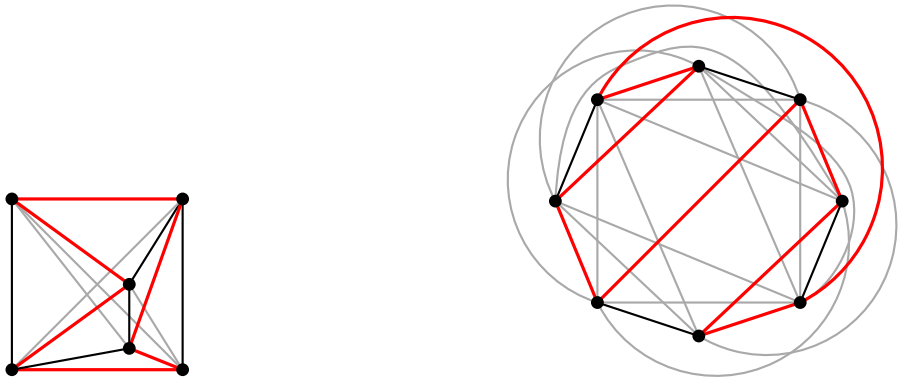

(a) (b)

Figure 5.5: (a) A plane Hamiltonian cycle (red) in a geometric drawing of K_6 which cannot be extended by a spanning star. (b) A plane Hamiltonian cycle in a drawing of K_8 (red) which can only be extended by 4 edges (black). Edges crossing the Hamiltonian cycle are drawn gray.

is not contained in any Hamiltonian cycle. Hence, prescribing an edge of a Hamiltonian cycle is not even possible in the geometric setting. Instead we only ask for a Hamiltonian path containing a prescribed edge. Again there is an easy example: Consider the edge $\{1, 5\}$ in $\mathcal{T}_5$ depicted in Figure 2.14(b). Since this edge has a crossing with all edges not sharing a common vertex, it is not contained in any plane Hamiltonian path. More generally this holds for the edge $\{1, n\}$ in $\mathcal{T}_n$. However, prescribing an edge for a plane Hamiltonian path is possible in convex drawings, in which $\mathcal{T}_5$ does not occur as a subdrawing. The proof follows from Theorem 5.2.2.

Theorem 5.2.3. *Let $\mathcal{D}$ be a convex drawing of K_n and let e be an edge of $\mathcal{D}$. Then $\mathcal{D}$ has a plane Hamiltonian path containing the edge e.*

Proof. Let $e = \{u, v\}$ be the prescribed edge in $\mathcal{D}$. By Theorem 5.2.2 there exists a plane Hamiltonian subgraph containing all edges adjacent to u. In Figure 5.6 we marked the Hamiltonian cycle red. Assume that the Hamiltonian cycle traverses $u, x_1, \ldots, x_{n-1}, u$ in this order with $v = x_i$ for some index i. If $i = 1$ or $i = n - 1$, the Hamiltonian cycle contains the edge $\{u, v\}$. Otherwise we start the Hamiltonian path at x_{i-1}, traverse $x_{i-2}, \ldots, x_1$, take the star edges $\{x_1, u\}$ and $e = \{u, x_i\} = \{u, v\}$, and finally traverse $x_{i+1}, \ldots, x_{n-1}$. The edges of the constructed path are marked blue in Figure 5.6. Since all traversed edges are part of the original plane Hamiltonian subgraph, the constructed Hamiltonian path is also plane. □

5.2.3 Hamiltonian Cycles avoiding a Matching

Another variant is to consider a prescribed matching and ask whether there is a Hamiltonian cycle which together with the matching builds a plane Hamiltonian substructure, i.e., the edges of the matching are not crossed by the Hamiltonian cycle (but possibly contained). In the geometric setting, this corresponds to the question whether the visibility graph of matching edges is Hamiltonian. Hoffmann and Tóth [HT03] showed that for every plane perfect matching M in a geometric drawing of K_n there exists a plane Hamiltonian cycle that does not cross any edge from M. In his PhD thesis Hoffmann [Hof05, Theorem 3.2] moreover showed that this holds for

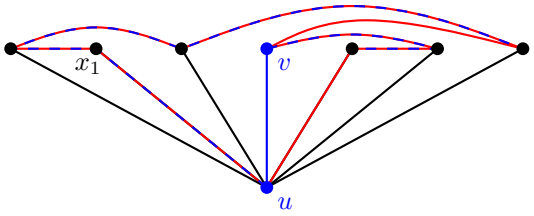

Figure 5.6: Illustration of the proof of Theorem 5.2.3. The blue edge is the prescribed edge. We choose one of the endvertices as star vertex which gives a Hamiltonian cycle (red) using Theorem 5.2.2. The Hamiltonian path (dashed blue) is constructed as in the proof containing the edge $\{u, v\}$.

all plane matchings, which are not necessarily perfect. While the statement does not generalize to simple drawings (Figure 5.7 shows the smallest example), it seems to generalize to convex drawings. We dare the following conjecture, which we verified for $n \leq 11$.

Conjecture 5.4. *For every plane matching M in a convex drawing of K_n there exists a plane Hamiltonian cycle that does not cross any edge from M.*

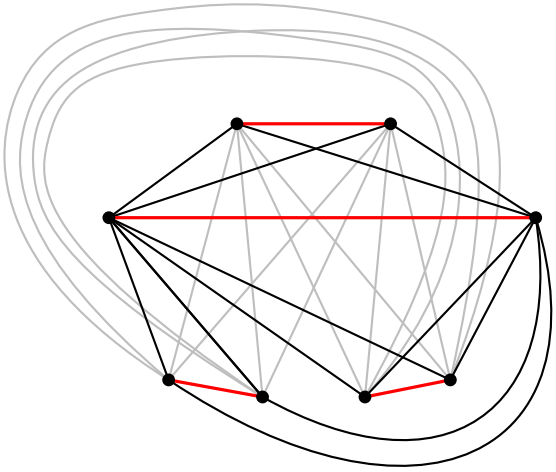

Figure 5.7: A perfect matching (red) in a non-convex drawing of K_8, which does not contain a plane Hamiltonian cycle not crossing the matching edges. Edges which cross matching edges are marked in gray.

5.2.4 Uncrossed Edges

In this section we focus on edges which are not crossed by any other edge of a given drawing of K_n. In 1964, Ringel [Rin64] proved that in every simple drawing of K_n there are at most $2n - 2$ edges without a crossing. Later, Harborth and Mengersen [HM74] studied the minimal number of uncrossed edges and showed that every simple drawing of K_n with $n \leq 7$ contains an uncrossed edge and constructed simple drawings for $n \geq 8$ such that every edge is crossed. The drawing of K_8 constructed by Harborth and Mengersen is depicted in Figure 5.8. For larger n the construction works the same using two cycles of length $\frac{n}{2}$ for even n. For odd n,

adding a vertex in the gray marked cell and carefully adding edges gives a drawing with the same properties. However, these drawings are not convex. In Figure 5.8 the red triangle has

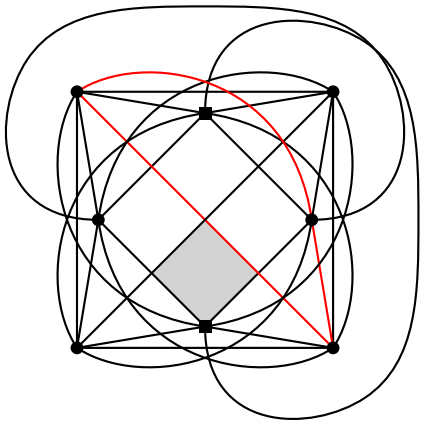

Figure 5.8: A drawing of K_8 without uncrossed edges. The red triangle has no convex side.

no convex side, which is witnessed by the square vertices which have an edge to a triangle vertex which does not stay in the corresponding side. Using the SAT framework, we confirmed these results. Moreover, when restricted to convex drawings, all drawings with $n \leq 10$ have an uncrossed edge. For $n = 11, \ldots, 21$, there are convex drawings where every edge is crossed. These examples are indeed h-convex. Kynčl and Valtr [KV09] showed that for sufficiently large n there is an h-convex drawing of K_n in which every edge is crossed. We conjecture:

Conjecture 5.5. *For every $n \geq 11$ there exists an h-convex drawing of K_n where every edge is crossed.*

Note that geometric drawings are of little interest in this context because the edges forming the boundary of the convex hull are always uncrossed.

5.3 Plane Hamiltonian cycles in convex drawings (Proof of Theorem 5.2.2)

We prove the existence of a plane Hamiltonian cycle in a constructive way and present a quadratic time algorithm to find it. For a given convex drawing $\mathcal{D}$ of the complete graph K_n and a fixed vertex $v_\star$ the algorithm computes a plane Hamiltonian cycle which does not cross edges incident to $v_\star$. Since this statement is independent from the labeling of the vertices, we assume throughout the section that $v_\star = n$ and that the other vertices are labeled from 1 to $n-1$ in cyclic order around $v_\star$, i.e., according to the rotation π_n. As usual we consider the vertices 1 to $n-1$ modulo $n-1$.
The convexity of a drawing in the plane and the containment of a plane Hamiltonian cycle is independent of the choice of the outer cell. For the figures and arguments, we choose a drawing where $v_\star$ is incident to the outer cell. The vertex $v_\star = n$ is denoted as the *star vertex* and edges incident to $v_\star$ as *star edges*. Note that every Hamiltonian cycle contains exactly two star edges. We let $\hat{E}$ be the set of non-star edges and call an edge $e \in \hat{E}$ *star-crossing* if it crosses

a star edge. For the Hamiltonian cycle we only use edges which are not star-crossing. Let $E^\circ = \hat{E} \setminus \{e \in \hat{E} : e \text{ is star-crossing}\}$ be the set of these candidate edges. The goal is to find a Hamiltonian path on the vertices $1, \dots, n-1$ using the edges of E°. For this we start at a vertex which we will determine later and successively add edges in such a ways that the endvertices u, v and u', v' of each pair of edges appear in the cyclic order u, v, u', v'. This ensures that the constructed path is plane.

Observation 5.3.1. *Let $e = \{u, v\}$ and $e' = \{u', v'\}$ be independent edges from E°. If u, v, u', v' appear in this cyclic order around $v_\star$, then e and e' do not cross.*

Particular focus will be on the edges $e = \{v, v+1\}$ with $1 \leq v < n$. Such an edge is called *good* if it is not star-crossing. Otherwise, if the edge $b = \{v, v+1\}$ crosses a star edge $\{w, v_\star\}$, then we say that b is a *bad edge* and w is a *witness* for the bad edge b.
If there is at most one bad edge $\{v, v+1\}$, then the $n-2$ good edges together with the two star edges $\{v, v_\star\}$ and $\{v+1, v_\star\}$ form a Hamiltonian cycle which visits the non-star vertices in the order of the rotation around $v_\star$.

Observation 5.3.2. *If $\hat{E}$ contains at most one bad edge, then $\mathcal{D}$ contains a plane Hamiltonian cycle which does not cross any star edges and visits the non-star vertices in the order of the rotation around the star vertex $v_\star$.*

An example of a drawing with two bad edges is illustrated in Figure 5.4(b) with the choice of $v_\star = 3$ and the two bad edges $\{4, 6\}$ and $\{6, 2\}$.
For the proof of the theorem it is essential to understand the structure of bad edges in a convex drawing. We start with an easy lemma concerning the convex side of the triangle spanned by $v_\star$ and a bad edge. If $b = \{v, v+1\}$ is a bad edge with witness w, then the side of the triangle spanned by $\{v, v+1, v_\star\}$ that contains w is not convex, since $v_\star$ and w both belong to this side but the edge $\{v_\star, w\}$ is not fully contained in this side.

Observation 5.3.3. *Let $b = \{v, v+1\}$ be a bad edge, then the side of the triangle spanned by $\{v, v+1, v_\star\}$ containing the witnesses is not convex.*

Every triangle in a convex drawing has at least one convex side. Thus, for every bad edge $b = \{v, v+1\}$ the triangle spanned by $\{v, v+1, v_\star\}$, denoted by T_b, has a unique convex side, which is the side not containing the witnesses.
The following lemma provides the layering structure of bad edges which is the key for our proof. Every bad edge has at least one witness. Hence except for the star vertex there are three additional vertices involved. To study the structure between two bad edges we need to investigate substructures of at most 7 vertices. Since it is a finite subconfiguration, we are able to use the SAT framework for the proof of this lemma. Note that this is possible since convex drawings are a hereditary structure, i.e., the drawing stays convex when a vertex and its adjacent edges are removed. In Section 5.4 we provide the full proof of this lemma without computer assistance.

Lemma 5.3.4. *Let $b = \{v, v+1\}$ and $b' = \{v', v'+1\}$ be two distinct bad edges with witnesses w and w', respectively. Then the following three properties hold:*

(i) $w \neq w'$;

(ii) w', w, v, v' *appear in this or the reversed cyclic order around* $v_\star$*;*

(iii) Each of the triangles $\{v, v+1, v_\star\}$ *and* $\{v', v'+1, v_\star\}$ *is in the convex side of the other.*

Proof. Assume towards a contradiction that a convex drawing of K_n contains two bad edges $b = \{v, v+1\}$ and $b' = \{v', v'+1\}$ with witnesses w and w', respectively, such that w', w, v, v', do not occur in this particular cyclic order or reversed. We may assume that $n \leq 7$ because the vertices $v, v+1, w, v', v'+1, w', v_\star$ (which are not necessarily distinct) induce a convex drawing on at most 7 vertices which has the desired property. Since every bad edge crosses at least one star edge, the subdrawing has at least two crossings. All simple drawings on $n \leq 4$ have at most one crossing and hence at most one bad edge. We used our SAT framework to enumerate all convex rotation systems on 5, 6, and 7 vertices, respectively. There are 3, 16, and 139 lexicographically minimal convex rotation systems on 5,6, and 7 vertices, respectively. For every convex rotation system, we test whether they fulfill the desired property. For this we fix two distinct vertices v, v' of our considered subdrawing. Moreover, we know that w is distinct from $v, v+1$ and w' distinct from $v', v'+1$. We prescribe the crossings $\{w, v_\star\}$ and $\{v, v+1\}$, respectively $\{w', v_\star\}$ and $\{v', v'+1\}$. Each of the drawings has the property that the vertices appear in the order w', w, v, v' or reversed around the vertex $v_\star$ and it holds $w \neq w'$. This is a contradiction to the assumption. Hence the properties (i) and (ii) hold.
To show (iii), assume without loss of generality that the cyclic order is $w', w, v, v+1, v', v'+1$, where possibly $v+1 = v'$ but all the other vertices are distinct. We show that the vertices $v', v'+1$ are contained in the convex side S of the triangle induced by $\{v, v+1, v_\star\}$. Recall that the side of the triangle containing w is not convex, see Observation 5.3.3. Assume towards a contradiction that at least one of the two vertices v' and $v'+1$ is in the interior of the non-convex side of T_b. Note that if $v' = v+1$, the vertex is in both sides of T_b. In all other cases not being in the convex side is equivalent to being in the non-convex side. Let $x \in \{v', v'+1\}$ be a vertex in the interior of the non-convex side of T_b. This vertex is a witness for the bad edge b. A contradiction since the order in the rotation around $v_\star$ does not correspond to one proven in (ii). Since both vertices v' and $v'+1$ are contained in S, the bad edge b' is fully contained in S. To show that the triangle spanned by $\{v, v+1, v_\star\}$ is contained in the convex side of the triangle spanned by $\{v, v+1, v_\star\}$ we change the roles of v and v'. □

This lemma immediately implies that there is at most one bad edge in every h-convex drawing.

Corollary 5.3.5. *Every h-convex drawing has at most one bad edge.*

Proof. Towards a contradiction assume, there are two bad edges $b = \{v, v+1\}$ and $b' = \{v', v'+1\}$ with witnesses w and w', respectively. Since h-convex drawings are convex, we can apply Lemma 5.3.4. Hence the cyclic order of the vertices around $v_\star$ is either w', w, v, v' or the reversed order and $v_\star, v, v+1$ are in the unique convex side of the triangle spanned by $\{v', v'+1, v_\star\}$ and vice versa. But this contradicts the property of h-convex drawings. □

Corollary 5.3.5 together with Observation 5.3.2 imply the moreover part of Theorem 5.2.2 for h-convex drawings. If a drawing has two or more bad edges Lemma 5.3.4 implies that there is a partition of the vertices $1, \ldots, n-1$ into two blocks such that in the rotation around $v_\star$ both blocks of the partition are consecutive, one contains the vertices of all bad edges and the other contains all the witnesses. Let $b = \{v, v+1\}$ be the bad edge whose vertices are

last in the clockwise order of its block. We cyclically relabel the vertices such that b becomes $\{n-2, n-1\}$. This makes the labels of all witnesses smaller than the labels of vertices of bad edges. In particular we then have the following two properties:

(sidedness) If $\{v, v+1\}$ is a bad edge with witness w, then $w < v$.

(nestedness) If $b = \{v, v+1\}$ and $b' = \{v', v'+1\}$ are bad edges with respective witnesses w and w' and if $v < v'$, then $w' < w$.

In addition we can apply a change of the outer cell (via stereographic projections) such that the vertex $v_\star$ and the initial segments of the edges $\{v_\star, 1\}$ and $\{v_\star, n-1\}$ belong to the outer cell. The nesting property implies that we can label the bad edges as $b_1, \ldots, b_m$ for some $m \geq 2$, such that if $b_i = \{v_i, v_i+1\}$, then $1 < v_1 < v_2 < \ldots < v_m = n-2$. Moreover, let w_i^L and w_i^R denote the leftmost (smallest index) and the rightmost (largest index) witness, respectively, of the bad edge b_i. Then $1 \leq w_m^L \leq w_m^R < w_{m-1}^L \leq w_{m-1}^R < \ldots < w_1^L \leq w_1^R$. Sidedness additionally implies $w_i^R < v_i$ for all $i = 1, \ldots, m$. Figure 5.9 shows the situation for two bad edges b_i and b_{i+1}. Note that $v_i + 1 = v_{i+1}$ is possible.

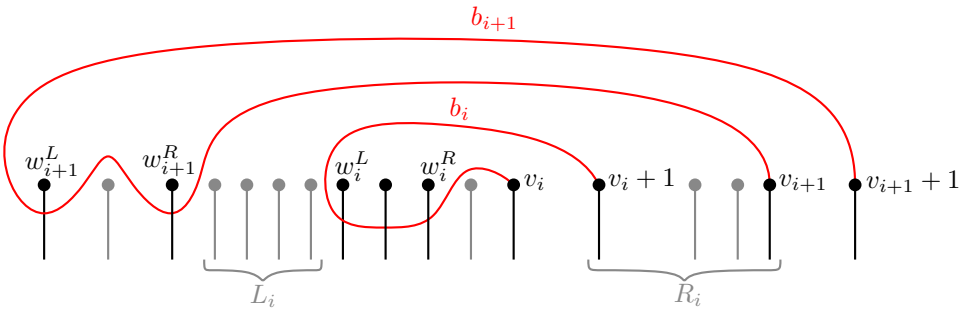

Figure 5.9: Illustration of sidedness and nestedness for two bad edges and together with the corresponding notation.

For $i = 1, \ldots, m-1$ let $L_i = \{x \in [n-1] : w_{i+1}^R < x < w_i^L\}$ and $R_i = \{x \in [n-1] : v_i + 1 \leq x \leq v_{i+1}\}$ denote the left and the right blocks of vertices between two consecutive bad edges b_i and b_{i+1}, see Figure 5.9. Note that R_i is non-empty since it always contains $v_i + 1$ and v_{i+1} but L_i might be empty.
In a first step, we consider edges between one of the two endvertices of the bad edge b_i and witnesses of b_i. In the following lemma we show that $\{w_i^L, v_i + 1\}, \{w_i^R, v_i\} \in E^\circ$ for all i.

Lemma 5.3.6. *For all $i \in [m]$ the edges $\{w_i^L, v_i + 1\}$ and $\{w_i^R, v_i\}$ are not star-crossing.*

Proof. For a fixed i, both edges are fully contained in the non-convex side of the triangle spanned by $\{v_i, v_i+1, v_\star\}$ since the induced subdrawing on the three vertices $v_\star, v_i, v_{i+1}$ and the considered witness already has a crossing. Assume $\{w_i^L, v_i + 1\}$ crosses a star edge $\{x, v_\star\}$. Then x has to be a witness of b_i with $x > w_i^L$. However, the side of the triangle $\{w_i^L, v_i + 1, v_\star\}$ that contains x is not convex due to the edge $\{x, v_\star\}$. Additionally, the other side is not convex due to the edge $\{v_i, v_i + 1\}$. A contradiction to the convexity. A similar argument holds for the edge $\{w_i^R, v_i\}$. Both situations are depicted in Figure 5.10. □

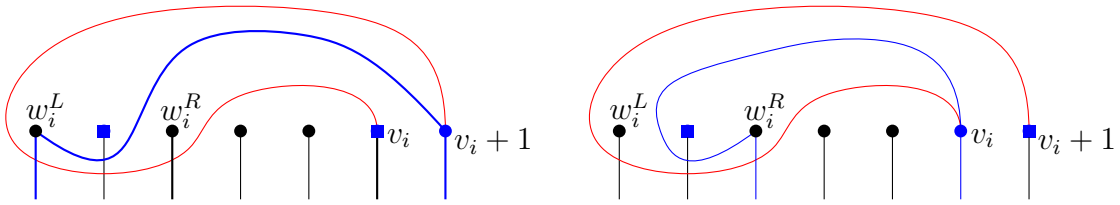

Figure 5.10: The blue edges $\{w_i^R, v_i\}$, $\{w_i^L, v_i + 1\}$ are not star-crossing. The star edges corresponding to the vertices marked with the squares show that the blue triangle is not convex.

Let us first consider the case, in which $L_i = \emptyset$ for all i. In this case, we construct a plane Hamiltonian cycle as follows: Begin with the edge $\{v_\star, v_1\}$. For $i = 1, \ldots, m-1$, when vertex v_i is visited, we go from v_i to w_i^R and then one by one with decreasing labels to w_i^L. From there we want to visit v_i+1 and then one by one in increasing order the vertices of R_i until we reach v_{i+1}. When we reach $v_m + 1 = n - 1$, we collect the remaining vertices x with $1 \leq x < w_m^L$ using the good edge $\{v_m + 1, 1\}$ and then one by one in increasing order to $w_m^L - 1$. A plane path is constructed. This path can be closed to a cycle with the edge $\{w_m^L - 1, v_\star\}$. These are all ingredients to find a plane Hamiltonian cycle in the special case where all $L_i = \emptyset$. Figure 5.11 shows an example for this special case. However in general there are vertices in L_i and the challenge is to visit all vertices in L_i.

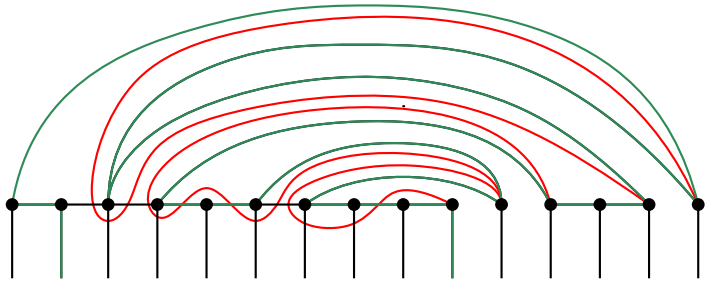

Figure 5.11: A plane Hamiltonian cycle (green) in the case where $L_i = \emptyset$ for all i.

The strategy to find the Hamiltonian cycle visiting all vertices of L_i is to identify edges in E° which connect a vertex in L_i with a vertex in R_i in such a way that we proceed in each step either one step to the left in L_i or one step to the right in R_i. These edges then allow constructing a path from v_i to v_{i+1} using edges from E°. In each step from v_i to v_{i+1} we visit all vertices from R_i and all vertices between w_i^L and w_i^R. However, it is possible that we do not visit all vertices from L_i. We proceed as follows: Starting at v_i we collect the remaining vertices from L_{i-1} and continue with the vertices from w_i^R to w_i^L with decreasing index as in the previous case where $L_i = \emptyset$. Additionally, we continue collecting some of the vertices in L_i until we reach one of the chosen edges in E° connecting a vertex from L_i to $v_i + 1$, which we use. In a second step we construct a path from $v_i + 1$ to v_{i+1} collecting all vertices in R_i and some of the vertices in L_i with the chosen edges of E° by jumping back and forth between L_i and R_i. During this procedure we proceed in each step either one step to the left in L_i or one step to the right in R_i. This yields a plane Hamiltonian cycle which has no crossing with a star edge.

In the following lemmas we describe which edges of E° we use to construct the Hamiltonian cycle. For this we consider edges from L_i to R_i and analyze which edges are not star-crossing. First, we show that the properties of a convex drawing imply that the edges between vertices of L_i and R_i stay in the region between the two bad edges b_i and b_{i+1}. This implies that the only star edges which can be crossed by those edges are $\{v_\star, x\}$ with $x \in L_i \cup R_i$.

Lemma 5.3.7. *All edges $\{u, v\}$ with $u, v \in L_i \cup R_i$ do not cross star edges $\{z, v_\star\}$ with $z \in V \backslash (L_i \cup R_i)$.*

Proof. The convex sides S_i and S_{i+1} of the triangles T_i and T_{i+1}, respectively, have a common intersection which is partitioned into three regions by the edges $\{w_{i+1}^R, v_\star\}$ and $\{w_i^L, v_\star\}$. Both vertices u, v are contained in the region that is bounded by both edges $\{w_{i+1}^R, v_\star\}$ and $\{w_i^L, v_\star\}$. Since the edge $\{u, v\}$ has to lie in S_i and S_{i+1} and can cross $\{w_{i+1}^R, v_\star\}$ and $\{w_i^L, v_\star\}$ at most once, it has to be fully contained in the same region. This shows that we cannot cross star edges $\{z, v_\star\}$ where z is outside of this region, i.e., $z \in V \backslash (L_i \cup R_i)$. □

Moreover, we show that an edge from a vertex in L_i to a vertex in R_i cannot cross star edges with vertices in R_i.

Lemma 5.3.8. *All edges $\{u, v\}$ with $u \in L_i$ and $v \in R_i$ do not cross star edges $\{z, v_\star\}$ with $z \in R_i$.*

Proof. Assume towards a contradiction that the edge $\{u, v\}$ crosses a star edges $\{z, v_\star\}$ with $z \in R_i$. We distinguish the following four cases which are illustrated in Figure 5.12. Let w_i, w_{i+1} be witnesses of the bad edges $b_i = \{v_i, v_i + 1\}$ and $b_{i+1} = \{v_{i+1}, v_{i+1} + 1\}$, respectively. If $\{u, v\}$ crosses a star edge $\{z, v_\star\}$ with $z \in R_i$ such that $z > v$, we are in Case 1 or Case 2. In both cases, we consider the subdrawing induced by $w_{i+1}, u, v, z, v_{i+1}, v_{i+1} + 1, v_\star$, which is a subdrawing on 7 vertices and u, v are adjacent in the rotation around $v_\star$. Hence $\{u, v\}$ is a bad edge in the subdrawing. This cannot happen in a convex drawing since the cyclic order of the vertices around $v_\star$ violates the statement of Lemma 5.3.4. If $z < v$, we consider the subdrawing induced by $u, w_i, v_i, v_i + 1, z, v, v_\star$. Again the edge $\{u, v\}$ is a bad edge with witness z since u and v are adjacent in the subdrawing. By Lemma 5.3.4 this order of vertices corresponding to two bad edges cannot happen. □

The previous lemmas show that if $\{u, v\}$ with $u \in L_i$ and $v \in R_i$ crosses a star edge $\{z, v_\star\}$, then $z \in L_i$. We now analyze crossings in L_i. The edge $\{u, v\}$ cannot cross two star edges $\{z_1, v_\star\}$ and $\{z_2, v_\star\}$ with $z_1 < u < z_2$ and $z_1, z_2 \in L_i$. This is because the two star edges cross the edge $\{u, v\}$ from different directions and hence are witnesses for non-convexity of the corresponding side of the triangle spanned by $\{u, v, v_\star\}$. For an illustration, see Figure 5.13.

Lemma 5.3.9. *The edge $\{u, v\}$ with $u \in L_i$ and $v \in R_i$ does not cross any two star edges $\{z_1, v_\star\}$ and $\{z_2, v_\star\}$ with $z_1 < u < z_2$ and $z_1, z_2 \in L_i$.*

Proof. Assume towards a contradiction, $\{u, v\}$ crosses both edges $\{z_1, v_\star\}$ and $\{z_2, v_\star\}$. Then z_1 and z_2 are on different sides of the triangle spanned by $\{u, v, v_\star\}$. Since both star edges $\{z_1, v_\star\}$ and $\{z_2, v_\star\}$ cross the triangle, there is no convex side. A contradiction to the convexity of the drawing. □

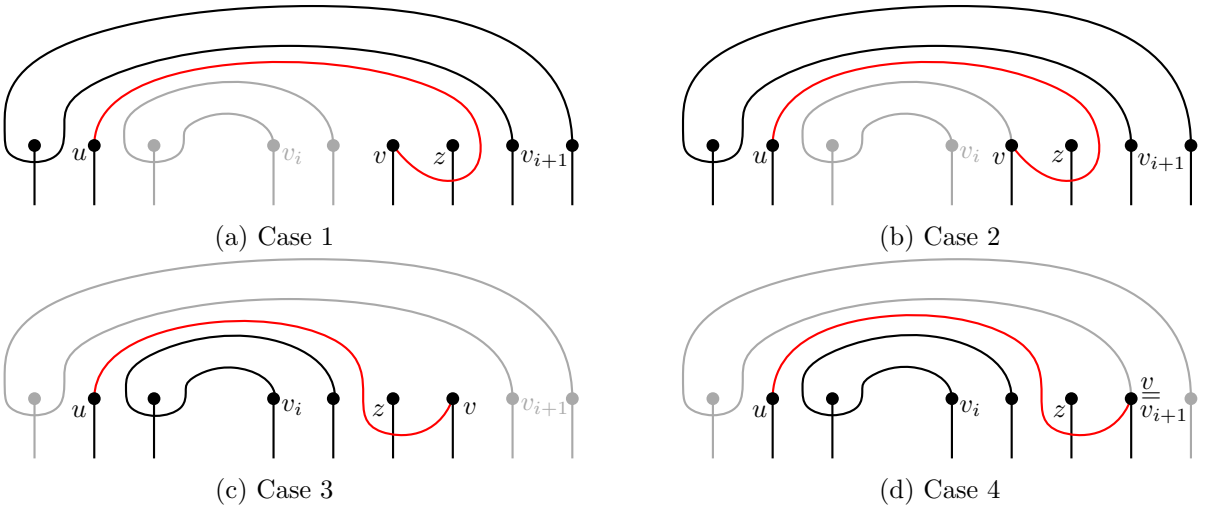

Figure 5.12: Illustration of the four forbidden configurations to prove Lemma 5.3.8. The red edges cannot cross the star edge $\{z, v_\star\}$ as depicted. The vertices (and incident edges) which are deleted to achieve a subdrawing contradicting the convexity are drawn gray.

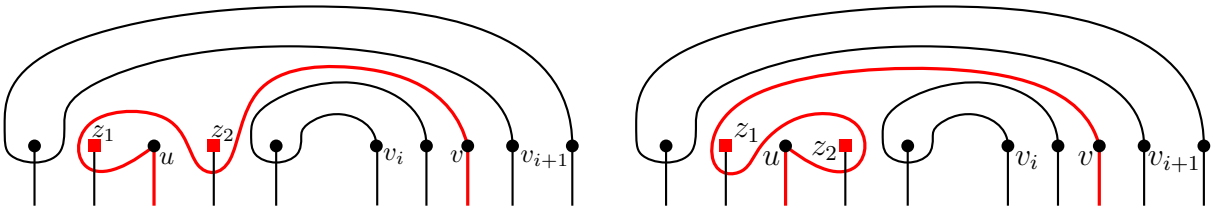

Figure 5.13: Illustration for the proof of Lemma 5.3.9. The red triangle $\{u, v, v_\star\}$ has no convex side. Witnesses for the non-convexity are the edges $\{z_1, v_\star\}$ and $\{z_2, v_\star\}$.

Even though edges from L_i to R_i cannot cross star edges incident to vertices in L_i with smaller and larger indices at the same time, crossing with one of them cannot be avoided. An edge from L_i to R_i whose endvertex in L_i is the vertex $w_{i+1}^R + 1$ can only cross star edges $\{z, v_\star\}$ where z is larger than the endvertex. The easiest case is that this edge is not star-crossing. In this case, we can visit all vertices of L_i in decreasing order and proceed similar as in the case for $L_i = \emptyset$. In the following, we study the case that it is star-crossing. In general, we focus on edges which only cross star-edges with larger indices than the endvertex in L_i. As the following lemma shows those edges help us to find edges from L_i to R_i which are not star crossing.

Lemma 5.3.10. *Let $u \in L_i$ and $v \in R_i$ and z be the largest index in L_i with $z > u$ such that the edge $\{u, v\}$ crosses the star edge $\{z, v_\star\}$. Then the following two statements hold:*

(a) The edge $\{z, v\} \in E^\circ$, i.e., is not star-crossing.

(b) The edge $\{z + 1, v\}$ does not cross the edges $\{x', v_\star\}$ with $x' \in L_i$ and $x' \leq z$.

Proof. To show (a), assume towards a contradiction that the edge $\{z, v\}$ crosses a star edge $\{x', v_\star\}$. From Lemma 5.3.7 and Lemma 5.3.8 we know that $x' \in L_i$. Moreover, in a simple drawing the edge $\{z, v\}$ has no crossing with the triangle T induced by $\{u, v, v_\star\}$ because the

edges $\{u, v\}$ and $\{z, v_\star\}$ already cross. Hence $\{z, v\}$ does not cross any star edge which is fully contained in the side of T which does not contain z. The choice of z implies that all edges $\{x, v_\star\}$ with $x \in L_i$ and $x > z$ do not cross $\{u, v\}$. Hence $\{v, z\}$ can only cross star edges $\{x', v_\star\}$ with $x' \in L_i$ and $x' < z$.
Now observe that the triangle induced by $\{z, v, v_\star\}$ is not convex. The side containing the vertex x' is not convex since the edge $\{x', v_\star\}$ crosses $\{z, v\}$. The other side contains the vertex u and is not convex since the edge $\{u, v\}$ crosses $\{z, v_\star\}$. This is a contradiction. Figure 5.14 gives an illustration. The figure shows the two cases $x' = x'_1 > u$ and $x' = x'_2 < u$, which we do not need to distinguish.

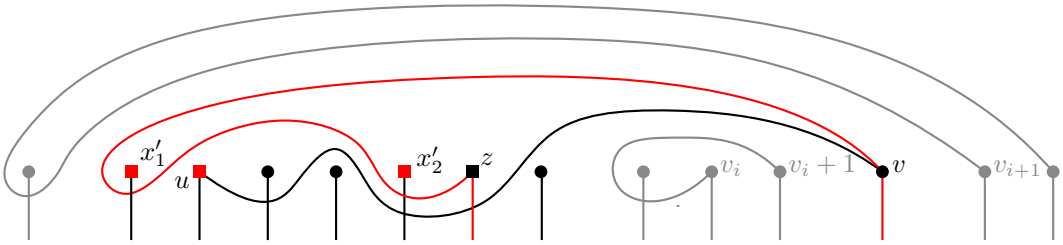

Figure 5.14: Illustration for the proof of Lemma 5.3.10(a). The red triangle $\{z, v, v_\star\}$ has no convex side. Witnesses for the non-convexity are the edges $\{u, v_\star\}$ and $\{x'_i, v_\star\}$.

To show (b), assume towards a contradiction that $\{z + 1, v\}$ crosses a star edge $\{x', v_\star\}$ with $x' \in L_i$ and $x' \leq z$. Since $\{z + 1, v\}$ is adjacent to $\{u, v\}$ and $\{v, v_\star\}$, the edge $\{z + 1, v\}$ has to cross $\{u, v_\star\}$ in order to cross a star edge $\{x', v_\star\}$ with $x' \in L_i$. From (a) we know that $\{z, v\}$ does not cross any star edges. Since $\{z, z+1\}$ is a good edge, the vertices u and $v_\star$ are contained in different sides of the triangle $\{z, z + 1, v\}$. This is a contradiction since both sides are not convex. Witnesses for the non-convexity are the star vertex $v_\star$ whose edge $\{z, v_\star\}$ crosses the boundary of the triangle and the edge $\{u, v\}$. An illustration is given in Figure 5.15. □

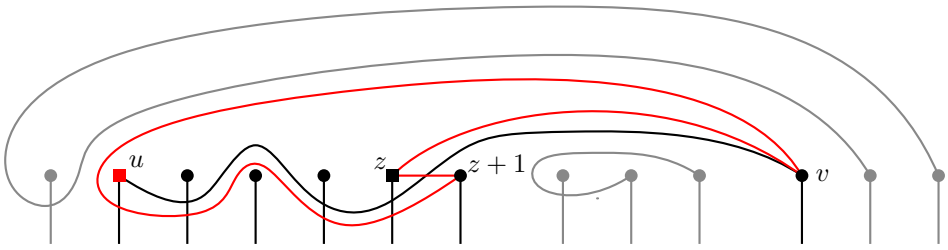

Figure 5.15: Illustration for the proof of Lemma 5.3.10(b). The red triangle has no convex side. Witnesses for the non-convexity are the edges $\{z, v_\star\}$ and $\{u, v\}$.

If $z \in L_i$ is the vertex with the largest index such that the star edge $\{z, v_\star\}$ is crossed by an edge from some $x \in L_i$ with $x < z$ to $r \in R_i$, then the edge $\{z + 1, r\}$ is not star-crossing. For this we define the vertex $l(r) \in L_i \cup \{-\infty\}$ for all $r \in R_i$. For all $r \in R_i$, let $l(r)$ denote the largest index in L_i such that the star edge $\{l(r), v_\star\}$ is crossed by an edge from a vertex $x < l(r)$ in L_i to r. More formally, it is

$$l(r) := \max\{z \in L_i : \text{ edge } \{z, v_\star\} \text{ crosses } \{u, r\} \text{ with } u \in L_i \text{ , } u < z\},$$

Note that a vertex $l \in L_i$ with the desired properties does not necessarily exist, in which case we have $l(r) = -\infty$. If one of the values satisfies $l(r) = -\infty$, we take the smallest r such that $l(r) = -\infty$ and construct a path from $l(r-1) \in L_i$ to v_{i+1} as follows: Since $l(r) = -\infty$, the edge $\{w_{i+1}^R + 1, r\}$ is not star-crossing. Hence we can go from $l(r-1)$ in L_i to the vertex with the smallest index in L_i which is $w_{i+1}^R + 1$, take the edge $\{w_{i+1}^R + 1, r\}$ to go to R_i and collect the remaining vertices one by one starting from r with increasing index to v_{i+1}.
With this definition and Lemma 5.3.10 it follows.

Lemma 5.3.11. *Let $r \in R_i$ with $l(r) \neq -\infty$. Then the edges $\{l(r), r\}$ and $\{l(r)+1, r\}$ are not star-crossing.*

In general we can show that the $l(r)$ have decreasing indices.

Lemma 5.3.12. *For $r, r' \in R_i$ with $r < r'$, we have $l(r) \geq l(r')$.*

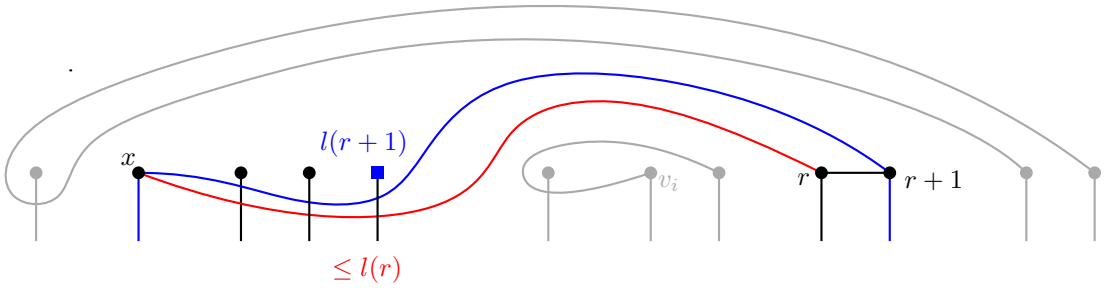

Figure 5.16: Illustration of the proof of Lemma 5.3.12.

Proof. We only consider the case $r' = r+1$. For $r' > r+1$ the claim follows by transitivity. Let T be the triangle induced by the vertices $\{v_\star, r+1, x\}$ such that $\{r+1, x\}$ crosses $\{l(r+1), v_\star\}$. See the blue triangle in Figure 5.16. The side of T containing $l(r+1)$ is not convex which is witnessed by $\{l(r+1), v_\star\}$. Since the drawing is convex, the side not containing $l(r+1)$ is convex. The edge $\{x, r+1\}$ does not cross star edges with vertices in R_i which shows that the vertex r is contained in the convex side of T. Hence the edge $\{x, r\}$ is fully contained in T. This implies that it crosses the star edge $\{l(r+1), v_\star\}$. This completes the proof that $l(r) \geq l(r+1)$. □

Similar to the case with $L_i = \emptyset$, we construct a Hamiltonian cycle starting with the edge $\{v_1, v_\star\}$. For $i = 1, \ldots, m-1$ we successively add paths from v_i to v_{i+1}. In the end we use good edges to traverse the remaining vertices and close the cycle with the edge $\{v_m + 1, v_\star\}$.
The first part is a path from v_i to $v_i + 1$. Starting from v_i, we go to the unvisited vertex in L_{i-1} with the largest index. Note that we set $L_0 = [w_1^R + 1, v_1 - 1]$. Then we visit them one by one with decreasing index until we reach the witness w_i^R. We proceed visiting vertices one by one with decreasing index until we reach w_i^L. Now we compute $l(v_i + 1)$. In the case $l(v_i + 1) = -\infty$, we proceed as described before and continue collecting all vertices in L_i one by one with decreasing index and then use the edge $\{w_{i+1}^R + 1, v_i + 1\}$ to go to R_i. In this case the remaining part of the path only consists of collecting the unvisited vertices in R_i with increasing index until reaching v_{i+1}.
If $l(v_i + 1) > -\infty$, we proceed from w_i^L to $l(v_i + 1) + 1$ one by one with decreasing index. By Lemma 5.3.11 the edge $\{l(v_i + 1) + 1, v_i + 1\}$ is not star crossing. We use this edge to get to

$v_i + 1$. Now we continue with the path to reach v_{i+1}. Let $r < v_{i+1}$ be the current vertex in R_i. We compute $l(r+1)$. If $l(r+1) = l(r)$, we use the good edge $\{r, r+1\}$ and continue with $r+1$ as current vertex in R_i. If $l(r+1) = -\infty$, we use the edge $\{r, l(r)\}$ which is not star crossing by Lemma 5.3.11. From $l(r)$ we continue collecting the remaining vertices with smaller index in L_i until $w_{i+1}^R + 1$, using the edge $\{w_{i+1}^R + 1, r+1\}$ and continue collecting the remaining vertices in R_i with increasing index. In the remaining case, i.e., $-\infty < l(r+1) < l(r)$, we use the edge $\{r, l(r)\}$ to go to L_i, continue collecting the vertices in L_i one by one with decreasing index until we reach $l(r+1)+1$. Then we use the edge $\{l(r+1), r+1\}$ which is not star crossing by Lemma 5.3.11. Now we proceed with $r+1$ as the current vertex in R_i.
For the last bad edge b_m, we construct the path to $v_\star$ as follows: Use the edge v_m to the largest vertex in L_{m-1} which was not used yet. Then proceed with decreasing index to reach vertex 1, and then add the good edge $\{1, v_m + 1\}$. Finally, we only have to add the star edge $\{v_m + 1, v_\star\}$ to close the path to a cycle.
For a formal description of the algorithm, see Algorithm 1.

Lemma 5.3.13. *Algorithm 1 finds a plane Hamiltonian cycle whose edges are not star-crossing in $O(n^2)$ time.*

Proof. The proof is divided into two parts. First we show that the algorithm indeed gives a plane Hamiltonian cycle. In the second part we give a proof for the quadratic runtime.
Correctness: In each step of Algorithm 1 we either progress to the left or to the right side without skipping vertices. Hence, every vertex is visited exactly once and the resulting cycle is Hamiltonian.
Moreover, since all the edges of the constructed path do not cross star edges and we construct the edges in such a way that the vertices of two independent edges $e = \{u, v\}$ and $e' = \{u', v'\}$ appear cyclically in the order u, u', v', v, they fulfill the condition of Observation 5.3.1. Hence the constructed Hamiltonian cycle is plane.
To see that no star-crossing edges are added, we analyze which edges are added by the algorithm:

- All edges that are added in lines 8, 10, 14, 17, 29, and 30 are between two consecutive vertices where both vertices lie in L_i or R_i or between w_i^L and w_i^R and hence they are good edges, i.e., they do not cross star edges.
- In lines 4 and 28 we add $\{v_i, u_i\}$: For $i = 1$, $\{v_1, u_1\}$ is a good edge because $u_1 = v_1 - 1$. For $i > 1$, we have either $u_i = w_i^R$ or $u_i = l(v_i)$. In the first case the edge is not star crossing by Lemma 5.3.6 and Lemma 5.3.11 implies that in the second case, the edge does not cross star edges.
- In line 9 we add $\{w_{i+1}^R + 1, r\}$: If we add an edge of this form, we are in the case where $l(r) = -\infty$. This implies that the edge $\{w_{i+1}^R + 1, r\}$ does not cross star edges.
- In line 15 we add $\{l(r) + 1, r\}$: In this case $l(r) \in [n-1]$ and by Lemma 5.3.11 this edge does not cross star edges.
- In line 19 we add $\{r', l(r')\}$: By Lemma 5.3.11 this edge does not cross star edges.

This shows the correctness of the algorithm since the edges added in Line 1 and Line 31 are star edges closing the path to a cycle.

Algorithm 1 Construction of a plane Hamiltonian cycle for convex drawings

Start the cycle with edge $\{v_\star, v_1\}$
Set $u_1 = v_1 - 1$
for $i = 1, \dots, m-1$ **do**
    Add edge $\{v_i, u_i\}$
    Set $r = v_i + 1$
    while $r \leq v_{i+1}$ **do**
        if $l(r) = -\infty$ **then**
            Add edges $\{u_i, u_i - 1\}, \dots, \{w^R_{i+1} + 2, w^R_{i+1} + 1\}$
            Add edge $\{w^R_{i+1} + 1, r\}$
            Add edges $\{r, r+1\}, \dots, \{v_{i+1} - 1, v_{i+1}\}$
            Set $u_{i+1} = w^R_{i+1}$
            Set $r = +\infty$
        else if $l(r) \in L_i$ **then**
            Add edges $\{u_i, u_i - 1\}, \dots, \{l(r) + 2, l(r) + 1\}$
            Add edge $\{l(r) + 1, r\}$
            Let $r' \in R_i$ be the largest index such that $l(r) = l(r+1) = \dots = l(r')$
            Add edges $\{r, r+1\}, \{r+1, r+2\}, \dots, \{r'-1, r'\}$
            if $r' < v_{i+1}$ **then**
                Add edge $\{r', l(r')\}$
                Set $u_i = l(r')$
            else if $r' = v_{i+1}$ **then**
                Set $u_{i+1} = l(v_{i+1})$
            end if
            Set $r = r' + 1$
        end if
    end while
end for
Add edge $\{v_m, u_m\}$
Add edges $\{u_m, u_m - 1\}, \{u_m - 1, u_m - 2\}, \dots, \{2, 1\}$
Add edge $\{1, v_m + 1\}$
Add star edge $\{v_m + 1, v_\star\}$

Running time: In the first preprocessing step, we compute the bad edges. This is possible in $O(n^2)$ time: for each of the $n-1$ edges $\{i, i+1\}$ there are $n-3$ potential witnesses which have to be tested. This directly determines the value m and all values v_i, w^L_i, w^R_i.

In the second preprocessing step, we compute the values of $l(r)$ for every r. We claim that this can be done in $O(n^2)$ time. To determine $l(r)$ for $r \in R_i$, we check if $l = l(r)$ for every $l \in L_i$. Recall that $l(r+1) \leq l(r)$ due to Lemma 5.3.12. Thus, once $l(r)$ is determined, we only need to check for vertices $l \in L_i$ where $l \leq l(r)$ to determine $l(r+1)$. We start with the smallest index r from R_i and with the largest index l from L_i, and iteratively either decrement l by one if $l \neq l(r)$, or we find $l = l(r)$ and increment r by one. In total, we consider a linear number of candidate pairs (l, r) to determine all values $l(r)$. For each such pair (l, r), we can test in linear

time whether $l = l(r)$ holds by checking whether the edge $\{l, v_\star\}$ crosses some edge $\{l', r\}$ with $l' < l$. Altogether, we can compute all values of $l(r)$ in $O(n^2)$ time.
Next observe that in each loop at least one edge is added to the cycle. Since in total there are exactly n edges added to the cycle, there are at most n iterations of the loop which takes $O(n)$ time. Hence, the total running time of Algorithm 1 is $O(n^2)$. □

This completes the proof of Theorem 5.2.2.

5.4 A second Proof of Lemma 5.3.4

In this section, we give the complete proof of Lemma 5.3.4 without computer assistance.

Lemma 5.3.4. *Let $b = \{v, v+1\}$ and $b' = \{v', v'+1\}$ be two distinct bad edges with witnesses w and w', respectively. Then the following three properties hold:*

(i) $w \neq w'$;

(ii) w', w, v, v' *appear in this or the reversed cyclic order around* $v_\star$;

(iii) Each of the triangles $\{v, v+1, v_\star\}$ *and* $\{v', v'+1, v_\star\}$ *is in the convex side of the other.*

In the following we prove the three properties separately starting with the first one. All of the arguments only consider the subdrawing induced by the vertices $\{w, w', v, v+1, v', v'+1, v_\star\}$ which is sufficient as described in the proof of Lemma 5.3.4 in Section 5.3. Throughout the section, we use the notation T_b for the triangle spanned by the two endvertices $v, v+1$ of a bad edge b and the star vertex $v_\star$ (see Observation 5.3.3). Moreover S_b denotes the convex side of T_b, which is the side not containing the witness w. For the figures in this section, we draw the triangle spanned by $\{v, v+1, v_\star\}$ red an the triangle spanned by $\{v', v'+1, v_\star\}$ blue.
In a first step we show that a vertex cannot be a witness for more than one bad edge, i.e., $w' \neq w$.

Proof of property (i). Assume towards a contradiction that $w = w'$, i.e., there is a vertex w which is a witness for both bad edges $b = \{v, v+1\}$ and $b' = \{v', v'+1\}$. Hence b and b' have a crossing with the edge $\{w, v_\star\}$. We assume without loss of generality, that the vertices w, v, v' appear in this cyclic order around $\pi_{v_\star}$. Otherwise they appear in the reverse order and the arguments work analogously. Note that possibly $v+1 = v'$.
If both vertices $v', v'+1$ lie in the convex side of T_b, the edge b' cannot cross $\{w, v_\star\}$ without leaving the convex side. A contradiction to the convexity of the drawing. Hence at least one of the two vertices $v', v'+1$ has to be in the non-convex side of T_b. In the same way we argue that not both vertices $v, v+1$ can lie in the convex side of $T_{b'}$. This shows that b has to cross at least one of the edges $\{v', v_\star\}$ or $\{v'+1, v_\star\}$ and b' has to cross at least one of the edges $\{v, v_\star\}$ and $\{v+1, v_\star\}$. We consider the three cases for b. Either b crosses exactly one of the two edges or both.

Case 1: b crosses $\{v', v_\star\}$ but not $\{v'+1, v_\star\}$.

In this case it clearly holds $v+1 \neq v'$. The vertex v' is in the interior of the non-convex side of T_b and $v'+1$ in the interior of the convex side of T_b. Since they are separated by T_b, the connecting edge b' has to cross T_b an odd number of times. In a simple drawing this is either once or three

times since every edge is crossed at most once. If b' crosses $\{v+1, v_\star\}$ it has to cross b as well. Hence we are in the situation with three crossings, which is depicted in Figure 5.17(a). In this case it is impossible to insert the edge $\{v+1, v'+1\}$ in the convex side of T_b, a contradiction to the convexity. Hence we assume from now on that b' does not cross $\{v+1, v_\star\}$.

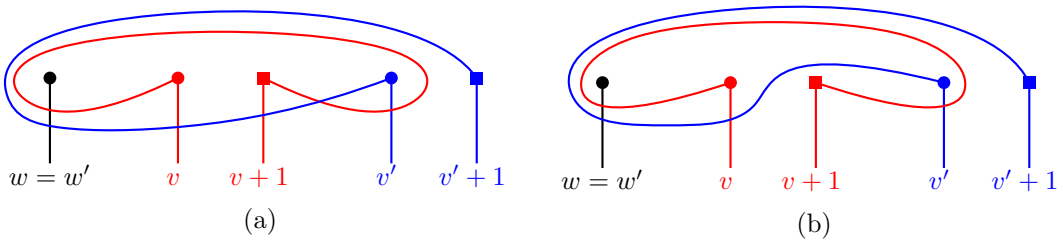

Figure 5.17: Illustration of two bad edges $b = \{v, v+1\}$ and $b' = \{v', v'+1\}$. The vertices marked with squares cannot be connected by an edge such that the drawing remains convex.

However, the edge b' has to cross at least one of the edges $\{v, v_\star\}$ and $\{v+1, v_\star\}$. Hence the remaining case is one crossing with the triangle T_b exactly at the edge $\{v, v_\star\}$. The situation is depicted in Figure 5.17(b). In this case $v+1$ is in the convex side of $T_{b'}$ but the edge $\{v+1, v'+1\}$ cannot stay in the intersection of both convex sides. Again a contradiction.

Case 2: b crosses $\{v'+1, v_\star\}$ but not $\{v', v_\star\}$.

In this case, $v'+1$ is in the interior of the non-convex side of T_b and v' is in the convex side. First consider the case $v+1 = v'$. The edge b' has to cross $\{v, v_\star\}$ which is not possible without crossing adjacent edges. Hence this situation cannot happen in a simple drawing. See Figure 5.18 for an illustration.

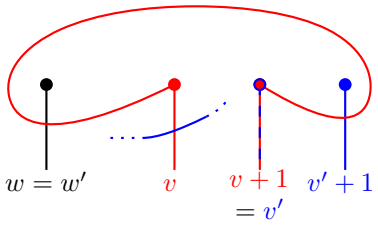

Figure 5.18: Illustration of two bad edges $b = \{v, v+1\}$ and $b' = \{v', v'+1\}$ with $v+1 = v'$.

From now on assume $v+1 < v'$. Again the edge b' has to cross T_b an odd number of times and at least one of the two edges $\{v, v_\star\}$ and $\{v+1, v_\star\}$. By the properties of a simple drawing, the edge has to cross either b or $\{v+1, v_\star\}$ since v' is in a region bounded by those two edges and the adjacent edge $\{v'+1, v_\star\}$. If b' crosses b, then it crosses all three boundary edges of T_b since it also has to cross at least one of the two star edges. The situation is depicted in Figure 5.19(a). The edge connecting v' and v has to lie completely in the convex side of T_b, which is impossible without crossing adjacent edges. A contradiction.
In the second case b' only crosses $\{v+1, v_\star\}$, see Figure 5.19(b). Since v is in the convex side of $T_{b'}$, the edge $\{v, v'\}$ has to stay in the intersection of both convex sides S_b and $S_{b'}$ which again is not possible.

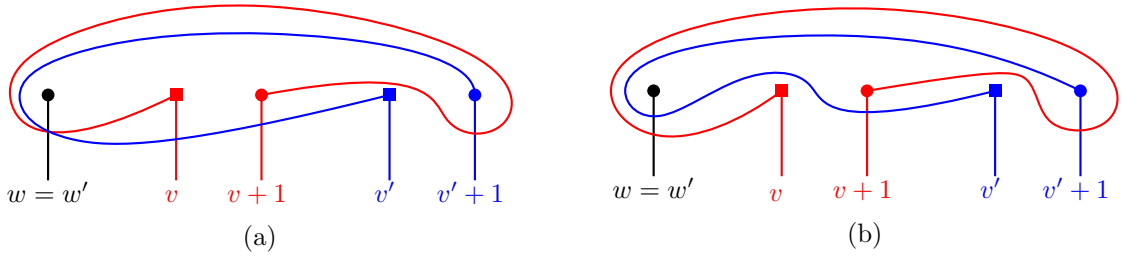

Figure 5.19: Illustration of two bad edges $b = \{v, v+1\}$ and $b' = \{v', v'+1\}$. The vertices marked with squares cannot be connected by an edge such that the drawing remains convex.

Case 3: b crosses both $\{v', v_\star\}$ and $\{v'+1, v_\star\}$.

In this case, it clearly is $v+1 \neq v'$ since both of the vertices v' and $v'+1$ are witnesses for the bad edge b and hence they have to be in the interior of the non-convex side of T_b. Therefore, the edge b' has to cross the triangle T_b an even number of times. As before, it has to cross at least one of the edges $\{v, v_\star\}$ or $\{v+1, v_\star\}$, which implies that b' crosses the triangle T_b exactly twice. Moreover b' cannot cross $\{v, v_\star\}$ and $\{v+1, v_\star\}$ at the same time without crossing b. See Figure 5.20 for an illustration. There are two cases remaining. By assumption $v', v'+1$ are in the non-convex side of T_b and exactly one of the vertices of $v, v+1$ is in the interior of the convex side of $T_{b'}$, while the other one in the interior of the non-convex side. Exchanging the roles of b and b' leads to the cases already considered (Case 1 and Case 2, see Figure 5.17(a) and Figure 5.19(a)). This concludes the proof that $w \neq w'$. □

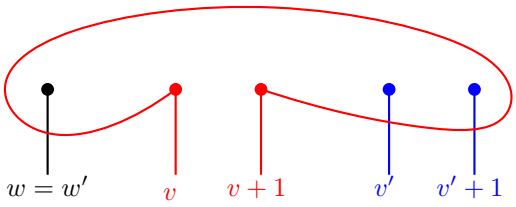

Figure 5.20: Illustration of the third case.

As a next step, we show that there is only one order (up to reversing) in which the vertices appear in the cyclic order around the star vertex $v_\star$.

Proof of property (ii). As already shown in (i), we have $w \neq w'$ and hence w cannot be a witness of b'. Similar w' cannot be a witness of b. Note that $w' \in \{v, v+1\}$, $w \in \{v', v'+1\}$ and $v+1 = v'$ are possible. Up to reflection, there are three different possibilities for the rotation around $v_\star$.

(5.1) w' w v v'

(5.2) w w' v v'

(5.3) w v w' v'

We want to show that the order in (5.1) is the only possibility for convex drawings. Hence we show that in the other two cases this cannot happen in a convex drawing. For this we

distinguish the two main cases. For each of them we consider several subcases depending on the edge crossings.

Case 1: Cyclic order w, w', v, v' around $v_\star$ as in (5.2)

We assume without loss of generality $w < w' \leq v < v+1 \leq v'$. Note that $v'+1$ might coincide with w. By assumption w is a witness of the edge $b = \{v, v+1\}$ and hence b crosses $\{w, v_\star\}$. We distinguish further subcases dependent on which star edges b crosses other than $\{w, v_\star\}$. By (i) the edge b does not cross $\{w', v_\star\}$.

Subcase (a): b crosses neither $\{v', v_\star\}$ nor $\{v'+1, v_\star\}$.
Note that this in particular implies $v'+1 \neq w$. Both vertices v' and $v'+1$ are in the interior of the convex side of T_b. Hence b' has to stay in the convex side of T_b, which implies that $w' \neq v$. Moreover, since w' is in a region bounded by the three edges $\{v, v_\star\}, \{w, v_\star\}, b$, it is impossible that b' crosses the star edge $\{w', v_\star\}$ without crossing $\{w, v_\star\}$. A contradiction. An illustration is given in Figure 5.21(a).

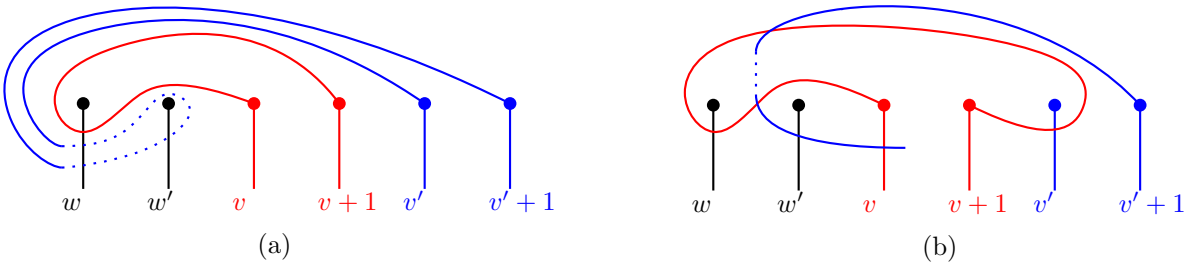

Figure 5.21: (a) The edge $b' = \{v', v'+1\}$ has to stay in the convex side of T_b and has to cross $\{w', v_\star\}$, which is not possible. (b) The edge b' cannot be drawn such that it crosses $\{w', v_\star\}$ but not $\{w, v_\star\}$.

Subcase (b): b crosses $\{v', v_\star\}$ but not $\{v'+1, v_\star\}$.
In this case it holds $v+1 \neq v'$ and $w \neq v'+1$. Since v' and $v'+1$ are in different sides of T_b, the edge b' has to cross T_b and odd number of times, either once or three times. Assume $w' \neq v$. Since the edge b' crosses $\{w', v_\star\}$, it has to cross two of the edges bounding the region in which w' is contained. These are the edges $\{w, v_\star\}, b, \{v, v_\star\}$. Moreover, b' does not cross $\{w, v_\star\}$. Hence there is only one possibility for b' and it has to cross $\{v, v_\star\}$ and b. Similar, in the case $w' = v$, the edge b' has to cross $\{v, v_\star\}$ and b. To connect to $v'+1$, the edge b' has to cross b again since this is the only edge incident to the region containing $v'+1$. This is impossible in a simple drawing. For an illustration, see Figure 5.21(b).

Subcase (c): b crosses $\{v'+1, v_\star\}$ but not $\{v', v_\star\}$.
If $v' \neq v+1$, the vertices v' and $v'+1$ are in different sides of T_b which implies that b' has an odd number of crossings with T_b. Since b' crosses $\{w', v_\star\}$ but not $\{w, v_\star\}$, there are at least two crossings with T_b which implies that there are exactly three. Hence every edge of T_b is crossed exactly once by b'. There is only one possibility to draw this, which is depicted in Figure 5.22(a).

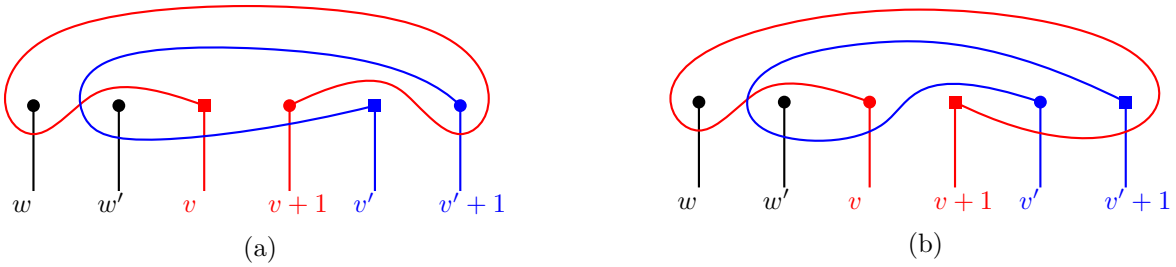

Figure 5.22: (a) The edge $\{v, v'\}$ whose vertices are marked with squares cannot be added in a convex way. (b) The edge $\{v+1, v'+1\}$ whose vertices are marked with squares cannot be drawn in a convex drawing.

The vertex v' which is in the convex side of T_b cannot be connected to v while staying in the convex side. This contradicts the property of convex drawings. Note that these also statements hold in the case $w' = v$ or $w = v' + 1$. If $v' = v + 1$, the edge b' has to cross b and $\{v, v_\star\}$. Since b and b' share an vertex, this is not possible in a simple drawing.

Subcase (d): b crosses both $\{v', v_\star\}$ and $\{v' + 1, v_\star\}$.
In this case it holds $v' \neq v + 1$ and both vertices v' and $v' + 1$ are in the non-convex side of T_b. However the vertex w' is in the convex side. Hence the edge b' crosses T_b twice. Both crossings are needed to enter and leave the cell containing w'. In order to obtain a simple drawing, b' has to cross $\{v, v_\star\}$ and b as illustrated in Figure 5.22(b). This implies that $v + 1$ is in the convex side of $T_{b'}$. Hence the edge $\{v + 1, v' + 1\}$ has to stay in the convex side. This is not possible in a simple drawing. A contradiction.

Hence this order cannot appear in convex drawings. We now consider the second order of the vertices around $v_\star$.

Case 2: Cyclic order w, v, w', v' around $v_\star$ as in (5.3)
In this case, we assume that it holds $w < v < v + 1 \leq w' < v'$. Note that this order implies that $v + 1 \neq v'$. However $v + 1 = w'$ and $v' + 1 = w$ are still possible. We again distinguish the following four subcases.

Subcase (a): b crosses neither $\{v', v_\star\}$ nor $\{v' + 1, v_\star\}$.
This case implies that $w \neq v' + 1$. In this case, both vertices, v' and $v' + 1$ are in the convex side of T_b and hence the edge b' has to stay in the convex side and does not cross T_b. Hence it has to be $v+1 \neq w'$. Now v' is in the convex side of T_b and v in the convex side of $T_{b'}$. This implies that the edge $\{v, v'\}$ has to stay in the intersection of both convex sides. The situation is depicted in Figure 5.23(a). The triangle induced by $\{v, v', v_\star\}$ has no convex side. The vertices w and w' are witnesses for this since their star edges connecting to $v_\star$ cross the boundary of this triangle.

Subcase (b): b crosses $\{v', v_\star\}$ but not $\{v' + 1, v_\star\}$.
This case implies again that $w \neq v' + 1$. The edge b' crosses $\{w', v_\star\}$. To guarantee this crossing, the edge has to cross b and $\{v + 1, v_\star\}$. The remaining edge of T_b, which can be crossed to leave this side of the triangle, is $\{v, v_\star\}$. However, we cannot connect to $v' + 1$, which is in

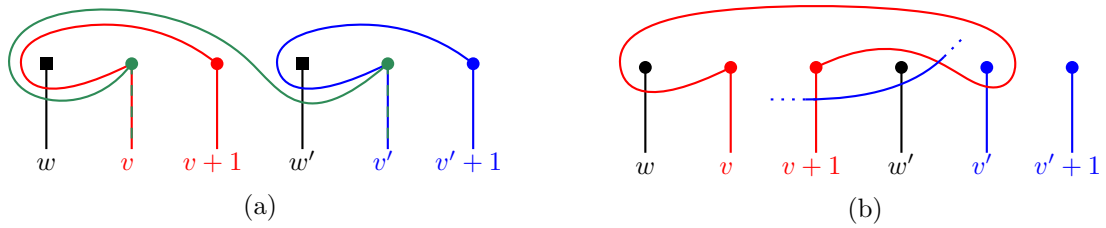

Figure 5.23: (a) The green edge connecting v and v' must not cross any of the blue or red edges. But in this case the green triangle is not convex due to $\{w, v_\star\}$ and $\{w', v_\star\}$. (b) In this convex drawing there cannot be an edge $b' = \{v', v'+1\}$, which crosses $\{w', v_\star\}$ but not $\{w, v_\star\}$.

the convex side of T_b, without crossing $\{w, v_\star\}$. A contradiction. The situation is depicted in Figure 5.23(b).

Subcase (c): b crosses $\{v'+1, v_\star\}$ but not $\{v', v_\star\}$.
As in the previous case, v' and $v'+1$ are in different sides of T_b and hence b' crosses T_b either once or three times. Assume it only crosses once, then the edge b' crosses either $\{v+1, v_\star\}$ or b in order to leave the region containing w'. First assume b' crosses only b. But then v and $v+1$ are in the convex side of $T_{b'}$ and the edge b does not stay in the convex side. Hence this cannot happen in a convex drawing. If b' crosses only $\{v+1, v_\star\}$, the vertex v is in the convex side of $T_{b'}$ and v' is in the convex side of T_b. This shows that the connecting edge $\{v, v'\}$ has to stay in the intersection of both convex sides. This is not possible, see Figure 5.24(a).
In the remaining case b' crosses all three boundary edges of T_b. Again this cannot happen in a convex drawing of the complete graph. To see this note that v' is in the convex side of T_b. As before, the edge $\{v, v'\}$ has to stay in the convex side of T_b and does not cross adjacent edges. This is impossible. The case is depicted in Figure 5.24.

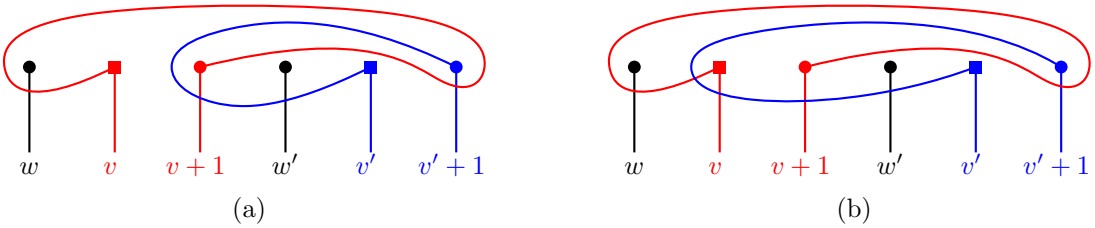

Figure 5.24: Two cases to draw the edge b'. In both cases the edge $\{v', v\}$, whose endvertices are marked with squares, cannot be added in a convex drawing.

Subcase (d): b crosses both $\{v', v_\star\}$ and $\{v'+1, v_\star\}$
The vertices v' and $v'+1$ are in the non-convex side of T_b. The edge b' has to cross $\{w', v_\star\}$, which is contained in the convex side of T_b. Hence b' has to cross exactly two edges of T_b, which are b and $\{v+1, v_\star\}$ as boundary edges of the region, which contains w'. This implies that the vertex v is contained in the convex side of $T_{b'}$. However, the edge $\{v, v'\}$ cannot be drawn in the convex side without crossing adjacent edges. This is a contradiction. For an illustration see Figure 5.25.

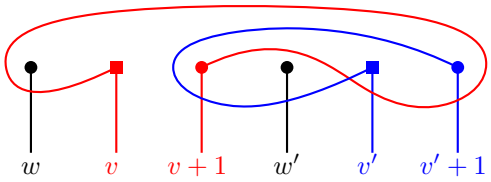

Figure 5.25: The edge $\{v, v'\}$, whose endvertices are marked with squares, cannot be drawn such that the drawing stays convex.

This shows that the only possible order of the vertices around the fixed star vertex $v_\star$ is w', w, v, v'. Note that this in particular implies that $w \notin \{v', v'+1\}$ and $w' \notin \{v, v+1\}$. □

It remains to show that the bad edges b and b' do not cross and are nested as claimed.

Proof of property (iii). From the two previous parts we know that $w \neq w'$ and that w', w, v, v' appear in this order (or reversed) in the rotation $\pi_{v_\star}$ around the star vertex $v_\star$. Without loss of generality we assume that the vertices appear in the order w', w, v, v' around $v_\star$. The other case is symmetric. Moreover, since $w' \neq w$ holds for all witnesses, a witness w of b cannot be a witness for w' and vice versa. In particular b does not cross $\{w', v_\star\}$ and b' does not cross $\{w, v_\star\}$. This implies that w is in the convex side of $T_{b'}$ and w' in the convex side of T_b.
To show the statement, we have to show that $v', v'+1$ are in the convex side of T_b and $v, v+1$ are in the convex side of $T_{b'}$. This is sufficient since the convexity implies that the edge b, respectively b', is completely contained in the corresponding convex side. We only show the first part that $v', v'+1$ are in the convex side of T_b. The other case works analogously. Assume towards a contradiction that at least one of the two vertices v' and $v'+1$ is in the interior of the non-convex side of T_b. Note that if $v' = v+1$, the vertex is in both sides of T_b. In all other cases not being in the convex side is equivalent to being in the non-convex side. If at least one of the two vertices $v', v'+1$ is in the interior of the non-convex side of T_b, this vertex is a witness of the bad edge b. A contradiction since the order in the rotation around $v_\star$ does not correspond to one proven in (ii). □

This concludes the proof of the lemma.

Chapter 6

Asymptotic Number and Fliples

In this chapter, we discuss the asymptotic number of r-signotopes and generalized signotopes. More specifically we give a proof of Proposition 2.2.14 showing that for $r \geq 3$ there are $2^{\Omega(n^{r-1})}$ r-signotopes on $[n]$. Moreover we make structural investigations of signotopes and give the first linear lower bound on the number of fliples in every r-signotope. More specifically we show that every r signotope on $[n]$ has at least $\frac{2n-2}{r}$ fliples. For generalized signotopes, we show that asymptotically there are $2^{\Omega(n^3)}$ many (Theorem 6.3.1), which strengthens a result by Knuth [Knu92] who proved a lower bound for the number of generalized signotopes. We improve his lower bound and give an asymptotically matching upper bound using Shearer's entropy lemma. Kynčl [Kyn13] showed that there are at most $2^{n^2\alpha(n)^{O(1)}}$ weak isomorphism classes of simple drawings of K_n, where $\alpha(n)$ is the extremely slow growing inverse of the Ackermann function. Hence there are essentially more generalized signotopes than simple drawings, which shows that there a generalized signotopes which do not come from simple drawings. Moreover we study the relation between simple drawings and generalized signotopes for small numbers in more detail.

Outline In the first part of this chapter, in Section 6.1, we consider r-signotopes and give a proof of Proposition 2.2.14. This part is based on [BFS23a]. In Section 6.2, we improve the lower bound of the minimum degree in the flip graph $G(n, r)$ from the constant number 2 to a linear bound $\frac{2n-2}{r}$, which is unpublished. In the remaining part of this chapter, Section 6.3 we determine the asymptotic number of generalized signotopes, improving a previous result by Knuth [Knu92] and in Section 6.4 we discuss the relation to simple drawings. These two sections are based on [BFS$^+$23b].

6.1 Asymptotic Number of Signotopes

It is well known that the number of oriented matroids of rank r on n elements is $2^{\Theta(n^{r-1})}$ [BLS$^+$99, Corollary 7.4.3]. As shown in Section 2.2.5, the set of r-signotopes is a subset of rank r oriented matroids. Balko showed that r-signotopes are indeed a rich subclass of oriented matroids of rank r.

Proposition 2.2.14 ([Bal19, Theorem 3])**.** *For $r \geq 3$, the number of r-signotopes on $[n]$ is $s(n, r) = 2^{\Theta(n^{r-1})}$.*

In ranks 1 and 2 there are 2^n and $n!$ signotopes on $[n]$, respectively. Rank 1 signotopes are mappings from $[n]$ to $\{+, -\}$ without any additional property and 2-signotopes are permutations. For rank $r \geq 3$, the precise number of r-signotopes on $[n]$ has been computed for small values of r and n; see A006245 (rank 3) and A060595 to A060601 (rank 4 to rank 10) on the OEIS.

6.1.1 Proof of the upper Bound

The upper bound follows immediately using the fact, that r-signotopes on n elements are rank r oriented matroids (cf. Section 2.2.5) and their number is upper bounded by $2^{c(n^{r-1})}$ [BLS+99, Chapter 7.4]. For completeness, however, we include an inductive proof.
For rank 3, there exists a constant $c > 0$ such that for every n there are at most $2^{cn^2(1+o(1))}$ signotopes on n elements. The currently best bound $c = 0.657$ is due to Felsner and Valtr [FV11].
For rank $r \geq 4$, we proceed by induction. Given an r-signotope σ on $[n]$, we compute its sequence of projections. For each $i \in [n]$, we project σ to i and obtain an $(r-1)$-signotope $\sigma \downdownarrows_i$ on $n-1$ elements. Since two distinct r-signotopes yield different sequences $(\sigma \downdownarrows_i)_{i\in[n]}$ of projections, we can bound the number of r-signotopes as

$$s(n,r) \leq (s(n-1,r-1))^n \leq \left(2^{c(n-1)^{r-2}}\right)^n \leq 2^{cn^{r-1}}.$$

6.1.2 Proof of the lower Bound

For convenience we assume $n = rm$ for some $m \in \mathbb{N}$. We partition $[n] = \bigcup_{k=1}^{r} N_k$ into r intervals $N_k = [(k-1)m+1, km]$ of size m.
For every r-subset $(x_1, \ldots, x_r)$ we define the weight $\phi(x_1, \ldots, x_r) = \left(\sum_{k=1}^{r-1} x_k\right) - x_r$. Note that, for r-subsets $X = (x_1, \ldots, x_{r+1})$ with $x_1 < \ldots < x_{r+1}$ as usual, it holds $\phi(X_1) > \ldots > \phi(X_r)$ and $\phi(X_r) < \phi(X_{r+1})$.
For a threshold T we now define a collection $\mathcal{S}_T$ of signotopes on $[n]$. A signotope σ is in $\mathcal{S}_T$ if σ has the following signs, where $\pm$ indicates that the sign can be chosen arbitrarily from $\{+,-\}$.

$$\sigma(x_1, \ldots, x_r) = \begin{cases} - & \text{if } x_{r-1} \notin N_r,\ x_r \in N_r, \text{ and } \phi(x_1, \ldots, x_r) > T \\ \pm & \text{if } x_{r-1} \notin N_r,\ x_r \in N_r, \text{ and } \phi(x_1, \ldots, x_r) = T \\ + & \text{otherwise.} \end{cases}$$

For the lower bound we show two properties:

(i) The elements of $\mathcal{S}_T$ are indeed signotopes.

(ii) For fixed r and a suitable chosen T there are $2^{\Omega(n^{r-1})}$ elements in $\mathcal{S}_T$.

To show (i), we check the monotonicity of all $(r+1)$-subsets $X = (x_1, \ldots, x_{r+1})$, that is, there is at most one sign-change in the sequence

$$(\sigma(X_1) \ \ldots \ \sigma(X_{r+1})).$$

If $x_{r+1} \notin N_r$, then $\sigma(X_j) = +$ for all $j = 1, \ldots, r+1$ and there is no sign change on the packet. Otherwise, there is some $k \in [r+1]$ such that $x_1, \ldots, x_{k-1} \notin N_r$ and $x_k, \ldots, x_{r+1} \in N_r$.
If $k < r$, then $x_{r-1}, x_r, x_{r+1} \in N_r$. Hence each X_j contains at least two elements from N_r, which implies $\sigma(X_j) = +$ for all $j = 1, \ldots, r+1$ and there is no sign change on the packet.
If $k = r$, then each X_j with $j < r$ contains two elements from N_r and thus $\sigma(X_j) = +$ for $j < r$. We also know that $\phi(X_r) < \phi(X_{r+1})$, therefore, if $\sigma(X_r) = -$ then $\sigma(X_{r+1}) = -$ as well. Hence, there is at most one sign change on the packet.
Finally, if $k = r+1$, then $\sigma(X_{r+1}) = +$. Since $\phi(X_1) > \phi(X_2) > \ldots > \phi(X_r)$ the sign sequence $(\sigma(X_1)\ \sigma(X_2)\ \ldots\ \sigma(X_r))$ is a sequence of $-$ signs followed by a sequence of $+$ signs possibly one $\pm$ in between. Again there is at most one sign change on the packet.
This completes the proof of (i) that all elements of $\mathcal{S}_T$ are signotopes.

It remains to show (ii), i.e., for some T the set $\mathcal{S}_T$ contains sufficiently many elements. Call an r-subsets $(x_1, \ldots, x_r)$ *splitted* if $x_k \in N_k$ for all $k = 1, \ldots, r$. Splitted r-subsets with $\phi(x_1, \ldots, x_r) = T$ are subsets where every $\sigma \in \mathcal{S}_T$ can be freely and independently assigned to a sign from $\{+, -\}$. For two non-determined r-subsets the choice can only affect each other if they appear in a common $(r+1)$-subset. This is the case if they share $r-1$ elements. However since only one element differs, the weight ϕ of the two r-subsets differs. Hence not both r-subsets have weight T. If there are a_T splitted r-subsets with $\phi(x_1, \ldots, x_r) = T$ then $|\mathcal{S}_T| \geq 2^{a_T}$.
For splitted r-subsets $(x_1, \ldots x_r)$, we can identify the elements $x_k \in N_k$ with its relativ position $y_k = x_k - (k-1)m$ in the set N_k. Hence the splitted r-subsets are in bijection with the set $[m]^r$ via $y_k = x_k - (k-1)m$. We first consider the r-tuples $(y_1, \ldots, y_r) \in [m]^r$ and then find the corresponding r-subsets $(x_1, \ldots, x_r)$.
There are $\binom{\ell-1}{r-2}$ possible ordered partitions of an integer ℓ into exactly $r-1$ positive integers. Hence for $r-1$ positive integers $y_1, \ldots, y_{r-1}$ there are $\binom{\ell-1}{r-2}$ solutions to the equation

$$\sum_{k=1}^{r-1} y_k = \ell.$$

We use this to determine the number of solutions for r elements $y_1, \ldots, y_r \in [m]$ such that

$$\sum_{k=1}^{r-1} y_k = y_r. \tag{6.1}$$

Since y_r is in $[m]$, the number of solutions is $\sum_{\ell=1}^{m} \binom{\ell-1}{r-2}$. By the hockey-stick identity for binomial coefficients this can be rephrased as:

$$\sum_{\ell=1}^{m} \binom{\ell-1}{r-2} = \sum_{\ell=r-2}^{m-1} \binom{\ell}{r-2} = \binom{m}{r-1} = \Theta(m^{r-1}) = \Theta(n^{r-1}).$$

In the next step, we determine a suitable threshold T to find the corresponding r-subsets $(x_1, \ldots, x_r)$. Hence we want to determine T such that $\phi(x_1, \ldots, x_r) = \sum_{k=1}^{r-1} x_k - x_r = T$ if and only if the corresponding $y_1, \ldots, y_r$ fulfill equation (6.1). It is

$$\begin{aligned}
0 &= \sum_{k=1}^{r-1} y_k - y_r \\
&= \sum_{k=1}^{r-1} (x_k - (k-1)m) - (x_r - (r-1)m) \\
&= \sum_{k=1}^{r-1} x_k - x_r - \sum_{k=1}^{r-1} m(k-1) + (r-1)m \\
&= \sum_{k=1}^{r-1} x_k - x_r - m \cdot \frac{(r-2)(r-1) - 2(r-1)}{2} \\
&= \sum_{k=1}^{r-1} x_k - x_r - m \cdot \frac{(r-4)(r-1)}{2}.
\end{aligned}$$

Hence $T = m \cdot \frac{(r-4)(r-1)}{2}$ is a constant which gives the lower bound.

6.2 Fliples in Signotopes

Felsner and Kriegel [FK99] showed that every Euclidean pseudoline arrangement with n pseudolines has at least $n-2$ triangular cells. Hence the minimum degree of $G(n,3)$ is at least $n-2$. Since the cyclic arrangement of rank 3 has exactly $n-2$ triangular cells, the lower bound is tight. Recently Alves Radtke et al. [AFO$^+$23] showed that $G(n,3)$ is $n-2$ connected. Felsner and Weil [FW01] conjectured that the minimum degree and the connectivity of $G(n,r)$ is $n-r+1$ for all $n \geq r \geq 3$. In particular this would show that the cyclic arrangement of rank r on n elements which has exactly $n-r+1$ fliples minimizes the number of fliples. Recently, together with Lukas Egeling from ETH Zürich we found a counterexample to this conjecture. There are eight rank 4 signotopes on 8 elements which only have 4 fliples. Those examples can be found using the SAT framework described in Section 3.6.1. As it turns out they are also examples which are not 2-extendable.

Since every r-signotope is contained in a maximum chain in $B(n,r)$, see Theorem 2.2.11, there exists in all signotopes except the cyclic and the reversed cyclic a r-subset which can be flipped from $+$ to $-$ and one which can be flipped from $-$ to $+$. Hence every signotope has at least 2 fliples. We show the first linear bound. As an intermediate step we show that every element is contained in a fliple.
In general pseudohyperplane arrangements, i.e., in oriented matroids, the question of the existence of simplicial cells remains open. Simplicial cells in terms of matroids are often called *mutations*. The existence of mutations for all oriented matroids is a famous conjecture by Las Vergnas, see [BLS$^+$99, Conjecture 7.3.10]. There are only partial results known. Bokowski and Rohls [BR01] showed that every rank 4 oriented matroid on $n \leq 12$ elements has a mutation. Moreover, in contrast to signotopes, there are examples in which one element is not incident to any simplicial cell. The first example of rank 4 with 20 element was presented by Richter-Gebert [Ric93]. More recently Bokowski and Rohls [BR01] found a smaller example of rank 4 with only 17 elements.

Theorem 6.2.1. *For $r \geq 2$ every r-signotope on $n \geq r+1$ elements has at least $\frac{2n-2}{r}$ fliples.*

Note that for $r = 1$ all n elements are fliples. Moreover, for $r = 2$ the fliples correspond to adjacent transposition and every permutation on n elements admits $n-1$ adjacent transposition. Moreover, for all $r \geq 1$ the graph $G(r,r)$ contains exactly 2 elements, both of them have degree exactly 1. The graph $G(r+1,r)$ is a $2(r+1)$ cycle (cf. Figure 2.5) in which every vertex has degree 2. This corresponds to the above bound.
From now on, we assume $r \geq 3$. The strategy for the proof is to show, that every element is contained in a fliple. For this, we first consider the element 1, which is the element at the first position. As in Section 3.5 (see page 54), we partition the $(r-1)$-element subsets into

$$\begin{aligned}
\mathcal{H}_1^\sigma &= \{\ I \subset [n] : |I| = r-1,\ 1 \in I\ \};\\
\mathcal{U}_1^\sigma &= \{\ I \subset [n] : |I| = r-1,\ 1 \notin I,\ \sigma(I \cup \{1\}) = +\ \};\\
\mathcal{D}_1^\sigma &= \{\ I \subset [n] : |I| = r-1,\ 1 \notin I,\ \sigma(I \cup \{1\}) = -\ \}.
\end{aligned}$$

Lemma 3.5.1 shows that $\mathcal{D}_1^\sigma$ is a down-set, and $\mathcal{U}_1^\sigma$ an up-set in the partial order $\prec$ corresponding to the r-signotope σ. We show that the minimal elements in the up-set and the maximal elements in the down-set together with the 1 are fliples.

Lemma 6.2.2. *There exists a fliple F of σ with $1 \in F$.*

Proof. Since $\binom{[n]}{r-1}$ contains sets which do not contain the 1, at least one of the two sets $\mathcal{D}_1^\sigma$ or $\mathcal{U}_1^\sigma$ is non-empty. For each of them which is non-empty, we take the closest element to 1 in the following sense:

- If $\mathcal{D}_1^\sigma$ is non-empty, we take a largest element $I_\mathcal{D}$ in $\mathcal{D}_1^\sigma$.
- If $\mathcal{U}_1^\sigma$ is non-empty, we take a smallest element $I_\mathcal{U}$ in $\mathcal{U}_1^\sigma$.

Note that the up- and down-sets might have more minimal or maximal elements. We show for both possibilities $I \in \{I_\mathcal{D}, I_\mathcal{U}\}$ that the r-subset $I \cup \{1\}$ is a fliple. We only discuss the case $I = I_\mathcal{U}$. The other case works analogously by changing the signs and corresponding orders. To show that it is a fliple, we show that it is flipable in each packet it is contained in. Let $I = (x_1, \dots, x_{r-1})$ and $P = \{1\} \cup I \cup \{y\}$ an $(r+1)$-subset containing $I \cup \{1\}$. Assume in the ordered sequence of P, the element y is at position $i \in \{2, \dots, r+1\}$, i.e., $P_i = I \cup \{1\}$. Note that $1 \in P_k$ for all $k = 2, \dots, r+1$. Since $I \in \mathcal{U}_1^\sigma$, the sign of this r-subset is

$$\sigma(P_i) = \sigma(I \cup \{1\}) = +.$$

We distinguish two cases. First assume $\sigma(P_1) = \sigma(I \cup \{y\}) = +$. This shows that for all $k < i$, it is $I = P_1 \backslash \{y\} \prec P_1 \backslash \{x_{k-1}\} = P_k \backslash \{1\}$, which implies that $P_k \backslash \{1\} \in \mathcal{U}_1^\sigma$ by the property of an up-set. Hence $\sigma(P_k) = +$. Moreover for all $k > i$ it is $I = P_1 \backslash \{y\} \succ P_1 \backslash \{x_{k-1}\} = P_k \backslash \{1\}$, which implies that $P_k \backslash \{1\} \in \mathcal{D}_1^\sigma$ by the minimality assumption of I. This shows that $\sigma(P_k) = -$. Hence the sign change is exactly between P_i and P_{i+1} which shows that P_i is flipable.
The second case, if $\sigma(P_1) = \sigma(I \cup \{y\}) = -$ works similar. For all $k > i$, it is $I \prec P_k \backslash \{1\}$, which implies that $P_k \backslash \{1\} \in \mathcal{U}_1^\sigma$ and hence $\sigma(P_k) = +$. Moreover for all $k < i$ it is $I \succ P_k \backslash \{1\}$ and hence $P_k \backslash \{1\} \in \mathcal{D}_1^\sigma$ by the minimality assumption of I. This shows that $\sigma(P_k) = -$. Hence the sign change is exactly between P_{i-1} and P_i. Again P_i is flipable, which completes the proof. □

Using the rotation operator and Lemma 6.2.2, we transfer this result to all elements. This yields a smaller lower bound on the number of fliples.

Proposition 6.2.3. *Let σ be an r-signotope on $n \geq r$ elements. For every $k \in [n]$, there is a fliple F with $k \in F$. In particular σ has at least $\frac{n}{r}$ fliples.*

Proof. By Lemma 6.2.2 there is a fliple containing the first element 1. Moreover, Lemma 3.3.2 shows that fliples are invariant under rotation. Hence with the rotation operator, we can make every element the first one. This shows that every element is contained in a fliple. Since every fliple contains r elements, there are at least $\frac{n}{r}$ fliples. □

In a next step, we show that there are at most 2 elements such that one of the two sets $\mathcal{U}_1^\sigma$, $\mathcal{D}_1^\sigma$ is empty. This shows that the remaining $n-2$ elements are contained in at least 2 fliples, which yields the statement of Theorem 6.2.1 since the total number of fliples is $\frac{2(n-2)+2}{r} = \frac{2n-2}{r}$.

Lemma 6.2.4. *For $n \geq r+1 \geq 4$, there are $n-2$ elements which are contained in at least 2 fliples.*

Proof. Let $k \leq n$ be a rotation of σ such that exactly one of the two sets $\mathcal{U}_1^\sigma$, $\mathcal{D}_1^\sigma$ is empty. If $\mathcal{U}_1^\sigma$ is empty, all subsets $I \in \binom{[n]}{r-1}$ which do not contain the 1 are in $\mathcal{D}_1^\sigma$, i.e., $\sigma_{\mathrm{rot}(k)}(I \cup \{1\}) = -$ for all $I \in \binom{[n]\setminus\{1\}}{r-1}$. Hence the sign of $(I \cup \{1\})_{\mathrm{rot}(-k)} = I_{\mathrm{rot}(-k)} \cup \{k+1\}$ in σ is

$$\sigma(I_{\mathrm{rot}(-k)} \cup \{k+1\}) = - \cdot (-)^x,$$

where x is the number of rotated elements in $I_{\mathrm{rot}(-k)}$, i.e, the number of elements in $I_{\mathrm{rot}(-k)}$ which are $\leq k$. We rephrase this as

$$\sigma(I \cup \{k+1\}) = - \cdot (-)^x,$$

for all I with $k+1 \notin I$ and $x = |\{i \in I : \ i \leq k\}|$. In the same way it follows for a rotation $k \leq n$ if $\mathcal{D}_1^\sigma$ is empty then

$$\sigma(I \cup \{k+1\}) = + \cdot (-)^x,$$

for all I with $k+1 \notin I$ and $x = |\{i \in I : \ i \leq k\}|$.
Denote the up-set from the k-fold rotation $\sigma_{\mathrm{rot}(k)}$ considered in the original signotope σ by $\mathcal{U}_{k+1}^\sigma = \left(\mathcal{U}_1^{\sigma_{\mathrm{rot}(k)}}\right)_{\mathrm{rot}(-k)}$ and similarly, the down-set by $\mathcal{D}_{k+1}^\sigma = \left(\mathcal{U}_1^{\sigma_{\mathrm{rot}(k)}}\right)_{\mathrm{rot}(-k)}$.

Claim 6.1. *Let $k, \ell \in [n]$ with $k < \ell$. If either $\mathcal{U}_k^\sigma = \mathcal{U}_\ell^\sigma = \emptyset$ or $\mathcal{D}_k^\sigma = \mathcal{D}_\ell^\sigma = \emptyset$, then $k = 1$ and $\ell = n$.*

Proof. Consider a subset $X \in \binom{[n]}{r}$ such that $k, \ell \in X$. For $k \neq 1$ or $\ell \neq n$, we may assume that the position of k and ℓ in the ordered set has an odd difference. If $\ell - k \leq r$ is odd, we consider the set X containing $k, k+1, \ldots, \ell-1, \ell$ with additional arbitrary element such that X has r elements. In the remaining cases, we choose X such that there is an even number of elements between k and ℓ which is always possible since $n \geq r+1$. Hence we can leave out elements in between. The only case where we cannot change the position of k and ℓ arbitrarily is for $k = 1$ and $\ell = n$. In this case k is always at the first and n is always at the r-th position. Hence if $r-1$ is even which is the case if r is odd, such a choice is not possible.

Let $s = -$ if $\mathcal{U}_k^\sigma = \mathcal{U}_\ell^\sigma = \emptyset$ otherwise if $\mathcal{D}_k^\sigma = \mathcal{D}_\ell^\sigma = \emptyset$ we set $s = +$. For the r-subset X as described above, it is

$$s \cdot (-)^i = \sigma(X) = s \cdot (-)^j$$

where i is the position of k in the ordered set X and j the position of ℓ. This is impossible if $j - i$ is odd. ■

For an illustration of two pseudolines for which the down-set is empty and hence there cannot be pseudolines above both or below both see Figure 6.1(a).
The claim shows that there exist no three distinct elements such that the up-set of all of them is empty. Moreover, there are no three distinct elements such that the down-set of all of them is empty.
In the case that there is one k such that up-set is empty and ℓ such that down-set is empty, we get the following relation. For an illustration in terms of pseudolines see Figure 6.1(b) showing that two such pseudolines have to be consecutive.

(a) (b)

Figure 6.1: (a) Two pseudolines with marked down-set. If the down-set of both pseudolines is empty, then there are no pseudolines starting above the blue one or below the red one. (b) Two pseudolines such that for the red one the up-set is empty and for the blue one the down-set is empty. In this case there is no pseudoline between the two.

Claim 6.2. *Let $k, \ell \in [n]$. If $\mathcal{U}_k^\sigma = \mathcal{D}_\ell^\sigma = \emptyset$, then $|k - \ell| = 1$.*

Proof. Consider an r-subset X which contains k, ℓ. Let i be the position of k and j the position of ℓ in the ordered set of X. It holds

$$- \cdot (-)^i = \sigma(X) = + \cdot (-)^j$$

which is impossible if $|i - j|$ is even. For every choice of $k, \ell \in [n]$ except $|k - \ell| = 1$, we find a set X such that $|i - j|$ is even. ■

Assume towards a contradiction that there are three elements for which either the up-set or the down-set is empty, then there are two elements of the same kind. Hence one of them is 1 and the other one n. Moreover, the third element must be different from 1 and n and at a distance of 1 from both of them. This is not possible for $n \geq 4$. □

6.3 Counting Generalized Signotopes

In this section we show that the number $g(n)$ of generalized signotopes on n elements is of order $2^{\Theta(n^3)}$. Knuth [Knu92] already showed a lower bound of $\log_2(g(n)) \geq \frac{1}{27}n^3$. We improve the constant to $\frac{1}{24}$ and give an asymptotic matching upper bound. For small n the exact number of generalized signotopes can be found at the sequence A328377 of OEIS.

Theorem 6.3.1. *The number $g(n)$ of generalized signotopes on $n \geq 8$ elements is between $2^{c_1 \cdot n^3 + O(n^2)}$ and $2^{c_2 \cdot n^3}$ for constants $c_1 = \frac{1}{24} \approx 0.0417$ and $c_2 \approx 0.1339$.*

6.3.1 Upper Bound for $g(n)$:

For $n \geq t$ we show that $g(n) \leq g(t)^{\binom{n}{t}/\binom{n-3}{t-3}}$ is an upper bound on the number of generalized signotopes on n elements. For this we use of Shearer's entropy lemma [CGFS86].

Lemma 6.3.2 (Shearer's Entropy Lemma [CGFS86])**.** *Let S be a finite set and let $A_1, \ldots, A_m$ be subsets of S such that every element of S is contained in at least k of the sets $A_1, \ldots, A_m$.*

If $\mathcal{F}$ is a collection of subsets of S and $\mathcal{F}_i = \{F \cap A_i \colon F \in \mathcal{F}\}$ for $1 \le i \le m$. Then

$$|\mathcal{F}|^k \le \prod_{i=1}^{m} |\mathcal{F}_i|.$$

Let $t \le n$. We consider the set $S = \binom{[n]}{3}$ of all triples from $[n]$ and, for each t-subset I of $[n]$, let $A_I = \binom{I}{3}$ be the set of triples of I. There are $m = \binom{n}{t}$ choices for I and as many sets A_I. Each triple in S belongs to $k = \binom{n-3}{t-3}$ sets A_I.
A generalized signotope on n elements is uniquely encoded by its $+$-triples, which form a subset of S. Let $\mathcal{F}$ be the family of all generalized signotopes on n elements given by their $+$-triples. For every I, let $\mathcal{F}_I = \{F \cap A_I \colon F \in \mathcal{F}\}$. Note that $\mathcal{F}_I$ is a family of generalized signotopes on I. Hence $|\mathcal{F}_I| \le g(t)$.
Lemma 6.3.2 implies for $m = \binom{n}{t}$ and $k = \binom{n-3}{t-3}$

$$g(n)^k = |\mathcal{F}|^k \le \prod_{I \in \binom{[n]}{t}} |\mathcal{F}_I| \le g(t)^m,$$

Therefore,

$$g(n) \le g(t)^{m/k} = 2^{c(t)\binom{n}{3}} \quad \text{with} \quad c(t) = \log_2(g(t)) / \binom{t}{3}.$$

Note that in the last equation, we used that $\binom{n}{3}/\binom{t}{3} = \binom{n}{t}/\binom{n-3}{t-3}$.
Using $g(8) = 35\,355\,434\,970\,848$ (cf. Table 6.1 or OEIS A328377), we obtain that the number $g(n)$ of generalized signotopes on $n \ge 8$ elements is at most $2^{c_2 \cdot \binom{n}{3}}$ where $c_2 = c(8) \approx 0.8036$. This is the same as $2^{c_2' \cdot \binom{n}{3}}$ with $c_2' = \frac{1}{6} \cdot c_2 \approx 0.1339$. In [BFS+23b] the largest available value was $g(7)$ which gave a constant of $c(7) \approx 0.8352$. From the above equation, it holds $c(n) \le c(t)$, that is, c is non-increasing. Thus, the factor c_2 can be expected to decrease if a value of $c(t')$ with $t' > 8$ becomes available.

6.3.2 Lower Bound for $g(n)$:

We give a recursive construction of a set $\mathcal{G}_{3n}$ of generalized signotopes on $3n$ elements. The set $\mathcal{G}_3$ consists of the two generalized signotopes on $[3]$.
In the next step, we construct $\mathcal{G}_{3n}$ based on $\mathcal{G}_n$. Let $A = \{1, \dots, n\}$, $B = \{n+1, \dots, 2n\}$, and $C = \{2n+1, \dots, 3n\}$. Pick three generalized signotopes γ_A, γ_B, γ_C from $\mathcal{G}_n$ and an arbitrary mapping $M : A \times B \times C \to \{+, -\}$. We define γ by the following rule: for $x < y < z$ we set

$$\gamma(x,y,z) = \begin{cases} \gamma_A(x,y,z) & \text{if } x,y,z \in A \\ \gamma_B(x,y,z) & \text{if } x,y,z \in B \\ \gamma_C(x,y,z) & \text{if } x,y,z \in C \\ M(x,y,z) & \text{if } x \in A, y \in B, z \in C \\ + & \text{otherwise.} \end{cases}$$

Claim 6.3. *γ is a generalized signotope on n elements.*

Proof. For any four elements $x < y < z < w$, at least two are from the same class $S \in \{A, B, C\}$. We look at the signs sequence $(\gamma(y,z,w)\ \gamma(x,z,w)\ \gamma(x,y,w)\ \gamma(x,y,z))$.
If all four elements are from S, then we use that γ_S is a generalized signotope.
If exactly three of the elements are from S, then there are at least three $+$ signs in the sequence. This shows that the forbidden patterns $+-+-$ and $-+-+$ do not occur. Now if exactly two of the elements are from S, then if the two elements are x, y the triples (x,y,z) and (x,y,w) map to plus and we have $++??$, where $? \in \{+,-\}$ is arbitrary. If y, z are from S, we have $+??+$, and if z, w are from S, we have $??++$. In any case, the forbidden alternating sign patterns cannot occur. ■

Since there are $|\mathcal{G}_n|^3 \cdot 2^{n^3}$ possibilities to choose $\gamma_A, \gamma_B, \gamma_C, M$, and no two such selections yield the same γ, we have

$$|\mathcal{G}_{3n}| = |\mathcal{G}_n|^3 \cdot 2^{n^3}.$$

Now, using the all-plus-extensions (cf. Lemma 6.3.3), we obtain sets $\mathcal{G}_{3n+1}$ and $\mathcal{G}_{3n+2}$ of generalized signotopes on $3n+1$ and $3n+2$ elements, respectively, with $|\mathcal{G}_{3n}| = |\mathcal{G}_{3n+1}| = |\mathcal{G}_{3n+2}|$. The name "all-plus-extension" comes from the fact, that we assign $+$ to each triple $a < b < c$ which is not completely contained in $[n]$.

Lemma 6.3.3 (All-plus-extension)**.** *Let γ be a generalized signotope on n elements and let $n' \geq n$ be an integer. Then the mapping $\gamma' : [n']_3 \to \{+,-\}$ with*

$$\gamma'(x,y,z) = \begin{cases} \gamma(x,y,z) & \text{if } x,y,z \in [n]; \\ + & \text{if } x<y<z \text{ or } y<z<x \text{ or } z<x<y; \\ - & \text{if } y<x<z \text{ or } x<z<y \text{ or } z<y<x; \end{cases}$$

is a generalized signotope on n' elements.

Proof. Consider four elements $x, y, z, w \in [n']$ with $x < y < z < w$. If $x, y, z, w \in [n]$, then the sequence $(\gamma'(xyz)\ \gamma'(xyw)\ \gamma'(xzw)\ \gamma'(yzw))$ avoids the forbidden patterns $+-+-$ and $-+-+$ because γ is a generalized signotope. Otherwise, the sequence $(\gamma'(x,y,z)\ \gamma'(x,y,w)\ \gamma'(x,z,w)\ \gamma'(y,z,w))$ contains at least three $+$-entries. □

Hence, for $f(n) = \log_2 |\mathcal{G}_n|$ we have

$$f(n) = 3f(\lfloor n/3 \rfloor) + \lfloor n/3 \rfloor^3.$$

Inductively assuming $f(n) \geq \frac{1}{24}n^3 - \frac{3}{8}n^2$, which is easy to check for $n = 1$ and $n = 2$, we obtain

$$\begin{aligned} f(n) &= 3f\left(\left\lfloor \frac{n}{3} \right\rfloor\right) + \left\lfloor \frac{n}{3} \right\rfloor^3 \\ &\geq 3\left(\frac{1}{24} \cdot \left\lfloor \frac{n}{3} \right\rfloor^3 - \frac{3}{8} \cdot \left\lfloor \frac{n}{3} \right\rfloor^2\right) + \left\lfloor \frac{n}{3} \right\rfloor^3 \\ &\geq 3\left(\frac{1}{24} \cdot \left(\frac{n-2}{3}\right)^3 - \frac{3}{8} \cdot \left(\frac{n}{3}\right)^2\right) + \left(\frac{n-2}{3}\right)^3 \\ &= \frac{1}{24}n^3 - \frac{3}{8}n^2 + \frac{1}{2}n - \frac{1}{3} \ \geq\ \frac{1}{24}n^3 - \frac{3}{8}n^2 \end{aligned}$$

for every $n \geq 3$. This completes the proof of the lower bound.

6.4 Generalized Signotopes and Simple Drawings

By introducing a notion of flips for generalized signotopes, we show that generalized signotopes indeed are a proper generalization of simple drawings. From the known estimates for the asymptotic number of simple drawings, it follows that most generalized signotopes do not come from simple drawings.

6.4.1 Flip-equivalent Generalized Signotopes

Let γ be a generalized signotope on $[n]$. A pair (i, j) of distinct elements of $[n]$ is said to be *edge-flipable* in γ if inverting the signs of all triples containing i and j yields a generalized signotope. If γ comes from a simple drawing and ij is an edge incident to the outer cell, then (i, j) is edge-flipable in γ. Moreover, the generalized signotope γ' obtained by inverting all triples containing i and j again comes from a drawing. Indeed, if $\mathcal{D}$ is a drawing corresponding to γ and the edge $e = ij$ is incident to the outer cell c_1, then there is a second cell c_2 which is separated from c_1 only by e. The drawing $\mathcal{D}'$ obtained by wrapping this edge around which makes c_2 the outer cell corresponds to γ'. Type $\mathrm{I_a}$ and type $\mathrm{I_b}$ of the simple drawings of K_4 (see Figure 2.13) differ by such a flip operation applied to the edge $\{3, 4\}$.
Two generalized signotopes γ, γ' are *edge-flip-equivalent* if there is a sequence $(i_1, j_1), \ldots, (i_k, j_k)$ of pairs and a sequence $\gamma_0, \ldots, \gamma_k$ of generalized signotopes with $\gamma = \gamma_0$, $\gamma' = \gamma_k$, and γ_ℓ is obtained from $\gamma_{\ell-1}$ by flipping the pair (i_ℓ, j_ℓ). This edge-flip-equivalence relation partitions the set of all generalized signotopes into *flip classes*, which we further consider to be closed under relabeling of the elements.
In the following, we show that two weakly isomorphic drawings yield flip-equivalent generalized signotopes. In fact, the following lemma will be the key to show that most generalized signotopes do not come from simple drawings.

Lemma 6.4.1. *Two weakly isomorphic drawings $\mathcal{D}$ and $\mathcal{D}'$ of K_n in the plane yield edge-flip-equivalent generalized signotopes.*

Proof. Gioan [Gio05, Gio22] proved that two weakly isomorphic drawings on the sphere can be transformed into each other using triangle-flips, i.e., the change of a cell bounded by three edges and without incident vertices by moving one edge past the crossing of the other two edges, see Figure 2.15. As already discussed earlier, an edge at the outer cell can be flipped which yields a generalized signotope of the same edge-flip equivalence class. In such a way we achieve two weakly isomorphic drawings with the same chosen outer cell. Hence we might assume both drawings $\mathcal{D}$ and $\mathcal{D}'$ are drawn in the plane with the same edges incident to the outer cell. Suppose we have $\mathcal{D} = \mathcal{D}_0, \mathcal{D}_1, \ldots, \mathcal{D}_m = \mathcal{D}'$, where $\mathcal{D}_i$ is transformed into $\mathcal{D}_{i+1}$ by a triangle-flip. We have to show that $\gamma(\mathcal{D}_i)$ and $\gamma(\mathcal{D}_{i+1})$ are edge-flip-equivalent generalized signotopes. Here $\gamma(\mathcal{D}_i)$ denotes the generalized signotope of the drawing $\mathcal{D}_i$. A crucial point is that generalized signotopes come from drawings in the plane while weak isomorphism is a property of spherical drawings. Hence, we have to allow triangle-flips with the triangle being the outer cell.
Let $\triangle_i$ be the triangular cell in $\mathcal{D}_i$ which is flipped to obtain $\mathcal{D}_{i+1}$. If $\triangle_i$ is a bounded cell, we are done because of $\gamma(\mathcal{D}_i) = \gamma(\mathcal{D}_{i+1})$. Otherwise, if $\triangle_i$ is the outer cell, apply an flip of an edge bounding the outer cell to obtain an isomorphic drawing $\mathcal{D}_i'$ in which another cell is the outer cell. Because of the edge-flip, $\gamma(\mathcal{D}_i')$ is edge-flip-equivalent to $\gamma(\mathcal{D}_i)$. □

	Gen.Sig.	Relabeling	Edge-Flip	Weak Isom.
3	2	1	1	1
4	14	2	2	2
5	544	6	3	5
6	173 128	167	16	102
7	630 988 832	63 451	442	11 556
8	35 355 434 970 848	?	?	5 370 725
9				7 198 391 729
⋮				
n	$2^{\Theta(n^3)}$	$2^{\Theta(n^3)}$	$2^{\Theta(n^3)}$	$2^{\widetilde{\Theta}(n^2)}$

Table 6.1: The first three columns show the number of generalized signotopes on n elements, equivalence classes up to relabeling, and flip classes, respectively. The last column shows the number of weak isomorphism classes of simple drawings of K_n from [ÁAF+15] (cf. OEIS A276110). The asymptotic bounds are provided in Theorem 6.3.1 and [Kyn13], respectively.

Note that the asymptotic number of $2^{\Theta(n^3)}$ generalized signotopes applies to the numbers of relabeling classes and edge-flip classes, respectively, because reflections and relabelings only give a factor of at most $2 \cdot n!$ and the number of elements in a edge-flip class is at most $2^{\binom{n}{2}}$. Moreover, there are at most $2^{\tilde{O}(n^2)} = 2^{n^2\alpha(n)^{O(1)}}$ weak isomorphism classes of simple drawings of the complete graph K_n [Kyn13]. Here α denotes extremely slow growing inverse of the Ackermann function. By Lemma 6.4.1, each weak isomorphism classes is contained in a edge-flip-equivalence class of generalized signotopes. Since the number of generalized signotopes in an edge-flip-equivalence class is at most $2^{\binom{n}{2}}$, we conclude that at most $2^{\tilde{O}(n^2)} \cdot 2^{\binom{n}{2}} = 2^{\tilde{O}(n^2)}$ generalized signotopes come from simple drawings of K_n.

6.4.2 Small Configurations

To get a better understanding of which generalized signotopes come from simple drawings, we enumerated all generalized signotopes and edge-flip classes up to $n = 7$ elements, see Table 6.1. Moreover, since drawings from the same weak isomorphism class induce edge-flip-equivalent generalized signotopes (Lemma 6.4.1), Table 6.1 also restates the number of weak isomorphism classes from [ÁAF+15].

In Section 2.4, we have seen that there are precisely two weak isomorphism classes of simple drawings of K_4, see Figure 2.13. Via relabeling and mirroring, all 14 generalized signotopes on $n = 4$ elements are realized by type I and type II. These 14 generalized signotopes partition into two relabeling classes and two edge-flip classes. One of the classes corresponds to drawings of type I (1 crossing) and the other one to drawings of type II (0 crossings). In particular, the edge-flip operation for generalized signotopes preserves the number of crossings in a 4-tuple. Therefore, we can define the *crossing number* of a generalized signotope γ on n elements as the number of induced 4-tuples which belong to the edge-flip class of the type I drawing.

For $n = 5$, there are 544 generalized signotopes, which belong to 6 relabeling classes and 3 edge-flip classes, respectively. There are five weak isomorphism classes of simple drawings of K_5, see

Figure 6.2. We have verified by computer that each of the 544 generalized signotope on $n = 5$

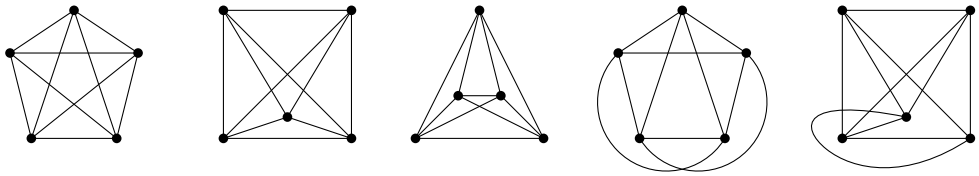

Figure 6.2: The five types of simple drawings of K_5.

elements is realized by a simple drawing of K_5. Since we can read whether a 4-tuple of vertices induces a crossing from the generalized signotope, it is clear that drawings with different number of crossings do not correspond to a common relabeling class of generalized signotopes. Indeed, the class with 24 generalized signotopes corresponds to type I and type V (both 5 crossings), the class with 280 generalized signotopes corresponds to type II and type IV (both 3 crossings), and the class with 240 generalized signotopes corresponds to type III (1 crossing). We conclude that generalized signotopes are not able to encode the weak isomorphism class. Also convexity is not encoded: type I and type V induce the same generalized signotope but type I is face-convex while type V is non-convex. Note that type I is $\mathcal{C}_5$ (cf. Figure 2.14(a)) and together with type II, type II they are the three geometric drawings of K_5. While type IV and type V are the two obstructions $\Pi^{\text{oc}}_{5,1}$ and $\Pi^{\text{oc}}_{5,2}$ to convexity (cf. Figure 2.18). Type V is the twisted drawing $\mathcal{T}_5$.

For $n = 6$, there are 173 128 generalized signotopes, 167 relabeling classes, and 16 edge-flip classes. We have verified by computer that 151 of the 167 relabeling classes are realized by a simple drawing of K_6. However, from each of the 16 edge-flip classes there is a representative which can be realized by a simple drawing of K_6. The non-realizable generalized signotopes on $n = 6$ belong to three edge-flip classes, which have 3, 4, and 5 crossings, respectively. Note that there is a unique edge-flip class with 3 crossings, a unique edge-flip class with 4 crossings, and two edge-flip classes with 5 crossings.

We now consider the edge-flip class F of generalized signotopes on $n = 6$ elements with 3 crossings. There is up to weak isomorphism a unique simple drawing $\mathcal{D}$ of K_6 which has the minimum of 3 crossings. Indeed since this drawing has no cell bounded by exactly three edges and no vertex, this is the unique drawing up to strong isomorphism. A drawing of the graph is given in Figure 6.3. Therefore, every drawing realizing a generalized signotope from F is

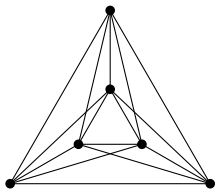

Figure 6.3: The unique simple drawing of K_6 which has the minimum of 3 crossings.

isomorphic to $\mathcal{D}$. Since the drawing $\mathcal{D}$ is highly symmetric, there are up to isomorphism only 3 choices for the outer cell, and hence only 3 of the 10 generalized signotopes from the edge-flip

class F are realized

$$\gamma^1_{\text{real}} = ----+----++++++++++$$
$$\gamma^2_{\text{real}} = +--------++++++++++$$
$$\gamma^3_{\text{real}} = --+---+--++++++++++$$

The remaining 7 generalized signotopes of that edge-flip class are not realizable.

$$\gamma^1_{\text{non}} = --+-+---++++++++++$$
$$\gamma^2_{\text{non}} = --+---+--++++++++++$$
$$\gamma^3_{\text{non}} = ------++--++++++++++$$
$$\gamma^4_{\text{non}} = -++--+-++-+++-++++++$$
$$\gamma^5_{\text{non}} = --+-----+-++++++++++$$
$$\gamma^6_{\text{non}} = -----+--+-++++++++++$$
$$\gamma^7_{\text{non}} = -+-------++++++++++$$

To lift the non-representable examples to higher number of elements we use the all-plus-extension of a generalized signotope. see lemma 6.3.3

Corollary 6.4.2. *For $n \leq 5$ all generalized signotopes on n elements are realizable as simple drawing of K_n. For $n \geq 6$ there exist non-realizable generalized signotopes on n elements.*

Proof. The first part follows from earlier discussions in this section. For the second part, consider the non-realizable generalized signotope γ on 6 elements from above. Now, for every integer n' with $n' \geq 6$, the all-plus-extension of γ (Lemma 6.3.3) is also non-realizable since it contains γ as an induced subconfiguration. □

Another interesting example is the generalized signotope on $n = 7$ elements.

$$\gamma_7 = +---++----+--++-+-+-+-++++++++-++++$$

This configuration is not representable by any simple drawing of K_7 because it has crossing number 7 while every drawing of K_7 has at least 9 crossings [Guy72].
It would be interesting to have non-trivial bounds for the minimum number of crossings of generalized signotopes on n elements.

Chapter 7

Conclusion and Open Problems

The main result of Chapter 3 is a generalization of Levi's extension lemma to signotopes of odd rank (cf. Theorem 3.1.2). Moreover, we present examples of rank $r = 4, 6, 8, 10, 12$ which are not 2-extendable. Based on this evidence, we conjecture that for every even rank $r \geq 4$ there is an r-signotope which is not 2-extendable (cf. Conjecture 3.1). In Section 3.6.3 we present a family of partial signotopes ρ_r for even r such that every r-signotope containing ρ_r is not 2-extendable. An affirmative answer to the following conjecture would solve Conjecture 3.1.

Conjecture 7.1. *For every even r there is an r-signotope containing ρ_r.*

One possibility to handle this question is to complete the partial signotope ρ_r by assigning additional signs without violating the monotonicity condition of signotopes. However in general such a completion does not necessarily exist. The decision problem whether a partial assignment can be completed to a full assignment is known as completion problem. For related structures such as uniform 3-chirotopes [Bai05, Tsc03], uniform acyclic 3-chirotopes [Knu92] and generalized signotopes [BSS23a] the problem is known to be NP-hard, while it is polynomial solvable for 2-signotopes, i.e., permutations. Most likely, the completion problem for 3-signotopes is also NP-hard as conjectured by [FGT05].

Moreover we showed that signotopes are generally not 4-extendable. The remaining case is extendability with three prescribed points.

Question 7.2. *Are signotopes of odd rank 3-extendable?*

Signotopes are a rich subclass of oriented matroids. Extendability for higher dimensions was previously studied in the setting of oriented matroids. Goodman and Pollack [GP81] showed that rank 4 oriented matroids do not provide an extension by a pseudohyperplane going through three prescribed points. Later Richter-Gebert [Ric93] showed that there is a rank 4 oriented matroid which is not 2-extendable. However it might be true that, similar as for signotopes, there is an extension theorem for oriented matroids of odd rank.

Question 7.3. *Is there an extension theorem for oriented matroids of odd rank?*

The rank 4 oriented matroid by Richter-Gebert which is not 2-extendable is part of a construction which provides an oriented matroid such that one element is not contained in a mutation. In the geometric sense this translates to a pseudoplane in $\mathbb{R}^3$ in a pseudoplane arrangement which is not incident to a simplicial cell. A famous conjecture by Las Vergnas is the existence of mutations in oriented matroids.

Conjecture 7.4 ([BLS$^+$99, Conjecture 7.3.10])**.** *Every oriented matroid admits a mutation.*

For oriented matroids of rank 4 and with $n \leq 12$ elements it is known to be true [BR01]. In contrast, the existence of fliples (which is the corresponding structure in signotopes) follows from the fact that every signotope is contained in a maximum chain [FW01]. In Chapter 6 we improved the lower bound to $\frac{2n-2}{r}$ fliples in every r-signotope on n elements, which gives a lower bound on the minimum degree in the flip graph. However the minimum degree of the flip graph $G(n,r)$ is not determined. Felsner and Weil conjectures it to be $n-r+1$, which corresponds to the degree of the constant + signotope. Recently, together with a Master student, Lukas Egeling, from ETH Zürich, we discovered that this conjecture does not hold. There are eight rank 4 signotope on 8 elements with 4 fliples, which is the minimal number of fliples.

Question 7.5. *What is the minimum degree of $G(n,r)$, i.e., the minimum number of fliples in every signotope?*

Moreover there are a lot of open problems concerning the structure of the flip graph such as the connectivity, Hamiltonicity and more, which we want to investigate in the future.
Similarly as for signotopes, one can define a flip graph of generalized signotopes. Note that in contrast to the edge-flip operation defined in Section 6.4, the flip is the sign change of an r-subset such that the new sign mapping remains a generalized signotope. In the flip graph for a fixed n the vertices are the generalized signotopes and two vertices are connected if they differ in a single sign. However very little is known about the flip graph.

Question 7.6. *Is the flip graph of generalized signotopes connected? Determine the minimum degree.*

In signotopes there is always an r-subset which can flip from $-$ to $+$ and one which can flip from $+$ to $-$ unless all signs are $+$ or $-$, respectively. This is not longer true for generalized signotopes. Manfred Scheucher (personal communication) found the following generalized signotope on 12 elements in which no $-$ can be flipped to $+$. Encoded in the reversed lexicographic order of its 3-subsets it is the following generalized signotope.

$$\gamma_{\text{noflip}} = +------+------+----------+--------+---+++----+$$
$$-----+------+--+--+--+---+----+--++------+---+-$$
$$-+-+-+------+-+-+--------------+-+--+------++--$$
$$--++--+--------------------+------+--+-+-+---++--++$$
$$++++++--++----+-+-+-----++--+---.$$

In this thesis generalized signotopes are mainly considered as a combinatorial encoding of triangle orientations of simple drawings. As shown in Section 6.4 not all generalized signotopes come from simple drawings. Hence it would certainly be nice to have a characterization of those generalized signotopes which come from a simple drawing. However, finding such a characterization might be challenging since there are several simple drawings yielding the same generalized signotope. An example is the generalized signotope corresponding to the constant + function. Both drawings $\mathcal{C}_n$ and $\mathcal{T}_n$ correspond to this generalized signotope, see Section 2.4. From the view point of simple drawings flipping the sign of a triple $\{a,b,c\}$ corresponds to moving a vertex $x \in \{a,b,c\}$ over the edge connecting the two remaining vertices. However, there might be up to three possibilities. It is not uniquely defined which of the three vertices is moved over the edge. For

example the two simple drawings $\mathcal{T}_5$ and $\mathcal{C}_5$ can be transformed into each other by two flip operations which corresponds to changing a triple to $-$ and back to $+$. However since there are different vertices involved this gives a different drawing.
A first step might be to restrict the setting to convex drawings where the generalized signotope might be unique since convex drawings are $\mathcal{T}_5$-free. In particular, besides the mentioned characterization of pseudolinear drawings as 3-signotopes [BFK15, Theorem 3.2], Balko, Fulek, and Kynčl provide a characterization of which generalized signotopes can be drawn as x-monotone simple drawings and which can be drawn as x-monotone semisimple drawings by forbidding finitely many subconfigurations [BFK15, Theorem 3.1]. In the spirit of their results, Kynčl's theorem [Kyn20], and the classification of h-convex and convex drawings [AMRS22], we pose the following question on characterizing drawable generalized signotopes. Recall that a generalized signotope is *drawable* if there exists a simple drawing whose triangle orientation is the generalized signotope.

Question 7.7. *Is there a finite number k such that all generalized signotopes are drawable if all k-subsets are drawable?*

Additionally it might be interesting to find a topological representation of all generalized signotopes.

Question 7.8. *Is there a geometric or topological representation of generalized signotopes?*

A related structure mentioned by Knuth [Knu92] are so called *transitive interior triple systems*, which are a proper subclass of generalized signotopes (Knuth called them interior triple systems) and contain all signotopes. Hence the number of transitive interior triple systems is in $2^{\Omega(n^2)}$ and $2^{O(n^3)}$. The precise asymptotic number remains unknown.

Question 7.9 ([Knu92])**.** *What is the asymptotic number of transitive interior triple systems?*

For signotopes we presented various topological representations in Chapter 2. The most recent one is by Miyata [Miy21] who showed that signotopes of arbitrary rank $r \geq 3$ can be represented in the plane by so called $(r-2)$-intersecting pseudoconfigurations of points. Those configurations are an abstraction of the interpolation polynomials spanned by $r-1$ points. Signotopes which can be represented by an $(r-2)$-intersecting pseudoconfiguration of points using polynomial functions are called *polynomially realizable*. Moreover in terms of pseudohyperplane arrangements a signotope is *realizable* if there is a hyperplane arrangement with the same combinatorics. A natural question is whether those two terms of realizability coincide.

Question 7.10. *Is an r-signotope realizable if and only if it is polynomially realizable?*

In Section 4.4 the main ingredient to show that sufficiently large convex drawings admit a 6-hole is Theorem 4.4.7 which states that the convex side of every minimal k-gon is f-convex. This makes it possible to transfer results, which do not depend on the outer cell, from pseudolinear drawings to convex drawings. For future research and to obtain better bounds on the minimal integer $h^{\text{conv}}(k)$ such that every convex drawing with more than $h^{\text{conv}}(k)$ vertices contains a k-hole, it would certainly be nice to determine the size of a largest k-gon and the size of a largest f-convex subdrawing in a convex drawing.

Question 7.11. *What is the largest f-convex subdrawing in every convex drawing of K_n?*

The currently best lower bound for the largest k-gon and hence for the largest f-convex drawing in K_n is of magnitude $k \geq (\log_2 n)^{1/2-o(1)}$ [SZ22]. The construction of Erdős–Szekeres [ES60] shows that there are geometric drawings and hence every convex drawings, which only contain k-gons of size $k \leq \lceil \log_2 n \rceil + 1$. However, we are not aware of any sublinear upper bound on the size of a largest f-convex subdrawing. In the case of h-convex drawings, Arroyo et al. [ARS21, Lemmas 5.2–5.6] showed that a partitioning into two parts which are both f-convex is possible.

In Chapter 5 we showed that every convex drawing of K_n admits a plane Hamiltonian cycle. Rafla [Raf88] conjectures that this is true in all simple drawings of K_n. Among various conjectures we stated, we want to emphasize the strengthening of Rafla's conjecture, see Conjecture 5.2.

Question 7.12. *Do all simple drawings of K_n contain a plane Hamiltonian subgraph of size $2n-3$?*

However it would certainly be nice to solve any of those conjectures in order to make progress on Rafla's conjecture.

Bibliography

[ÁAF+15] B. M. Ábrego, O. Aichholzer, S. Fernández-Merchant, T. Hackl, J. Pammer, A. Pilz, P. Ramos, G. Salazar, and B. Vogtenhuber. All good drawings of small complete graphs. In *Proceedings of the 31st European Workshop on Computational Geometry (EuroCG 2015)*, pages 57–60, 2015.

[ABB+09] J. L. Arocha, I. Bárány, J. Bracho, R. Fabila, and L. Montejano. Very colorful theorems. *Discrete & Computational Geometry*, 42(2):142–154, 2009.

[ABR21] A. Arroyo, J. Bensmail, and R. B. Richter. Extending drawings of graphs to arrangements of pseudolines. *Journal of Computational Geometry*, 12(2):3–24, 2021.

[ACH+23] O. Aichholzer, M. Chiu, H. P. Hoang, M. Hoffmann, J. Kyncl, Y. Maus, B. Vogtenhuber, and A. Weinberger. Drawings of complete multipartite graphs up to triangle flips. In *Proceedings of the 39th International Symposium on Computational Geometry (SoCG 2023)*, volume 258 of *LIPIcs*, pages 6:1–6:16. Schloss Dagstuhl, 2023.

[ADKP22a] P. Ágoston, G. Damásdi, B. Keszegh, and D. Pálvölgyi. Orientation of convex sets. arXiv:2206.01721, 2022.

[ADKP22b] P. Ágoston, G. Damásdi, B. Keszegh, and D. Pálvölgyi. Orientation of good covers. arXiv:2206.01723, 2022.

[AFO+23] Y. Alves Radtke, S. Felsner, J. Obenaus, S. Roch, M. Scheucher, and B. Vogtenhuber. Flip graph connectivity for arrangements of pseudolines and pseudocircles. arXiv:2310.19711, 2023. To appear at ACM-SIAM Symposium on Discrete Algorithms (SODA24).

[AGT+22] O. Aichholzer, A. García, J. Tejel, B. Vogtenhuber, and A. Weinberger. Twisted ways to find plane structures in simple drawings of complete graphs. In *Proceedings of the 38th International Symposium on Computational Geometry (SoCG 2022)*, volume 224 of *LIPIcs*, pages 5:1–5:18. Schloss Dagstuhl, 2022.

[AHH+10] O. Aichholzer, T. Hackl, C. Huemer, F. Hurtado, and B. Vogtenhuber. Large bichromatic point sets admit empty monochromatic 4-gons. *SIAM Journal on Discrete Mathematics*, 23(4):2147–2155, 2010.

[AHP+15] O. Aichholzer, T. Hackl, A. Pilz, P. Ramos, V. Sacristán, and B. Vogtenhuber. Empty triangles in good drawings of the complete graph. *Graphs and Combinatorics*, 31:335–345, 2015.

[AK92] N. Alon and D. J. Kleitman. Piercing convex sets and the Hadwiger-Debrunner (p, q)-problem. *Advances in Mathematics*, 96(1):103–112, 1992.

[AMRS17] A. Arroyo, D. McQuillan, R. B. Richter, and G. Salazar. Drawings of K_n with the same rotation scheme are the same up to Reidemeister moves (Gioan's Theorem). *Australasian J. Combinatorics*, 67:131–144, 2017.

[AMRS18] A. Arroyo, D. McQuillan, R. B. Richter, and G. Salazar. Levi's lemma, pseudolinear drawings of K_n, and empty triangles. *Journal of Graph Theory*, 87(4):443–459, 2018.

[AMRS22] A. Arroyo, D. McQuillan, R. B. Richter, and G. Salazar. Convex drawings of the complete graph: topology meets geometry. *Ars mathematica contemporanea*, 22(3), 2022.

[AOV24] O. Aichholzer, J. Orthaber, and B. Vogtenhuber. Towards crossing-free hamiltonian cycles in simple drawings of complete graphs. *Computing in Geometry and Topology*, 3(2):5:1–5:30, 2024.

[ARS21] A. Arroyo, R. B. Richter, and M. Sunohara. Extending drawings of complete graphs into arrangements of pseudocircles. *SIAM Journal on Discrete Mathematics*, 35(2):1050–1076, 2021.

[Bai05] P. Baier. NP-completeness of partial chirotope extendibility. arXiv:math/0504430, 2005.

[Bal19] M. Balko. Ramsey numbers and monotone colorings. *Journal of Combinatorial Theory, Series A*, 163:34–58, 2019.

[Bár82] I. Bárány. A generalization of Carathéodory's theorem. *Discrete Mathematics*, 40(2):141–152, 1982.

[BF87] I. Bárány and Z. Füredi. Empty simplices in Euclidean space. *Canadian Mathematical Bulletin*, 30(4):436–445, 1987.

[BFK15] M. Balko, R. Fulek, and J. Kynčl. Crossing numbers and combinatorial characterization of monotone drawings of K_n. *Discrete & Computational Geometry*, 53(1):107–143, 2015.

[BFMS23] H. Bergold, S. Felsner, M. M. Reddy, and M. Scheucher. Using SAT to study plane Hamiltonian substructures in simple drawings. arXiv:2305.09432, 2023.

[BFS+20] H. Bergold, S. Felsner, M. Scheucher, F. Schröder, and R. Steiner. Topological drawings meet classical theorems from convex geometry. In *Proceedings of 28th International Symposium on Graph Drawing and Network Visualization (GD 2020)*, LNCS 12590, pages 281–294. Springer, 2020.

[BFS23a] H. Bergold, S. Felsner, and M. Scheucher. An extension theorem for signotopes. In *39th International Symposium on Computational Geometry (SoCG 2023)*, volume 258 of *LIPIcs*, pages 17:1–17:14, 2023. Supplemental data: `https://github.com/manfredscheucher/supplemental-signotope-extension`.

[BFS+23b] H. Bergold, S. Felsner, M. Scheucher, F. Schröder, and R. Steiner. Topological drawings meet classical theorems from convex geometry. *Discrete & Computational Geometry*, 70:1121–1143, 2023.

[BFZ19] P. V. Blagojević, F. Frick, and G. M. Ziegler. Barycenters of polytope skeleta and counterexamples to the topological tverberg conjecture, via constraints. *Journal of the European Mathematical Society*, 21(7):2107–2116, 2019.

[Bie19] A. Biere. CaDiCaL at the SAT Race 2019. In *Proceedings of SAT Race 2019 – Solver and Benchmark Descriptions*, volume B-2019-1 of *Department of Computer Science Series*, pages 8–9. University of Helsinki, 2019.

[Bir59] B. J. Birch. On $3N$ points in a plane. *Mathematical Proceedings of the Cambridge Philosophical Society*, 55(4):289–293, 1959.

[BLS+99] A. Björner, M. Las Vergnas, B. Sturmfels, N. White, and G. M. Ziegler. *Oriented Matroids*, volume 46 of *Encyclopedia of Mathematics and its Applications*. Cambridge University Press, 2 edition, 1999.

[BMP05] P. Brass, W. O. J. Moser, and J. Pach. *Research Problems in Discrete Geometry*. Springer, 2005.

[BR01] J. Bokowski and H. Rohlfs. On a mutation problem for oriented matroids. *European Journal of Combinatorics*, 22(5):617–626, 2001.

[BS18] I. Bárány and P. Soberón. Tverberg's theorem is 50 years old: a survey. *Bulletin of the AMS*, 55:459–492, 2018.

[BSS81] I. Bárány, S. B. Shlosman, and A. Szücs. On a topological generalization of a theorem of Tverberg. *Journal of the London Mathematical Society*, s2-23(1):158–164, 1981.

[BSS23a] H. Bergold, M. Scheucher, and F. Schröder. Using SAT to find NP-hardness proofs for 41 completion problems. arXiv:2402.06397, 2023. submitted.

[BSS23b] H. Bergold, M. Scheucher, and F. Schröder. Holes in convex drawings. In *Proceedings of the 39th European Workshop on Computational Geometry (EuroCG 2023)*, pages 10:1–10:7, 2023.

[BW88] A. Bachem and A. Wanka. Separation theorems for oriented matroids. *Discrete Mathematics*, 70(3):303–310, 1988.

[CFS23] F. Cortés Kühnast, S. Felsner, and M. Scheucher. Improved lower bounds for the number of pseudoline arrangements, 2023. personal communication.

[CGFS86] F. Chung, R. Graham, P. Frankl, and J. Shearer. Some intersection theorems for ordered sets and graphs. *Journal of Combinatorial Theory, Series A*, 43(1):23–37, 1986.

[DM19] A. Dumitrescu and R. Mandal. New lower bounds for the number of pseudoline arrangements. In *Proceedings of the 30th Annual ACM-SIAM Symposium on Discrete Algorithms (SODA'19)*, pages 410–425. SIAM, 2019.

[Erd78] P. Erdős. Some problems on elementary geometry. *Australian Mathematical Society*, 2:2–3, 1978.

[ES35] P. Erdős and G. Szekeres. A combinatorial problem in geometry. *Compositio Mathematica*, 2:463–470, 1935.

[ES60] P. Erdős and G. Szekeres. On some extremum problems in elementary geometry. *Annales Universitatis Scientiarium Budapestinensis de Rolando Eötvös Nominatae, Sectio Mathematica*, 3–4:53–63, 1960.

[Fel04] S. Felsner. *Geometric Graphs and Arrangements - Some Chapters from Combinatorial Geometry.* Advanced lectures in mathematics. Vieweg+Teubner, 2004.

[FG17] S. Felsner and J. E. Goodman. Pseudoline arrangements. In Toth, O'Rourke, and Goodman, editors, *Handbook of Discrete and Computational Geometry.* CRC Press, third edition, 2017.

[FGT05] S. Felsner, B. Gärtner, and F. Tschirschnitz. Grid orientations, $(d, d+2)$-polytopes, and arrangements of pseudolines. *Discrete & Computational Geometry*, 34(3):411–437, 2005.

[FK99] S. Felsner and K. Kriegel. Triangles in Euclidean arrangements. *Discrete & Computational Geometry*, 22(3):429–438, 1999.

[FL78] J. Folkman and J. Lawrence. Oriented matroids. *Journal of Combinatorial Theory, Series B*, 25(2):199–236, 1978.

[FR13] R. Fulek and A. J. Ruiz-Vargas. Topological graphs: Empty triangles and disjoint matchings. In *Proceedings of the 29th Annual Symposium on Computational Geometry (SoCG 2013)*, pages 259–266. ACM, 2013.

[FS09] J. Fox and B. Sudakov. Density theorems for bipartite graphs and related Ramsey-type results. *Combinatorica*, 29:153–196, 2009.

[FS20] F. Frick and P. Soberón. The topological Tverberg problem beyond prime powers. arXiv:2005.05251, 2020. The authors state in v2 that the proof of Theorem 1.1 is incomplete.

[Ful14] R. Fulek. Estimating the number of disjoint edges in simple topological graphs via cylindrical drawings. *SIAM Journal on Discrete Mathematics*, 28(1):116–121, 2014.

[FV11] S. Felsner and P. Valtr. Coding and counting arrangements of pseudolines. *Discrete & Computational Geometry*, 46(3), 2011.

[FW00] S. Felsner and H. Weil. A theorem on higher Bruhat orders. *Discrete & Computational Geometry*, 23(1):121–127, 2000.

[FW01] S. Felsner and H. Weil. Sweeps, arrangements and signotopes. *Discrete Applied Mathematics*, 109(1):67–94, 2001.

[Ger08] T. Gerken. Empty Convex Hexagons in Planar Point Sets. *Discrete & Computational Geometry*, 39(1):239–272, 2008.

[Gio05] E. Gioan. Complete graph drawings up to triangle mutations. In *Proceedings of the International Workshop on Graph-Theoretic Concepts in Computer Science (WG 2005)*, volume 3787 of *LNCS*, pages 139–150. Springer, 2005.

[Gio22] E. Gioan. Complete graph drawings up to triangle mutations. *Discrete & Computational Geometry*, 67(4):985–1022, 2022.

[GNT00] A. García Olaverri, M. Noy, and J. Tejel. Lower bounds on the number of crossing-free subgraphs of K_n. *Computational Geometry*, 16(4):211–221, 2000.

[Goo80] J. E. Goodman. Proof of a conjecture of Burr, Grünbaum, and Sloane. *Discrete Mathematics*, 32(1):27–35, 1980.

[GP80] J. E. Goodman and R. Pollack. On the combinatorial classification of nondegenerate configurations in the plane. *Journal of Combinatorial Theory, Series A*, 29(2):220–235, 1980.

[GP81] J. E. Goodman and R. Pollack. Three points do not determine a (pseudo-) plane. *Journal of Combinatorial Theory, Series A*, 31(2):215–218, 1981.

[GP82] J. E. Goodman and R. Pollack. Helly-type theorems for pseudoline arrangements in $\mathcal{P}^2$. *Journal of Combinatorial Theory, Series A*, 32(1):1–19, 1982.

[GP84] J. E. Goodman and R. Pollack. Semispaces of configurations, cell complexes of arrangements. *Journal of Combinatroial Theory, Series A*, 37(3):257–293, 1984.

[GP93] J. E. Goodman and R. Pollack. *Allowable Sequences and Order Types in Discrete and Computational Geometry*, pages 103–134. Springer, 1993.

[GPP+17] X. Goaoc, P. Paták, Z. Patáková, M. Tancer, and U. Wagner. Bounding Helly numbers via Betti numbers. In *A Journey Through Discrete Mathematics: A Tribute to Jiří Matoušek*, pages 407–447. Springer, 2017.

[Grü80] B. Grünbaum. *Arrangements and Spreads*, volume 10 of *CBMS Regional conference series in mathematics*. American Mathematical Society, 1972 (reprinted 1980).

[GTP21] A. García Olaverri, J. Tejel Altarriba, and A. Pilz. On plane subgraphs of complete topological drawings. *Ars Mathematica Contemporanea*, 20(1):69–87, 2021.

[GTVW22] A. García, J. Tejel, B. Vogtenhuber, and A. Weinberger. Empty triangles in generalized twisted drawings of K_n. In *In Proceedings of Graph Drawing and Network Visualization (GD 2022)*, volume 13764 of *LNCS*, pages 40–48. Springer, 2022.

[Guy72] R. K. Guy. Crossing numbers of graphs. In *Graph Theory and Applications: Proceedings of the Conference at Western Michigan University*, pages 111–124. Springer, 1972.

[Har78] H. Harborth. Konvexe Fünfecke in ebenen Punktmengen. *Elemente der Mathematik*, 33:116–118, 1978.

[Har98] H. Harborth. Empty triangles in drawings of the complete graph. *Discrete Mathematics*, 191:109–111, 1998.

[Hel30] E. Helly. Über Systeme von abgeschlossenen Mengen mit gemeinschaftlichen Punkten. *Monatshefte für Mathematik Band 37*, pages 281–302, 1930.

[HKK23] W. Hochstättler, S. Keip, and K. Knauer. Kirchberger's theorem for complexes of oriented matroids. *Linear Algebra and its Applications*, 2023.

[HM74] H. Harborth and I. Mengersen. Edges without crossings in drawings of complete graphs. *Journal of Combinatorial Theory, Series B*, 17(3):299–311, 1974.

[HMPT20] A. F. Holmsen, H. N. Mojarrad, J. Pach, and G. Tardos. Two extensions of the Erdős–Szekeres problem. *Journal of the European Mathematical Society*, pages 3981–3995, 2020.

[Hof05] M. Hoffmann. *On the existence of paths and cycles.* Doctoral thesis, ETH Zurich, Zürich, 2005.

[Hol16] A. F. Holmsen. The intersection of a matroid and an oriented matroid. *Advances in Mathematics*, 290:1–14, 2016.

[Hor83] J. D. Horton. Sets with no empty convex 7-gons. *Canadian Mathematical Bulletin*, 26:482–484, 1983.

[HPT08] A. F. Holmsen, J. Pach, and H. Tverberg. Points surrounding the origin. *Combinatorica*, 28(6):633–644, 2008.

[HT03] M. Hoffmann and C. D. Tóth. Segment endpoint visibility graphs are Hamiltonian. *Computational Geometry*, 26(1):47–68, 2003.

[Kes22] B. Keszegh. Discrete Helly-type theorems for pseudohalfplanes. *European Journal of Combinatorics*, 101:103469, 2022.

[Kes23] B. Keszegh. A new discrete theory of pseudoconvexity. *Discrete Mathematics & Theoretical Computer Science*, 25:1, 2023.

[Kir03] P. Kirchberger. Über Tschebycheffsche Annäherungsmethoden. *Mathematische Annalen*, 57:509–540, 1903.

[Kli22] J. Kliem. *Applications of topology, combinatorics and algorithms to discrete geometry.* PhD thesis, Freie Universität Berlin, 2022.

[KM05] G. Kalai and R. Meshulam. A topological colorful Helly theorem. *Advances in Mathematics*, 191(2):305–311, 2005.

[Knu92] D. E. Knuth. *Axioms and Hulls*, volume 606 of *LNCS*. Springer, 1992.

[KST18] C. Keller, S. Smorodinsky, and G. Tardos. Improved bounds on the Hadwiger–Debrunner numbers. *Israel Journal of Mathematics*, 225:925–945, 2018.

[KV91] M. M. Kapranov and V. A. Voevodsky. Combinatorial-geometric aspects of polycategory theory: Pasting schemes and higher Bruhat orders (list of results). *Cahiers de Topologie et Géométrie Différentielle Catégoriques*, 32:11–27, 1991.

[KV09] J. Kyncl and P. Valtr. On edges crossing few other edges in simple topological complete graphs. *Discrete Mathetmatics*, 309(7):1917–1923, 2009.

[Kyn13] J. Kynčl. Improved enumeration of simple topological graphs. *Discrete & Computational Geometry*, 50(3):727–770, 2013.

[Kyn20] J. Kyncl. Simple realizability of complete abstract topological graphs simplified. *Discrete & Computational Geometry*, 64(1):1–27, 2020.

[Lev26] F. Levi. Die Teilung der projektiven Ebene durch Gerade oder Pseudogerade. *Berichte über die Verhandlungen der Sächsischen Akademie der Wissenschaften zu Leipzig, Mathematisch-Physische Klasse*, 78:256–267, 1926.

[Mat02] J. Matoušek. *Lectures on Discrete Geometry*, volume 212 of *Graduate texts in mathematics*. Springer, 2002.

[Miy21] H. Miyata. On combinatorial properties of points and polynomial curves. arXiv:1703.04963, 2021.

[Mnë88] N. E. Mnëv. The universality theorems on the classification problem of configuration varieties and convex polytopes varieties. In *Topology and Geometry-Rohlin Seminar*, pages 527–544. Springer, 1988.

[MS89] Y. I. Manin and V. V. Schechtman. Arrangements of hyperplanes, higher braid groups and higher Bruhat orders. *Advanced Studies in Pure Mathematics*, 17:289–308, 1989. Algebraic Number Theory – in honor of K. Iwasawa.

[MW14] I. Mabillard and U. Wagner. Eliminating tverberg points, i. an analogue of the whitney trick. In *Proceedings of the thirtieth annual symposium on Computational geometry*, pages 171–180, 2014.

[Nic07] C. M. Nicolás. The Empty Hexagon Theorem. *Discrete & Computational Geometry*, 38(2):389–397, 2007.

[NM80] M. M. Newborn and W. O. J. Moser. Optimal crossing-free Hamiltonian circuit drawings of K_n. *Journal of Combinatorial Theory, Series B*, 29(1):13–26, 1980.

[OEI] OEIS Foundation Inc. The On-Line Encyclopedia of Integer Sequences. Published electronically at `http://oeis.org`.

[Ort22] J. Orthaber. Crossing-free Hamiltonian cycles in simple drawings of the complete graph (and what we found along the way). Master's thesis, Graz University of Technology, 2022.

[Ove03] M. H. Overmars. Finding sets of points without empty convex 6-gons. *Discrete & Computational Geometry*, 29(1):153–158, 2003.

[Öza87] M. Özaydin. Equivariant maps for the symmetric group. Unpublished preprint, University of Wisconsin-Madison, 1987. `http://minds.wisconsin.edu/bitstream/handle/1793/63829/Ozaydin.pdf`.

[Pat20] Z. Patáková. Bounding Radon number via Betti numbers. In *36th International Symposium on Computational Geometry (SoCG 2020)*, volume 164 of *LIPIcs*, pages 61:1–61:13. Schloss Dagstuhl, 2020.

[PST03] J. Pach, J. Solymosi, and G. Tóth. Unavoidable configurations in complete topological graphs. *Discrete & Computational Geometry*, 30(2):311–320, 2003.

[PT05] J. Pach and G. Tóth. Disjoint edges in topological graphs. In *Combinatorial Geometry and Graph Theory*, volume 3330 of *LNTCS*, pages 133–140. Springer, 2005.

[Raf88] N. H. Rafla. *The good drawings D_n of the complete graph K_n*. PhD thesis, McGill University, Montreal, 1988.

[Ric93] J. Richter-Gebert. Oriented matroids with few mutations. In *Discrete & Computational Geometry*, volume 10, pages 251–269. Springer, 1993.

[Rin56] G. Ringel. Teilungen der Ebene durch Geraden oder topologische Geraden. *Mathematische Zeitschrift*, 64:79–102, 1956.

[Rin64] G. Ringel. Extremal problems in the theory of graphs. In *Theory of Graphs and its Applications (Proceedings of the Symposium Smolenice, 1963)*, volume 8590. Publishing House Czechoslovak Academy of Sciences, 1964.

[Rou88] J.-P. Roudneff. Tverberg-type theorems for pseudoconfigurations of points in the plane. *European Journal of Combinatorics*, 9(2):189–198, 1988.

[Rui17] A. J. Ruiz-Vargas. Many disjoint edges in topological graphs. *Computational Geometry*, 62:1–13, 2017.

[RZ94] J. Richter-Gebert and G. M. Ziegler. Zonotopal tilings and the Bohne-Dress theorem. *Contemporary Mathematics*, 178:211–211, 1994.

[Sch19] M. Schaefer. A proof of Levi's extension lemma. arXiv:1910.05388, 2019.

[Sch23] M. Scheucher. A SAT Attack on Erdős–Szekeres Numbers in $\mathbb{R}^d$ and the Empty Hexagon Theorem. *Computing in Geometry and Topology*, 2(1):2:1–2:13, 2023.

[SP06] G. Szekeres and L. Peters. Computer solution to the 17-point Erdős–Szekeres problem. *Australia and New Zealand Industrial and Applied Mathematics*, 48(2):151–164, 2006.

[SSW13] M. Sharir, A. Sheffer, and E. Welzl. Counting plane graphs: Perfect matchings, spanning cycles, and Kasteleyn's technique. *Journal of Combinatorial Theory, Series A*, 120(4):777–794, 2013.

[Sta84] R. P. Stanley. On the number of reduced decompositions of elements of Coxeter groups. *European Journal of Combinatorics*, 5:359–372, 1984.

[Suk12] A. Suk. Disjoint edges in complete topological graphs. In *Proceedings of the 28th Annual Symposium on Computational Geometry (SoCG 2012)*, pages 383–386. ACM, 2012.

[Suk17] A. Suk. On the Erdős–Szekeres convex polygon problem. *Journal of the American Mathematical Society*, 30:1047–1053, 2017.

[SZ22] A. Suk and J. Zeng. Unavoidable patterns in complete simple topological graphs. In *Graph Drawing and Network Visualization (GD 2022)*, volume 13764 of *LNCS*, pages 3–15. Springer, 2022.

[Tho03] H. Thomas. Maps between higher Bruhat orders and higher Stasheff-Tamari posets. In *Proceedings of the International Conferences on Formal Power Series and Algebraic Combinatorics*. Linköping, Sweden, 2003. full version:arXiv:math/0212097.

[Tsc03] F. Tschirschnitz. *LP-related properties of polytopes with few facets*. PhD thesis, ETH Zürich, 2003.

[Tve66] H. Tverberg. A generalization of radon's theorem. *Journal of the London Mathematical Society*, 1(1):123–128, 1966.

[WHH14] N. Wetzler, M. J. H. Heule, and W. A. Hunt. DRAT-trim: Efficient checking and trimming using expressive clausal proofs. In *Theory and Applications of Satisfiability Testing (SAT 2014)*, volume 8561 of *LNCS*, pages 422–429. Springer, 2014.

[Wil23] N. J. Williams. The first higher Stasheff-Tamari orders are quotients of the higher Bruhat orders. *Electronic Journal of Combinatorics*, 30(1), 2023.

[YO69] T. Yanagimoto and M. Okamoto. Partial orderings of permutations and monotonicity of a rank correlation statistic. *Annals of the Institute of Statistical Mathematics*, 21:489–506, 1969.

[Zie93] G. M. Ziegler. Higher Bruhat orders and cyclic hyperplane arrangements. *Topology*, 32(2):259–279, 1993.

[Zie11] G. M. Ziegler. $3N$ colored points in a plane. *Notices of the AMS*, 48(4):550–557, 2011.

Zusammenfassung

In dieser Arbeit untersuchen wir Vorzeichenabbildungen, die für einen festen Rang r Teilmengen von $\{1, \ldots, n\}$ der Mächtigkeit r auf eines der beiden Vorzeichen $+$ und $-$ abbilden, wobei Vorzeichenmuster auf induzierten Teilstrukturen vermieden werden. Insbesondere betrachten wir Signotope und verallgemeinerte Signotope, die aus Pseudohyperebenen Arrangements und einfachen Zeichnungen hervorgehen. Unter Verwendung dieser kombinatorischen Kodierungen für topologische Objekte beweisen wir verallgemeinerte Aussagen klassischer Ergebnisse.

Wir betrachten Levis Erweiterungslemma für Pseudogeraden Arrangements und beweisen, dass es sich auf Signotope ungeraden Ranges r verallgemeinern lässt. Levi zeigte 1926, dass jedes Pseudogeraden Arrangement durch eine zusätzliche Pseudogerade erweitert werden kann, welche zwei vorgeschriebene Punkte enthält. Eine Verallgemeinerung auf die Dimension 3 ist nicht möglich. Goodman und Pollack entdeckten 1981 ein Beispiel eines Pseudoebenen Arrangements und drei vorgeschriebene Punkte, das nicht erweiterbar ist, obwohl es eine Erweiterung durch d Punkte für Hyperebenen Arrangements in Dimension d gibt. Später zeigte Richter-Gebert (1993), dass sogar eine Erweiterung durch zwei vorgeschriebene Punkte in Dimension 3 nicht möglich ist. Wir zeigen, dass für Signotope, die eine Teilklasse von Pseudohyperebenen Arrangements bilden, ein Erweiterungssatz in geraden Dimensionen (ungerader Rang r) gilt. Außerdem geben wir Signotope von Rang 4, 6, 8, 10 und 12 an, welche nicht erweiterbar sind.

Zudem betrachten wir klassische Ergebnisse der konvexen Geometrie wie beispielsweise den Satz von Carathéodory, Helly und Kirchberger und untersuchen diese im Kontext einfacher Zeichnungen des vollständigen Graphen. Insbesondere bestimmen wir, in welcher Ebene der von Arroyo et al. (2022) eingeführten Konvexitätshierarchie die Aussagen gelten und ab welcher Ebene es Gegenbeispiele gibt. Die Konvexitätshierarchie beschreibt mehrere Teilklassen von Zeichnungen zwischen Punktmengen in der Ebene und einfachen Zeichnungen unter Verwendung eines verallgemeinerten Konvexitätsbegriffs. Für den Beweis des Satzes von Kirchberger spielen verallgemeinerte Signotope eine wesentliche Rolle. Diese kodieren die Dreiecksorientierungen von einfachen Zeichnungen. Zusätzlich zu den genannten Sätzen betrachten und definieren wir Löcher im Rahmen einfacher Zeichnungen ein. Löcher werden klassischer Weise in der Forschung von Punktmengen betrachtet. Wir zeigen, dass sich konvexe Zeichnungen ähnlich wie Punktmengen verhalten, da jede hinreichend große konvexe Zeichnung ein 6-Loch enthält, während es beliebig große Zeichnungen ohne 7-Löcher gibt.

Zu guter Letzt zeigen wir, dass die Vermutung von Rafla (1988) für konvexe Zeichnungen wahr ist. Die Vermutung besagt, dass jede einfache Zeichnung des vollständigen Graphen einen planaren Hamiltonkreis enthält. Bis jetzt ist nur die Existenz von planaren Pfaden der Länge $\Omega\left(\frac{\log(n)}{\log\log(n)}\right)$ (Suk, Zeng und Aichholzer et al. 2022) und planaren Matchings der Größe $\Omega(\sqrt{n})$ (Aichholzer et al. 2022) bekannt. Wir untersuchen Variationen und Verallgemeinerungen dieser

Vermutung. Insbesondere beweisen wir, dass jede konvexe Zeichnung eine planare Teilstruktur zulässt, die aus einem planaren Hamiltonkreis und zusätzlichen $n - 2$ Kanten besteht.